Natural Resources Canada | Ressources naturelles Canada

GEOLOGICAL SURVEY OF CANADA

OPEN FILE 7858

Geology and petrology of the Schultz Lake Intrusive Complex and its relationship to unconformity uranium deposits: Schultz Lake, NTS 66-A/5 and Aberdeen Lake, NTS 66-B/8, Western Churchill Province

A.R. Miller and T.D. Peterson

2015

Canada

GEOLOGICAL SURVEY OF CANADA

OPEN FILE 7858

Geology and petrology of the Schultz Lake Intrusive Complex and its relationship to unconformity uranium deposits: Schultz Lake, NTS 66-A/5 and Aberdeen Lake, NTS 66-B/8, Western Churchill Province

A.R. Miller and T.D. Peterson

2015

doi:10.4095/296600

This publication is available for free download through GEOSCAN (http://geoscan.nrcan.gc.ca/).

Recommended citation

Miller, A.R. and Peterson, T.D., 2015. Geology and petrology of the Schultz Lake Intrusive Complex and its relationship to unconformity uranium deposits: Schultz Lake, NTS 66-A/5 and Aberdeen Lake, NTS 66-B/8, Western Churchill Province; Geological Survey of Canada, Open File 7858, 1 .zip file. doi:10.4095/296600

Table of Contents

Geology and petrology of the Schultz Lake Intrusive Complex and its relationship to unconformity uranium deposits: Schultz Lake, NTS 66-A/5 and Aberdeen Lake, NTS 66-B/8, Western Churchill Province

Introduction

In 1994, A.R. Miller, then Regional Metallogenist for the Western Churchill Province, Mineral Deposits Division, Geological Survey of Canada, was approached by Dr. Jean Mondy, then Vice President Exploration Canada for COGEMA Resources Inc. to suggest mineralization-related mapping projects under the Geological Survey of Canada's Industrial Partners Program (IPP) in the Schultz Lake map area on land under exploration permit to COGEMA Resources. A. Miller had devoted parts of eighteen summer field seasons, 1977 to 1994, to mapping the western half of the Schultz Lake map area and evaluating the metallogeny of uranium and other metals.

The project that was selected for the 1995 field work was one proposed by Dr. J. Mondy: the basement terrain south of the Thelon Fault and southwest of Kiggavik in an area that encompassed the Context and Contact exploration grids. The focus of this project was to map the geology of this basement terrain, ascertain its position with respect to the sub-Thelon paleoweathered zone and appraise the potential for basement-hosted unconformity uranium mineralization.

As mapping progressed in the summer of 1995, it became evident that there was little evidence of the sub-Thelon paleoweathered zone; however, a polyphase alkaline-granitic intrusive complex was identified. The size and complexity of this intrusive complex had not been identified by previous GSC mapping (Donaldson, 1966). The first author introduced the term Schultz Lake Intrusive Complex (SLIC) in his 1996 report (Appendix 1).

Subsequently, the term SLIC was informally used during GEM-U activities (Jefferson et al., 2011a,b) and broadened by Tschirhart et al. (2013) to encompass the terrain south of the Thelon Fault as defined by Miller (this document) and a comparable terrain along strike north of the Thelon Fault.

The results from the 1995-1996 collaborative private sector – government geological program have provided a modern data base for recent and ongoing government geosciences programs and supported basement-hosted uranium and rare earth exploration programs in the greater Schultz Lake area, Nunavut since approximately 2006.

A. Miller, 87 Findlay Avenue, Ottawa K1S2V1

oredeposits@yahoo.com

The report generated by A. Miller in 1996 is Appendix 1 of this Open File - a PDF version of a photocopy of the original Industrial Partners Program (IPP) document. Appendix 1 is an extensive geological, petrographic and geochemical study of a mixed Dubawnt minette – Hudson Suite granitoid complex (see Peterson et al., 2002 for descriptions of these suites). An intrusive unit termed the Martell Syenite by Donaldson (1965) has since been more closely defined by Scott et al. (2015) as frozen magma that was a mixture of the minette and granite melts. The SLIC therefore can now be described as dominated by rocks lying within the Martell Syenite spectrum, with the end member phases evident at some outcrops.

The whole rock analyses and most mineral analyses require no further comment than is given in the original report. The exception is the amphibole analyses. In his report, Miller referred to the amphiboles generically as hornblende, and only performed end member recalculations on the more calcic analyses. Primary calcic amphiboles (in this case, dominantly edenite) are typical of the Hudson Suite granitoids. However, amphiboles in the minettes (Peterson, 2006) and in most Martell syenites are substantially more alkaline and are frequently K-richterite. A substantial number of the amphibole analyses of this report fall within that compositional range. A spreadsheet of recalculated amphibole analyses (after Locock, 2013) is included here as Appendix 2.

T. Peterson

Acknowledgments

Dave Quirt (AREVA Resources Canada, Inc.) and C.W. Jefferson are thanked for facilitating the broader distribution of this legacy report, and Jefferson for reviewing a draft of the Open File components.

References

Donaldson, J.A. 1965. The Dubawnt Group, Districts of Keewatin and Mackenzie. Geological Survey of Canada, Paper 64-20, 11 p.

Donaldson, J A. 1966. Geological Survey of Canada, Preliminary Map 7-1966; 1 sheet, doi: 10.4095/107734.

Jefferson, C., Pehrsson, S., Peterson, T., Chorlton, S., Davis, B., Keating, P., Gandhi, S., Fortin, R., Buckle, J., Miles, W., Rainbird, R., Lecheminant, T., Tschirhart, V., Tschirhart, P., Morris, W., Scott, J., Cousens, B., McEwan, B., Bethune, K., Riemer, W., Calhoun, L., White, J., MacIsaac, D., Leblon, B., Lentz, D., LaRocque, A., Shelat, Y., Patterson, J., Enright, A., Stieber, C., Riegler, T., 2011a. Northeast Thelon region geoscience framework - new maps and data for uranium in Nunavut. Geological Survey of Canada Open File 6950.

Jefferson, C.W., Chorlton, S.J., Pehrsson, S.J., Peterson, T.D., Wollenberg, P., Scott, J., Tschirhart, V., McEwan, B., Bethune, K., Calhoun, L., White, J.C., Leblon, B., LaRocque, A., Shelat, Y., Lentz, D., Patterson, J., Riegler, T., Skulski, T., Robinson, S., Paulen, R., McClenaghan, M.B., Layton-Matthews, D., MacIsaac, D., Riemer, W., Stieber, C., Tschirhart, P., 2011b. Northeast Thelon Region: geomapping for uranium in Nunavut. Geological Survey of Canada Open File 6962.

Locock, A.J., 2013. An Excel spreadsheet to classify chemical analyses of amphiboles following the IMA 2012 recommendations. Computers and Geosciences 62, 1-11.

Peterson, T.D., van Breemen, O., Sandeman, H. and Cousens, B. 2002. Proterozoic (1.85–1.75 Ga) igneous suites of the Western Churchill Province: granitoid and ultrapotassic magmatism in a reworked Archean hinterland. Precambrian Research, **119**: 73–100.

Peterson, T.D., 2006. Geology of the Dubawnt Lake area, Nunavut-Northwest Territories. Geological Survey of Canada Bulletin 580.

Scott, J.M., Peterson, T.D., Davis, W.J., Jefferson, C.W., and Cousens, B.L., 2015. Petrology and geochronology of Paleoproterozoic intrusive rocks, Kiggavik uranium camp, Nunavut. Canadian Journal of Earth Sciences, in press.

Tschirhart, V., Morris, W.A., Jefferson, C.W. 2013. Framework geophysical modelling of granitoid vs. supracrustal basement to the northeast Thelon Basin around the Kiggavik uranium camp, Nunavut. Canadian Journal of Earth Sciences, **50**: 667–677. doi: org/10.1139/cjes-2012-0149.

Geology and Petrology of the Schultz Lake Intrusive Complex and its relationship to unconformity related uranium deposits Schultz Lake, NTS 66A/5 and Aberdeen Lake 66B/8 Western Churchill Province

by
@A.R. Miller
MAY 27, 1996

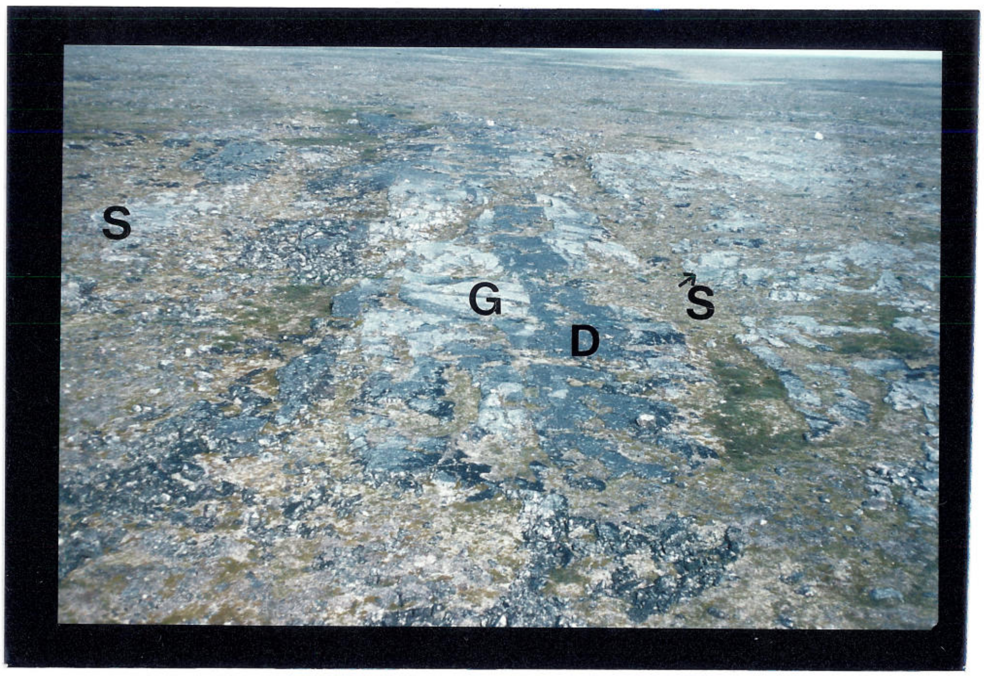

* Contribution to the 1995-1996 IPP Project between the Geological Survey of Canada and Cogema Resourses Inc., PNC Exploration (Canada) Co. and Daewoo Corp.

FRONTISPIECE

Aerial view, looking west, of east northeast-trending linear syenite dykes (D) which cut the agmatitic phase {syenite (S) - light blue gray in the photo and granite (G) - whitish in the photo} of the Schultz Lake Intrusive Complex. Location: about 1 km north of "Mushroom Lake".

ABSTRACT

The Paleoproterozoic Schultz Lake Intrusive Complex (SLIC) is one of five major aeromagnetic anomalies in the Archean basement on the north side of the Paleoproterozoic Baker Lake subbasin. The SLIC intrudes Archean gneissic granitoids and supracrustal rocks belonging to the 2.68 Ga Woodburn Lake Group. This complex is subdivided into three phases in order of increasing younging: syenites, granites and lamprophyre-fine grained syenite.

The mode of emplacement of each of these phases is different. The syenite complex stoped into the Archean granitoid gneisses and supracrustal rocks whereas the granitic complex intruded older syenites in a series of sheets or sills with discordant dykes. This mode of intrusion is similiar to metalliferous Hercynian granites. Lamprophyre - fine-grained syenite dykes are younger than the granite-syenite complex and are controlled by east and east northeast regional fault zones.

The syenite complex is comprised of coarse-grained oikocrystic potassic feldspar cumulates and a diverse array of meso-, melano and leucocratic, even grained to porphyritic syenites. The granitic complex is predominantly comprised of coarse-grained leucocratic granite with subordinate fine-grained leucocratic granite and aplite.

The SLIC is dissected by several fault system, the most prominent set being a east to east-northeast set. Northwest and northeast fault cut the complex. The overall northeast trend of the complex and the association of northeast-trending faults suggests that the complex may have been focused by crustal-scale northeast-trending faults.

Whole rock and mineral petrochemistry link the syenitic phase to the ultrapotassic-potassic magmatic event in the Western Churchill Province and the source region based on geochemistry is the upper mantle. The granitic phase is interpreted to belong to I-type granites and is interpreted to be the product of fusion of the lower crust due to rising geotherms caused by the intrusion of ultrapotassic-potassic magmas.

The lamprophyre-syenite dykes that cut the complex are identical to and belong to the regional 1.84 - 1.83 Ga lamprophyre/minette dykes swarm that is coeval with Christopher Island Formation. Thus the SLIC represent an early ultrapotassic-potassic - granitic event that preceded the main 1.84-1.83 ultrapotassic volcanic event. It is postulated that this magmatic event may be as old as 1.9 Ga.

Differentiation and fractionation in the syenite and granitic complexes did not lead the formation of hydrothermal uranium concentrations. The association of world-class uranium deposits near the margin of the SLIC are interpreted to be the product of Mesoproterozoic, 1.4 Ga, reactivation of the western Churchill crust and the focusing of those fluids along fault zone. selected geophysical surveys should be done over selected targets in the SLIC in order to investigate the potential for unconformity-type uranium deposits in the SLIC.

CONTENTS

LIST of FIGURES

LIST of APPENDICES

INTRODUCTION

Metallogenic comparisons between the Thelon and Athabasca basins have been drawn on the basis of two types of unconformity-related uranium deposits adjacent to and beneath these basins as well as to broadly similar sedimentological and diagenetic features. The two basins lie peripheral to and overlie structural-metamorphic domains that have undergone Proterozoic thermotectonism.

The Thelon Basin lies northwest of the Snowbird Tectonic Zone (Figure. 1) and this basin overlies and is displaced by numerous crustal-scale greenschist-grade mylonite zones. In the Schultz Lake map area, the Archean basement beneath and adjacent to the southeastern margin of the Thelon Basin underwent extensive early Proterozoic, ca 1.9 Ga, thermotectonism followed by deposition of ca 1.84 Ga continental sedimentary and volcanic rocks and coeval intrusions. The protracted uplift history has resulted in the development and/or reactivation of several fault systems that record multiple movements. Deciphering the Proterozoic movement histories on these fault systems is critical to understanding the geometry and genesis of basement-hosted unconformity-related uranium deposits.

In the Schultz Lake map area, the eastern margin of the Thelon Basin is in part-faulted against an Archean basement terrane dominated by ca 2.8 Ga Woodburn Lake Group supracrustal rocks and by Archean ortho- and paragneisses. This basement terrane was intruded by a circa 1.9 Ga Paleoproterozoic syenite-granite complex that has an exposed surface area of approximately 300 sq. km. Basement-hosted unconformity-related uranium deposits are present in the Archean supracustal rocks but they display a close spatial relationship to this Paleoproterozoic intrusive complex. The question commonly debated about these deposits is whether the uranium is genetically related to the granitic intrusion and subsequently modified by younger, 1.4 Ga, hydrothermal episodes, or whether the intrusive contact between the Paleoproterozoic intrusive complex and Archean supracrustal rocks represents a rheological inhomogeneity about which long-lived faulting was focused and along which 1.4 Ga uranium-bearing hydrothermal fluids migrated.

SCOPE OF THE PROJECT

Three weeks were spent mapping the intrusive complex and immediately adjacent Archean country rocks in portions of 66A/5

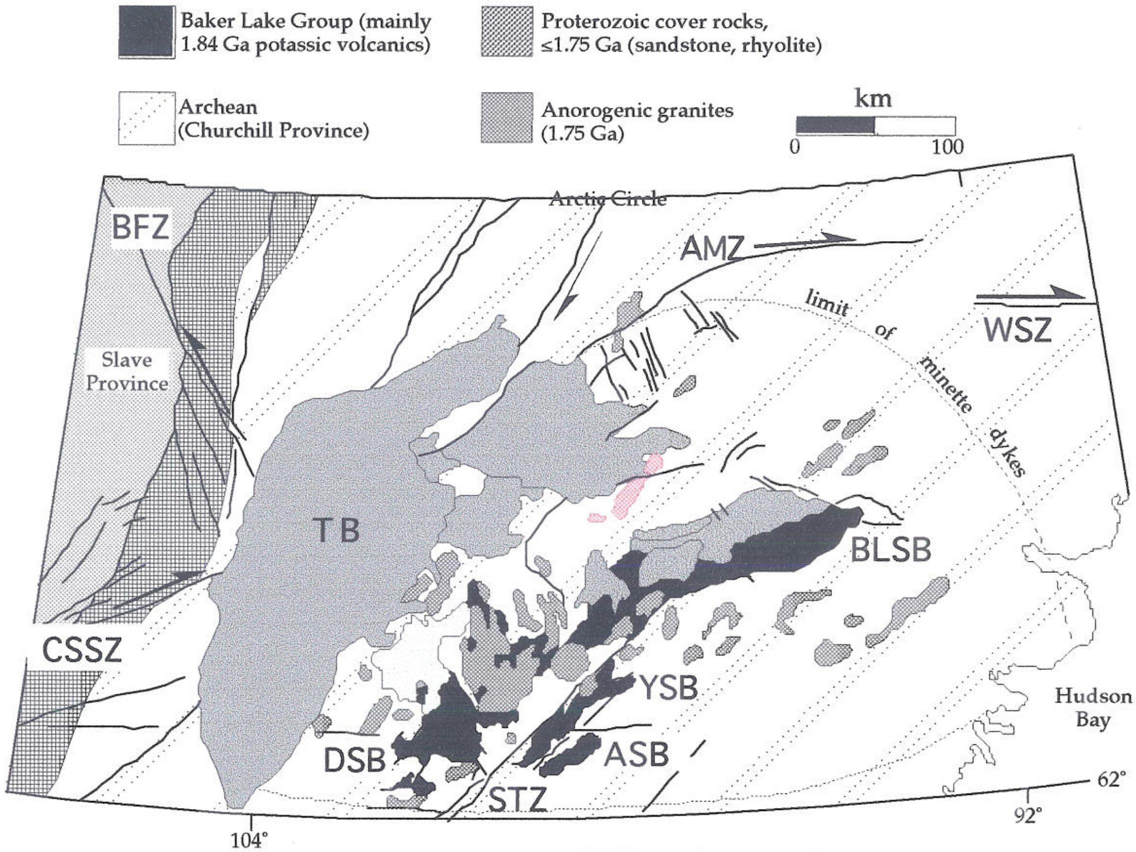

TB	Thelon Basin	CSSZ	Great Slave Shear Zone
ASB	Angikuni Subbasin	BFZ	Bathurst Fault Zone
YSB	Yathkyed Subbasin	STZ	Snowbird Tectonic Zone
DSB	Dubawnt Subbasin	WSZ	Wager Shear Zone
BLSB	Baker Lake Subbasin	AMZ	Amer Mylonite Zone
			Schultz Lake Intrusive Complex

Figure 1. Location of the Schultz Lake Intrusive Complex in relation to Paleoproterozoic subbasins and principal structural elements, western Churchill Province.

and 66B/8 and that data was compiled at 1:50000 scale. The objectives of this project were

a) mapping the intrusive complex and immediately adjacent Archean country rocks in portions of 66A/5 and 66B/8 and compile at 1:50000 scale;

b) identify the intrusive relationships with respect to the Archean basement and identify the individual phases of the complex;

c) the style of emplacement of various phases of the intrusive complex;

d) post-emplacement structures in the pluton;

e) petrographic and geochemical studies on each phase of the intrusive complex.

GEOLOGICAL SETTING

1.84 - 1.76 Ga Paleoproterozoic Basins

At circa 1.84-1.83 Ga the central portion of the western Churchill Province underwent extension and that crustal-scale extensional event is recorded by the preservation of three correlative continental basins that are spatially associated with the northeast-trending Snowbird Tectonic Zone and subparallel structures. These continental basins lie principally to the west of the Snowbird Tectonic Zone. The alignment of these three distinctive and correlative Paleoproterozoic lithostratigraphic sequences defines a 750 Km long northeast-trending extensional terrane in the central western Churchill Province (Figure 1). The three correlative basins are 1) the Martin Group of the Martin Basin and its correlative outliers, northern Saskatchewan, 2) an unnamed sequence that forms a small outlier at the north end of Snowbird Lake and 3) the multiple subbasins in the central part of the western Churchill Province. The multiple subbasins in the central part of the western Churchill Province, Baker Lake, Dubawnt Lake, Angikuni and Yathkyed subbasins, have a combined northeast-tending strike length of approximately 400 Km and attain widths of 50-70 km; the subbasins were filled with continental sedimentary and volcanic rocks that belong to the Baker Lake and Wharton groups, Dubawnt Supergroup.

Stratigraphy of the lower Dubawnt Supergroup - A Review

Wright (1955) was the first to propose the term Dubawnt Group for the flat-lying unfossiliferous Precambrian sedimentary and volcanic rocks in the Baker - Yathkyed - Kamilukuak lakes area.

Donaldson (1969) refined the Dubawnt Group into five formations: red clastics of the South Channel and Kazan formations, ultrapotassic volcanic and volcaniclastic rocks of the Christopher Island Formation, felsic volcanic and volcaniclastic rocks of the Pitz Formation and the Thelon Formation dominated by siliciclastic rocks with very minor limestone and mafic volcanic rocks. This subdivision was based on stratigraphic analysis of the type section south and southeast of Baker Lake, eastern end of the Baker Lake subbasin, and analysis of the entire Thelon Basin which lies primarily west and northwestern of the Snowbird Tectonic Zone.

The type section of the lower Dubawnt Group is subdivided into a flat-lying basal redbed clastic sequence comprised of the South Channel and Kazan formations overlain by the mafic volcanic sequence, Christopher Island Formation. This subdivision was based on sedimentological and compositional characteristics within the redbed sequence and the stratigraphic relations between the redbed sequence and overlying ultrapotassic volcanic sequence. The critical features for constructing this stratigraphic column were: 1) an unconformity between the boulder conglomerate and reworked Archean basement; 2) conformable relationship between the South Channel conglomerate and Kazan sandstone facies; 3) conformable relationship between the red Kazan sandstone sequence and Christopher Island ultrapotassic volcanic rocks 4) most importantly, the red clastic sediments of the South Channel and Kazan formations do not contain clasts of Christopher Island volcanic rocks in the eastern most subbasin and 5) the Christopher Island Formation is defined by the first appearance of volcanic detritus in red clastic sediments or the first volcanic flow-pyroclastic unit. Donaldson (1969) recorded that the red clastic sequence thins rapidly towards the west and is unconformably overlain by ultrapotassic volcanics and derived volcaniclastic sediments of the Christopher Island Formation.

Over the next one and a half decades, renewed regional mapping west and southwest of Donaldson's type area, refined the internal stratigraphy of the Dubawnt Group in the Tebesjuak - Yathkyed - Kamilukuak - Dubawnt lakes area. New stratigraphic units and stratigraphic relationships were recognized: 1) the lack of or only thin aerially restricted veneers of red clastic sediments, conglomerate-sandstone sequences, void of ultrapotassic volcanic clasts at the base of the Dubawnt Group; 2) Christopher Island Formation rocks lying unconformably on basement with no red clastic sediments beneath; 3) a new stratigraphic unit, Kunwak

Formation, a conglomerate-sandstone sequence derived principally from the Christopher Island Formation but lacking in ultrapotassic flow or pyroclastic rocks and 4) bimodal volcanism associated with the felsic-dominated volcanism of the Pitz Formation and 5) the first definition of the petrochemical stratigraphy, lamproite-minette, of the Christopher Island ultrapotassic volcanism in the Dubawnt Lake area. In 1992 the Dubawnt Group was tentatively reassign to supergroup status and that nomenclature tabulated below will be utilized in this report (Figure 2).

DUBAWNT SUPERGROUP

Barrensland Group	**Alkali basaltic volcanism**
Lookout Point Fm	
Kuungmi Fm →	post 1.72 Ga
Thelon Fm	
~~	**High-silica, F-rich volcanism**
Wharton Group	
Pitz Fm →	circa 1.76 Ga
~~	
Baker Lake Group	
Kunwak Fm	**Ultrapotassic volcanism**
Christopher Island Fm →	
Kazan Fm	
South Channel Fm	circa 1.84 -1.83 Ga
~~ Unconformity	
Archean, Early Proterozoic	

Figure 2. Stratigraphy of the Dubawnt Supergroup (after Gall et al, 1992)

The onset of subaerial Christopher Island ultrapotassic volcanism with coeval intrusive rocks, associated mass wasting epiclastic deposits and volcaniclastic sedimentary rocks represents volumetrically and aerially the most extensive lithostratigraphic unit in the Baker Lake Group. Secondly this formation represents the largest or possibly the second largest ultrapotassic-potassic magmatic province in the world. The thickness of the Christopher Island Formation varies from northeast to southwest. In the central and southwestern portions of the Baker Lake subbasin, shingled wedges range up to 10000 feet in total thickness. Following the cessation of ultrapotassic volcanism, faulting continued and a series of small isolated basins were formed. These were filled with continental fluvial sediments, Kunwak Formation, derived principally by denudation of Christopher Island strata.

The upper most formation of the Baker Lake Group, Pitz Formation, rests disconformably to unconformably on older strata. Sediments belonging to this formation indicate the continuation of fluvial continental deposystem, however the fluvial sediments are interbedded and derived in part from high-silica, fluorite- and topaz-bearing ignimbrites and rhyolitic - dacite flows. Pitz volcanism and coeval plutons define a second magmatic event, separate from but as distinctive as the ultrapotassic magmatism that defines the Christopher Island volcanism.

Importantly these two volcanic sequences, the mafic ultrapotassic volcanism of the Christpher Island Formation and the silicic volcanism of the Pitz Formation, are accompanied by their respective plutonic equivalents. A spectrum of intrusive rocks have been recognized within the Archean basement and within the redbeds and volcaniclastic rocks that fill these structurally-controlled subbasins. The Archean basement on the southern side of the Baker Lake subbasin hosts diversified potassic-ultrapotassic intrusions. This diversified array of intrusive rocks is represented by layered ultrapotassic complexes, composite syenite-mafic syenite plutons and lamprophyre-syenite dyke complexes near the basal unconformity of the Baker Lake Group. This diversity in composition, size and geometry of intrusions in the basement on the southern side of the Baker Lake subbasin suggests that a crustal section is preserved through which ultrapotassic magmas ascended. This section is on the order of 70 km thick. Within the redbed and ultrapotassic volcanic sequences, lamprophyre-syenite dykes interpreted as feeders to Christopher Island volcanic rocks, discordant polyphase syenitic complexes up to 250 - 350 sq. km in exposed area and fractionated sills dykes and laccoliths that vary in composition from monzonite to highly fractionated syenitic intrusive rocks, bostonite (felsic minette) are the synvolcanic equivalents to the volcanic rocks in the Christopher Island Formation.

The diversity and number of ultrapotassic intrusions present in the basement on southern side of the Baker Lake subbasin are not present in the Archean basement rocks on the northern side of the

Baker Lake subbasin, Schultz and Aberbeen lakes map. Felsic magmatism represented by the Pitz volcanic rocks and its consanguineous and diverse suite of fine- to coarse-grained flourite-bearing granitoid plutons followed voluminous potassic-ultrapotassic magmatism. Silicic volcanic rocks and related plutonic equivalents are focused on the northwestern side of the Snowbird Tectonic Zone. This distribution must be controlled by the translithospheric Snowbird Tectonic Zone and must reflect fundamental differences in the thermal regime, melting in the lower crust-upper mantle, on the northwestern side of the Baker Lake subbasin.

Numerous circular to ellipsoidal high-intensity aeromagnetic anomalies are present north and northwest of the northwestern edge of the Baker Lake subbasin (Figure 3). These anomalies are attributed to magnetite-bearing Paleoproterozoic intrusions and these intrusions are hosted in Archean gneisses and supracrustal rocks and can be buried by Thelon Formation sandstone. The level of emplacement of these plutons must have been different when evaluated with respect to the present erosional surface and Paleoproterozoic and Mesoproterozoic uplift histories. The largest of these anomalies, termed the Judge Sissons Anomaly, which is ellipsoidal in form, is centred on and trends eastwards from Judge Sissons Lake and has not breached the Archean gneisses and supracrustal rocks known to be present in that area. A second northeast-trending anomaly, termed the Schultz Lake Intrusive Complex (SLIC) is approximately 75 km along its northeast-southwest strike and a width of approximately 10-15 km. The southern half of this intrusive complex is the focus of this project.

Age of Paleoproterozoic volcanism-plutonism, Western Churchill Province

The ages on Christopher Island ultrapotassic and Pitz silicic rocks in the central western Churchill Province are too few to indicate any temporal relationships from west to east along the 400 km strike of this magmatic province. However a few ages constrain ultrapotassic magmatism to circa 1850-1830 Ma with a concentration in the 1840-1830 Ma period. A syenitic pluton in the Amer Lake area dated at 1850 +30/-10 Ma was assumed to approximate the age of ultrapotassic magmatism; however this pluton is distant from the main centre of ultrapotassic magmatism. Ages of 1832+/-28, Pb/Pb apatite, and 1825 +/- 12 Ma, Ar^{39}-Ar^{40} hornblende, from a diamondiferous lamprophyre in the basement beneath the Baker

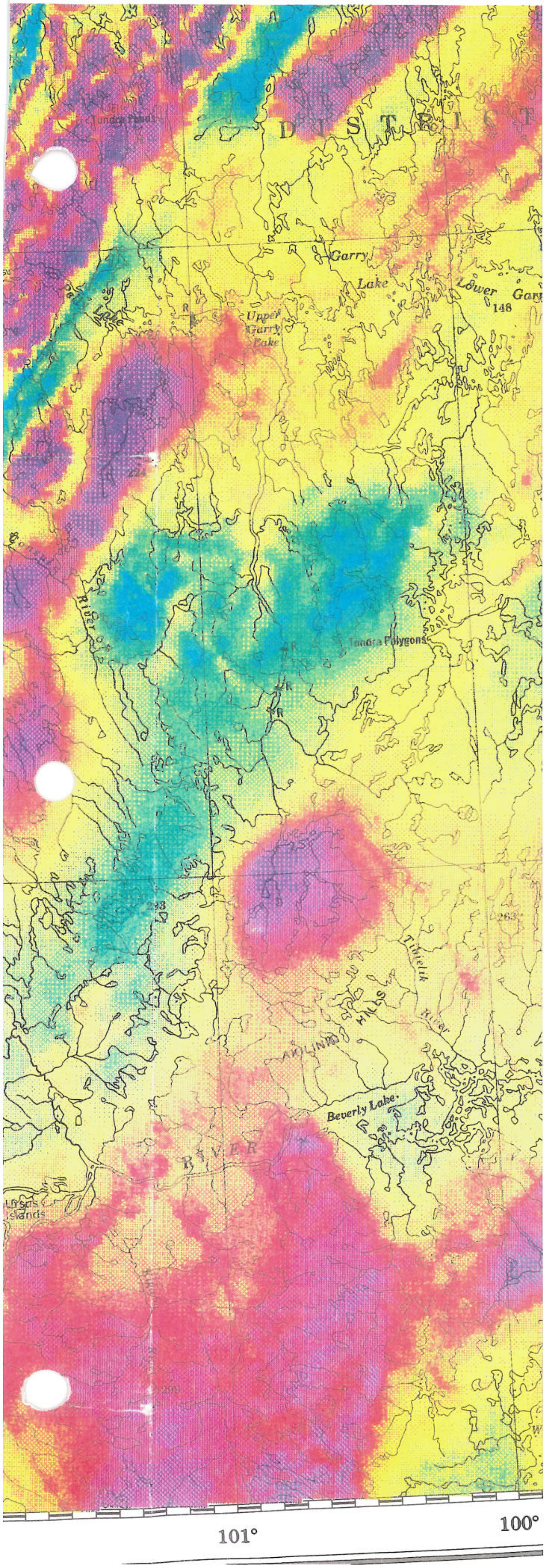

Figure 3. Aeromagnetic anomaly map of the Schultz-Aberbeen lakes area, 1:1,000,000 scale.

1. **Schultz Lake Intrusive Complex**
2. **Judge Sissons Anomaly**
3. **Mallery Anomaly**
4. **Marjorie Hills Anomaly**
5. **Aberdeen Lake Anomaly**

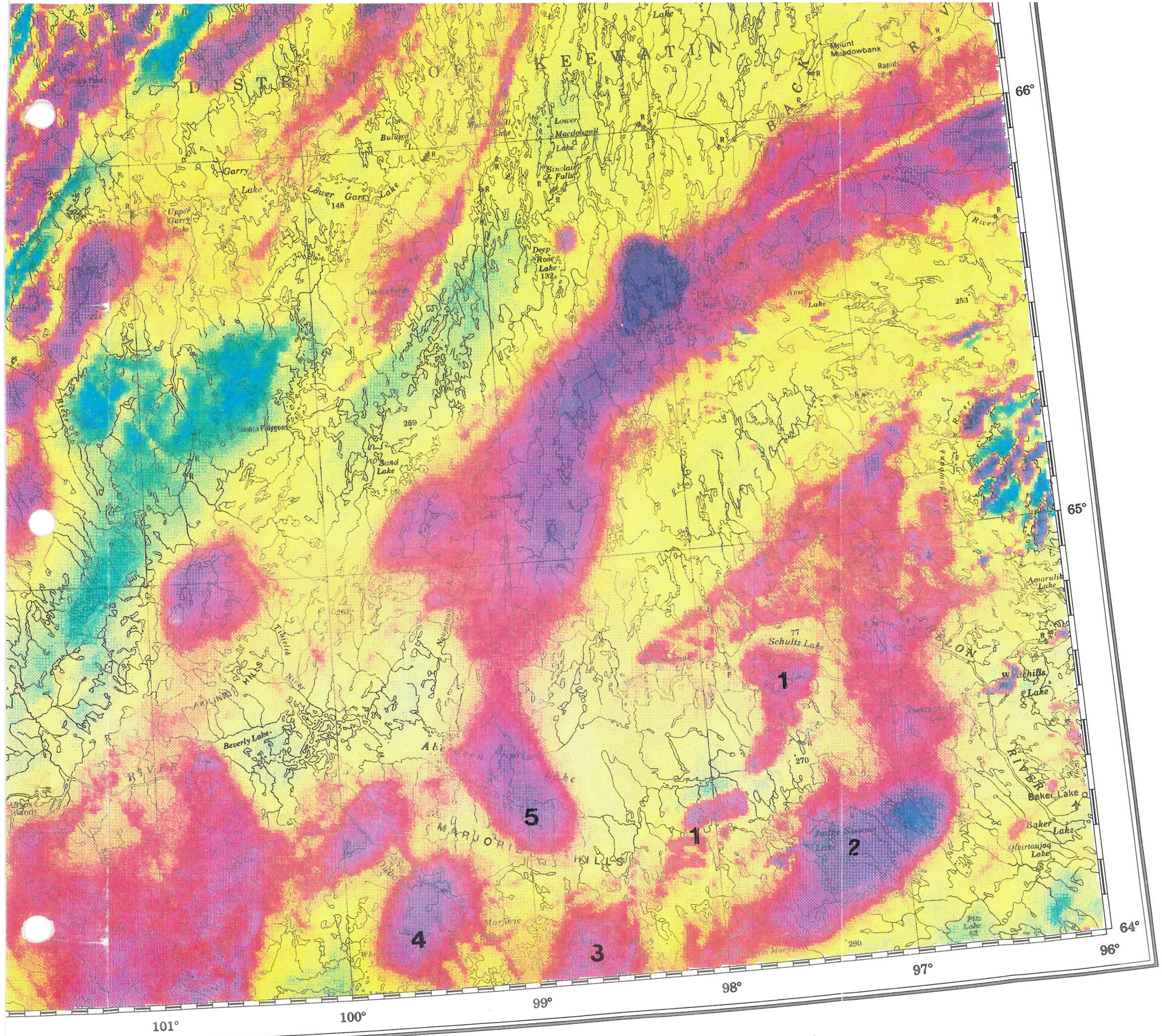

DISTRICT OF KEEWATIN
Mount Meadowbank
Rapids
Lower Macdougall Lake
Sinclair Falls
Garry Lake
Lower Garry Lake
Upper Garry Lake
148
Deep Rose Lake
132
Tundra Ponds
Tundra Polygons
Sand Lake
259
253
River
Schultz Lake
77
1
270
Beverly Lake
Aberdeen Lake
MARJORIE HILLS
5
1
2
3
4
Baker Lake
Amarulik Lake
Whitehills Lake
290
66°
65°
64°
101°
100°
99°
98°
97°
96°

lake subbasin and a syenitic intrusion in the basement beneath the Dubawnt subbasin better contrain ultrapotassic magmatism to circa 1840 - 1830 Ma. This age is in agreement with the maximum age range of 1836 Ma, whole rock and mineral K-Ar ages, on lamprophyres from the southwestern side of the Baker Lake subbasin. However the ages from lamprophyres is less well contrained due to large error limits

The younger magmatic episode dominated by high silica fluorine-rich granite and Pitz rhyolite yield a magmatic peak at 1.76 Ga. If these two magmatic peaks are accepted, circa 1840 - 1830 Ma for ultrapotassic and 1760 Ma for silicic magmatism, then the Baker Lake Group evolved over 70 - 80 Ma. The author considers this time interval to be too long and argues that ultrapotassic and felsic magmatism may be more compressed based on the following argument. First, the rock record of the sedimentary and volcanic rocks that comprise the Baker Lake and Wharton groups indicate a continental tectonic setting with subaerial volcanism and fluvial sedimentation. Secondly, in this continental setting, paleosols of markedly different ages are recognized. The presence of a locally preserved paleosol beneath certain subfacies of the South Channel Formation dictates tectonic stabilization of the western Churchill Province and continental weathering. Following silicic magmatism-volcanism at 1.76 Ga, tectonic stability returned to the western Churchill based on the presence of a thick aerially-extensive lateritic-like paleosol developed on Baker Lake, Wharton group strata and Archean gneisses. The age of this paleosol is bracketed between 1.76 Ga and 1.72 Ga, the latter represents the earliest diagenetic age in the Thelon Formation. Between cessation of Christopher Island ultrapotassic and the onset of Wharton silicic volcanism, a series of small fault-controlled basins were formed and were filled with continental alluvial-fluvial sedimentary rocks belonging to the Kunwak Formation. Considering the continental and subaerial setting of these fault-controlled basins and the 70 - 80 Ma within which the Kunwak Formation must have been deposited, it would seem plausible that one or more paleosols would have been formed during this period. However and most importantly, no paleosols have been recorded prior to or following Kunwak deposition. Thus the two magmatic episodes may span a narrower time interval than suggested by the available geochronological data and by the absence of either pre- or post-Kunwak paleosols. This age argument is considered relevant to the SLIC because the principal phases of this intrusive complex bears many similiarities to plutonic rocks related to both the Christopher Island and Pitz igneous events and the relative temporal relationships observed between the various major intrusive phases are in part consistent with intrusive relationships observed on a regional scale.

REGIONAL STRUCTURE

The western Churchill Province is characterized by a northeast-trending structural fabric and this fabric is highlighted by numerous parallel and subparallel northeast-trending high strain zones (Figures 1, 3). On a regional basis, one important and little recognized attribute of these high strain zones is the overlapping en echelon geometry that produces a gradual shift from northeast to east-trending high strain zones along the structural grain of the western Churchill Province. Examples are the Amer Mylonite - Wager Fault zones and the northeast-trending Snowbird Tectonic Zone - various east to northeast-trending mylonite zones along the southern margin of the Baker Lake subbasin. It is the latter that is important in the Schultz Lake map area and to macro structures in the project area.

In the Schultz Lake map area, east northeast-trending faults and mylonite zones are the most prominent structural element; these are expressed as topographic linears and on regional and detailed aeromagnetic maps by linear zones having lower magnetic susceptibility (Figure 3). The southern most of these faults truncates the northern margin of the Baker Lake subbasin against Archean gneisses. Numerous parallel faults are recognized across the one hundred and twenty kilometer north-south dimension of the Schultz Lake map area. In particular, the SLIC is faulted with dextral sense into two segments by a major structure that has been informally termed the Thelon Fault (Figure 3, 4). South of the Thelon fault, the intrusive complex is dissected by parallel and subparallel second and third order faults that have the same dextral fault motion. One of these faults has been informally termed the North Sissons Fault Zone (NSFZ) (Figure 4). The deformational history of this fault family is unresolved and it is unknown if there is an Archean component. However the faulted geometry of the intrusive complex dictates post-intrusion and certainly some of that motion is post-Thelon Formation.

SCHULTZ LAKE INTRUSIVE COMPLEX

Intrusive Phases

The aeromagnetic anomaly defined as the Schultz Lake Intrusive Complex trends north northeast and is anvil-shaped (Figure 3). The eastern edge of this anomaly is linear and trends north northeast. This intrusive complex is approximate 70 km along its north northeast strike and the width varies from a maximum of 20 km across the northern portion to 10 km across the southern portion of the complex. A east northeast-trending dextral fault, Thelon Fault, divides the intrusive complex into approximately equal segments and the southern segment is the focus of this project (Figures 3, 4).

The complex is divisible into three intrusive phases, syenitic, granitic and lamprophyre - fine-grained syenite; these phases are listed from oldest to youngest based on crosscutting intrusive relationships that were observed throughout the project area. The syenitic and granitic phases were subdivided based on grain size, colour index, and the presence of xenoliths and xenocrysts. Three subtypes from the syenitic phase, cognate and non-cognate xenolithic syenite, fine- and medium grained leucocratic and melanocratic syenitic and melanocratic oikocrystic syenite are depicted in Figure 4. The granitic phase is dominated by salmon to orangy red medium-grained leucocratic flourite-bearing granite with subordinate white fluorite-bearing medium- to fine-grained granite and aplite. The youngest intrusive phase, represented by lamprophyre and fine grained syenite dykes clearly crosscut syenitic rocks which have been intruded by medium- to coarse-grained leucogranite. These dykes chill against the former two rock units and vary from black lamprophyre with very coarse-grained mica, presumed to be xenocrystic mica to fine-grained syenite containing micro-xenoliths. Dykes with these features are reminiscent of primitive lamprophyre and syenite dykes in the basement on the south side of the Baker Lake subbasin.

Mode of emplacement

Syenitic Phase

The interpreted mode of emplacement differs between the three phases of the complex. Contact relations between the complex and Archean granodioritic to granitic gneisses are poorly exposed. and gneissic rocks in the "Buzzard" lake area, east of the eastern margin of the map Figure 4, contains sparsely distributed syenite dykes. However from limited outcrops west of Andrew Lake and in the west of Jane Lake, it is inferred that the syenitic phase stoped into Archean gneisses (Figure 5). Contacts zones are comprised of discordant and concordant units of melanocratic to leucocratic syenite.

Granitic Phase

Discordant and concordant relationships between the granite and syenitic phases are consistent throughout the project area and support the interpretation that the granitic phase is post-syenite. Aplite and fine-grained granitic dykes and sills crosscut all phases of the syenite complex and occasionally a decrease in grain size, chilled contacts, were observed on the margins of some granitic sheets that were intrusive into leucrocratic to melanocratic, oikocrystic and xenolithic syenite.

Sills of granitic composition at all scales were recognized in syenite and basement. West of Andrew Lake, at the contact between the basement and intrusive complex, sheets of flourite-bearing granite passively intruded along the foliation in shallowly east dipping quartzofeldspathic gneisses, (see photo in Beaudemont report, 1994). This passive intrusive style without brecciation nor stoping of the earlier syenitic phase is typical of the granitic phase.

The granitic phase of the complex is interpreted to occur as discordant bodies and as sheets within the earlier syenitic rocks. Subhorizontal sills of aplite, fine-grained granite and coarse-grained granite were observed at all scales in the syenitic phase of the complex. The smallest scale of sill is recorded by narrow, 10-15 cm wide, true thickness, aplite in mafic and oikocrystic syenite (Figure 6) and by fine- to medium grained granite which occurs as sheets and irregular discordant bodies with agmatitic portions of the complex (Figure 7). In areas of low relief with poor outcrop or moderate outcrop with undulating topography, the sill-like geometry of coarse- and fine-grained granite can be discerned by examining colour variations presented by the distribution of dark syenite and light granite. In these areas, contact have tight arcuate forms and can close on themselves forming ellipsoidal-shaped and gently domical areas of granite. These are interpreted as large-scale sills measuring up to 1-2 km in longest dimension and 0.5 km wide. regardless of the scale of these sill-like intrusions, the longest dimension is oriented about a north to northeast direction, a direction that mimics the regional north to northeast trend of the Schultz Lake Intrusive Complex. The sheeted geometry of Schultz Lake complex granites is similiar to Hercycian sheeted granite complexes that are associated

Figure 5. Heterolithic xenolithic medium-grained syenite from the margin of the Schultz Lake Intrusive Complex; xenoliths are dominated by rounded subequant and elongated gneissic xenoliths (G) and minor cognate equant mafic phlogopite clinopyroxenite xenoliths (CM).

Figure 6. Subhorizontal aplite sills, approximately 10 cm thick, in oikocrystic syenite; these small-scale sills typify the intrusive style of the granitic phase into the earlier syenitic phase of the Schultz Lake Intrusive Complex.

Figure 7. Agmatitic phase of the Intrusive Complex, located immediately north of "Mushroom Lake". Outcrop area is comprised of approximately equal proportions of syenite (dark) and medium- to coarse-grained salmon coloured granite (light). Note the shallow dipping sill-like sheet of granite in syenite. This outcrop area illustrates the second order sill-like intrusive style of the granitic phase of the complex.

with greisen-type tin and tungsten mineralization. The greisen-sulfosalt-wolframite occurrence north of Lone Gull may be of this type or possibly related to a specialized cupola or inflection on a granitic sill.

Lamprophyre - fine-grained syenite Phase

The third phase of the intrusive complex, lamprophyres and fine-grained syenite dykes, trend east to east northeast-trending, are subvertical and are always clustered in and near east northeast-trending fault zones. These faults displace the complex in a dextral sense. The width of these dykes vary from as narrow as 20 cm to 20 metres (Figure 8) and importantly these dykes chill against granite and syenite (Figure 9). Well developed chilled margins on these dykes suggest cooler syenite-granite country rocks compared with the poorly formed or non-existence of chilled contacts between the granite and syenite. This suggests that these dykes are significantly younger than the broadly time equivalent syenitic and granitic phases. Also since there are grain size variations were observed in the granite against syenite these relationships suggest that there may be several generations or pulses of granitic intrusion into a syenite complex and chilled margins formed on later granitic sheets that intruded cooler portions of the syenite complex. At present time, there is no evidence to suggest that grain size variations in granitic sheets are related to emplacement at different structural levels in the complex.

Structure -Schultz Lake Intrusive Complex

Macrosstructure

~~The~~ The association of dykes in and periperal to east northeast-trending faults is considered a most important feature that defines crustal blocks in the Schultz-Aberdeen map area. This has implications for Paleoproterozoic, circa 1.85-1.80 Ga deformation and Mesoproterozoic circa 1.4 Ga deformation and its relationship to uranium mineralization. There appears to be a relationship between the number and size of dykes and the size of the east northeast-trending fault zones. For example, the dyke complex in and immediately north of "Mushroom Lake" is the largest identified in the project area and is associated with the North Sissons Fault Zone. This deformation zone has a protracted deformation history

Figure 8. Dykes of fine-grained syenite intruding agmatitic granite (light) - syenite (dark). Dykes widths are variable; the number of dykes and size may be a function of the size and importance of the tectonic breaks that these intruded are associated with. Photo (**A**) is located just north of "Mushroom Lake" in the North Sissons Fault Zone, a major zone of deformation, brecciation with accompanying silicification and hematitization whereas (**B**) is located approximately 2 km to the north northeast of the site in (**A**) on a subparallel narrower east northeast-trending fault.

(**A**)

(**B**)

Figure 9. Chilled margins of a fine-grained syenite dyke (A) and east northeast-trending (075°) black lamprophyre (B) against leucocratic granite. Note in (B) a xenolith of fine-grained granite near the inner contact of the chill zone in the lamprophyre dyke. These dykes are distant from known fault traces and the contacts are undeformed; by contrast see Figure 10A.

(A)

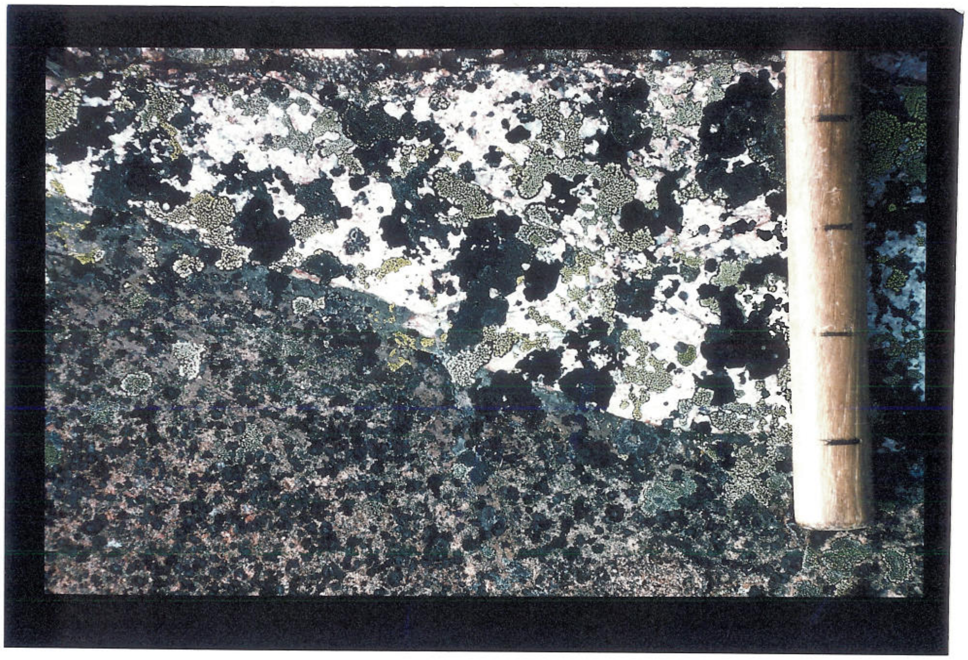

(B)

exhibited by polyphased breccias with accompanying silicification and hematitization. Additional zones of subparallel dykes were located (Figure 4) north and south of the North Sissons Fault Zone and these were inferred to be peripheral to fault zones. In some cases, silicification and hematitization were recognized in the vicinity which strengthens the interpretation. But these dykes and degree of silicification and hematitization were not neccessarily on the scale or as intense as in and adjacent to the North Sissons Fault Zone. Thus zones of narrower dykes and hydrothermal alteration are considered second or possibly third order fault zones that parallel major crustal brakes in the Schultz-Aberbeen map area.

A prominent aeromagnetic feature in the Schultz Lake area is the northwest-trending Mackenzie diabase swarm. The lateral continuity of these dykes across the Schultz Lake map area and regionally is impressive but the most important feature of these dykes is the pinch out and overlap on any one dyke. This regionally consistent geometrical form of pinch out-overlap zones is not due to faults but is due a primary intrusive process related to stress regimes during 1267 Ma emplacement. These pinch out-overlap zones coincide with major east-west to east northeast crustal-scale discontinuities, the same structures exploited by the lamprophyre-fine-grained syenite dykes in the Schultz Lake Intrusive Complex. Thus dyke complexes, ultrapotassic dykes of the SLIC and the tholeiitic Mackenzie swarm in the Schultz-Aberdeen map area delineate two directions of crustal discontinuities in the Schultz-Aberdeen lake area. These northwest and east northeast-trending structures which host dykes of different ages and type subdivide the Archean basement with its overlying Thelon Formation into parallelograms.

Three sets of faults dissect the SLIC and are recognized through a combination of regional-scale aeromagnetic linears combined with topographic linears and geological mapping. They are east northeast, northeast and northwest faults (Figures 3, 4) and each is manifested by a decreased magnetic signature compared to adjacent intrusive rocks (Figures 3). In Figure 4, faults are designated as observed or inferred and the criteria utilized for the observed category include silicification caused by the presence by quartz microveinlets or wide, up to 10-30 metre composite quartz+/-hematite stockworks and breccias and the presence of lamprophyre and fine-grained syenite dykes. Inferred faults are based on a combination of low intensity aeromagnetic linears, topographic linears and the projection from identified fault zones.

Silicification with variable hematitization characterize the east to east northeast-trending faults. The outcrop expression of some of these faults can be subtle if an entire cross section of the fault is not exposed. Narrow and few quartz microveinlets in granite or lamprophyre (Figure 10A, B) and/or a weakly developed penetrative fabric are subtle indications of the presence of these east northeast trending structures. As the fault trace is approached, silicification and hematitization intensify towards the centre of these faults (Figure 10C).

Similiarly cognate ultramafic xenolith-bearing syenite near but south of the projected trace of the Thelon Fault contain bands of quartz +/-hematite veins that are constrained to zones of well developed fracture cleavage (Figure 11A) as well as second order stockwork zones in granite from the Granite Grid area (Figure 12). Polyphased movement histories are recorded by brecciated quartz vein systems (Figure 11B, C) which are similiar to polyphased brecciation textures in the North Sisson Fault zones and quartz stockwork zones that extend from the Andrews Lake deposit area northeastward through END and BONG grids.

These quartz stockwork zones all exhibit textures and structures indicative of polyphase quartz fluxing, brecciation, silicification and hematitization, red through ochre orange, of the wallrock. Angular altered wallrock within veins, ghost-like wallrock inclusions in veins represent intensely silicified early incorporated fragments and cockscomb quartz textures are all indicative of polyphased hydraulic fracturing with open space filling (Figure 13A, B, C). Ultra fine-grained fibrolitic quartz and chalcedonic quartz implies syn-deformation quartz crystallization (Figure 13D, E).

The subvertical east northeast-trending faults, as the Thelon Fault, North Sissons Fault Zone and subparallel second and third order derivatives are part of one family of crustal-scale faults that traverse the western Churchill Province and extend from south of the Baker Lake subbasin northward across the Schultz Lake map area into the Amer Lake map area, a north-south distance of about 200 km. In the project area, these two most prominent dextral faults and subsidiary faults slices the southern half of the SLIC into a series of parallelogram-shaped blocks. The decreasing size of the parallelogram-shaped blocks towards the southwest may reflect post-intrusion uplift and erosion of the complex and adjacent Archean gneisses.

Figure 10. Variations in the types of alteration associated with east northeast-trending fault zones. (**A**) Thin quartz veinlets in fine grained syenite and granite and weak penetrative fabric along the granite-syenite contact are subtle manifestations that this outcrop is on the periphery of a fault zone, location - north shore of "Mushroom Lake", northern margin of the North Sissons Fault Zone.
(**B**) Photomicrograph of quartz microveinlets in leucogranite.

(**A**)

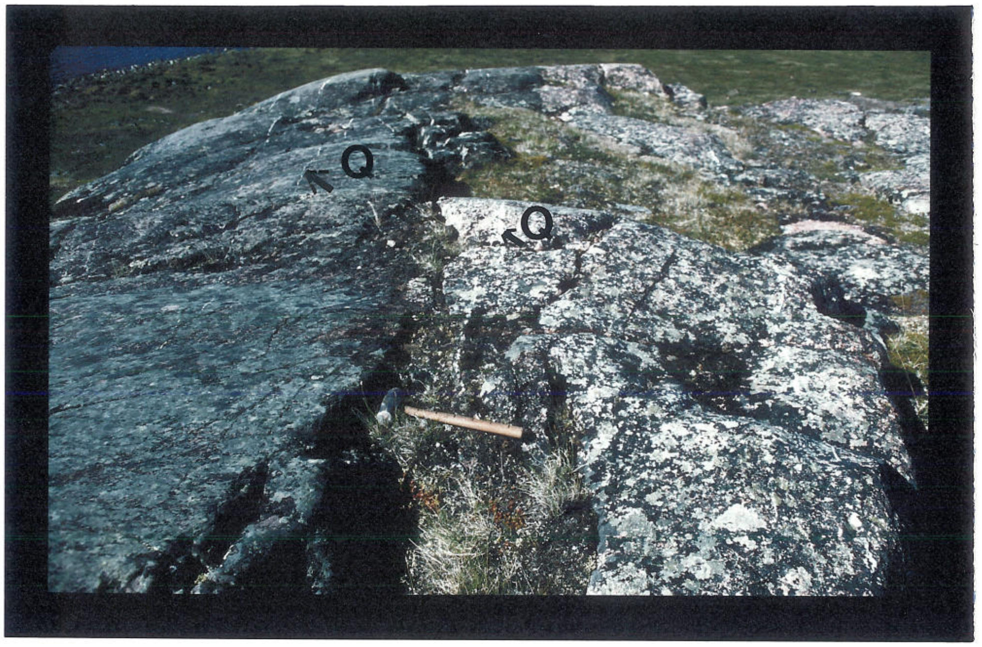

(**B**)

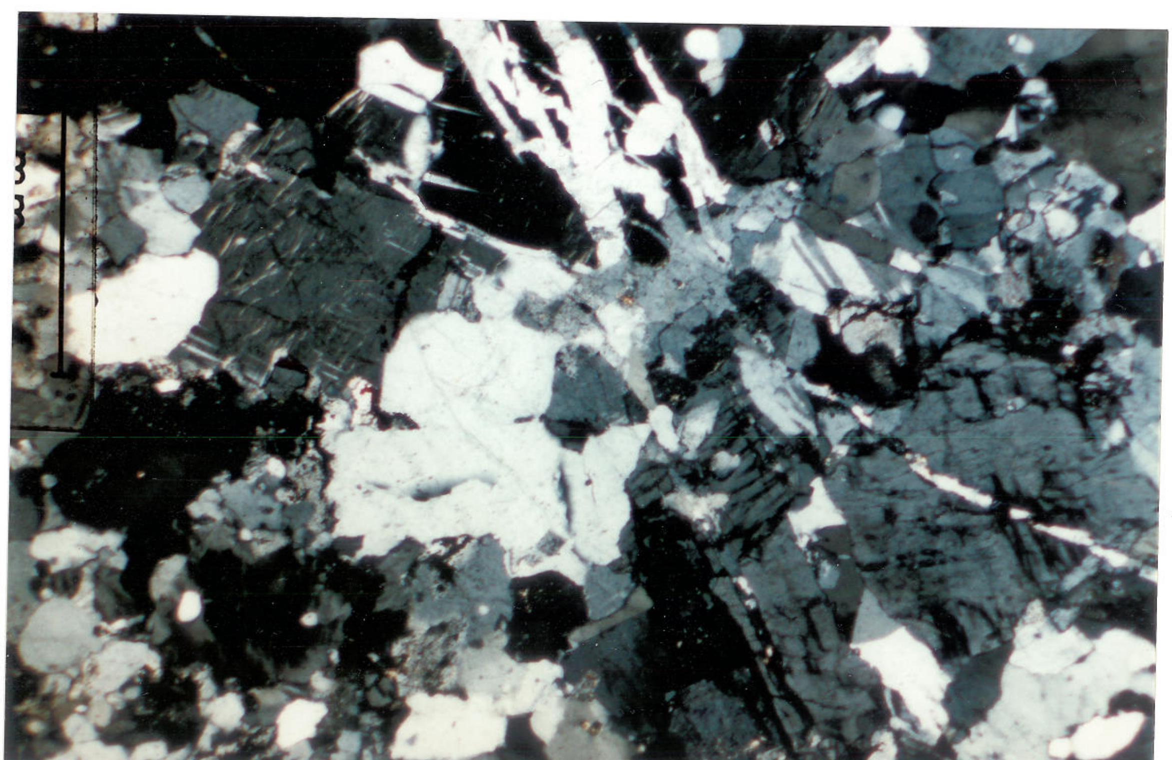

Figure 10 (C) John Learn is standing on the well cleaved strongly silicified and hematitized granite and fine-grained syenite , location on the cliff face immediately south of (A).

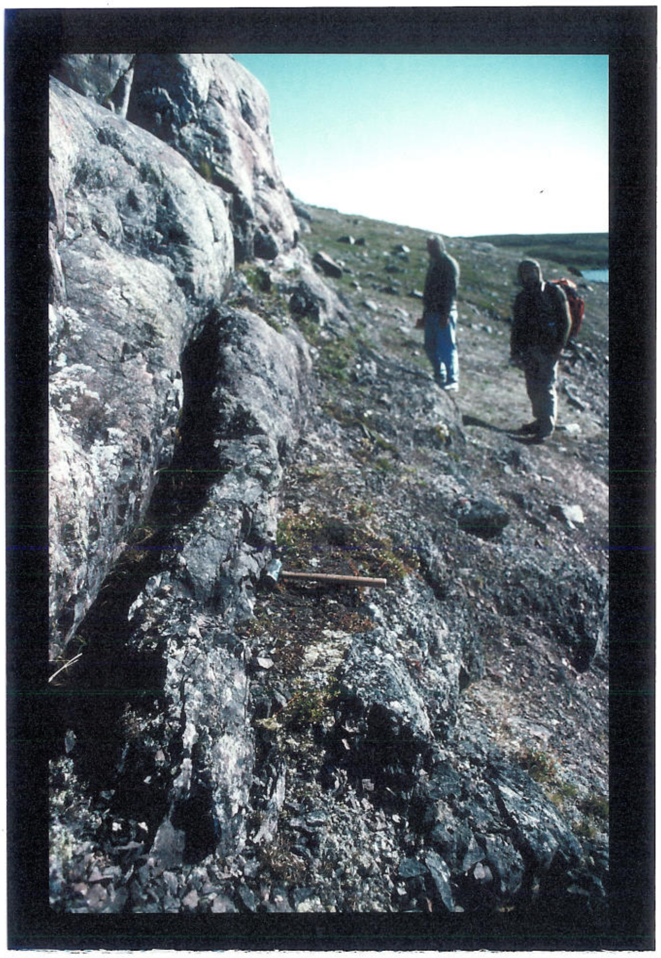

Figure 11. Polyphase quartz + hematite stockworks associated with the Thelon Fault.

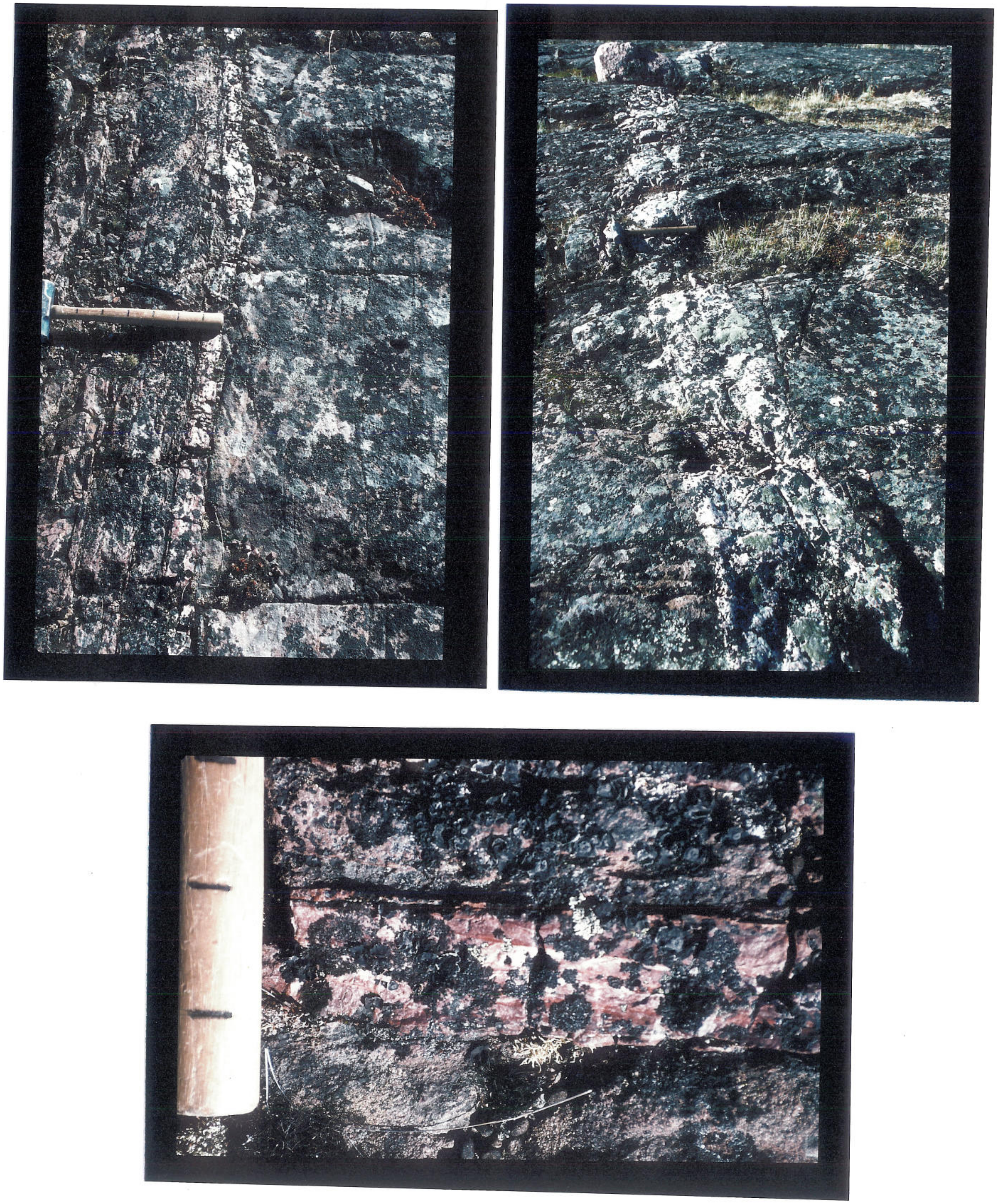

Figure 12. East-trending 10 metre wide quartz stockwork zone in granite near the faulted margin of the Intrusive Complex, Granite Grid area. Photo looking east from the faulted granite and in the background the low lying outcrops are comprised of Woodburn Group greywacke and orthoquartzite.

Figure 13. Textures of quartz+hematite in stockworks associated with east-northeast fault zones. (**A, B, C**) - Cockscomb quartz textures and hematitized and differentially silicified wallrock fragments in veins.

(A

B)

(C)

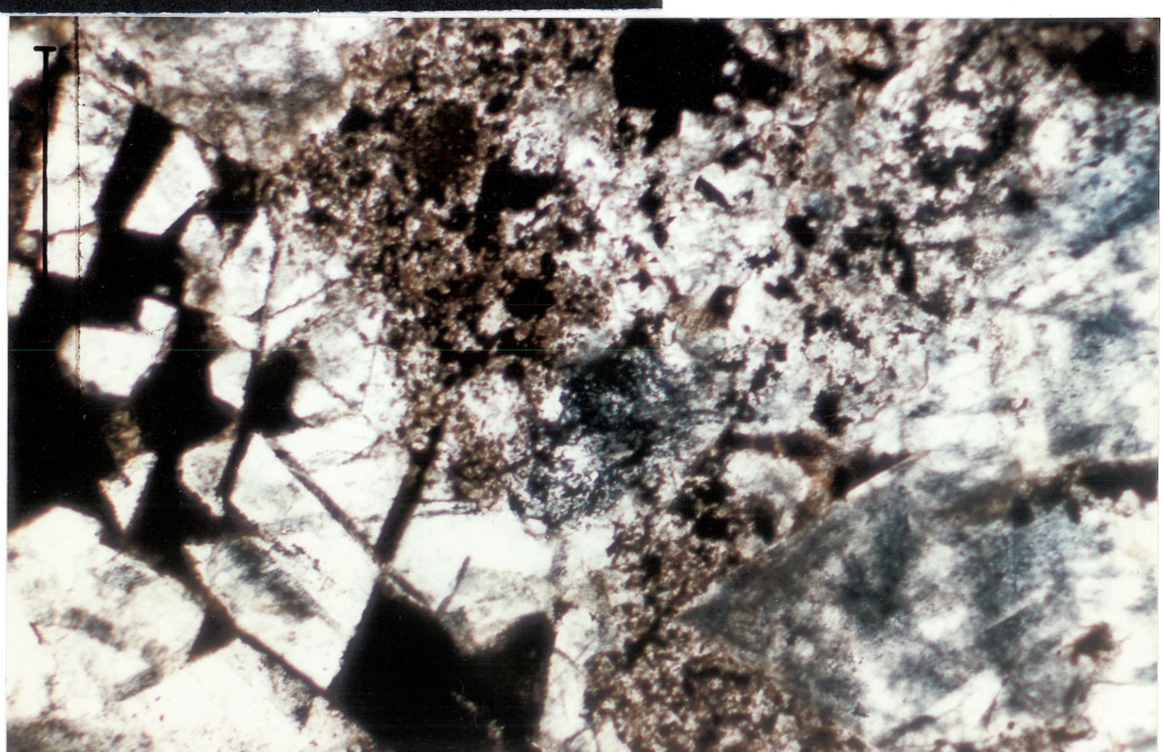

(D) Fibrolitic quartz and chalcedony in banded fault rock.

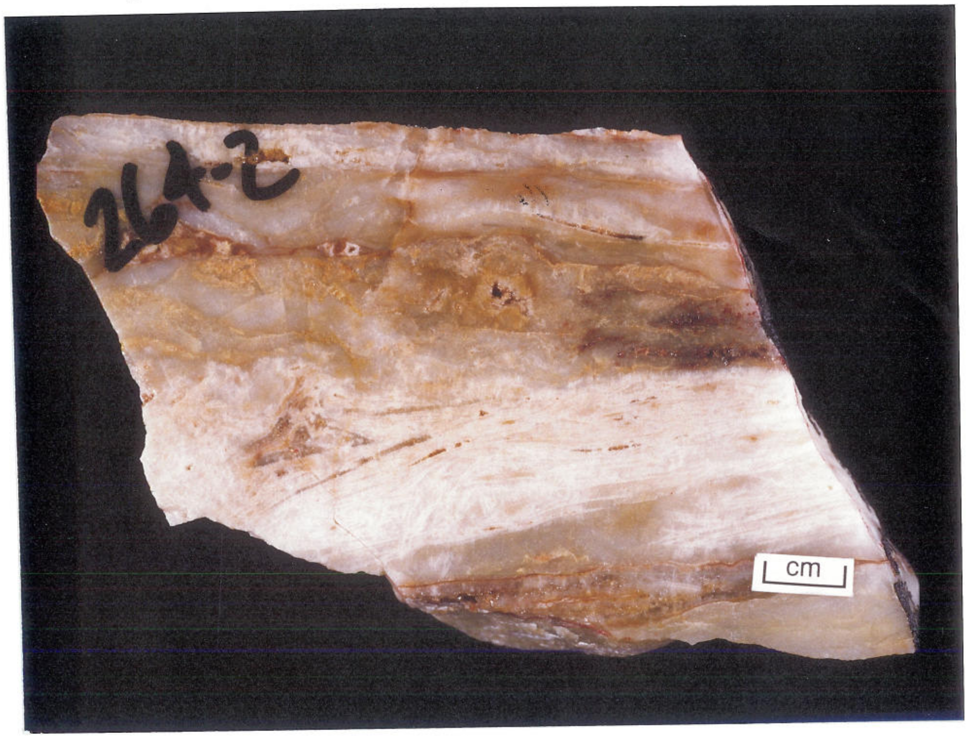

(E) Photomicrograph of D - fibrolitic quartz with hematite

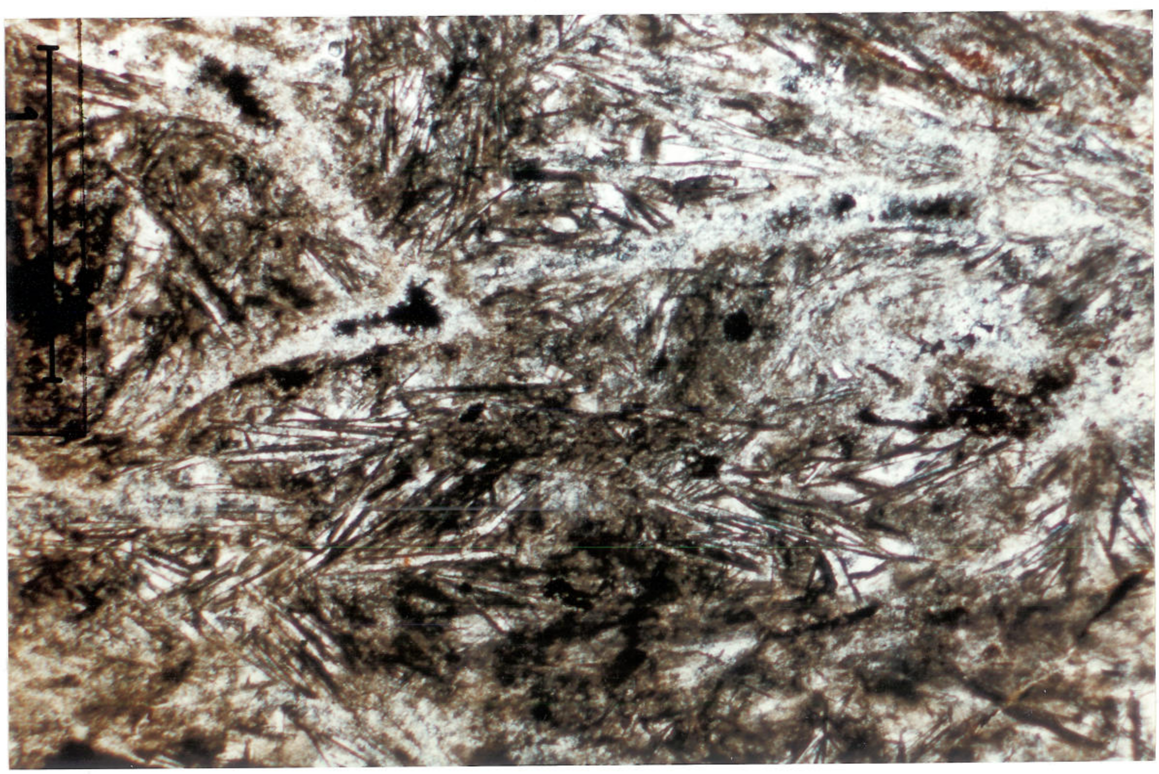

Subvertical northwest-trending faults are inferred from topographic linears and by zones having an increased fracture density. This characteristic of increasing fracture density towards the fault plane is a feature common to the conjugate set of northwest and northeast-trending brittle faults that are recognized throughout the 1.84 Ga Paleoproterozoic subbasins of the western Churchill Province. Displacement along these northwestern faults is uncertain even though there appears to be a minor dextral offset with respect to east northeast-trending faults.

Northeast to north northeast-trending faults are the least abundant of the three fault sets but this trend may have had a fundamental influence on the emplacement of known syenitic-granitic intrusions and anomalies in the Schultz and Amer Lakes map areas. North of Schultz Lake, a northeast-trending fault zone abruptly juxtaposes terranes of markedly different magnetic intensity. Southeast of this crustal discontinuity, several intense magnetic anomalies have a northeast strike. The eastern margin of the Schultz Lake Intrusive Complex has an overall north northeast strike and the ellipsoidal form of the intense aeromagnetic anomaly, termed the Judge Sissons Anomaly, is elongated along a northeast axis. It is posssible that the SLIC and other anomalies were controlled by northeast to northeast-trending crustal-scale fault zones; however even though a fault was inferred between granite and greywacke-orthoquartzite northeast of Sleek Lake, no definitive observations were made that would address this question. However the northeast-trending linear distribution of uranium deposits, Andrews Lake through End, Bong to Kiggavik, strongly suggests that uranium mineralization is controlled in part by this structural trend.

It is important to note that all three phases of the SLIC do not possess a penetrative fabric. However granitic rocks display the effects of proximal fault zones by the development of undulatory polydomainal quartz grains (Figure 14).

PETROGRAPHY and PETROLOGY

SYENITE COMPLEX

Petrography and mineral chemistry

Variations in colour index, grain size and types of cognate xenoliths and xenocrysts were use to subdivide and assemble an intrusive sequence for the syenitic phase of the SLIC. Coarse-grained oikocrystic syenite is one of two very distinctive rock units belonging

Figure 14 Photomicrograph of weak recrystallized leucogranite. Large quartz grain in the centre of the photo has developed subdomains due to its proximity to a zone of strain.

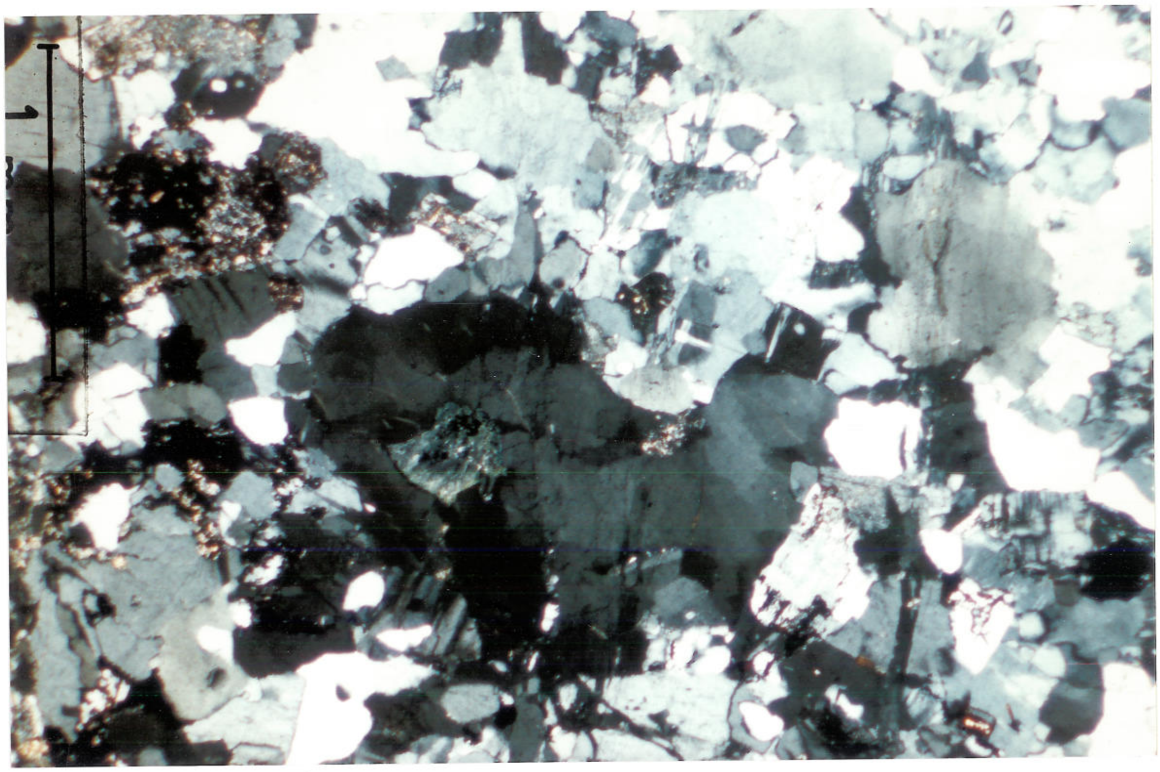

to the syenitic complex. It is intruded by meso- and leucocratic fine- to medium grained syenites and by granitic dykes. The weathered surface of this unit is very distinctive because of the positive domical weathering pattern of megacrystic, up to 3 cm, euhedral potassic feldspar oikocrysts (Figure 15A). Oikocrystic syenite contains ultrapotassic clinopyroxene+mica (biotite) cognate xenoliths (Figure 15B). Oikocrystic potassic feldspar can be spectacularly zoned (Figure 15C) and poikilitic with inclusions of clinopyroxene, mica (biotite) and trace sphene and fluorite (Figure 15D). These same phases occur interstitial to macrocrysts. Locally, irregular-shaped coarse-grained pegmatitic segregation pods consisting of pink K-feldspar+hornblende+/-quartz are present interstitial to oikocrystic potassic feldspar (Figure 15E). The tightly packed nature of the oikocrystic feldspars suggest this rock unit may be a cumulate and that the pegmatitic segregations represent fractionated intercumulus liquid.

The second most distinctive lithology in the syenitic phase of the SLIC is medium-grained mesocratic syenite with cognate ultrapotassic xenoliths that commonly weather recessively (Figure 16 A) This unit is best exposed along the northwestern portion of the SLIC, immediately south of the Thelon fault. Xenoliths geometry varies from equant rounded to elongate subrounded, egg-shaped, and a size range from 5 cm to less than 5 mm. Many of these xenoliths have a jacket of fine-grained mica (biotite) and this feature outwardly resembles glimmerite nodules present in lamprophyres and lavas that belong to the Christopher Island Formation. Some xenoliths are mica-rich like glimmerite nodules and are associated with subordinate clinopyroxene and trace fluorite (Figure 17). However the mica textures, unoriented and fine-grained do not resemble the jacketed, layered and curved textures of coarse-grained phlogopite in glimmerites (Peterson and LeCheminant, 1993, Canadian Mineralogist) Modal compositional variations of xenoliths from clinopyroxene-rich to mica-rich suggest that these xenoliths represent a continuum derived from a fractionating ultrapotassic magma. These xenoliths resemble layered ultrapotassic intrusions mapped by the author in the basement complex on the south side of the Baker Lake subbasin. Xenoliths of this compositional range have been observed in a variety of lithologies in the SLIC, oikocrystic syenite (Figure 14) and xenolithic syenite present on the margin of the complex, labelled as CM - cognate mafic xenolith (Figure 5). Because these xenoliths are widely distributed and the mineralogy of individual phases in the xenoliths are similiar to host rock these

Figure 15 (**A**) Outcrop photo of oikocrystic K-feldspar syenite; macrocrysts are 2-3 cm in size and intra-macrocryst segregation of hornblende (arrow). (**B**) Oikocrystic syenite with cognate ultrapotassic xenoliths (biotite clinopyroxenite).

(**A**)

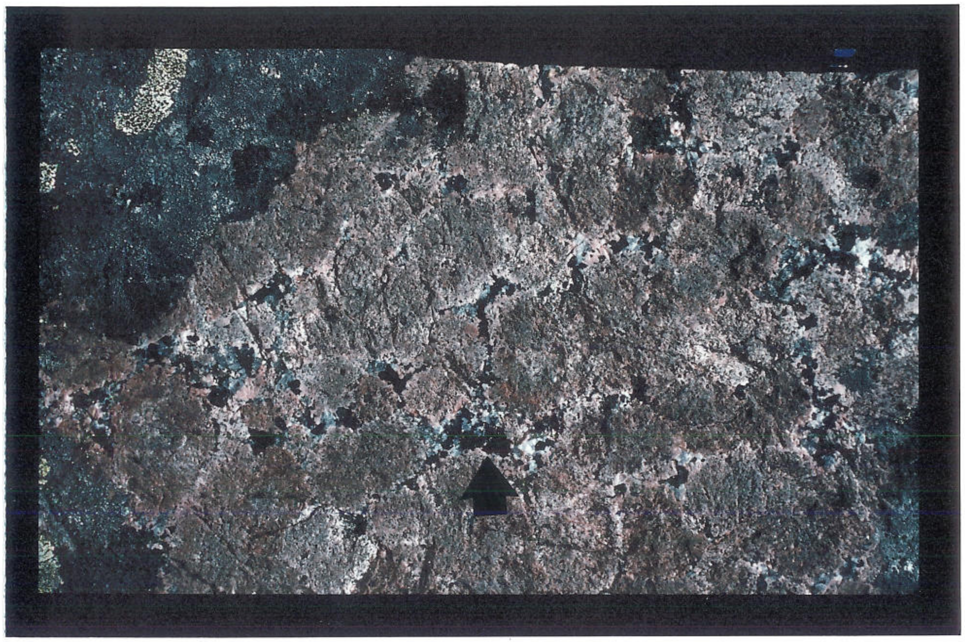

(**B**)

Figure 15C. Photomicrograph of complexly zoned oikocrystic potassic feldspar. Black band is an ink mark used for location identification during microprobe analysis.

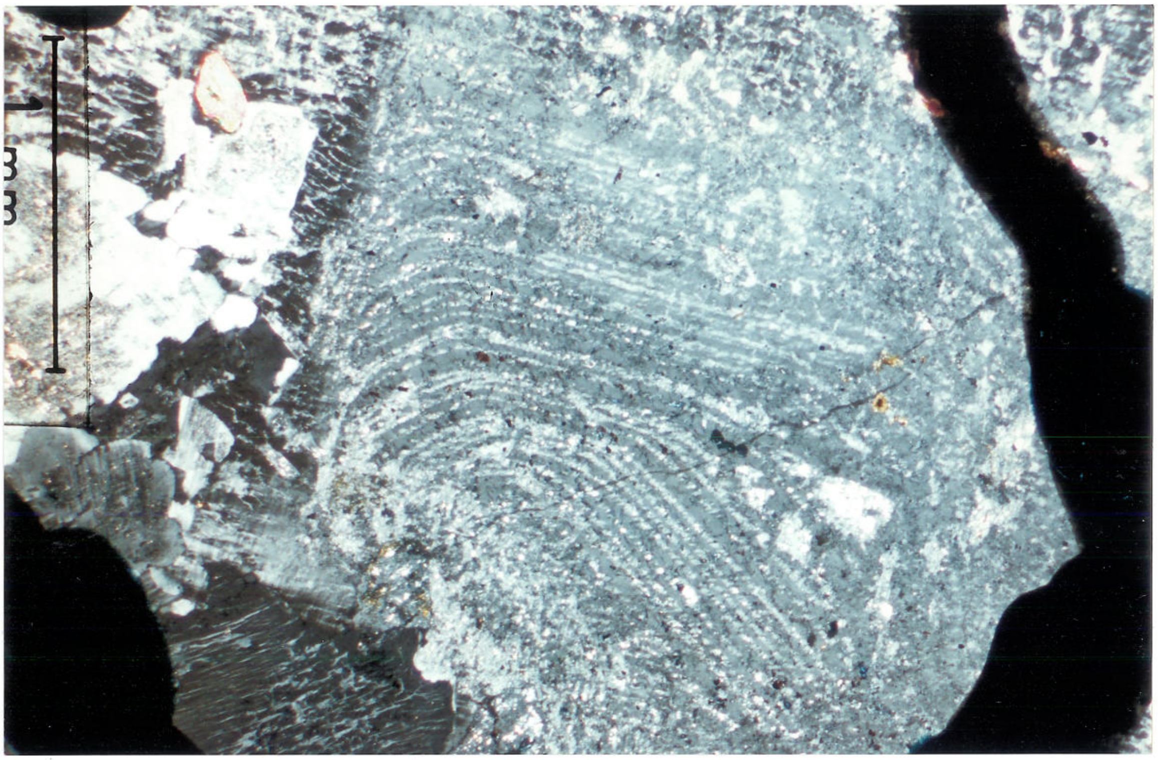

Figure 15D. Photomicrograph of coarse grained oikocrystic potassic feldspar with inclusions of clinopyroxene (C), biotite (B), sphene (S) and purple flourite (F).
Figure 15E. Photomicrograph of coarse-grained hornblende with subhedral magnetite hosted in alkali feldspar.

(D)

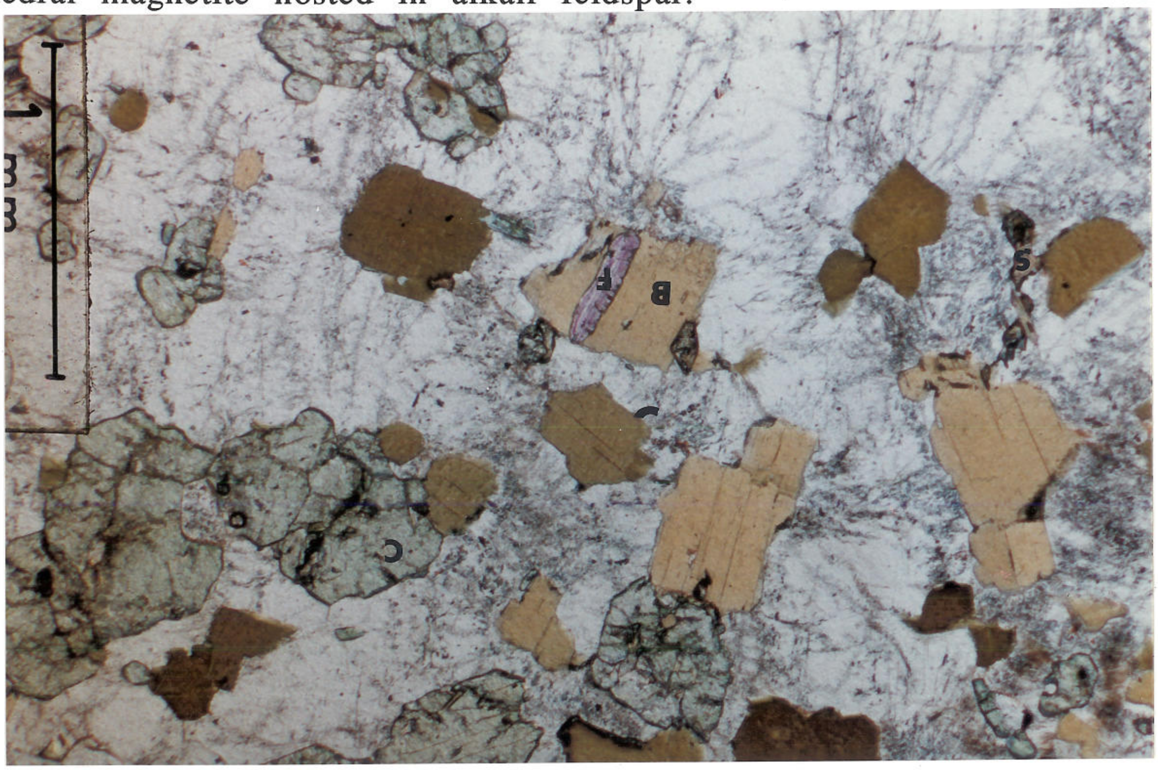

(E)

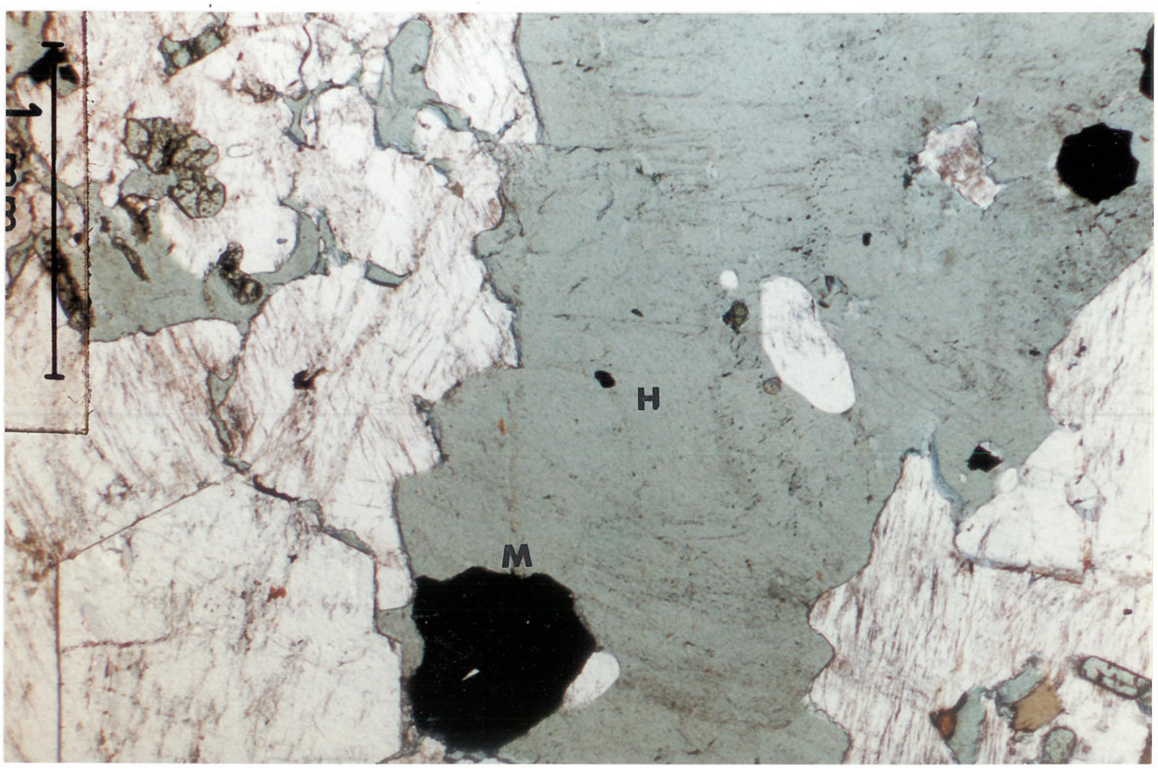

Figure 16. (A) Medium-grained clinopyroxene+phlogoite-bearing syenite with cognate biotite-bearing clinopyroxenite xenoliths. (B) Photomicrograph of (A) depicts the fine-grained biotite jacket on the phlogopite+clinopyroxene xenolith and the host which consists of potassic feldspar(K) +clinopyroxene (C) +biotite (B) + magnetite(M) +apatite (A).

(A)

(B)

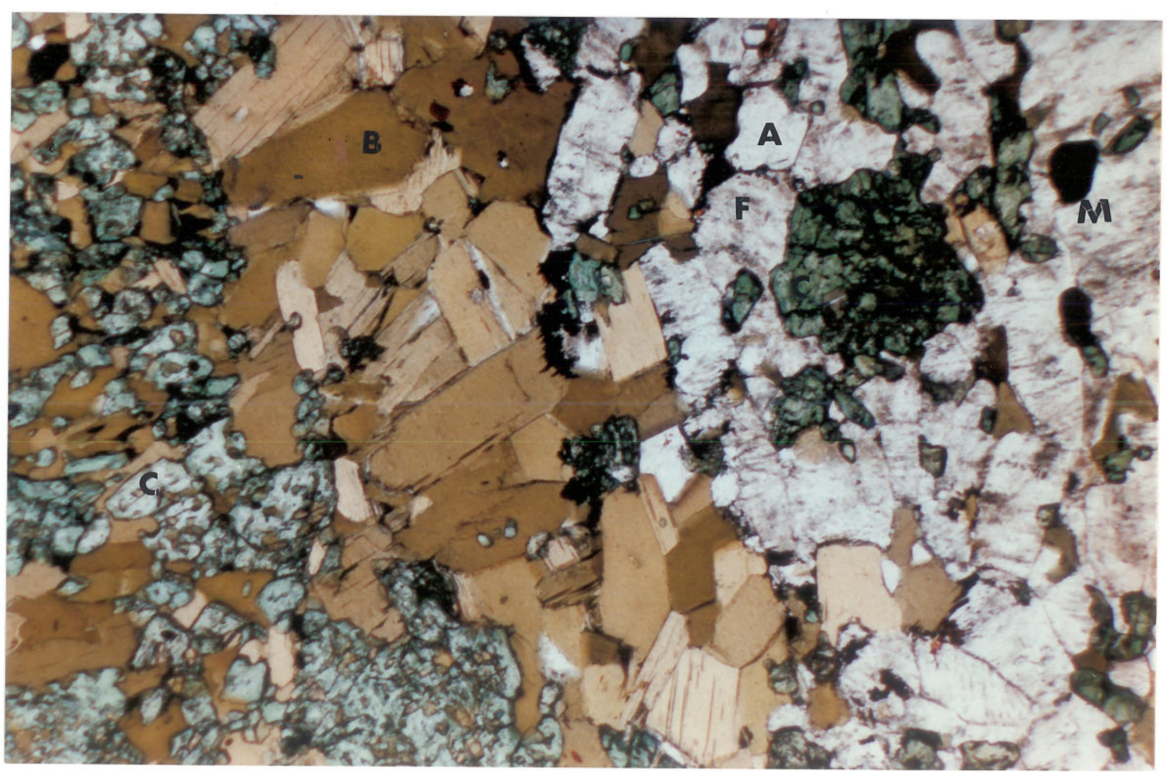

Figure 17. Photomicrograph of a portion of a biotite-rich xenolith with minor clinopyroxene (C), trace interstitial purple flourite (F) and euhedral magnetite.

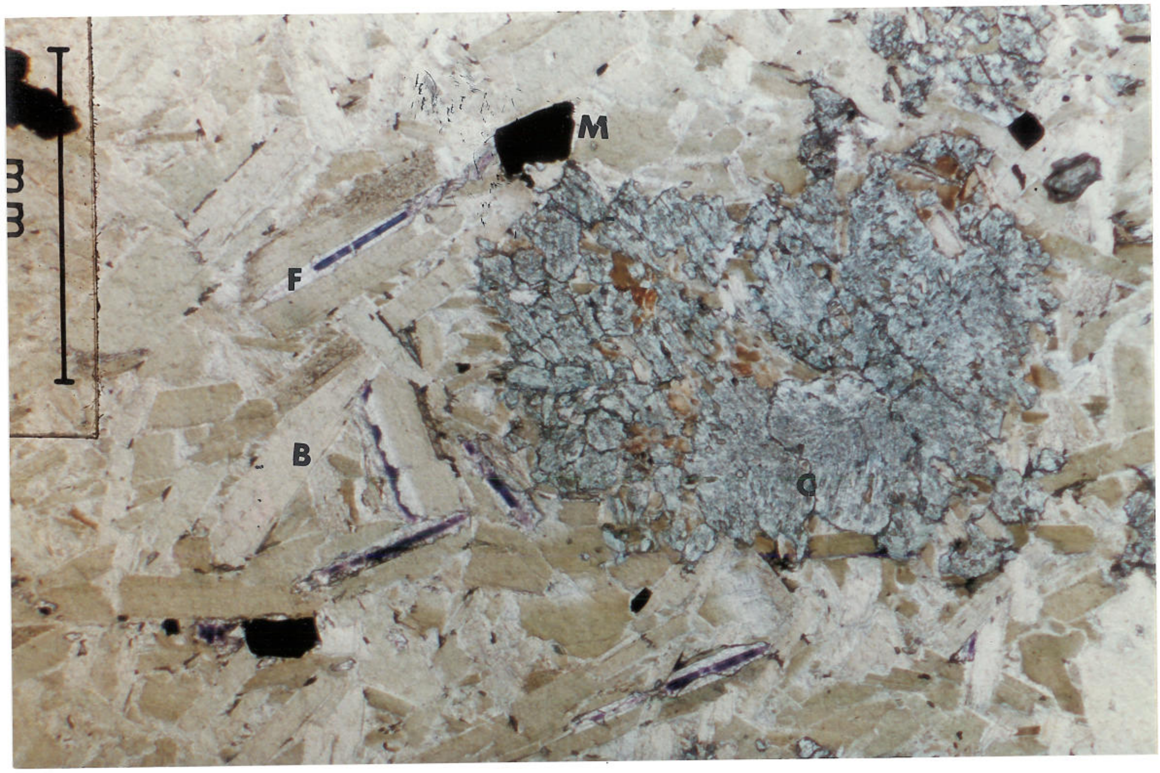

xenoliths are interpreted as being genetically related to the complex and are therefore considered to be cognate xenoliths.

The remaining rock types that comprise the syenitic portion of the complex represent a textural and mineralogical continuum from mesocratic through to leucocratic syenite and quartz-bearing syenite-monzonite. Textures in this undersaturated rock series range from medium- to fine-grained, even grained through to subporphyritic and porphyritic (Figure 18) and the porphyritc phases include potassic feldspar, albite and hornblende. Potassic feldspar is the most abundant phenocrystic phase and closely packed zoned phenocrysts can form a weakly developed trachytoid texture. Colour indices vary from 1-2 in feldspar-rich phases, commonly fine-grained syenite dykes to 10-15 in clinopyroxene + hornblende + mica-bearing phases. Assessory mineral as sphene, magnetite, flourite and apatite are ubiquitous and rare zircon (Figure 19).

Clinopyroxene

Clinopyroxene, the most abundant mafic mineral in this phase of the SLIC, and in some of the ultrapotassic cognate xenoliths. Texturally clinopyroxene occurs as phenocrysts and as equigranular individual grains and glomeroporphyritic aggregates distributed through one and two feldspar-bearing syenite. Macrocrysts are zoned with multiple growth bands whereas medium and fine grained clinopyroxene exhibit undulatory extinction. This undulatory extinction is representive of cryptic zoning. Overall the textures in medium to fine-grained clinopyroxene suggest equilibrium crystallization whereas zoned macrocrysts display disequilibrium textures.

The composition of all clinopyroxene analyses listed in Appendix 1 are represented in Figure 20. Analyses represent essentially one clinopyroxene type, salite with a small percentage of the analyses lying on and just within the ferrosalite compositional field. Zoning from centre to rim within individual macrocrysts and fine- to medium-grained clinopyroxene are normal with moderate to minor increases in iron. However oscillatory zoning patterns are present and represent reversals from the normal iron enrichment (Figure 21). These are interpreted as disequilibrium textures due to mixing of fractionated and more primative ultrapotassic magmas.

Figure 18. Outcrop photo of subporphyritic leucocratic syenite.

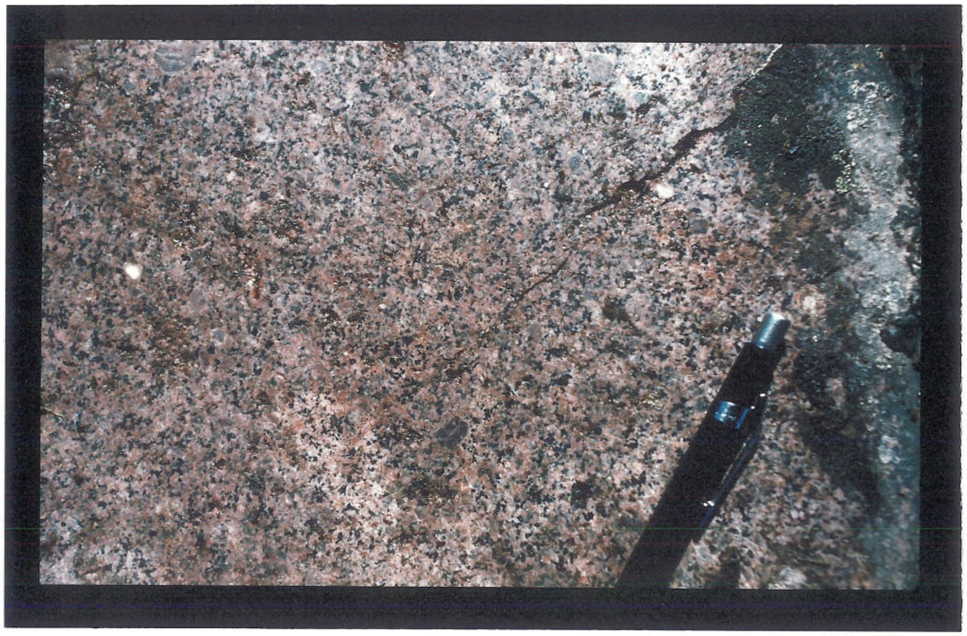

Figure 19. A series of photomicrographs to illustrate the range in mineralogy, texture and grain size of medium- to fine-grained, even grained through to subporphyritic and porphyritic and mesocratic to leucocratic syenite.

(A) Medium-grained hornblende (H) syenite. Poikilitic hornblende contains finer grains of potassic feldspar (K) + trace sphene (S) and disseminated magnetite (M).

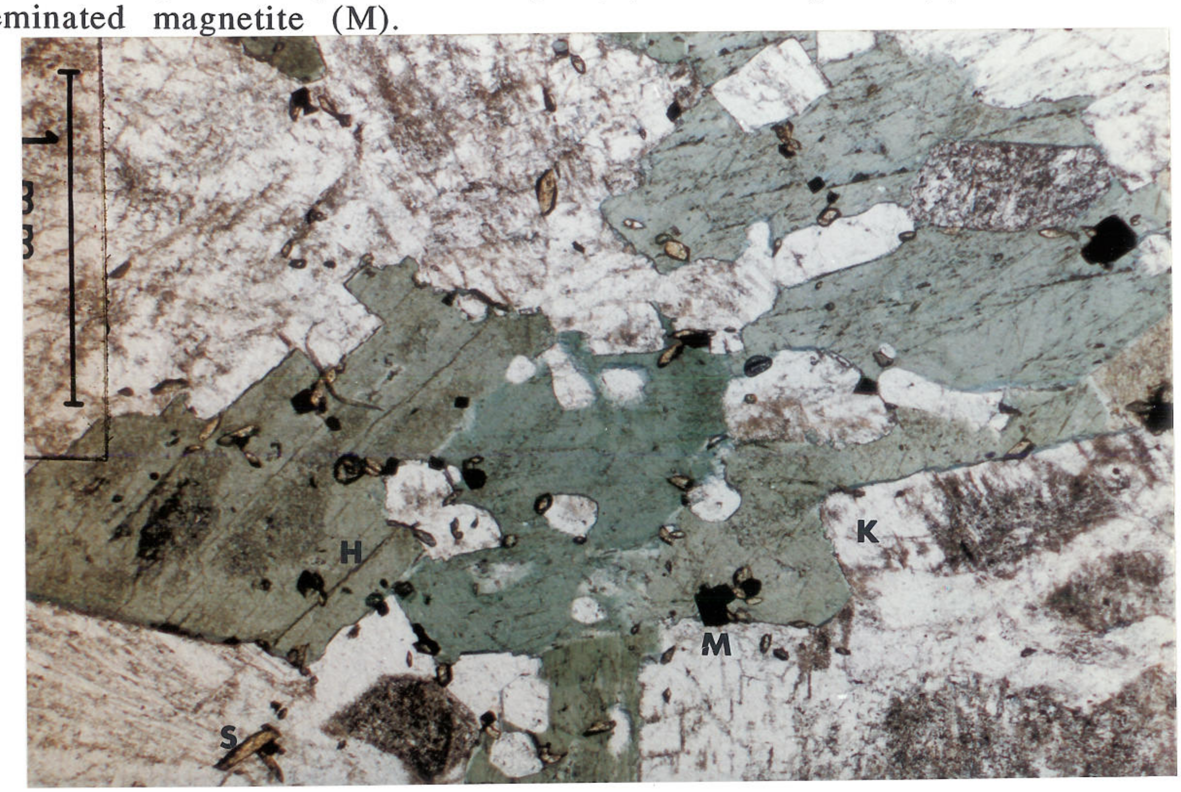

(B) Cluster of fine-grained hornblende (H) with sphene (S), magnetite (euhedral opague) in fine-grained potassic feldspar + albite.

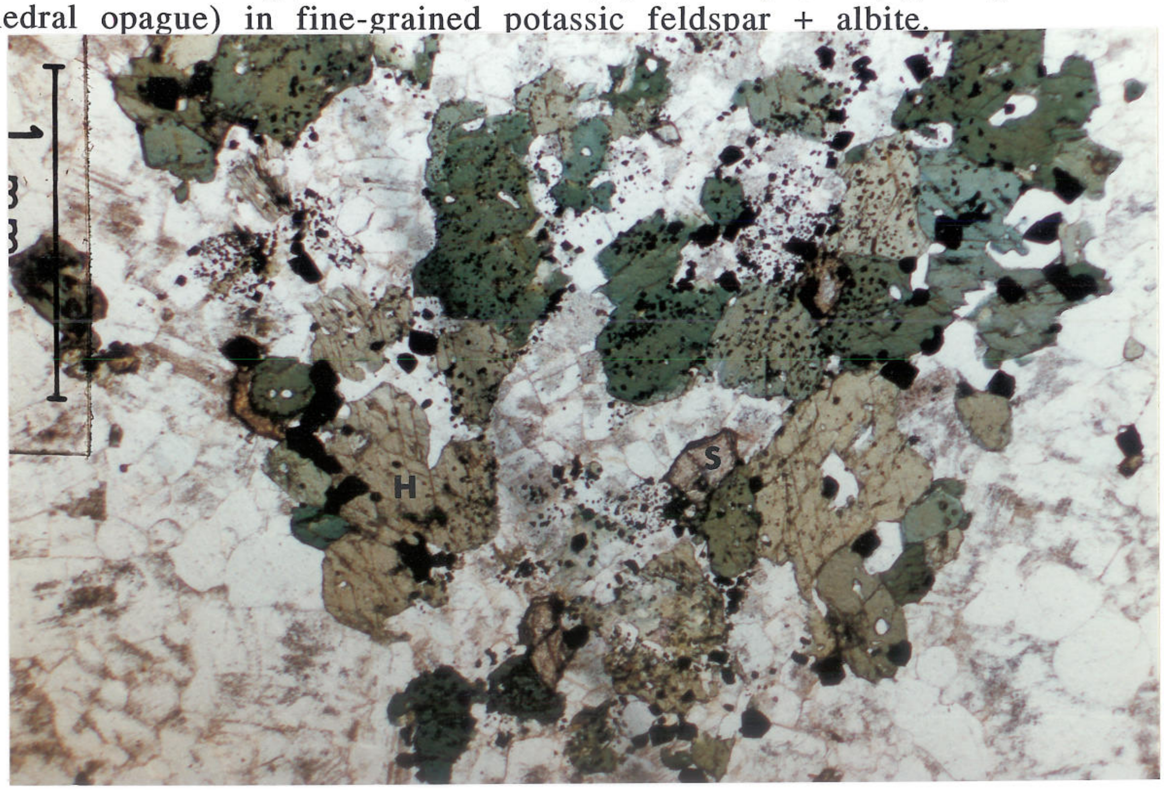

(C) Clinopyroxene (C) + biotite (B) syenite with euhedral apatite (A) and trace magnetite euhedra (black opaque).

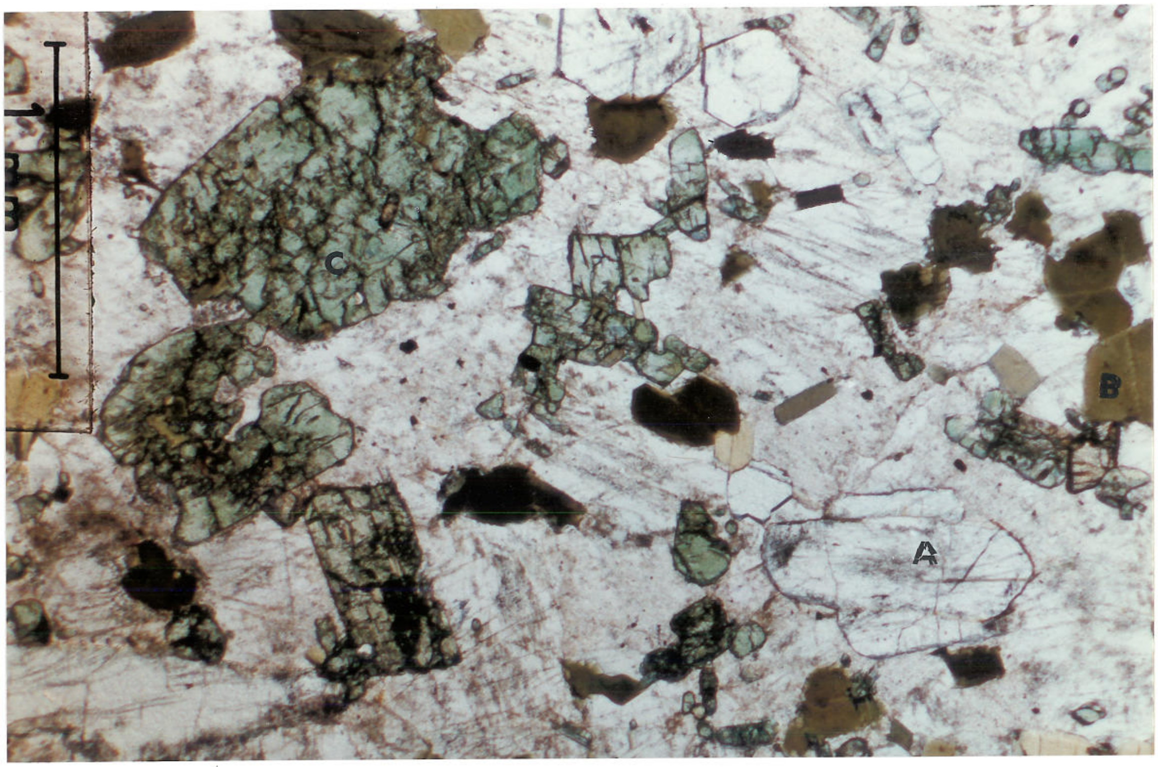

(**D**) Coarse-grained hornblende (H) syenite with trace magnetite and biotite (B); plane and polarized light.

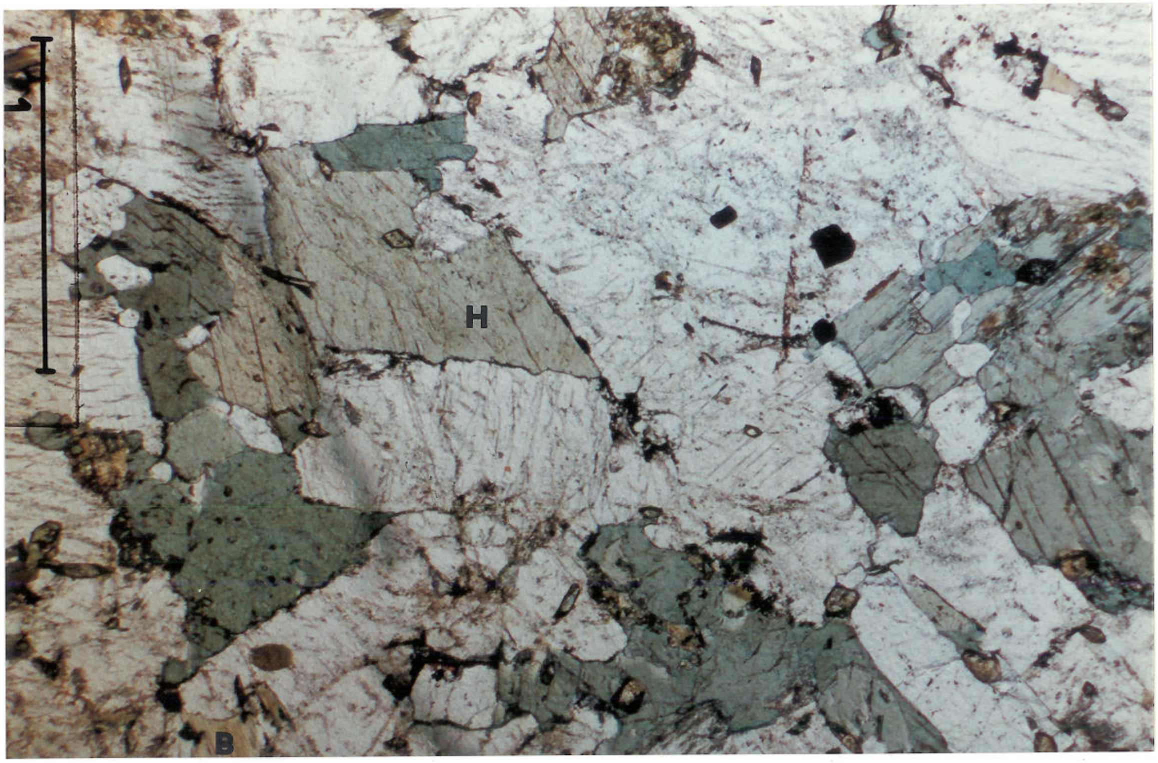

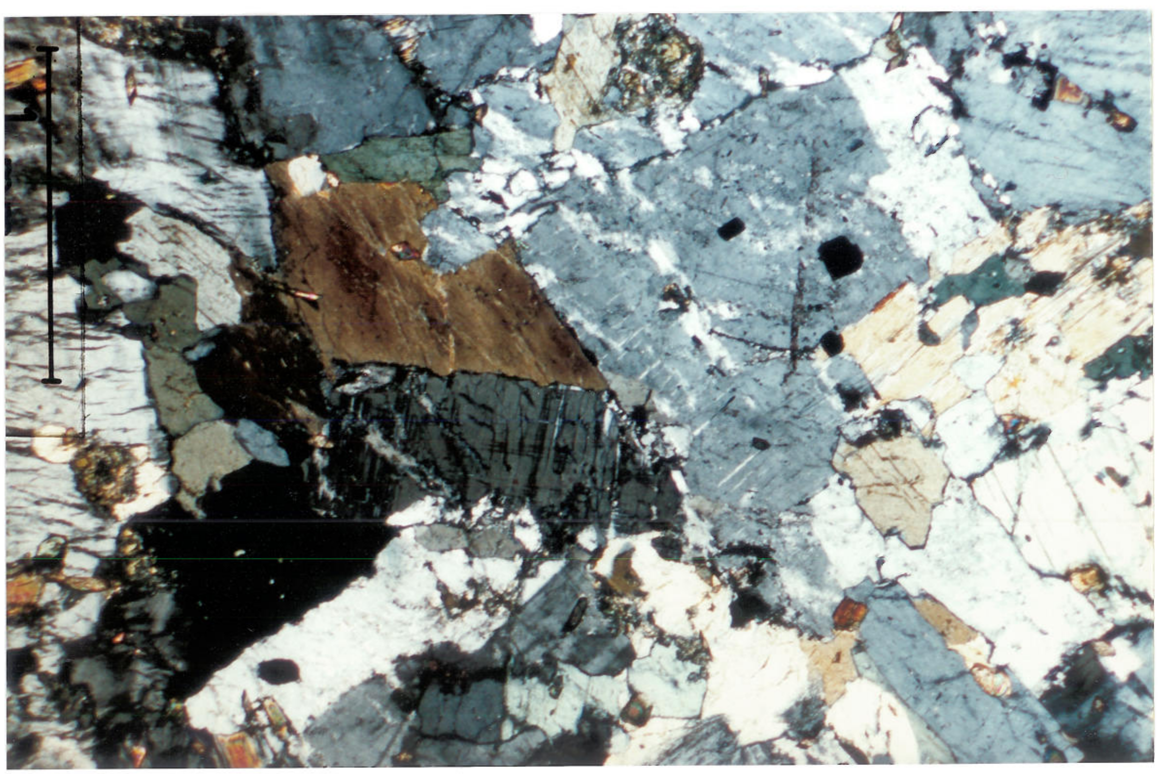

(E) Coarse-grained biotite (B) two feldspar syenite with magnetite (opaque), sphene (S), muscovite (M) and flourite (F); plane and polarized light.

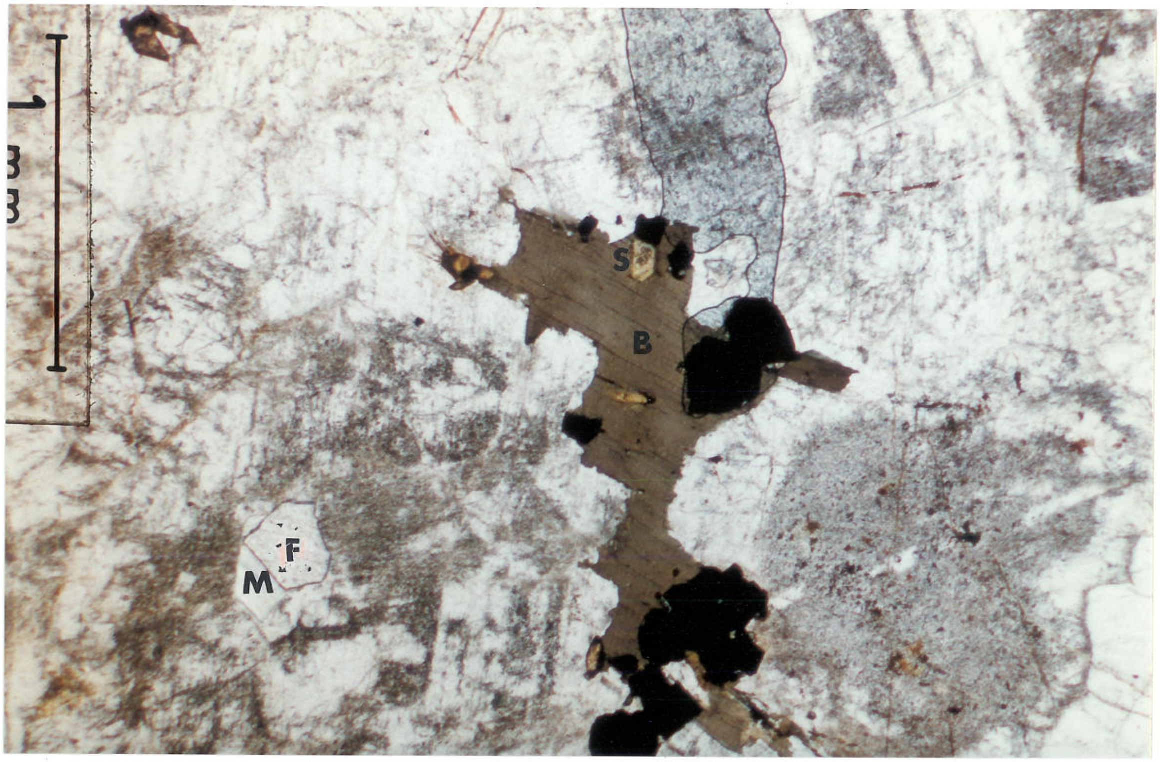

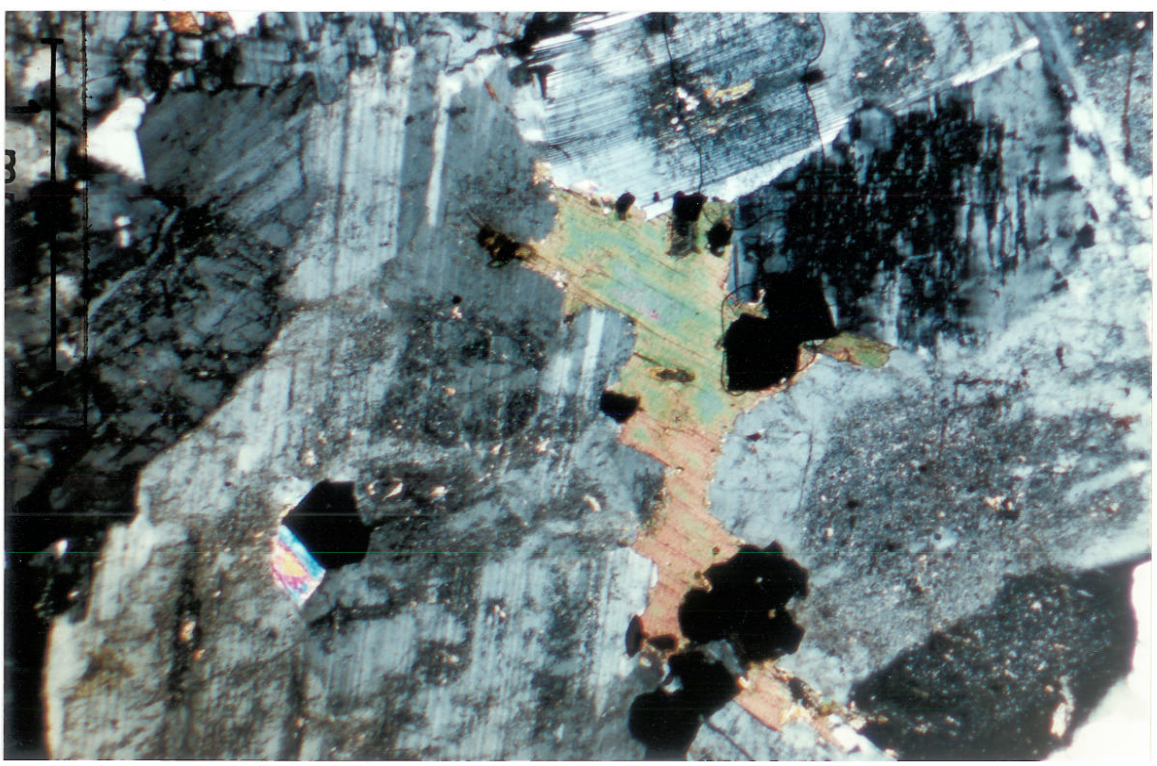

(**F**) Coarse-grained quartz syenite; coarse potassic feldspar (K), interstitial quartz (Q) and subhedral apatite (A), trace hornblende (H); plane and polarized light.

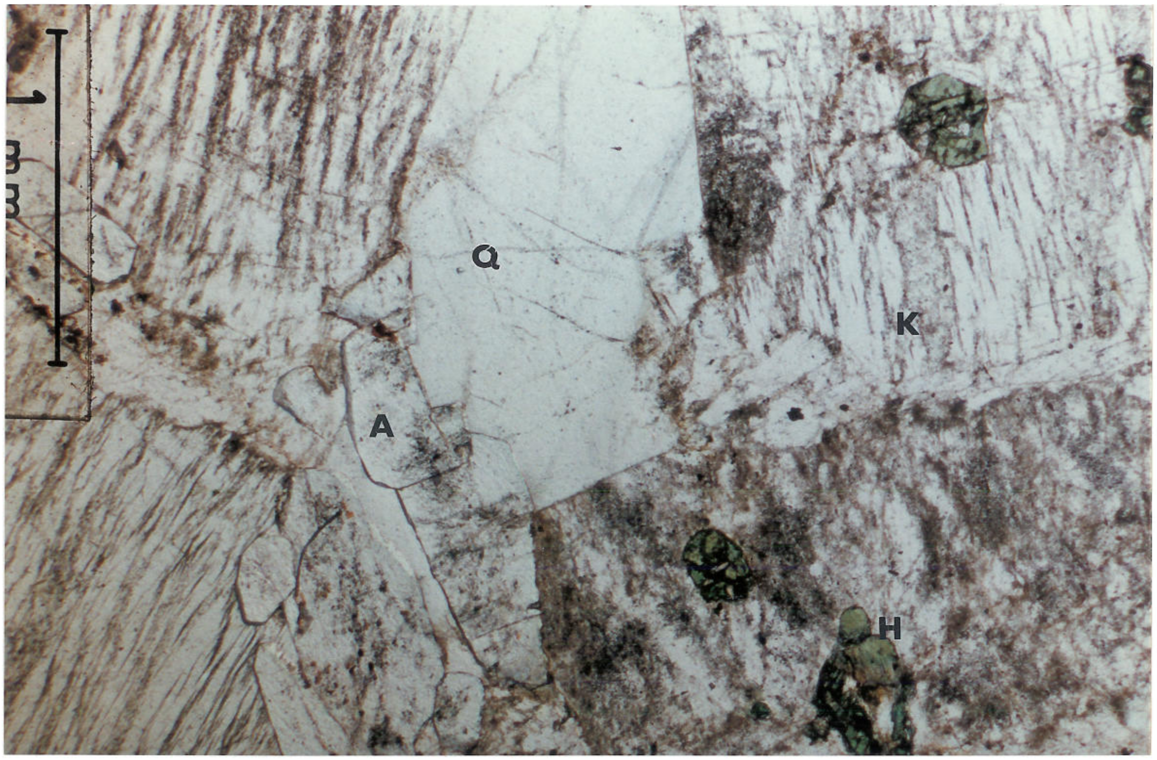

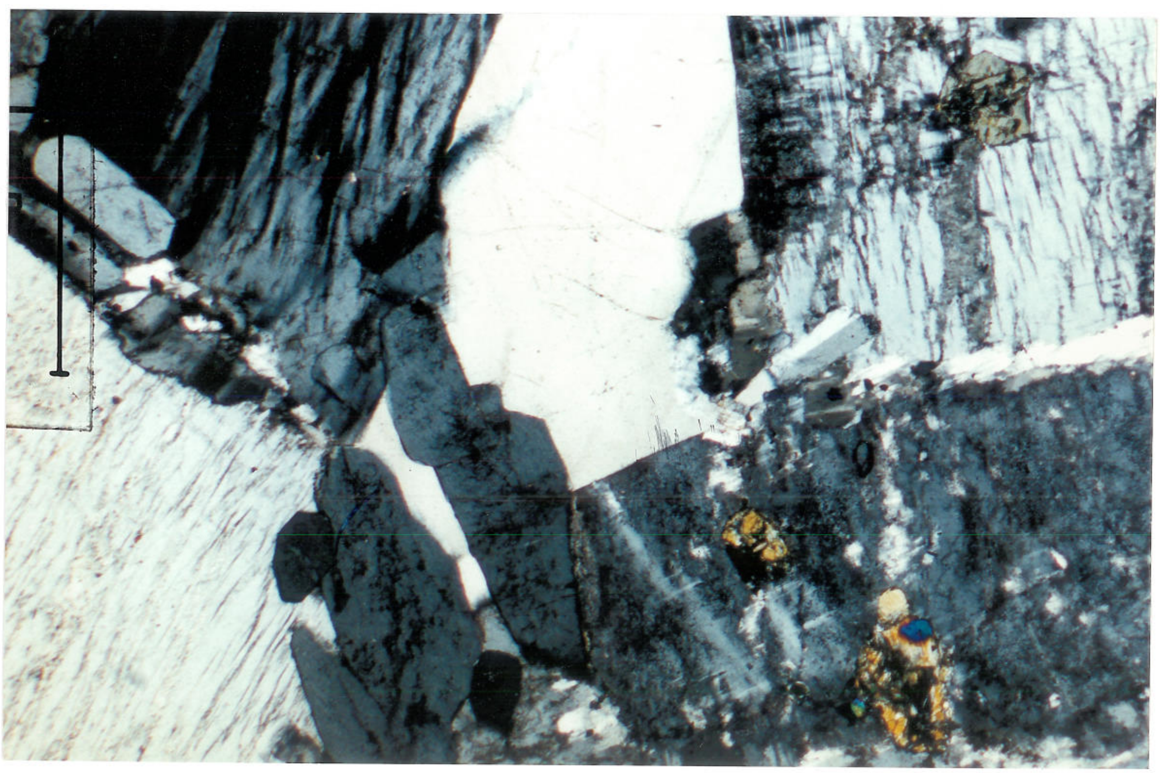

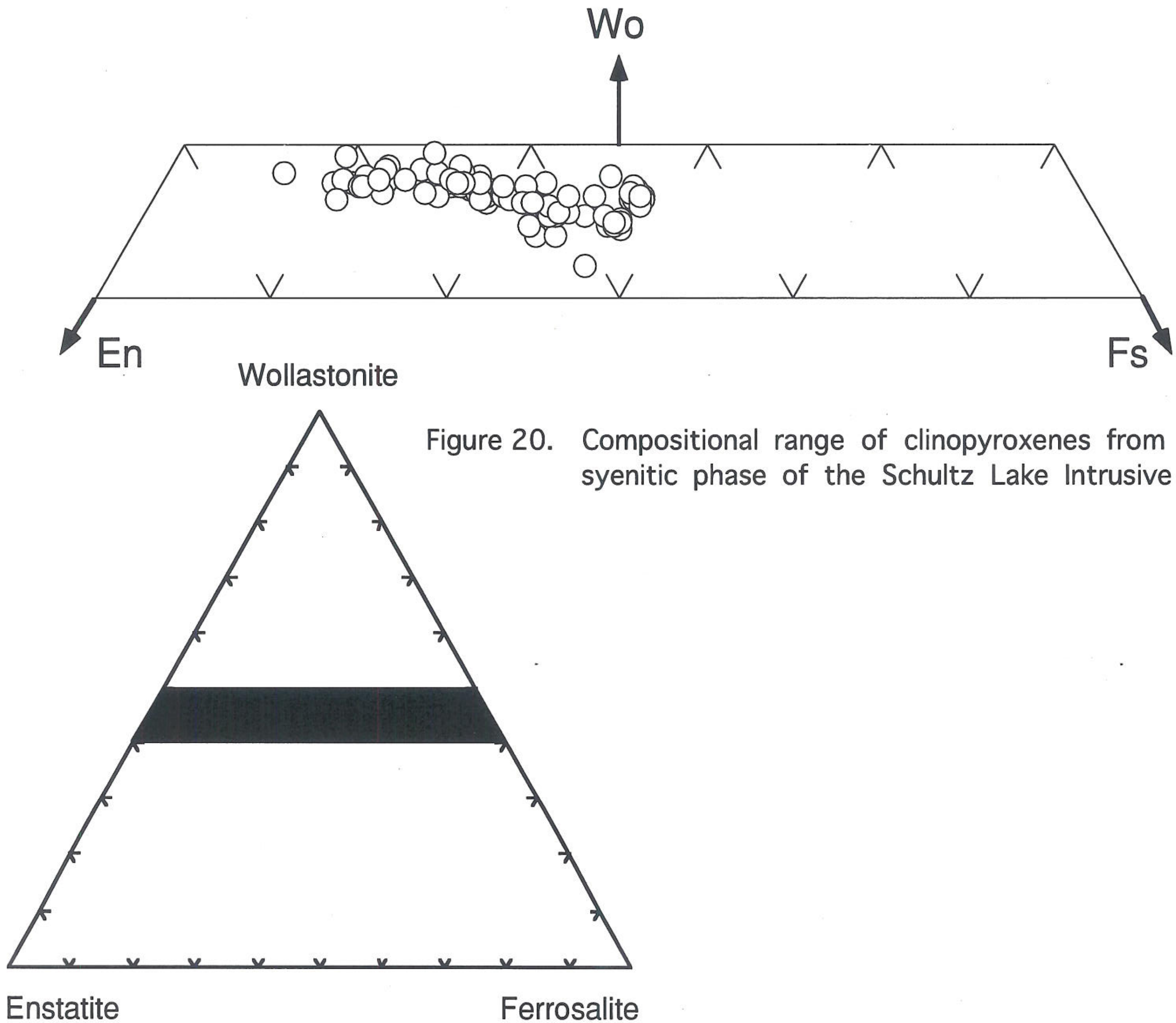

Figure 20. Compositional range of clinopyroxenes from the syenitic phase of the Schultz Lake Intrusive complex.

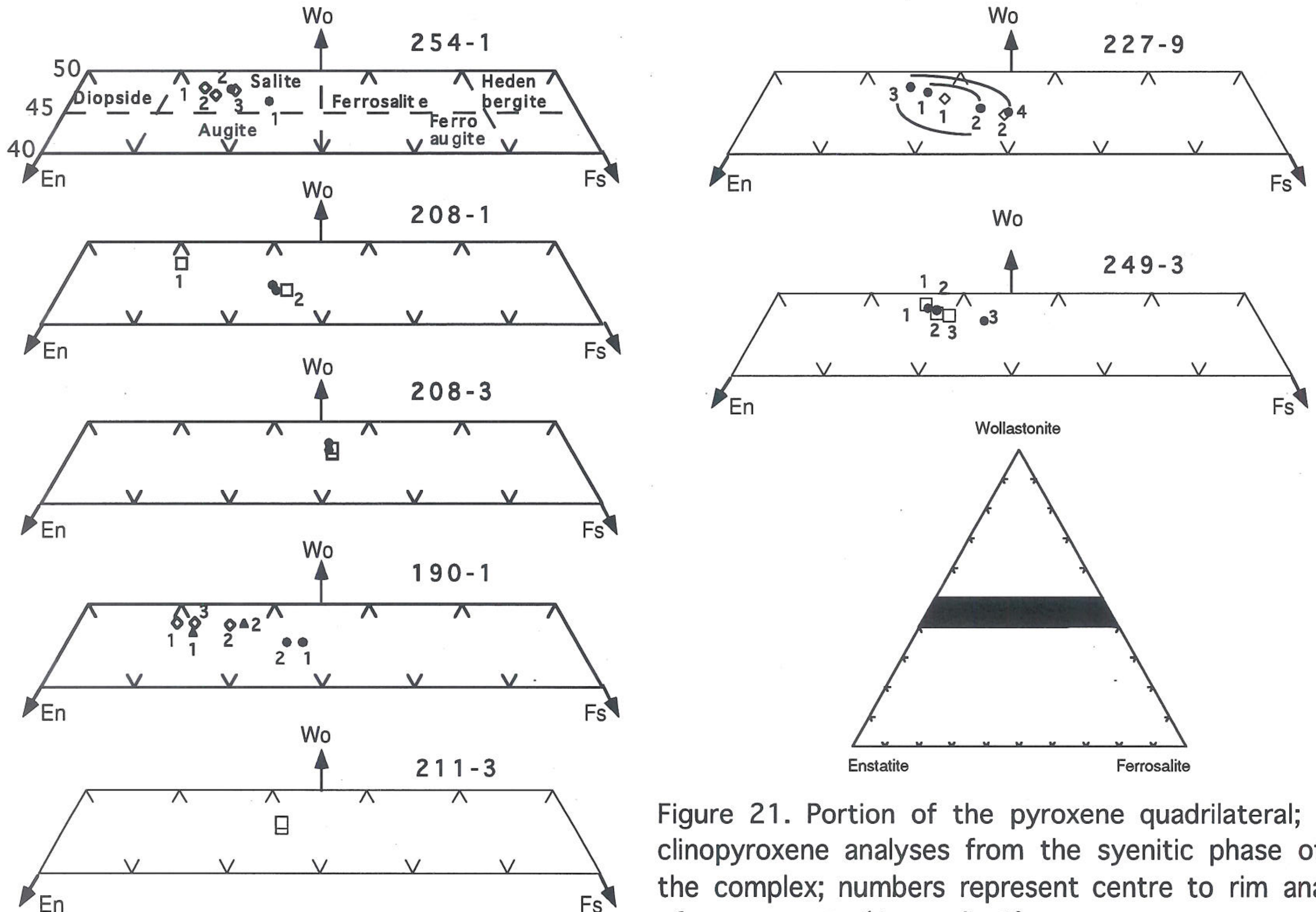

Figure 21. Portion of the pyroxene quadrilateral; clinopyroxene analyses from the syenitic phase of the complex; numbers represent centre to rim analyses of macrocrysts (Appendix 1).

Hornblende

Hornblende is the third most abundant mafic mineral in the syenitic phase of the SLIC. Textural variations of hornblende from a variety of syenitic rocks ~~suggests~~ suggests that it formed at different times through different processes. Coarse-grained hornblende interstitial to megacrystic potassic feldspar in oikocrystic syenite and its association with coarse-grained salmon pink K-feldspar and quartz indicates that this hornblende is the product of fractional crystallization of intercumulus liquid. Coarse-grained poikilitic and non-poikilitic hornblende associated with syenites having varied grain size and varied proportions of clinopyroxene and mica (biotite), mark the transition into more hydrous syenitic phases.

The composition of hornblende in syenitic rocks shows a trend of increasing iron, decreasing Mg/Mg+Fe in Figure 22, which is compatible with the prevalent trend of increasing iron in coexisting clinopyroxene. From Appendix 2, multiple analyses from centre to end in hornblende show no significant variations in the oxides of calcium, magnesium and iron. The lack of zoning in hornblende suggests equilibrium crystallization.

Mica

Analyses of mica from different syenitic phases and cognate mica+clinopyroxene xenoliths are listed in Appendix 3. Using the following nomenclature: phlogopite, Mg:Fe = >2:1; biotite, Mg:Fe = <2:1, all mica regardless of textural association is classified as biotite. Mica from cognate xenoliths, jackets on cognate xenoliths and as essential phase associated with clinopyroxene+hornblende+ potassic feldspar +/- albite have approximately equal MgO and FeO (wt%) abundances which average about 15 wt% for both oxides. However mica from clinopyroxenitic cognate xenoliths have MgO>FeO and tend towards more phlogopitic compositions. Slight variations in colour were recognized in plane polarized light and these vary from very pale yellow, brownish green to brown (Figure 15, 16, 17, 19). Biotite with lighter hues in plane light have slightly higher MgO contents and are present in mica-rich cognate xenoliths.

There are textural and chemical feature of biotite that suggest its petrological lineage to mantle-derived magmas and similiarities to ultrapotassic-potassic Christopher Island magmatism, especially Ti, Ba and F. These three elements are higher than macrocrysts in lamprophyre/minette but this association is diagnostic of mantle-

Figure 22. COMPOSITION OF CALCIC AMPHIBOLES FROM THE SYENITIC AND GRANITIC PHASES OF THE SCHULTZ LAKE INTRUSIVE COMPLEX.

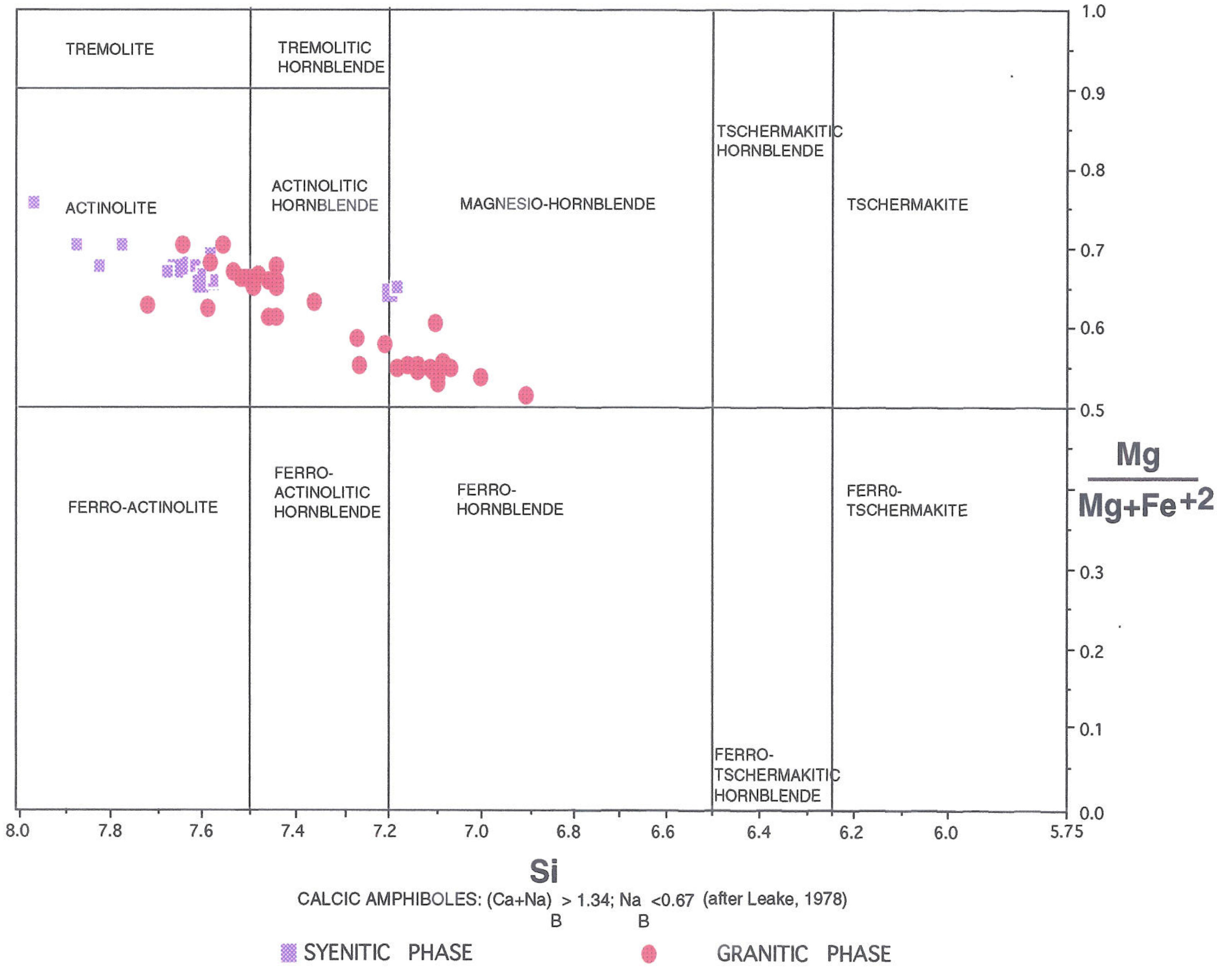

derived magmas. High TiO_2 to 2.4 wt%, BaO as high as 1.88 wt% with an average of approximately 0.5 wt% and F as high as 3.2 wt% are higher than mica macrocrysts in Christopher Island lamprophyres/minette. However negligible Cr_2O_3 and markedly different MgO and FeO abundances separate these biotite from phlogopite in lamprophyres/minette. However macrocrystic biotite are commonly observed in syenite and these macrocrysts can exhibit kink textures even though the host rock does not carry a penetrative fabric (Figure 23). Note the pale yellow-pale brown hue in plane light and the color zonation from centre to edge. This deformed texture is identical to deformed macrocrystic phlogopite in undeformed Christopher Island formation lavas equivalent lamprophyres/ minettes and the latter are interpreted as xenocrysts. Similiar biotite textures from syenites in the SLIC suggest that these are xenocrystic as well.

Feldspars

Feldspars in the syenitic phase of the complex are of two types, predominantly Na-poor K-feldspar, microcline and microcline perthite with variable Ba and low Fe in oikocrystic syenite and mafic syenite and albite with negligible Ba and Fe is present with microcline in mesocratic and leucocratic syenite. The presence of megacrystic and fine-grained groundmass high-Ba potassic feldspar in mafic and oikocrystic syenite is noteworthy, especially with contents as high as 7.7 wt% BaO and the zoning variations within grains. The presence of high-Ba microcline, 2 wt% BaO and greater, with low-Ba microcline, <1wt% BaO, microcline in the same rocks implies that there are several generations of microcline in early mafic and porphyritic syenites. Sector and concentric zoning patterns indicate the strong partition of Ba into interpreted early feldspar crystals and decreased BaO abundances between centre and edge records continued feldspar nucleation in magmas of markedly lower Ba contents. This zoning distribution of BaO in microcline is similiar to zoned BaO, centre to edge, in coarse-grained biotite within the same rock types. Barium distribution and contents in feldspar from the SLIC are comparable to Ba distribution in feldspar from Christopher Island volcanic rocks and lamprophyre/minette; the implication is that the syenitic phase of the Intrusive Complex most probably was generated in the same source region as the magmas represented by the Christopher Island lavas and dykes but underwent fractionation compared to quenching in the Christopher Island lavas and dykes.

Figure 23. Photomicrograph of kinked macrocrystic/xenocrystic biotite in a fine grained clinopyroxene+K-feldspar syenite; plane and polarized light.

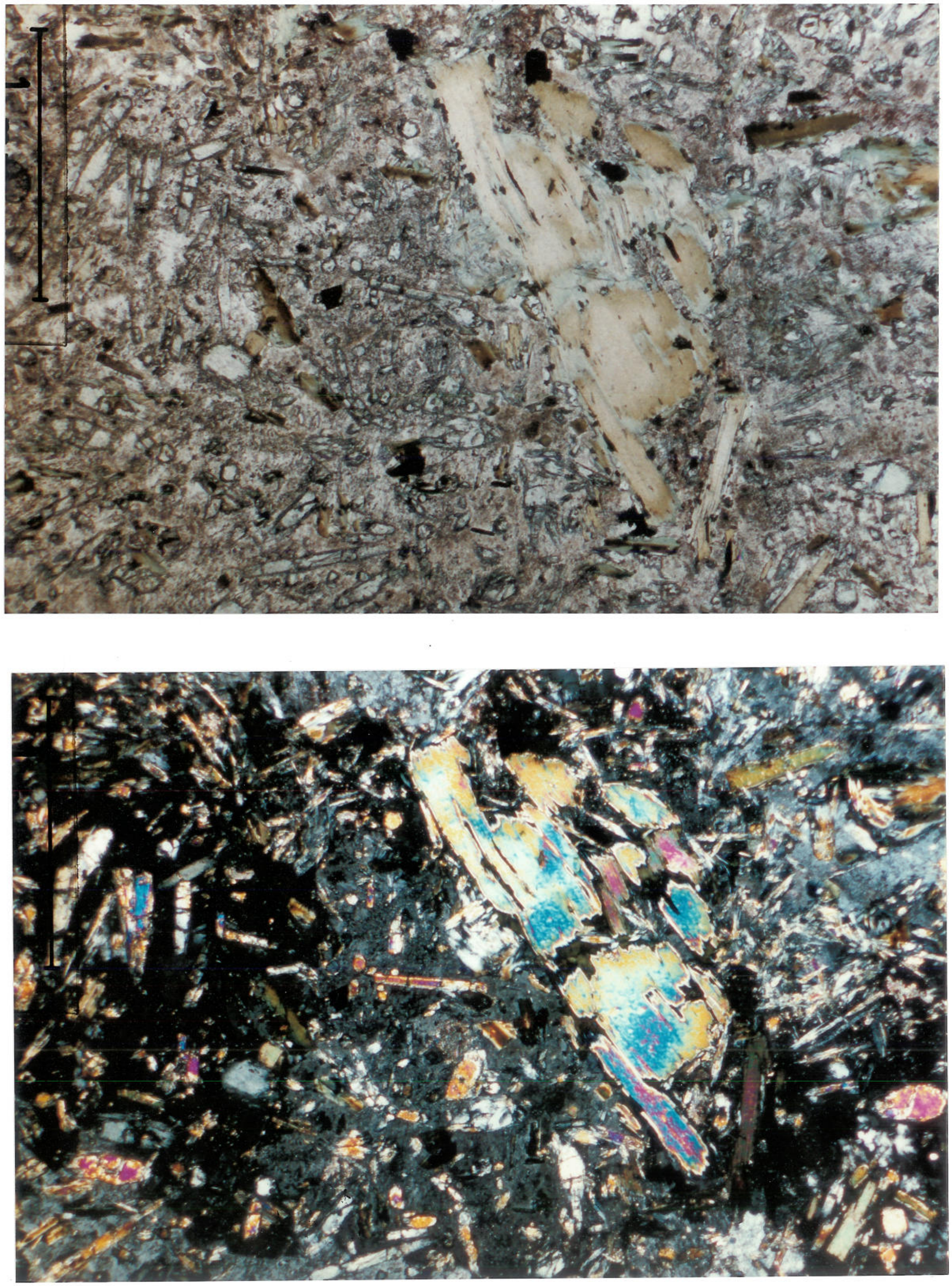

GRANITIC COMPLEX

Petrography and mineral chemistry

The most abundant unit that comprises the granitic phase of the complex is a salmon-coloured, coarse-grained leucocratic glomeroporphyritic quartz fluorite-bearing granite. The type area for this rock unit lies north of Mushroom Lake in the area designated as the agmatitic zone in Figure 4. White fine-grained white granite and aplitic dykes intrude and chill against syenitic rocks. Deuteric alteration of biotite to chlorite, hornblende to chlorite and fiberous amphibole and sericitization of albite in granitic rocks is pervasive and contrasts with the little altered syenitic rocks.

The estimated modal mafic mineral component of granitic rocks is 1-2% with biotite being the most abundant phase. A common macroscopic and microscopic feature of granitic rocks is the association of biotite with purple fluorite and both minerals occur as knots, 1 mm and less, intergranular to coarse-and medium-grained quartz and feldspars. Optical properties of sepia biotite, brown to red-brown distinguish it from the pale yellow - pale brown biotite in the syenitic rocks (Figure 24, 25).

Grain size, zoning and euhedralism of microcline, perthitic microcline and albite are the most diagnostic petrographic features of granitic rocks. Graphic intergrowth textures are not common but megacrystic complexly zoned microcline macrocrysts (Figure 26), poikilitic coarse-grained potassic feldspar with inclusions of albite (Figure 27) and subhedral feldspars (Figure 28) are common. These textures may suggest that the granitic rocks are not eutectic granites

Assessory minerals include purple flourite, sphene, zircon, apatite, magnetite and rare muscovite, and pyrite. Muscovite is considered a primary phase in the granite and its presence indicates that the granitic phase of the SLIC can be considered as a two mica granite complex. The Lone Gull granite that hosts the Main Zone of the Kiggavik ore body is a two mica granite and this granite is considered part of the granitic phase of the SLIC. Primary fine-grained muscovite is associated with interstitial biotite+fluorite or interstitial to quartz+feldspar and contrasts with very fine-grained white mica that is a replacement of the cores of zoned albite and to a lessor extent after microcline. The identification of a two mica granitic complex is directly genetically important and related to the

Figure 24. Coarse-grained granite: photomicrographs, **A**-plane light; **B**-crossed nicols, of interstitial aggregate of sepia brown biotite (B), hornblende (H) with prismatic sphene (S) and magnetite (euhedral opaque). Colour variations in biotite represent compositionally different domains.

(A)

(B)

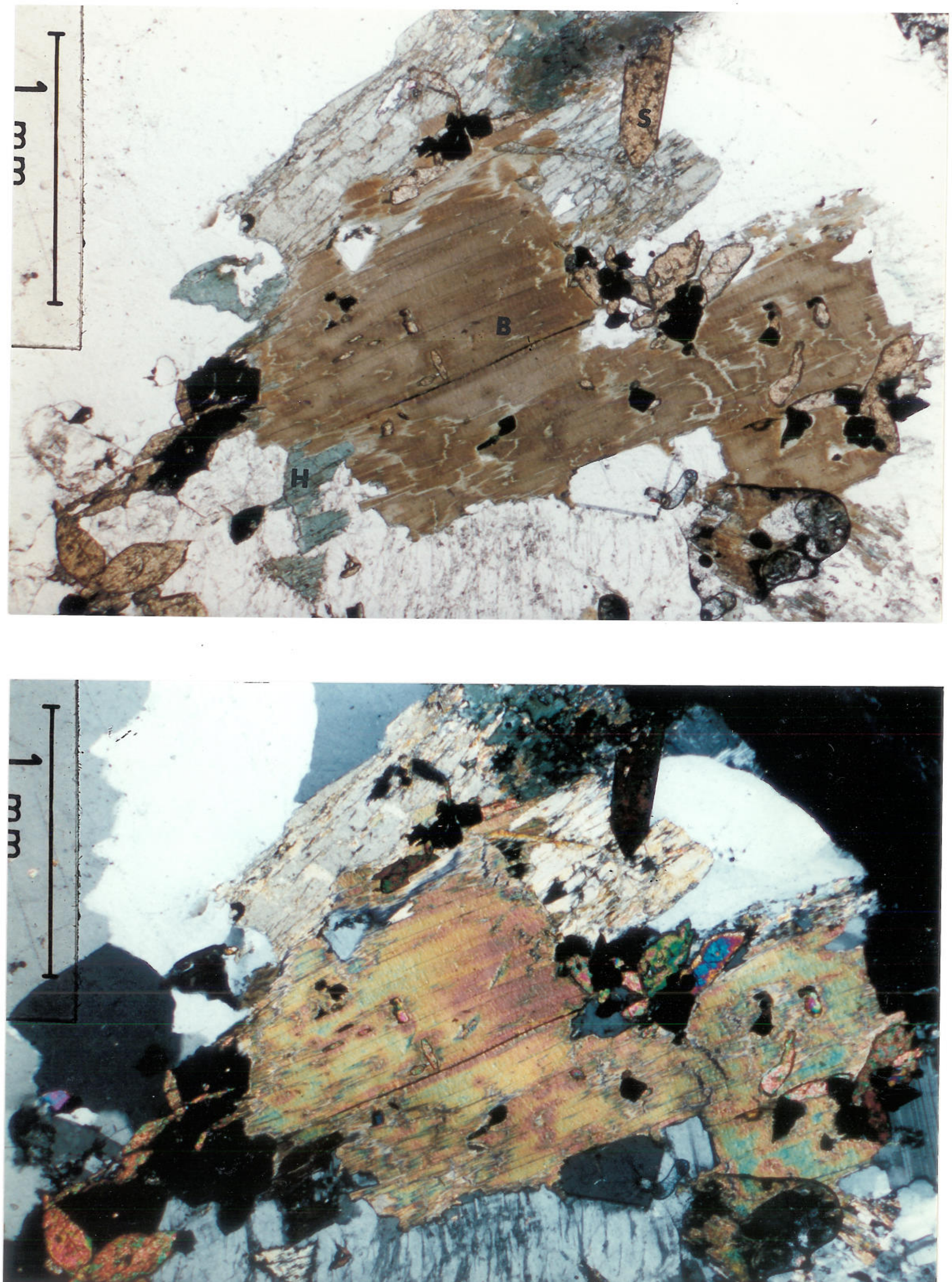

Figure 25. Coarse-grained granite at the contact with Archean gneisses, west of Andrew Lake: photomicrograph of chloritized red brown biotite interstitial to coarse-grained quartz+feldspar.

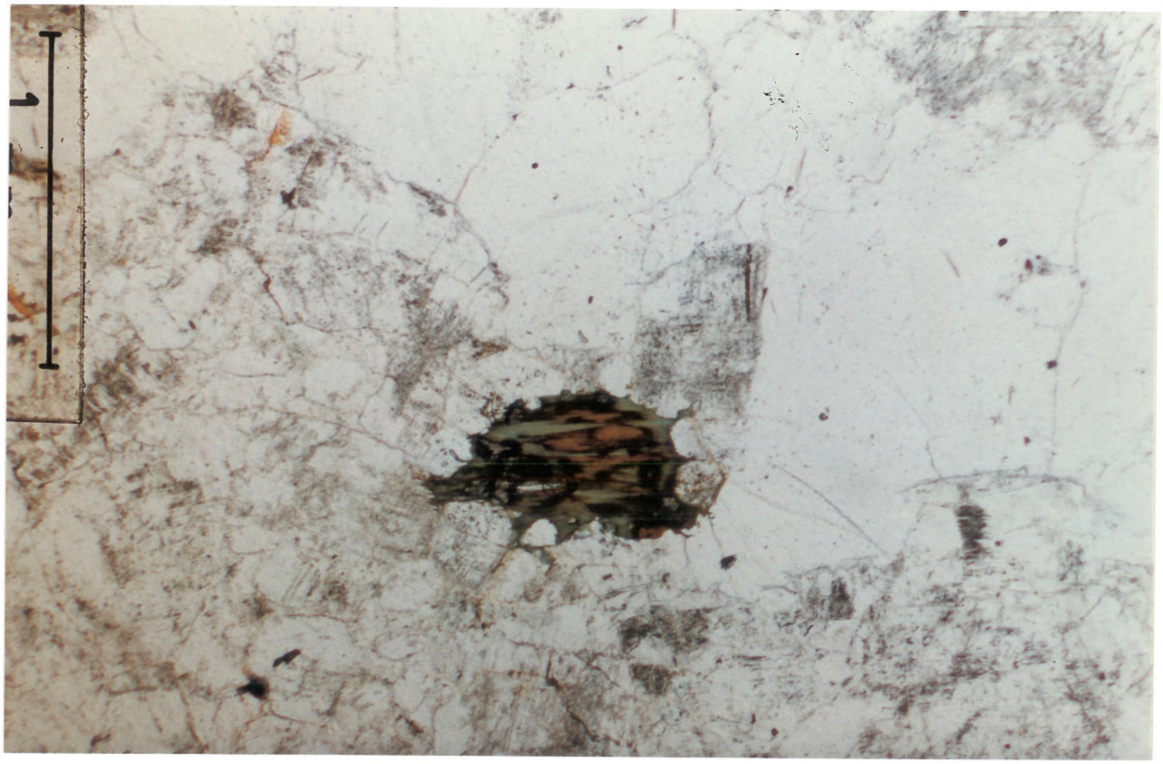

Figure 26. Photomicrograph, A-plane light; B-crossed nicols, of a portion of a microcline macrocrysts illustrating the complex zoning and inclusions of euhedral albite. This texture is identical to that in Figure 15C, from oikocrystic syenite

(A)

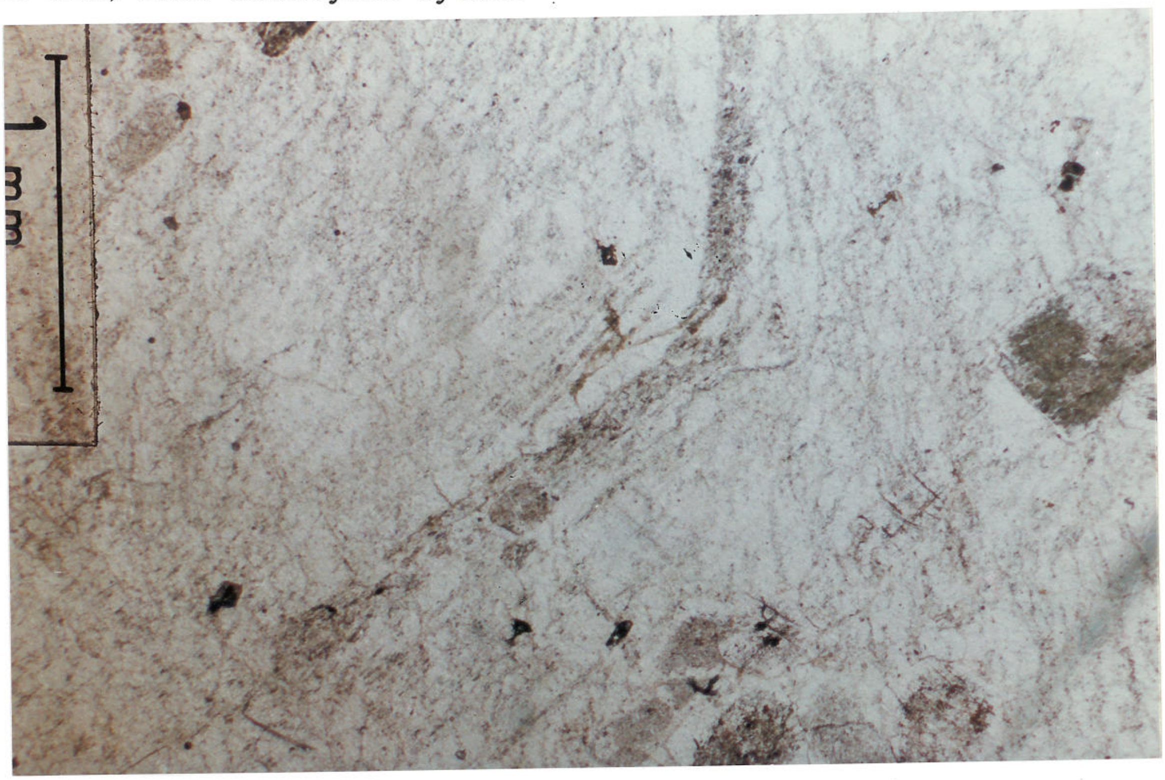

(B)

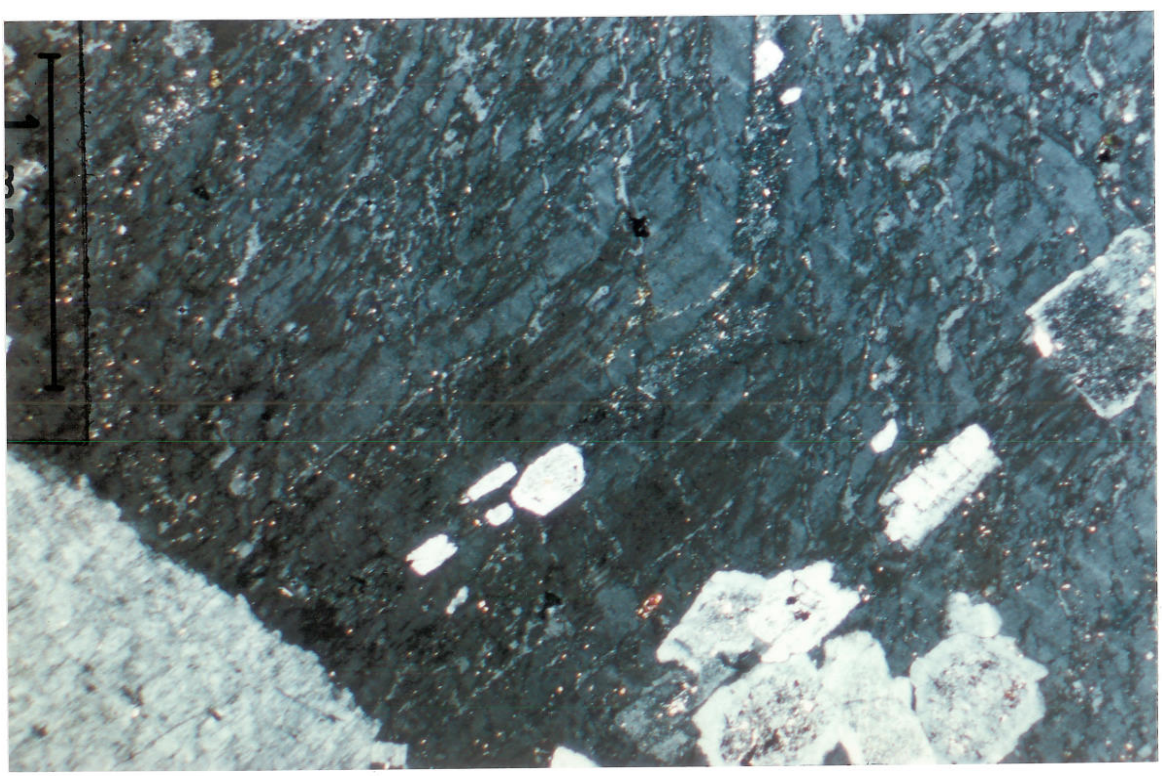

Figure 27. Photomicrograph of polikilitic microcline with variably sericitized zoned albite (A).

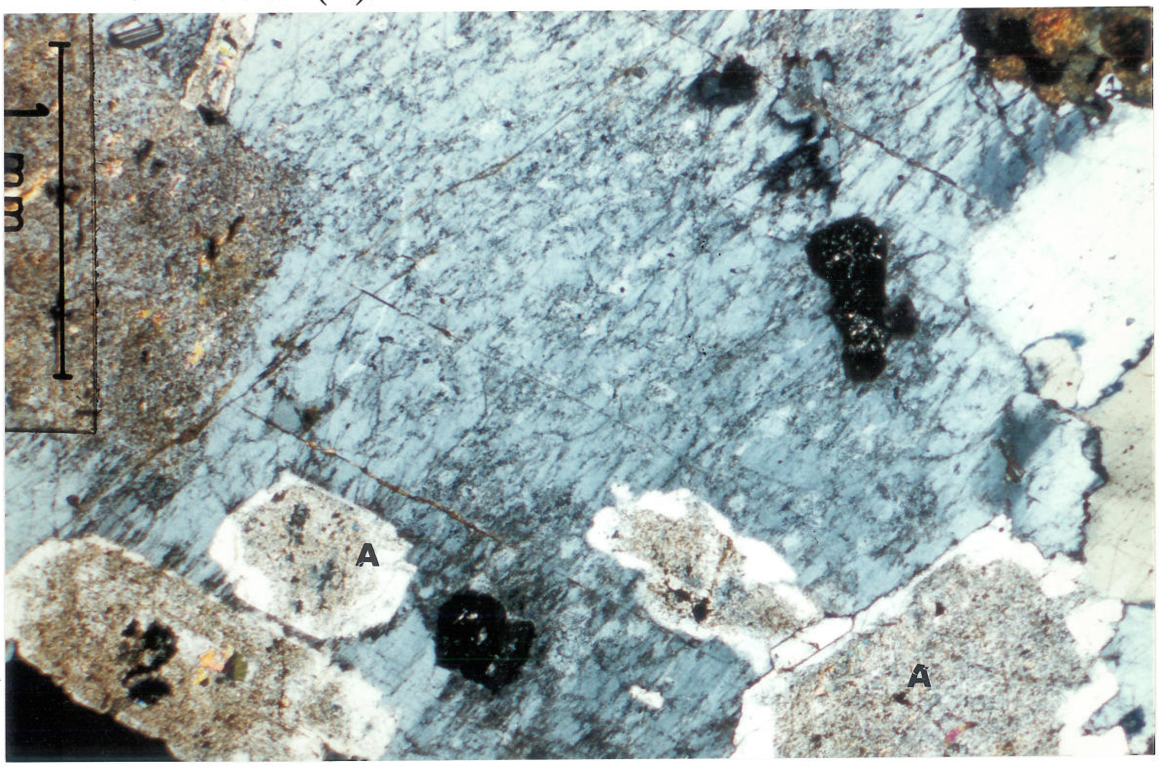

Figure 28. Photomicrograph of equigranular subhedral and euhedral microcline (K) and zoned albite with interstitial quartz (Q), sphene (S) and magnetite (M).

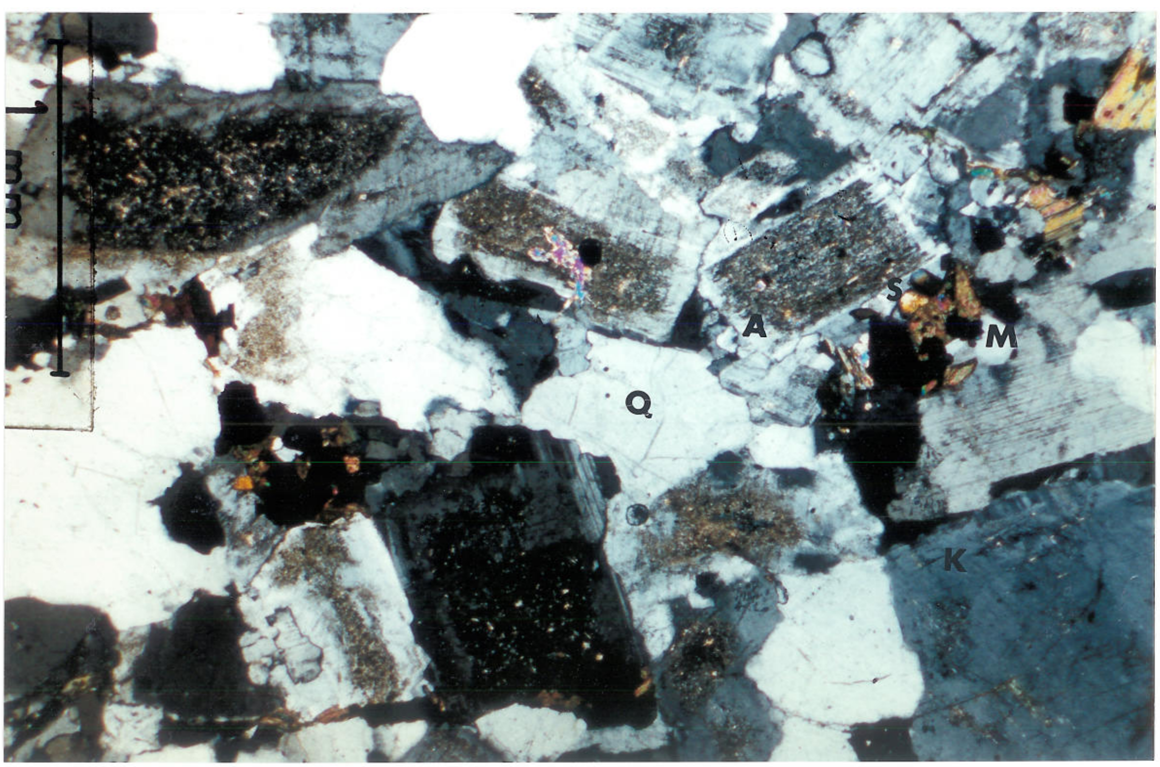

greisen mineralization. Magnetite is ubiquitous throughout the granitic phase as it is in the syenitic phase of the complex and this accounts for the high aeromagnetic signature of the complex. Sulphides are ~~very~~ very rare except for the most eastern margin of the complex north of Sleek Lake. This margin of the complex contains disseminated pyrite with rare molybdenite, hydrothermal quartz veins, the latter unrelated to quartz+hematite vein systems associated with faults and is interpreted to be related to the evolved sulphide-bearing granite in the Main Zone, Kiggavik deposit.

Micas

Analyses of red brown and brown biotite from granite are fluoro-biotites with up to 4.13 wt% F, a consistently greater abundance than in flourine-bearing biotite from syenitic rocks and less BaO when compared to biotite from syenitic rocks (Appendix 3).

Feldspars

Megacrystic complexly zoned microcline in coarse-grained granite (Figure 26) are highly anomalous in their BaO and Na_2O contents compared to analyses of microcline with typical compositions (Appendix 4). The complex zoning and megacrystic texture draw comparisons to megacrystic and polikilitic microcline in mafic and oikocrystic syenites and perhaps these highly anomalous microcline megacrysts are xenocrysts. It is not suggested that these are xenocrysts from the syenitic phase of the complex but rather these are xenocrysts that may reflect the site of magma generation/source region. Mineral chemistry and whole rock chemistry strongly suggest that the syenitic phase were derived by partial melting in the upper mantle. The presence of Ba-rich microcline similiar to those in syenite suggests that the source region for these granitic rocks may be the lower crust; silicic melt generation followed the formation of potassic-ultrapotassic melts. Melting in the lower crust was the result of a rising geotherm gradient caused by the transmission of potassic-ultrapotassic melts through the lower crust. Melting of a F-rich granulitic lower crust could produce F-enriched granites.

POST-GRANITE LAMPROPHYRE, FINE-GRAINED SYENITE DYKES

Two important field relationships should be reiterated: 1) these dykes are spatially related to east and east northeast trending fault zones and 2) these dykes chill against the granite. This later field relationship indicates that there is a thermal gradient or time difference between these two rock units whereas even though the the granite intrudes the syenite and was seen to chill against the syenite the overall interpretation is that the syenite-granite are more closely related in time.

Three undeformed lamprophyre-syenite dykes were chosen as representative of this igneous event and they are located: 1) north of Mushroom Lake and about 0.75 km north of the fault zone; 2) immediately east of Garhard Lake and 3) west of Jane Lake.

These undeformed lamprophyre-fine-grained syenite dykes have sustained minor deuteric alteration, principally chlorite after biotite and phlogopite. The groundmass of these dykes is comprised of fine-grained potassic feldspar and albite. Importantly, all dykes contain two generations of mica, clinopyroxene and feldspar.

Porphyritic mica are either individual grains or glomeroporphyritic aggregates and display kinked textures identical to porphyritic biotite in the syenitic phase of the SLIC (Figure 29). This texture in a undeformed host rock indicates these are xenocrysts and the deformation textures may be either to strain in the source region or due to deformation during assent

Clinopyroxene is present as zoned macrocrysts, glomeroporphyritic aggregates and as fine-grained anhedra in the groundmass (Figure 30). Textural variations of groundmass feldspar are highly variable and result from magmas that have had different petrological evolutionary paths. Groundmass feldspar can be very fine-grained or subhedral fine-grained albite and K-feldspar (Figure 31A, B), and cantain glomeroporphyritic pokilitic K-feldspar (Figure 31A). The latter are assumed to be cumulate xenocrysts.

The dykes commonly contain macro-xenoliths of basement gneiss, and granite from the SLIC as well as micro-xenoliths of quartz which can have very fine reaction rims with groundmass feldspar (Figure 32).

Mineral Chemistry: mica, clinopyroxene, feldspars

The porphyritic and glomeroporphyritic micas are phlogopitic in composition within 25.38 - 19.37 wt% MgO and 2.24 - 5.53 wt% FeO with anomalously high abundances of TiO_2, BaO, Cr_2O_3 and F

Figure 29. Textures of biotite and phlogopite from lamprophyre-syenite dykes. (**A**) Dyke north of Mushroom Lake: crossed nicols, partially chloritized porphyritic phlogopite in a fine-grained K-feldspar+albite groundmass. (**B**) Dyke west of Jane Lake: crossed nicols, kinked porphyritic phlogopite in two feldspar matrix

(A)

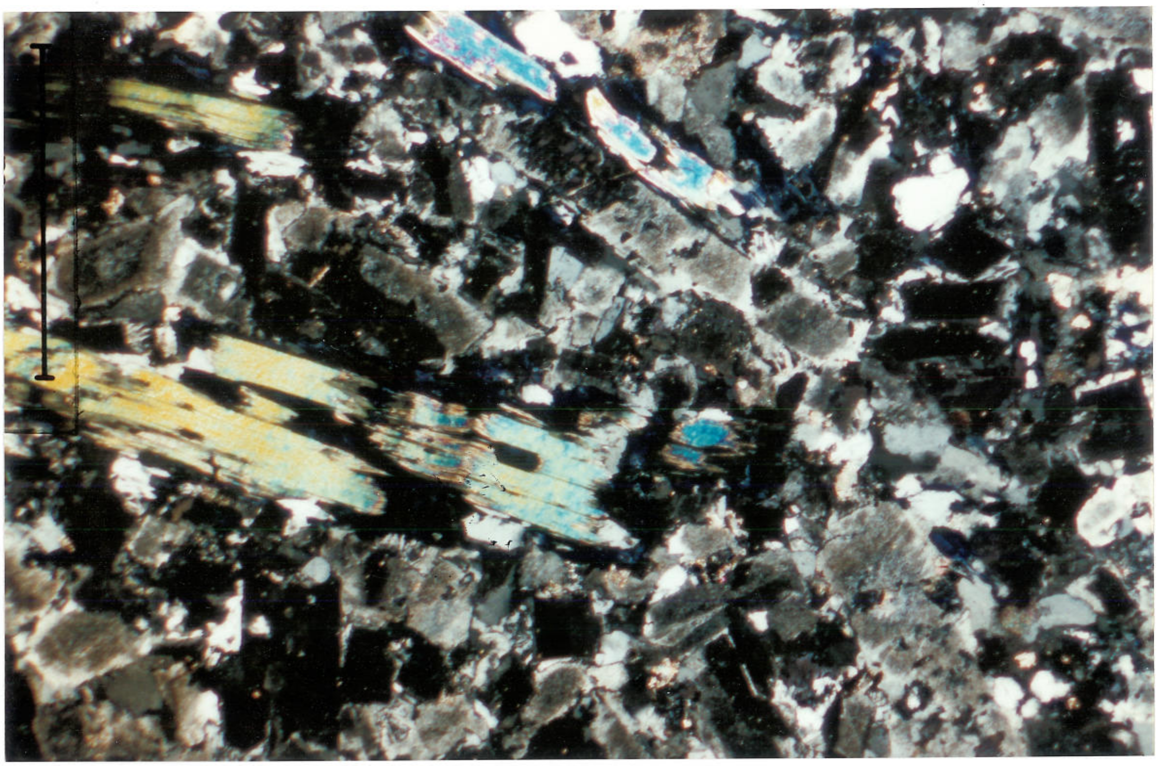

(B)

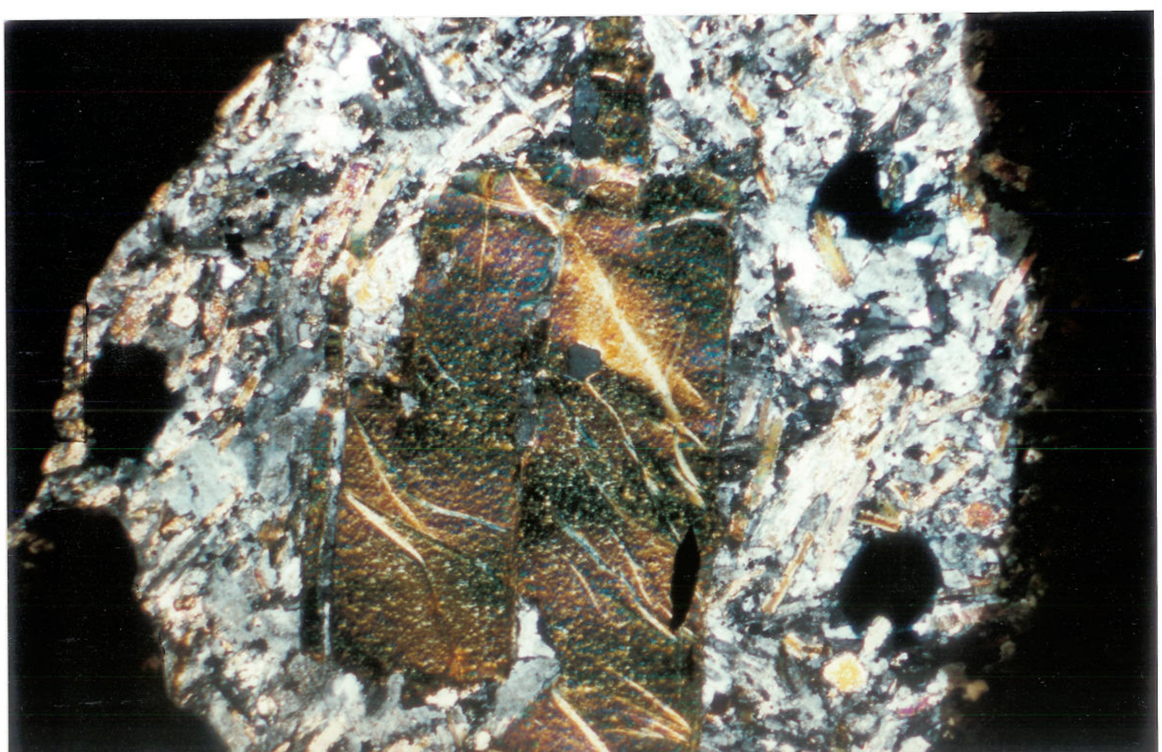

Figure 29C. Dyke east of Gårhard Lake: **A** - plane and **B** - crossed polarized light, glomeroporphyritic phlogopite (P) in a groundmass of K-feldspar+albite and clinopyroxene (C - high relief anhedra in groundmass) and second generation mica, biotite (B).

A

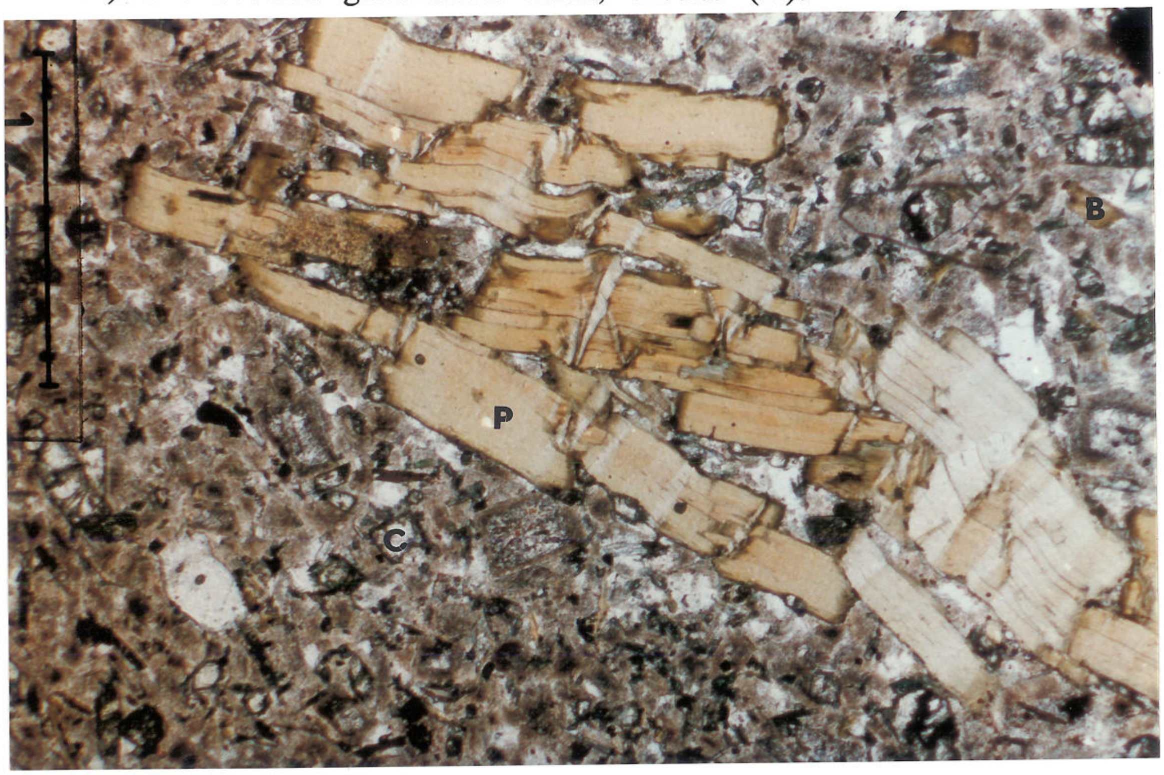

B

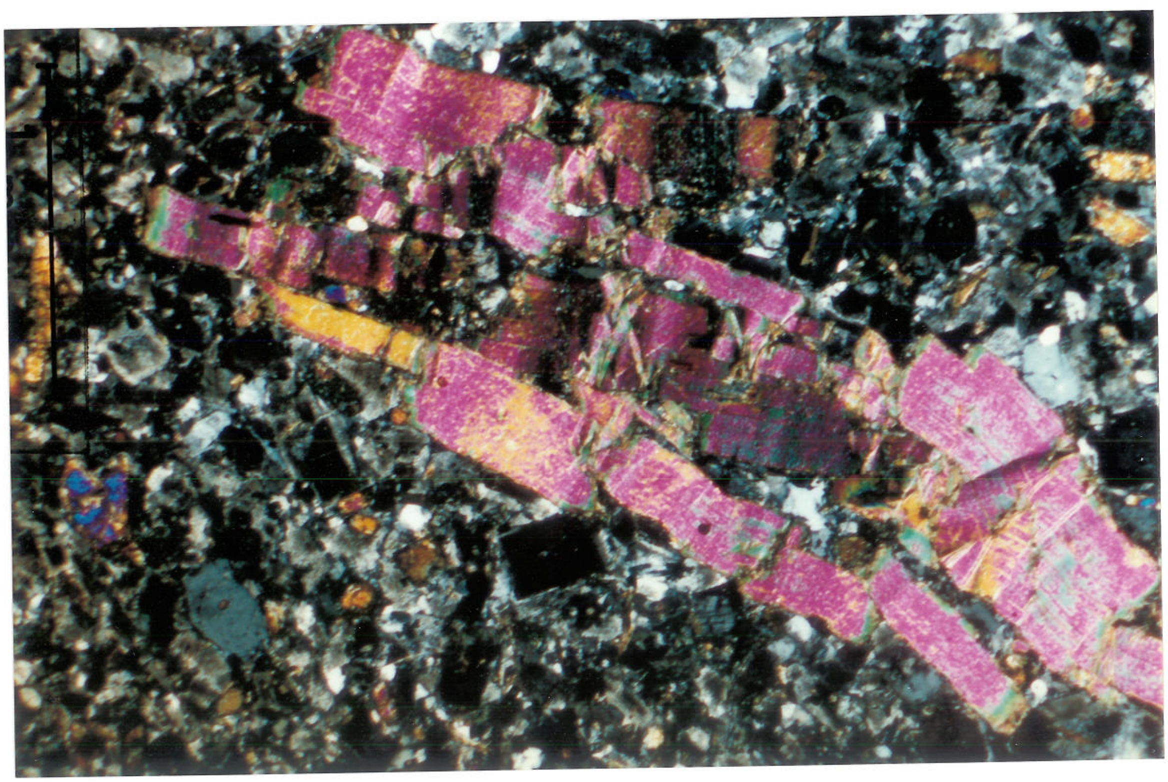

Figure 30. Clinopyroxene textures from a syenitic dyke, north of Mushroom Lake. (**A**) Two generations of clinopyroxene, zoned glomeroporphyritic macrocrysts (MC) and fine-grained anhedra in groundmass (C); (**B**) Zoned clinopyroxene macrocryst

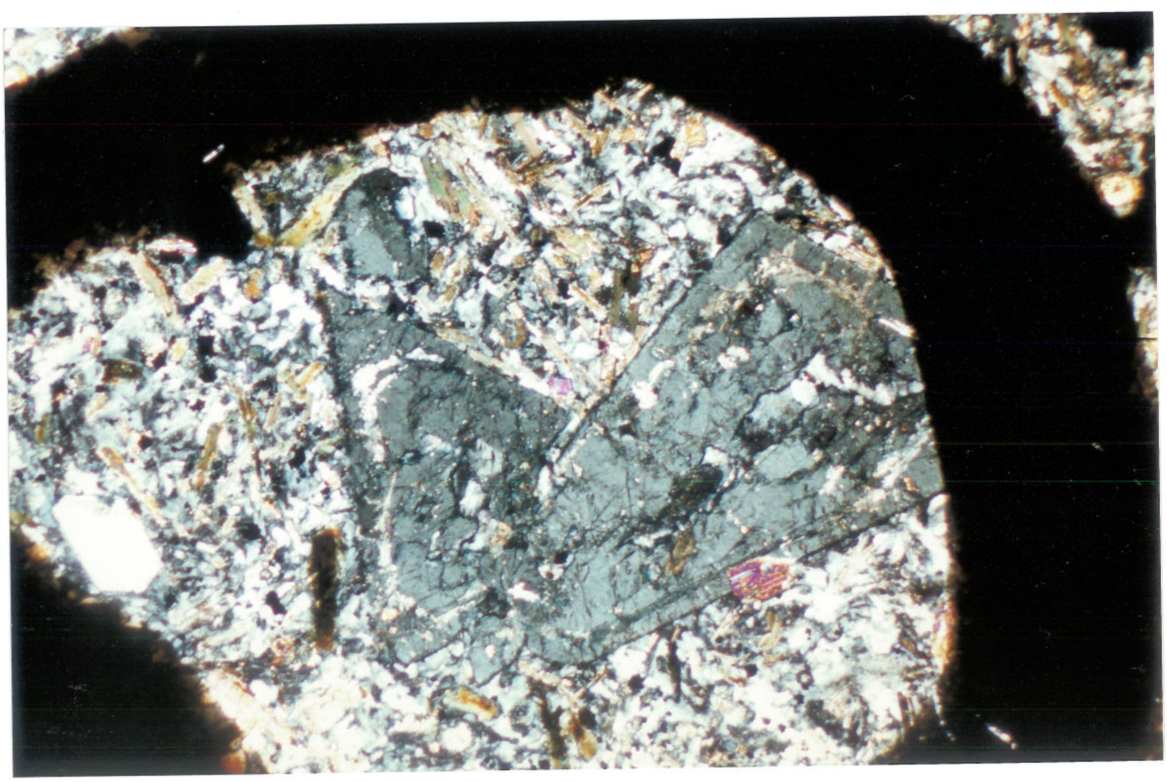

Figure 31A. Dyke east of Garhard Lake. Feldspar textures in lamprophyre-syenite dykes, plane and crossed polarized light. Very fine-grained feldspar groundmass hosting glomerporphyritic K-feldspar (K). Sphene (S), albite (A) and biotite (B) inclusions in glomerporphyritic K-feldspar. This texture resembles textures in the syenitic phase of the SLIC.

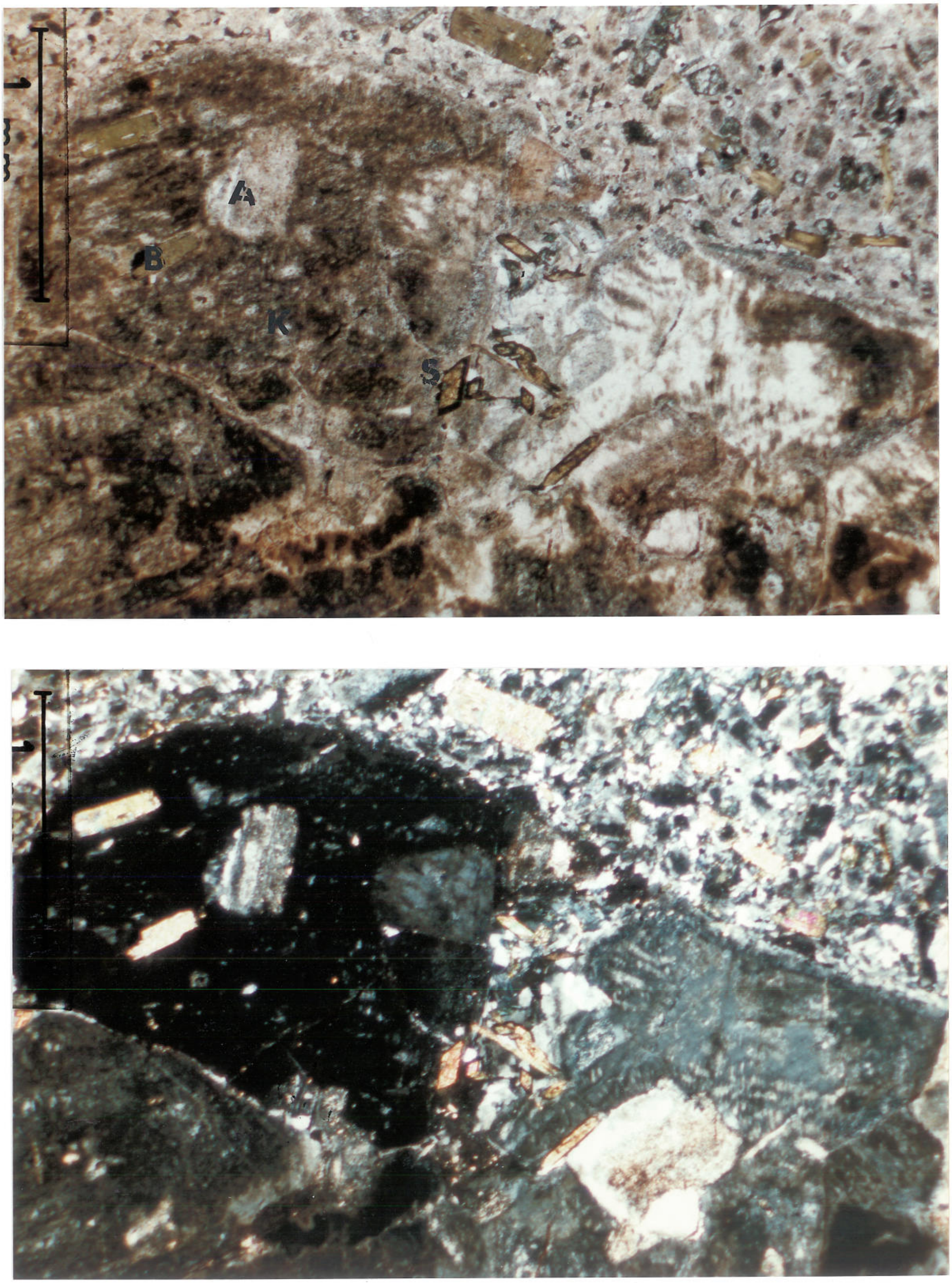

Figure 31B. Dyke west of Jane Lake. Feldspar textures in lamprophyre-syenite dykes, plane and crossed polarized light. Euhedral fine-grained albite and K-feldspar with interstitial completely and partially chloritized phlogopite (P).

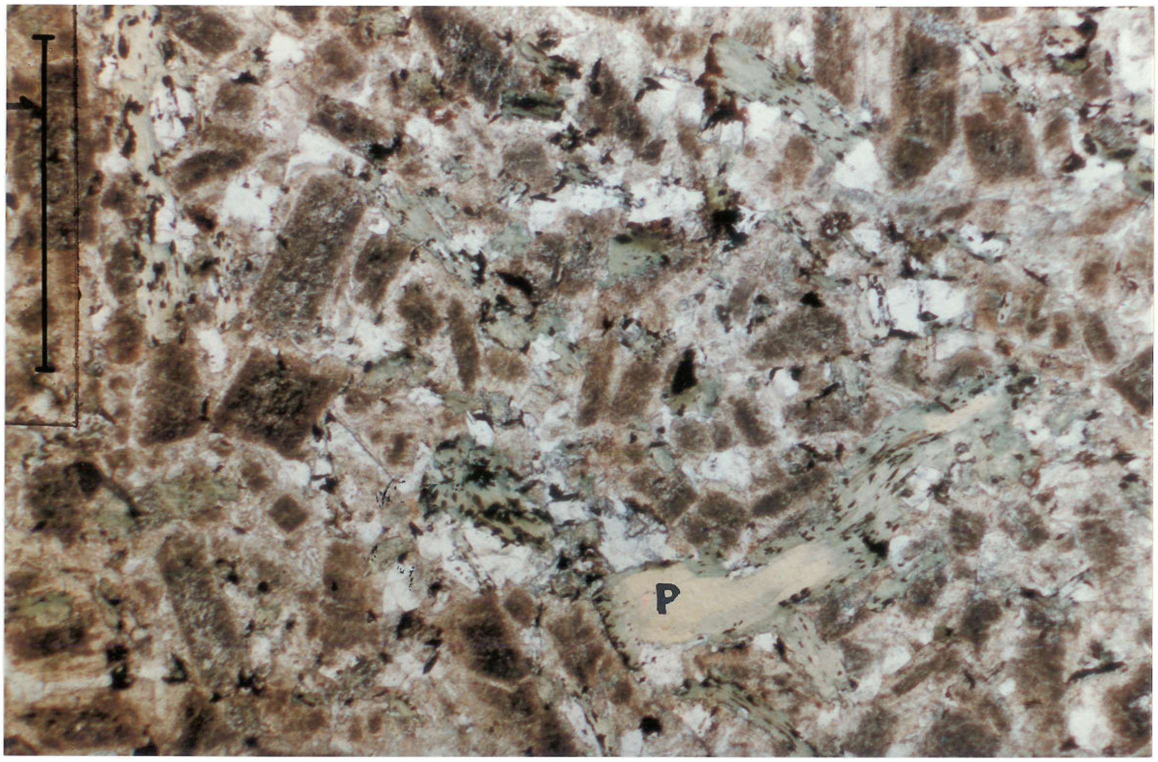

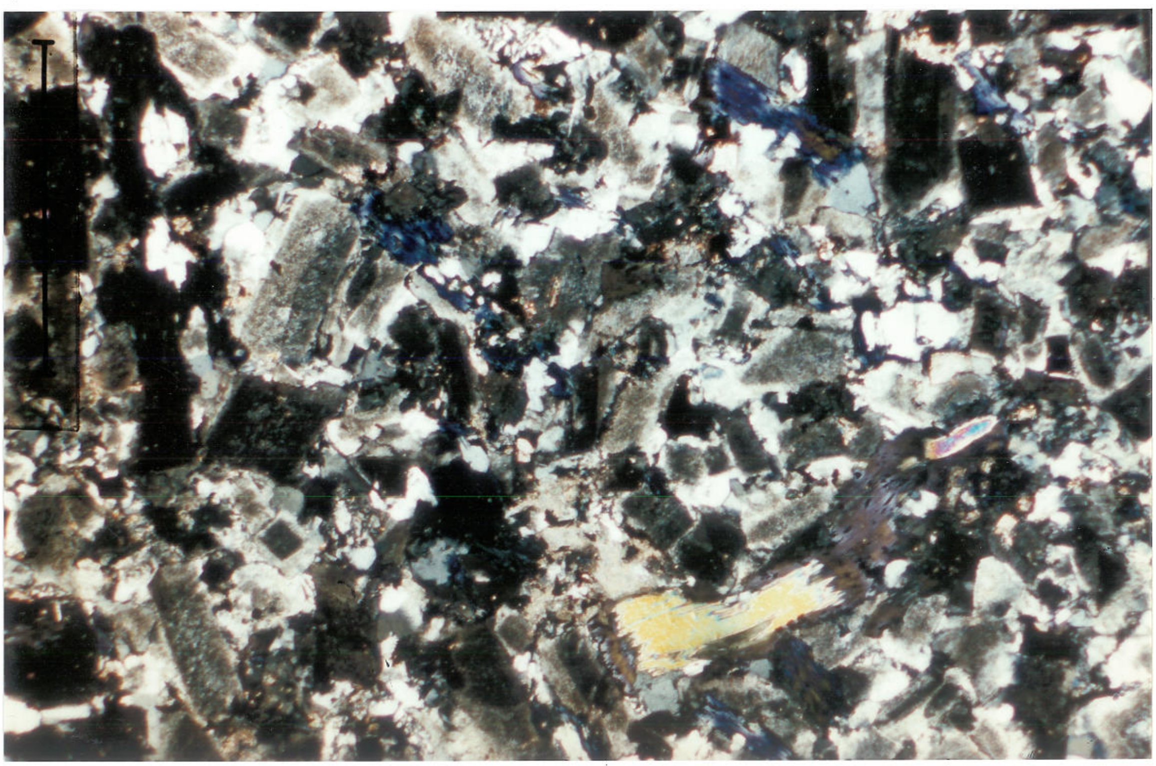

Figure 32. Photomicrographs of micro-xenolithic quartz in lamprophyre-syenite dykes. (**A**) Very fine-grained reaction rim between micro-xenolithic quartz (Q) and groundmass feldspar. (**B**) Rounded quartz micro-xenolith (Q).

(**A**)

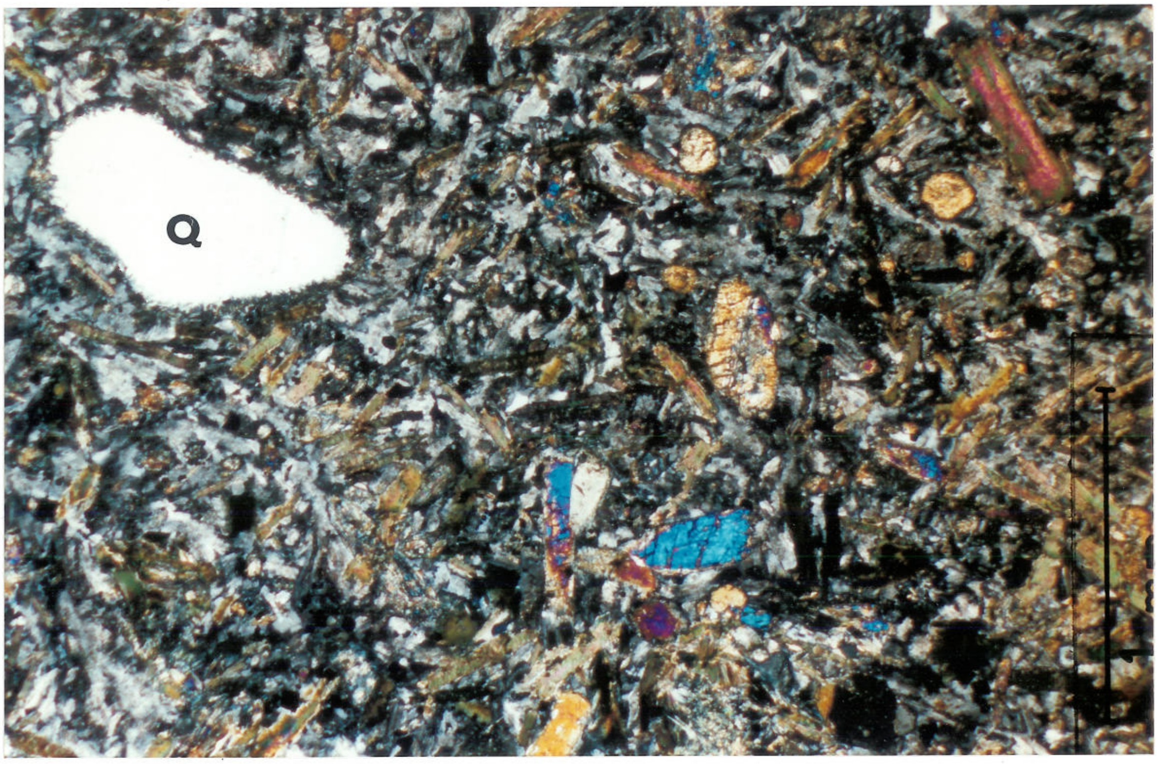

(**B**)

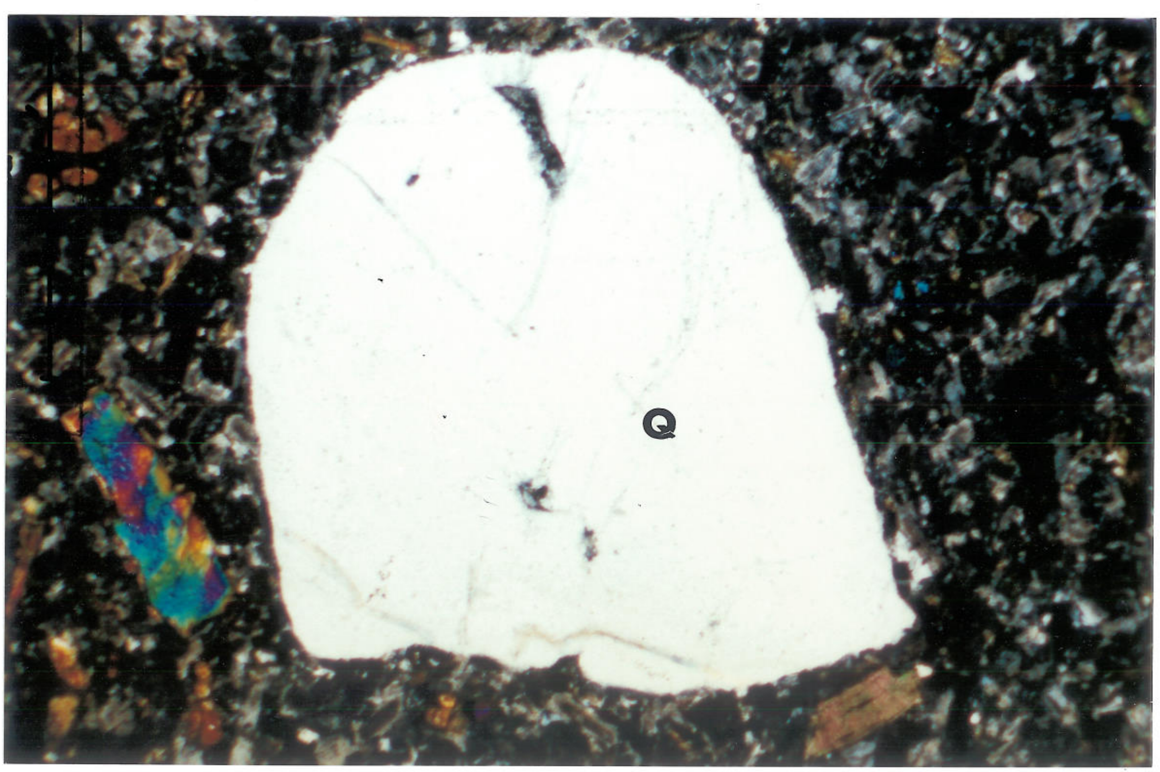

(Appendix 5A). These geochemical features along with core and rim chemical variations are identical to macrocrystic mica in minettes associated with Christopher Island Formation ultrapotassic magmatism. Groundmass mica is biotite and resembles biotite from the syenitic phase of the SLIC.

Clinopyroxene lie within the diopside and salite fields of the pyroxene quadrilateral and exhibit reverse zoning identical to clinopyroxene in Christopher Island Formation minettes. Reverse magmatic zoning is interpreted to be due to magma mixing in crustal reservoirs.

Microcline in the groundmass displays dramatic Ba zoning identical to early formed microcline in Christopher Island Formation minette (Appendix 5C; Figure 33). Coexisting albite contains negligible BaO. In summary the mineralogy and textural from the lamprophyre and fine-grained syenites that cut the SLIC are equated with the regional lamprophyre-minette swarm identified in the western Churchill Province (Figure 1).

GEOCHEMISTRY

CIPW norm were calculated using the whole rock chemistry in Appendix 6 and the program IGPET2 for Macintosh computers. The calculated normative components quartz-orthoclase-anorthite+albite (Q-OR-AN+AB) were used in conjunction with Streckeisen's (1976) plutonic rock classification to analyze the distribution of igneous rocks in the SLIC. In Figure 34, the syenitic rocks of the complex cluster in the syenite-quartz syenite field but range from undersaturated alkali-feldspar syenite to quartz monzonite. This corresponds to the rock variation of oikocrystic mafic syenite to leucocratic quartz syenite. Granitic rocks cluster very tightly in the granite 2B field. Lamprophyre-syenite dykes lie in the granite-monzonite-quartz monzonite fields. Except for the sample that lies within the granite 2A field, the other two dykes lie within the compositional range of syenitic rocks. Precautions were taken to not include xenoliths in dyke samples, however compositions might be influenced by micro-xenoliths.

Since the igneous rocks of the SLIC have in part affinities to Christopher Island Formation intrusive and extrusive rocks, the SLIC was compared to the latter on a total alkali vs silica diagram (Figure 35). Syenitic rocks and lamprophyre-syenite dykes in the SLIC lie

Figure 33. Backscatter electron photograph showing concentric and sector Ba-zoning in euhedral groundmass K-feldspar from the dyke east of Garhard Lake.

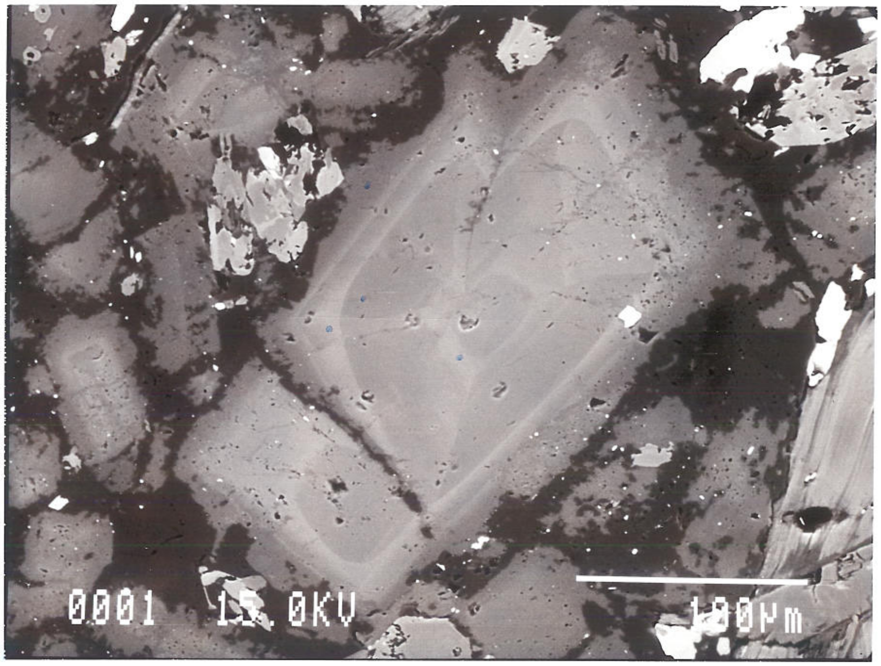

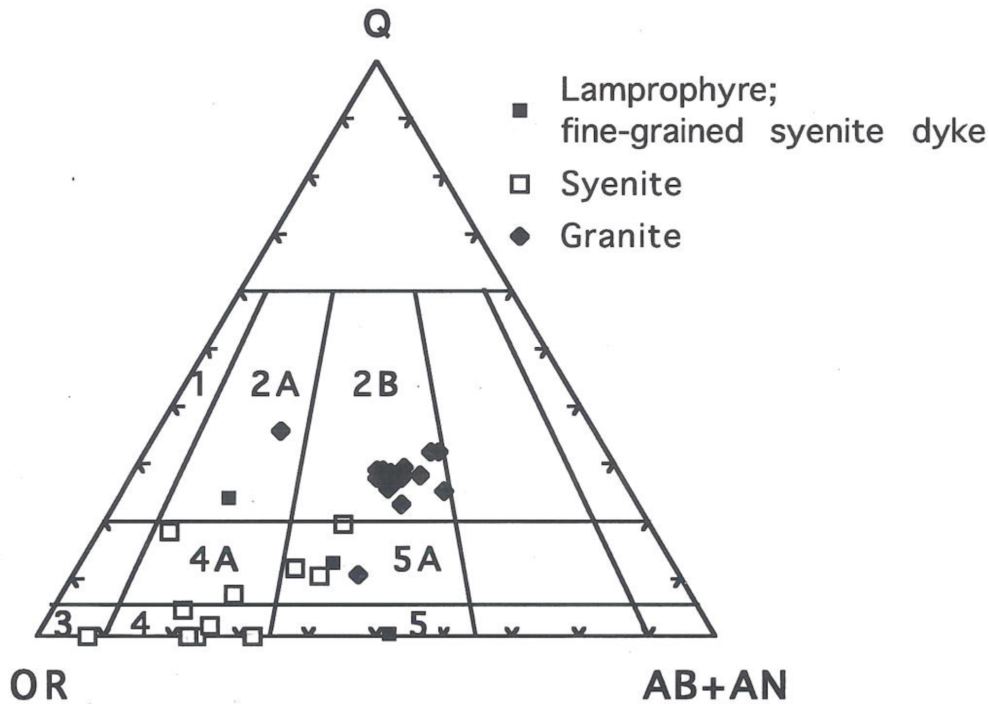

Figure 34. CIPW normative compositions for intrusive rocks that comprise the Schultz Lake Intrusive Complex (after Streckeisen, 1976).

1	Alkali-feldspar granite
2A,2B	Granite
3	Alkali-feldspar syenite
4, 4A	Syenite, quartz syenite
5, 5A	Monzonite, quartz monzonite

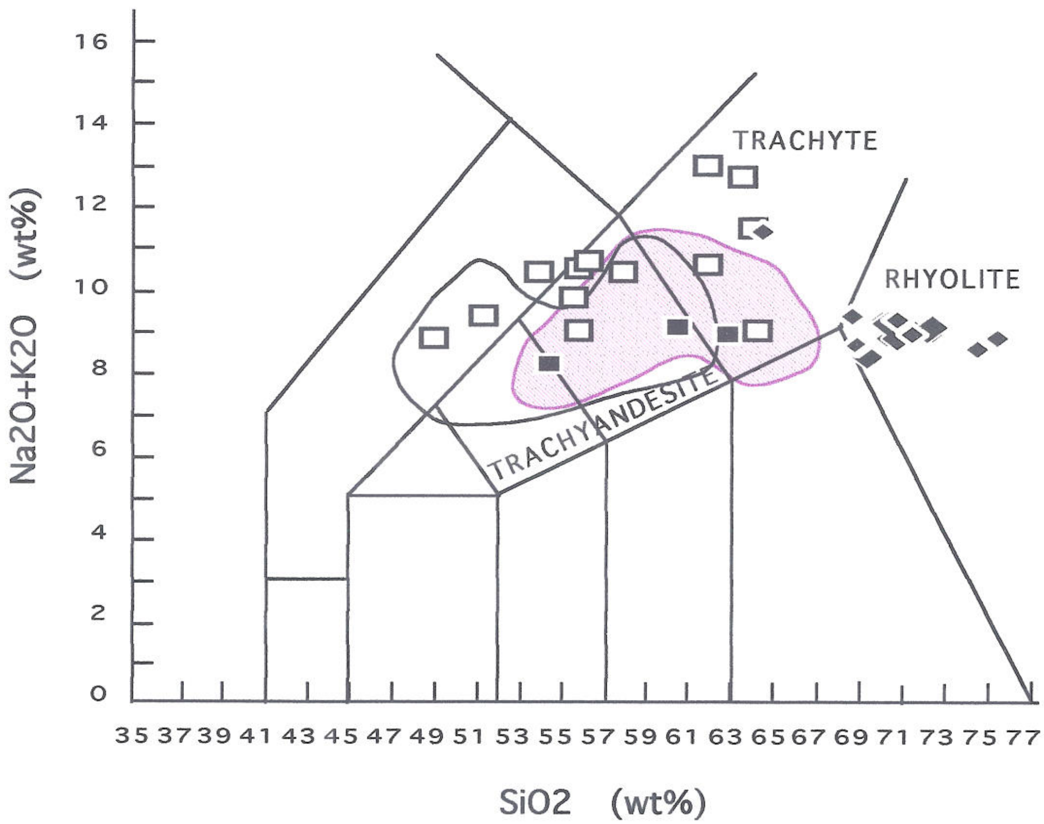

■ Phlogopite-phyric lamprophyre

◆ Fine- to coarse-grained fluorite granite and aplite

□ Hornblende+clinopyroxene, fine- to coarse-grained syenites

Field of Christopher Island syenites (from LeCheminant et al., 1987)

Field of Christopher Island mica-rich lamprophyres (from LeCheminant et al., 1987)

Figure 35. Total alkali-silica diagrams for various intrusive lithologies from the Schultz Lake Intrusive Complex plotted on discriminant diagram for potassic-ultrapotassic volcanic rocks (after LeMaitre, 1986)

within the distribution of intrusive CIF rocks (REE-bearing syenite, mesocratic to leucocratic syenites, highly fractionated syenites-bostonite, lamprophyres and trachyandesite volcanic rocks) (LeCheminant, Miller, LeCheminant, 1987; Miller, 1980; Miller and Blackwell, 1992) are considered to be genetically related to this ultrapotassic-potassic Paleoproterozoic igneous event in the western Churchill province. The granitic phase of the complex which is cut by syenite-lamprophyre cluster very tightly in the rhyolite field. However the relative timing of these two rock types, ie syenites cut by lamprophyre with an intervening granite event, is a very unusual feature and will be addressed in the Discussion section.

Lithophile and ferrromagnesium elements were plotted against silica in an attempt to evaluate whether the syenite-granite phases of the complex represent a continuous fractionation trend (Figure 36). Syenites and lamprophyre-syenite dykes overlap and form a continuous fractionation trend from 49 to 65 wt% SiO_2. A marked gap is present between 65 to 69 wt% SiO_2 and this gap separates the syenites/lamprophyre-syenite dykes from granitic rocks that lie in the range of 69 to 75 wt% SiO_2.

Normalized rare earth element (REE) patterns were used to examine the petrogenetic relationships between the three intrusive phases of the SLIC and to REE patterns in other ultrapotassic-potassic rocks belonging to the Christopher Island igneous event. All SLIC and comparison datum were normalized against Taylor and McLennan's chondrite values. REE patterns will be controlled by the following assessory minerals, primarily sphene, apatite and zircon, of which the former two are ubiquitous in syenitic rocks and all three minerals in granitic rocks but at markedly lower modal percentages. In Figure 37A, REE analyses of three dykes from the SLIC have similiar steep strongly LREE-enriched patterns with no infections. These patterns are identical to Christopher Island volcanic rocks from the Dubawnt Lake (Peterson et al., 1994) as well as to minettes in the Baker Lake subbasin (LeCheminant et al., 1987). The REE patterns are compatible with the interpretation that the east to northeast-trending lamprophyre-syenite dykes in the SLIC are part of the regional 1.84 Ga minette-lamprophyre swarm in the western Churchill Province.

The REE pattern for oikocrystic, mesocratic and leucocratic syenitic rocks, (Figure 37B) is identical to that of lamprophyre-syenite dykes. This is further confirmation that the syenitic phase of

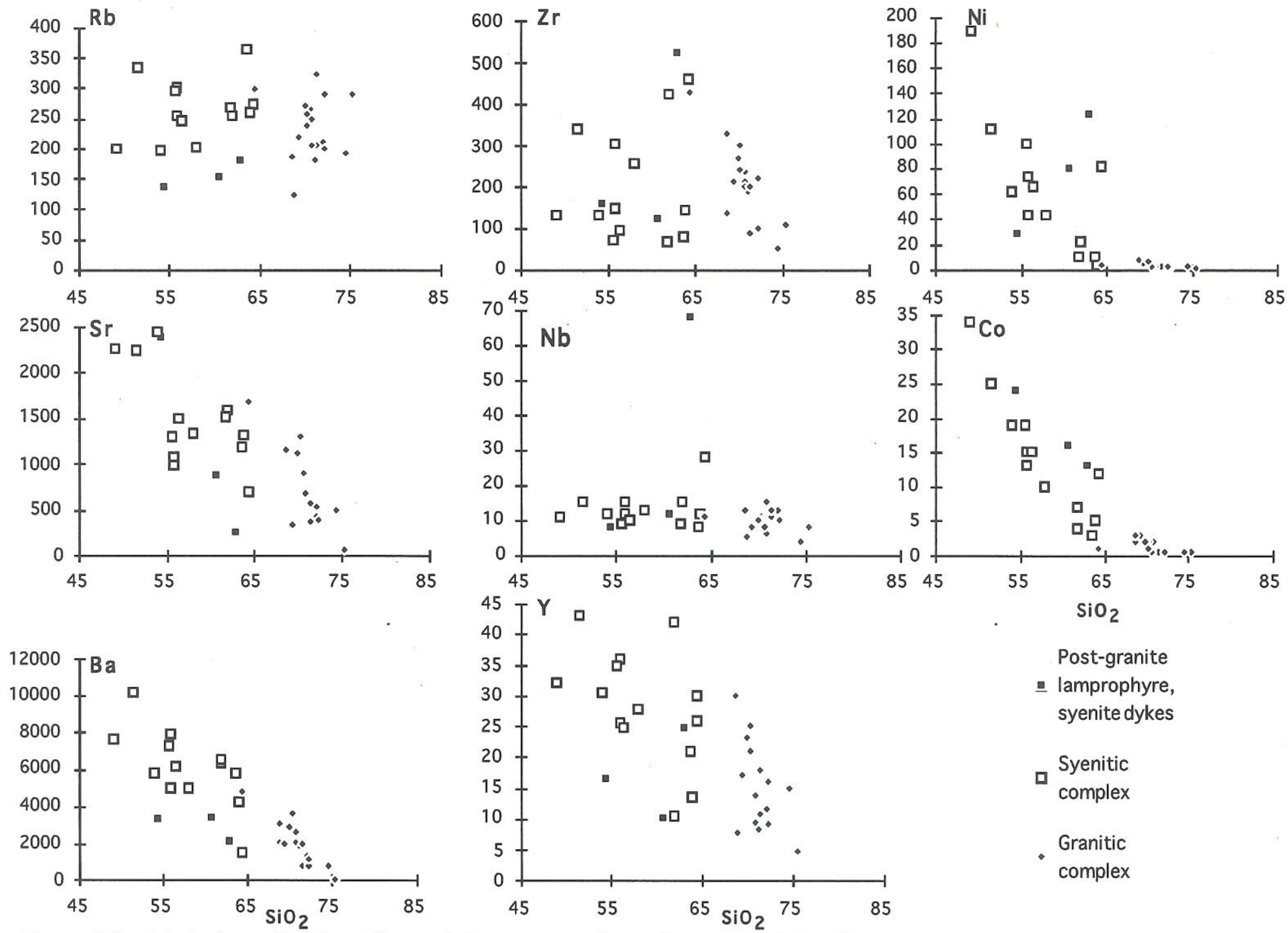

Figure 36. Variation of lithophile and ferromagnesium elements with silica for lithologies in the Schultz Lake Intrusive Complex.

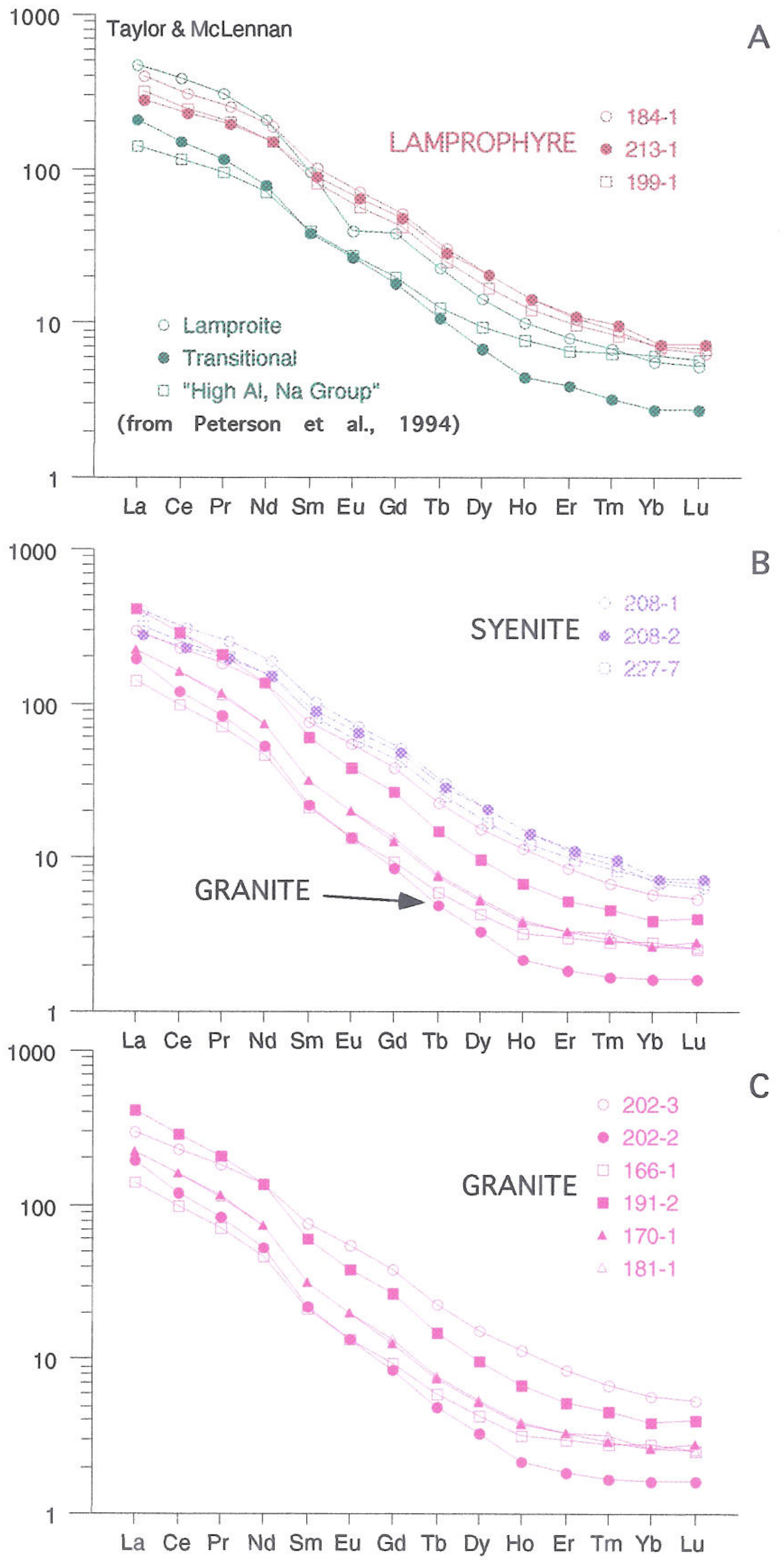

Figure 37. REE plots for the three phases of the Schultz Lake Intrusive Complex with comparisons to Christopher Island Formation volcanic rocks.

the intrusive complex and the later dykes are genetically related. Granitic rocks exhibit REE patterns in granitic rocks display steep strongly LREE-enriched patterns similiar to the syenitic rocks but shifted to lower absolute values. This pattern suggests that the granitic rocks ~~are~~ may be related not petrogenetically but through physical processes in the source region.

The REE patterns of SLIC syenitic rocks is compared to REE-enriched syenitic plutons from the Enekatcha and Carey lakes plutonic complexes. The latter plutonic complex are hosted with Archean granitic gneisses south southeast of Dubawnt Lake and has been dated at 1828 +/-12Ma. This pluton has highly fractionated phases that are enriched in many incompatible elements (Miller and Blackwell, 1992). Again SLIC lamprophyre-syenite are similiar to dykes in the Carey lake area and the Enekatcha syenitic rocks are similiar to the SLIC syenite except for the REE-enriched syenites (Figures 38, 37).

In Figure 36, the silica gap between the syenitic and granitic rocks suggests that the SLIC is not a product of fractionation. Since the granitic rocks were formed in a different source region than the syenitic rocks, plots of incompatible elements against SiO_2 were employed in order to better define the type of granitoid, orogenic versus anorogenic. In Figure 39, the various types of granitic rocks from the SLIC cluster in the I-type field. This classification as I-type is compatible with interpretation that the SLIC granites were derived by melting dehyrated continental crust. The SLIC granitic phases is similiar to other granitic subvolcanic plutonic complexes in the Baker Lake subbasin

DISCUSSION

Uranium Metallogeny and the Intrusive Complex

Developement of the crustal-scale uranium province in the central western Churchill Province can be viewed as a trinity that began at circa 2.45 - 2.1 Ga and culminated with the formation of unconformity-type uranium deposits between 1.4 - 1.2 Ga. This trinity is comprised of three elements that include each of the major time-lithostratigraphic units in the western Churchill. These are: 1) the Amer Group with its stratabound and stratiform uranium occurrences, 2) continental volcanic and sedimentary rocks in the Baker Lake and Wharton groups and 3) the Thelon Basin and

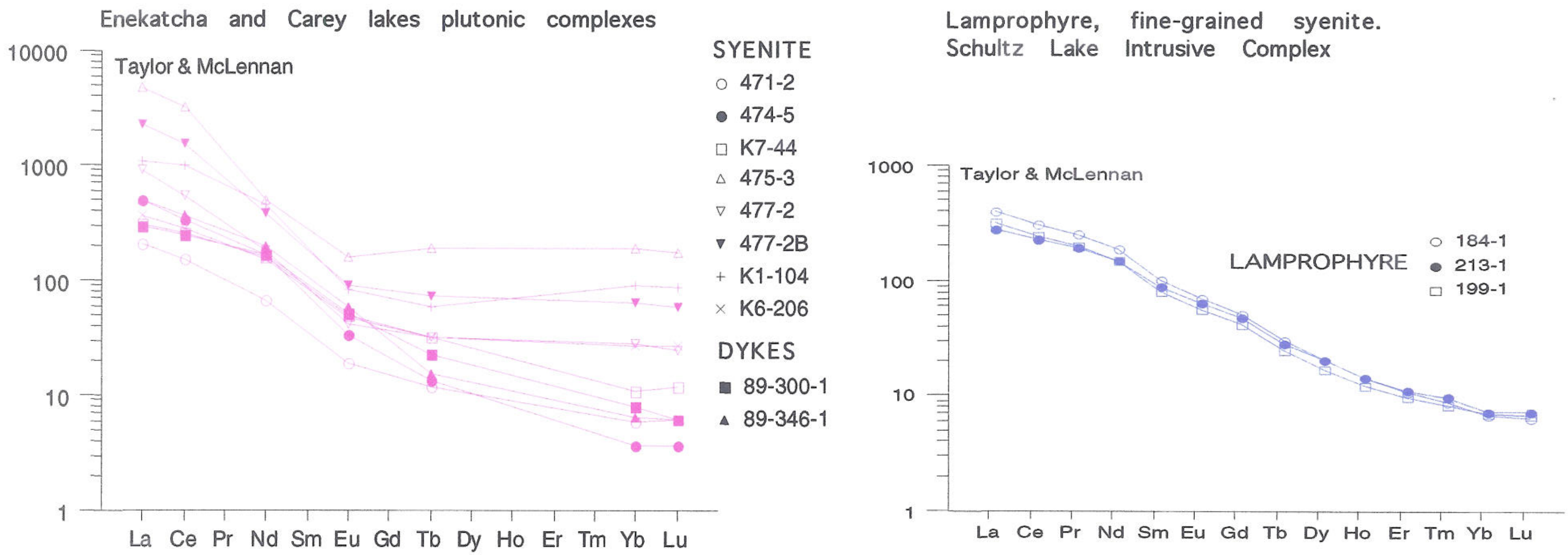

Figure 38. Comparison of normalized REE patterns from the Enekatcha and Carey lakes plutonic complexes and lamprophyre - fine-grained syenite dykes from the Schultz Lake Intrusive Complex.

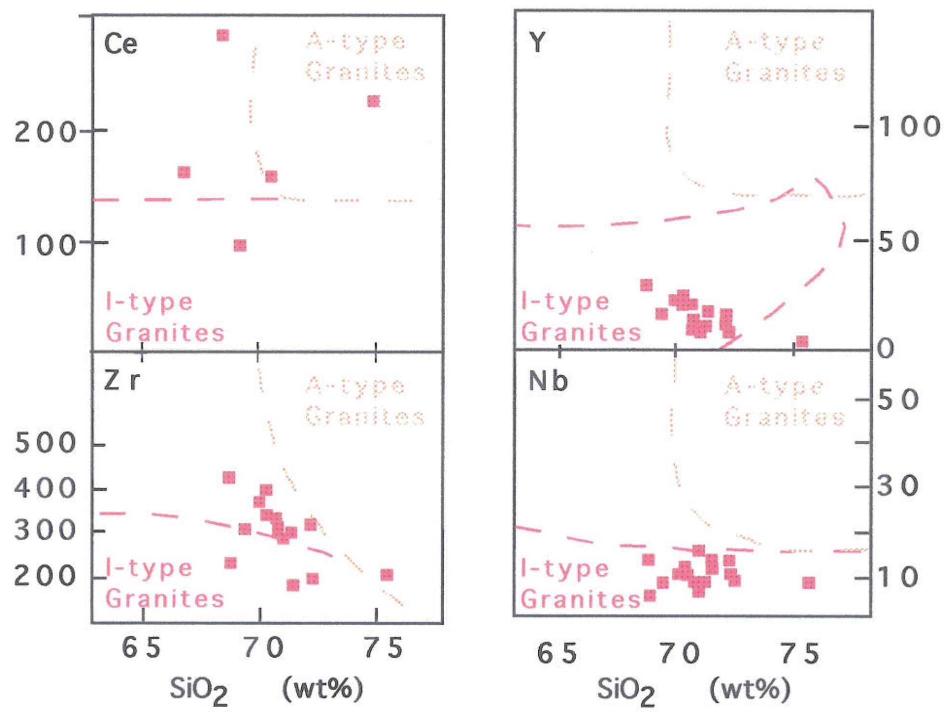

Figure 39. Plots of Ce, Zr, Y, Nb against SiO_2 to illustrate the I-type chemistry of the granitic rocks from the Schultz Lake Intrusive Complex. (Field boundaries from Collins et al., 1982)

underlying basement which host unconformity-type uranium deposits.

These unmetamorphosed and undeformed ultrapotassic and silicic magmatic events of the Christopher Island and Wharton groups represent the second element in the uranium trinity that defines the crustal-scale uranium province in the central western Churchill Province. Magma generation associated with extensional tectonics at 1.84 Ga in the western Churchill Province resulted in the voluminous generation and transmission of mantle-derived ultrapotassic magmas followed by lower crustal-derived uraniferous siliceous magmas into and onto the western Churchill crust. Magmatic processes, diagenesis of these volcano-sedimentary piles, syn- to post-volcanism, coupled with ongoing block faulting lead to a spectacular array of uranium deposit types hosted in Baker Lake and Wharton groups and basement to these subbasins.

Fractionation and differentiation processes associated with Christopher Island intrusive rocks has lead to incompatible element enrichment, notably Th>U, on average 3:1 with Zr, Ce La bearing minerals. Examples of this mineral deposit type are the bostonite sills and dykes in Christopher Island Formation rocks and underlying gneissic basement, Baker Lake and Dubawnt Lake subbasin areas and Enekatcha-like deep seated plutonic complexes. Uranium is enriched by these processes but it is held in refractory minerals and not associated with pitchblende vein systems. Pitchblende vein systems can be associated with quartz syenite plutons in the Baker Lake subbasin but these plutons are high level possible synvolcanic plutons. The syenitic and granitic phases of the SLIC are interpreted to be deep seated plutons because the granite phase does not display textures as myrolitic cavities that are indicative of high level plutons and commonly seen in granitic plutons that are intrusive into volcanics and sediments in the Baker Lake subbasin.

Thorium contents of rocks from the SLIC are: syenites, 5 - 21 ppm, granites, 13 - 50ppm and lamprophyre/syenite dykes, 14-75ppm. It is assumed that uranium abundances will be equal or less than thorium contents. All outcrops were examined with a discriminating scintillometer. Syenitic rocks have a variable scintillation due to different feldspar and assessory mineral contents. whereas the granitic rocks are higher and more uniform. Absolutely no evidence was found of either hydrothermal alteration zones, greisen-type or uranium vein systems that would suggest the presence of syngenetic hydrothermal pitchblende veins were associated with either the syenitic or granitic phases of the SLIC. Even the sulphide-bearing and quartz veined portion of the granite north of Sleek Lake does not carry uranium-bearing veins.

Model for the Schultz Lake Intrusive Complex

The syenitic phase and the post-granite lamprophyre/syenite dykes of the SLIC possess the geochemical and mineralogical characteristics that link them to mantle-derived melts akind to those that characterize the Christopher Island ultrapotassic-potassic magmatic event in the western Churchill Province. However the features of a discordant-concordant granite event between SLIC syenite and lamprophyre dyking is unusual. The Wharton silicic magmatic-volcanic event is post-Christopher Island magmatism and therefore crosscuts ultrapotassic-potassic rocks. The question arises: what is the age of the SLIC and is the granitic phase of the SLIC related to the Wharton Group igneous event? The author thinks not.

The aeromagnetic map of Schultz-Aberdeen lakes area displays numerous large magnetic anomalies which are assumed to be magnetite-bearing syenite, granite or complexes like the SLIC. The size and presumed volume of these intrusions indicates that a most significant melting event occurred in the mantle-lower crust over an area greater than 20,000 sq. km. on the north side of the Baker Lake subbasin.

Initial melting in the mantle produced the syenitic phase of the SLIC. This melt or multiple melts ascended into but became arrested in the lower crust. Fractionation processes were active as indicated by biotite- and clinopyroxene-rich cognate xenoliths and the wide spectrum of syenitic rocks. Geothermal gradients were elevated in the lower crust due to the volume of ultrapotassic-potassic magma that was ponded in the lower crust. With an increased geothermal gradient in the lower crust, a dehyrated lower continent crust melted to form the flourine-rich I-type granite. Even though the granite was seen to chill against the syenite locally, chilled contacts are not prevalent in the agmatitic complex just not of Mushroom Lake. Thus the granite is later than the syenite but it was intruded into still "warm" syenite in the lower to middle crust. Upward migration of these magmas may have been controlled by northeast-trending crustal scale fault.

Lamprophyre/syenite dykes represent the next igneous event and these chill against the syenite-granite. Field observations and petrogemistry are used to define the relative timing between syenite-granite and lamprophyre/syenite dykes. Petrochemistry of these dykes strongly indicates that these dykes belong to the regional lamprophyre/minette swarm associated with Christopher Island volcanism. These dykes are controlled by a family of east to east northeast faults which are parallel to subparallel to the Baker Lake subbasin. It is proposed that with the onset of extensional tectonics and regional faulting, the first ultrapotassic magmas, lamprophyres, intruded into the crust. Regional block faulting during graben formation may have uplifted the complex and lamprophyre dykes chilled against syenite-granite. The implication of this is that the syenite-granite of the SLIC must be older than the age of Christopher Island volcanism-plutonism established at circa1.84 - 1.83 Ma. Pre- and post-Thelon uplift probably unroofed the intrusive complex.

As a point of spectulation, the complex excluding lamprophyre may be as old as circa1.9 Ga. At circa 1.94 Ga, this portion of the western Churchill Province was undergoing a major uplift event which is recorded in granulite-grade mylonites east of Baker Lake. Melting in the mantle and lower crust may have occurred at this time (Figure 40A).

EXPLORATION GUIDELINES

From the petrochemistry of the SLIC, there is no evidence that igneous processes were responsible in any way for the world-class uranium deposits that are distributed along the eastern side of the complex. These deposits are interpreted as basement-hosted unconformity-type uranium deposits, albeit there are numerous features that set them apart from the classical Athabasca type deposits.

Structure is of paramount importance in these formation of these deposits along with lithological units that are highly susceptible to hydrolysis, feldspar alteration. With these two features it is possible that unconformity-type uranium mineralization could be hosted in the SLIC. The fault zones that dissect the complex display hallmark alteration assemblages that indicate silica mobility and argillization of feldspars (Figure 40B). In Figure 4, three "chrysler" symbols, pentagon with a star, are positioned on fault zones that

Figure 40A. Possible age for the SLIC in relation to Baker Lake and Wharton Group rocks.

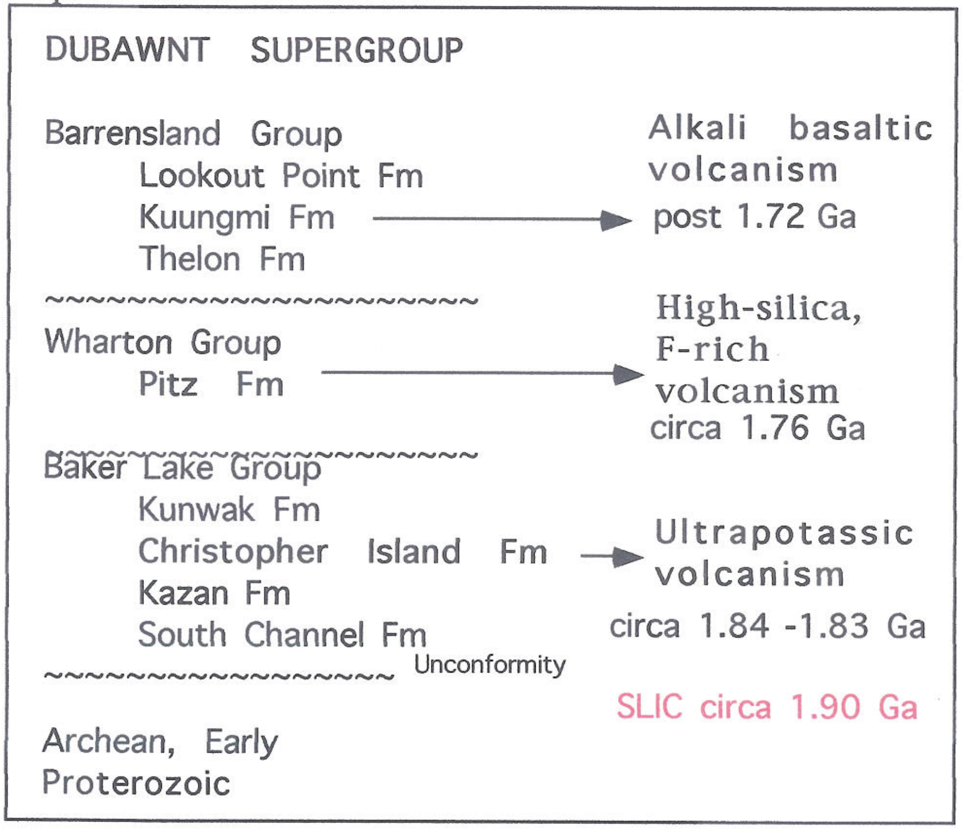

Figure 40B. Photomicrograph of argillic alteration on feldspar in SLIC granite

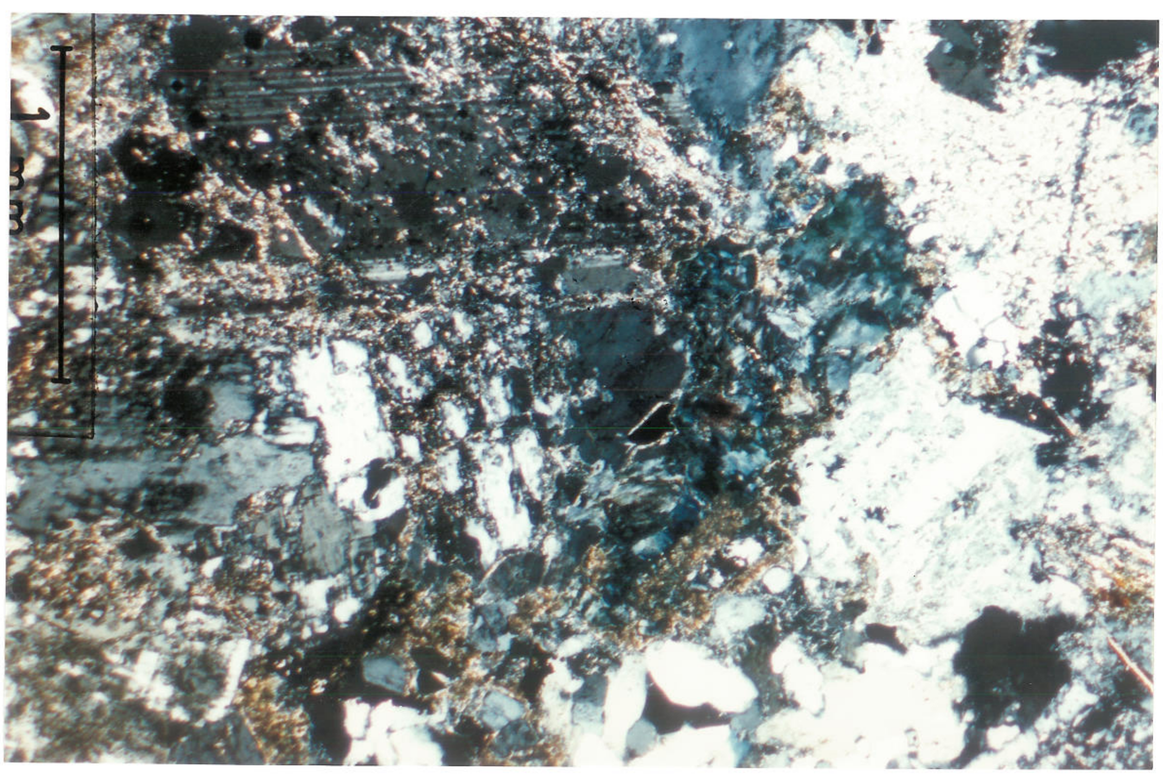

record multiple movements, are filled with quartz stockworks, and are mantled by hematitized and argillitized granite-syenite of the SLIC. This is a potential host rock for unconformity-type uranium deposits as indicated by the Kiggavik Main Zone, End and Andrew deposits.

It is proposed that gravity and resistivity surveys be conducted over these altered zones in order to assess the potential for uranium mineralization. The geophysical signature of these surveys from deposits like Kiggavik and Andrew can be used as a template in order to assess the merits of the three chosen fault zones as potential structures to host uranium mineralization. It should be kept in mind that 10 to 15 years ago no one would have explored for unconformity-type uranium deposits unless the targets was in lower Proterozoic metasedimentary rocks and associated with graphitic conductors, graphitic metapelite. The deposits in the Schultz Lake uranium camp are different and therefore new deposit types may be found in unconventional lithologies.

ACKNOWLEDGMENTS

The author is greatful to the IPP Industrial Partners for the opportunity to persue this geological problem. Electron microprobe analyses were determined on a JEOL 8600 electron superprobe at Barnett Geological Consulting, Lambeth, Ontario and on a CAMABAX electron microprobe at the Geological survey of Canada, Ottawa. G. Lemieux, Geological Survey of Canada, is thanked for the making of colour prints from slides.

	1	2	3	4	5	6	7	8	9
	"CLI 95MYAA	"CLI 95MYAA	"CLI 95MYAA	"CLI 95MYAA	"CLI 95MYAA	"CLI 95MYAA	"CLI 95MYAA	"CLI 95MYAA	"CLI 95MYAA
	190-1	190-1	190-1	190-1	190-1	190-1	190-1	190-1	190-1
	A3	A3	A3	A3	A4	A6	A6	A6	A6
	CPX, CENTRAL	AT MARGIN	SMALL CPX	AT MARGIN	CPX, CENTRAL	ZONED CPX WITH PHLOGOPIT	INTERIOR	AT MARGIN	ANOTHER CPX, CENTRAL
Rock Type	Syenite	Syenite	Syenite	Syenite	Syenite	Syenite	Syenite	Syenite	Syenite
SiO2	52.59	52.51	52.43	52.73	52.83	54.57	53.66	53.62	54.13
TiO2	0.16	0.21	0.23	0.11	0.16	0	0	0	0
Al2O3	0.72	0.68	0.93	0.52	0.8	0.17	0.35	0.38	0.29
Cr2O3	0.04	0	0	0	0	0	0	0.05	0.07
FeO	14.41	13.76	12.85	13.19	13.41	6.69	9.98	7.66	7.88
MgO	9.36	10.12	10.56	10.45	9.98	14.42	12.22	13.45	13.84
MnO	0.18	0.23	0.25	0.26	0.18	0.15	0.21	0.23	0.17
CaO	20.18	20.59	21.39	21.19	20.61	23.04	22.38	22.4	22.41
K2O	0	0	0.02	0.01	0	0	0.03	0.03	0.03
Na2O	2.5	2.17	1.68	1.92	2.27	1.23	1.23	1.51	1.52
TOTAl	100.14	100.27	100.34	100.38	100.24	100.27	100.06	99.33	100.34
	1	2	3	4	5	6	7	8	9
	"CLI	"CLI	"CLI	"CLI	"CLI	"CLI	"CLI	"CLI	"CLI
	95MYAA	95MYAA	95MYAA	95MYAA	95MYAA	95MYAA	95MYAA	95MYAA	95MYAA
	190-1	190-1	190-1	190-1	190-1	190-1	190-1	190-1	190-1
	A3	A3	A3	A3	A4	A6	A6	A6	A6
	CPX, CENTRAL	AT MARGIN	SMALL CPX	AT MARGIN	CPX, CENTRAL	ZONED CPX WITH PHLOGOPIT	INTERIOR	AT MARGIN	ANOTHER CPX, CENTRAL
	"	"	"	"	"	"	"	"	"
Si	2.011	2.001	1.99	2.003	2.008	2.014	2.014	2.009	2.008
Al	0	0	0.01	0	0	0	0	0	0
Total	2.011	2.001	2	2.003	2.008	2.014	2.014	2.009	2.008
Al	0.032	0.031	0.031	0.023	0.036	0.007	0.015	0.017	0.013
Ti	0.005	0.006	0.007	0.003	0.005	0	0	0	0
Cr	0.001	0	0	0	0	0	0	0.001	0.002
Fe	0.461	0.438	0.408	0.419	0.426	0.207	0.313	0.24	0.244
Mg	0.533	0.575	0.597	0.592	0.565	0.793	0.684	0.751	0.765
Mn	0.006	0.007	0.008	0.008	0.006	0.005	0.007	0.007	0.005
Ca	0.827	0.84	0.87	0.862	0.839	0.911	0.9	0.899	0.891
Na	0.185	0.16	0.124	0.141	0.167	0.088	0.09	0.11	0.109
K	0	0	0.001	0	0	0	0.001	0.001	0.001
Total	2.05	2.057	2.046	2.048	2.044	2.011	2.01	2.026	2.03
Enst	29.29	31	31.86	31.59	30.88	41.51	36.04	39.73	40.27
Wo	45.4	45.34	46.39	46.04	45.84	47.68	47.45	47.57	46.87
Fesil	25.3	23.65	21.75	22.37	23.28	10.81	16.51	12.7	12.86
Fe/Mg	0.875	0.776	0.696	0.722	0.764	0.266	0.468	0.329	0.326
Fe/Fe+Mg	0.467	0.437	0.41	0.419	0.433	0.21	0.319	0.248	0.246

Appendix 1, Electron microprobe analyses of clinopyroxene from syenites, SLIC.

10	11	12	13	14	15	16	17	18	19
"CLI 95MYAA	"CLI 95MYAA	"CLI 95MYAA	"CLI 95MYAA	"CLI 95MYAA	"CLI 95MYAA	"CLI 95MYAA	"CLI 95MYAA	"CLI 95MYAA	"CLI 95MYAA
190-1	190-1	190-1	190-1	190-1	190-1	199-2	199-2	199-2	199-2
A6	A7	A7	A7	A7	A7	A1	A1	A1	A1
AT MARGIN	CPX	AT MARGIN	ANOTHER CPX, CENTRAL	AT END	AT END	CPX WITH AMPHIBOLE	AT MARGIN	AT MARGIN	AT MARGIN
Syenite	Syenite	Syenite	Syenite	Syenite	Syenite	Syenite	Syenite	Syenite	Syenite
52.87	54.65	54.94	54.94	53.81	53.46	53.33	53.4	52.44	53.09
0.02	0	0	0	0.04	0.04	0.13	0.07	0.07	0.15
1.01	0.3	0.22	0.24	0.41	0.41	0.57	0.58	0.58	0.58
0.09	0	0	0	0.04	0	0	0	0	0.03
10.62	6.09	7.05	6.33	11.48	11.33	10.73	11.52	10.68	10.36
11.44	14.95	13.98	14.63	11.55	11.48	11.86	11.61	11.38	11.98
0.32	0.14	0.2	0.11	0.27	0.31	0.27	0.31	0.27	0.18
21.97	23.1	23	23.13	21.63	21.8	22.26	22.49	21.92	22.24
0.02	0.09	0.03	0.04	0.01	0.03	0.01	0.02	0	0
1.55	1.12	1.14	1.06	1.55	1.75	1.12	1.2	1.21	1.12
99.91	100.44	100.56	100.48	100.79	100.61	100.28	101.2	98.55	99.73
10	11	12	13	14	15	16	17	18	19
"CLI	"CLI	"CLI	"CLI	"CLI	"CLI	"CLI	"CLI	"CLI	"CLI
95MYAA	95MYAA	95MYAA	95MYAA	95MYAA	95MYAA	95MYAA	95MYAA	95MYAA	95MYAA
190-1	190-1	190-1	190-1	190-1	190-1	199-2	199-2	199-2	199-2
A6	A7	A7	A7	A7	A7	A1	A1	A1	A1
AT MARGIN	CPX	AT MARGIN	ANOTHER CPX, CENTRAL	AT END	AT END	CPX WITH AMPHIBOLE	AT MARGIN	AT MARGIN	AT MARGIN
"	"	"	"	"	"	"	"	"	"
1.996	2.009	2.023	2.018	2.016	2.009	2.004	1.997	2.007	2.003
0.004	0	0	0	0	0	0	0.003	0	0
2	2.009	2.023	2.018	2.016	2.009	2.004	2	2.007	2.003
0.041	0.013	0.01	0.01	0.018	0.018	0.025	0.023	0.026	0.026
0.001	0	0	0	0.001	0.001	0.004	0.002	0.002	0.004
0.003	0	0	0	0.001	0	0	0	0	0.001
0.335	0.187	0.217	0.194	0.36	0.356	0.337	0.36	0.342	0.327
0.644	0.819	0.767	0.801	0.645	0.643	0.664	0.647	0.649	0.674
0.01	0.004	0.006	0.003	0.009	0.01	0.009	0.01	0.009	0.006
0.889	0.91	0.907	0.91	0.868	0.878	0.896	0.901	0.899	0.899
0.113	0.08	0.081	0.075	0.113	0.128	0.082	0.087	0.09	0.082
0.001	0.004	0.001	0.002	0	0.001	0	0.001	0	0
2.037	2.017	1.989	1.995	2.015	2.035	2.017	2.031	2.017	2.019
34.47	42.75	40.56	42.03	34.44	34.26	35	33.91	34.35	35.47
47.58	47.48	47.97	47.77	46.36	46.77	47.23	47.21	47.56	47.33
17.95	9.77	11.48	10.2	19.2	18.97	17.77	18.88	18.09	17.21
0.537	0.234	0.291	0.247	0.571	0.569	0.521	0.572	0.54	0.494
0.349	0.19	0.225	0.198	0.363	0.363	0.342	0.364	0.351	0.331

Appendix 1, Electron microprobe analyses of clinopyroxene from syenites, SLIC.

20	21	22	23	24	25	26	27	28
"CLI 95MYAA	"CLI 95MYAA	"CLI 95MYAA	"CLI 95MYAA	"CLI 95MYAA	"CLI 95MYAA	"CLI 95MYAA	"CLI 95MYAA	"CLI 95MYAA
199-2	206-1	206-1	206-1	208-1	208-1	208-1	208-1	208-3
A1	A4	A4	A4	A1	A1	A3	A3	A1
ANOTHER GRAIN, CENTRAL	CPX, CENTRAL	AT MARGIN	CPX WITH AMPHIBOLE	CPX, CENTRAL	AT MARGIN	CPX, CENTRAL	AT MARGIN	CPX, CENTRAL
Syenite	Syenite	Syenite	Syenite	Syenite	Syenite	Syenite	Syenite	Syenite
52.64	53.1	53.23	52.84	53.41	53.54	54.16	53.06	51.28
0.45	0.36	0.16	0.22	0.13	0.1	0.18	0.19	0.03
0.92	0.82	0.9	0.47	0.5	0.46	1.27	0.54	0.68
0	0	0.02	0.08	0.06	0.01	0	0.1	0
9.77	8.73	13.23	14.53	12.86	12.81	6.92	13.3	15.95
12.56	12.7	10	9.42	10.25	10.6	14.17	9.81	8.16
0.19	0.1	0.18	0.2	0.12	0.19	0.05	0.18	0.63
22.83	23.08	19.8	17.89	19.25	20.11	22.6	18.9	20.82
0.01	0.01	0.02	0.01	0	0.01	0	0.01	0.01
0.77	1.01	2.78	3.95	2.96	2.66	1.14	3.31	1.72
100.14	99.91	100.32	99.61	99.54	100.49	100.49	99.4	99.28
20	21	22	23	24	25	26	27	28
"CLI	"CLI	"CLI	"CLI	"CLI	"CLI	"CLI	"CLI	"CLI
95MYAA	95MYAA	95MYAA	95MYAA	95MYAA	95MYAA	95MYAA	95MYAA	95MYAA
199-2	206-1	206-1	206-1	208-1	208-1	208-1	208-1	208-3
A1	A4	A4	A4	A1	A1	A3	A3	A1
ANOTHER GRAIN, CENTRAL	CPX, CENTRAL	AT MARGIN	CPX WITH AMPHIBOLE	CPX, CENTRAL	AT MARGIN	CPX, CENTRAL	AT MARGIN	CPX, CENTRAL
"	"	"	"	"	"	"	"	"
1.976	1.989	2.017	2.028	2.033	2.022	1.992	2.03	2
0.024	0.011	0	0	0	0	0.008	0	0
2	2	2.017	2.028	2.033	2.022	2	2.03	2
0.017	0.025	0.04	0.021	0.022	0.02	0.047	0.024	0.031
0.013	0.01	0.005	0.006	0.004	0.003	0.005	0.005	0.001
0	0	0.001	0.002	0.002	0	0	0.003	0
0.307	0.273	0.419	0.466	0.409	0.405	0.213	0.426	0.52
0.703	0.709	0.565	0.539	0.582	0.597	0.777	0.559	0.474
0.006	0.003	0.006	0.007	0.004	0.006	0.002	0.006	0.021
0.918	0.926	0.804	0.736	0.785	0.814	0.891	0.775	0.87
0.056	0.073	0.204	0.294	0.218	0.195	0.081	0.246	0.13
0	0	0.001	0	0	0	0	0	0
2.02	2.019	2.045	2.071	2.026	2.04	2.016	2.044	2.047
36.46	37.15	31.59	30.95	32.74	32.88	41.31	31.79	25.44
47.63	48.53	44.96	42.26	44.2	44.83	47.37	44.03	46.66
15.91	14.33	23.45	26.79	23.05	22.29	11.32	24.18	27.9
0.445	0.39	0.753	0.878	0.711	0.688	0.276	0.771	1.141
0.308	0.281	0.429	0.467	0.415	0.408	0.216	0.435	0.533

Appendix 1, Electron microprobe analyses of clinopyroxene from syenites, SLIC.

29	30	31	32	33	34	35	36	37	38
"CLI 95MYAA	"CLI 95MYAA	"CLI 95MYAA	"CLI 95MYAA	"CLI 95MYAA	"CLI 95MYAA	"CLI 95MYAA	"CLI 95MYAA	"CLI 95MYAA	"CLI 95MYAA
208-3	208-3	208-3	208-3	208-3	208-3	208-3	208-3	208-3	208-3
A1	A1	A1	A1	A1	A1	A2	A2	A2	A3
RAGGED CPX AT MARGIN	RAGGED CPX AT MARGIN	CPX AT MARGIN	CENTRAL	CENTRAL	CENTRAL	CPX, CENTRAL	INTERIOR	AT MARGIN	CPX, CENTRAL
Syenite	Syenite	Syenite	Syenite	Syenite	Syenite	Syenite	Syenite	Syenite	Syenite
51.1	51.85	52.02	52.18	52.52	52.03	52.28	51.71	51.94	51.7
0.08	0.03	0.11	0.11	0.08	0.05	0.06	0.1	0.08	0.08
0.66	0.64	0.74	0.58	0.62	0.67	0.64	0.9	0.66	0.64
0.02	0	0	0	0.03	0	0	0.02	0.01	0
15.72	15.45	15.66	15.93	15.83	15.57	15.63	14.99	15.82	16.17
8.23	8.37	8.35	8.24	8.24	8.23	8.39	8.8	8.1	8.29
0.39	0.45	0.5	0.51	0.65	0.57	0.6	0.43	0.71	0.47
20.91	20.6	20.8	20.99	21.3	21.26	21.15	22.12	20.56	21.01
0.02	0	0.01	0	0.02	0	0.02	0.02	0.01	0.01
1.74	1.74	1.78	1.68	1.59	1.56	1.53	1.23	1.85	1.53
98.87	99.13	99.97	100.22	100.88	99.94	100.3	100.32	99.74	99.9
29	30	31	32	33	34	35	36	37	38
"CLI	"CLI	"CLI	"CLI	"CLI	"CLI	"CLI	"CLI	"CLI	"CLI
95MYAA	95MYAA	95MYAA	95MYAA	95MYAA	95MYAA	95MYAA	95MYAA	95MYAA	95MYAA
208-3	208-3	208-3	208-3	208-3	208-3	208-3	208-3	208-3	208-3
A1	A1	A1	A1	A1	A1	A2	A2	A2	A3
RAGGED CPX AT MARGIN	RAGGED CPX AT MARGIN	CPX AT MARGIN	CENTRAL	CENTRAL	CENTRAL	CPX, CENTRAL	INTERIOR	AT MARGIN	CPX, CENTRAL
"	"	"	"	"	"	"	"	"	"
1.999	2.015	2.007	2.011	2.01	2.009	2.01	1.987	2.012	2.002
0.001	0	0	0	0	0	0	0.013	0	0
2	2.015	2.007	2.011	2.01	2.009	2.01	2	2.012	2.002
0.03	0.029	0.034	0.026	0.028	0.03	0.029	0.028	0.03	0.029
0.002	0.001	0.003	0.003	0.002	0.001	0.002	0.003	0.002	0.002
0.001	0	0	0	0.001	0	0	0.001	0	0
0.514	0.502	0.505	0.513	0.507	0.503	0.503	0.482	0.512	0.524
0.48	0.485	0.48	0.473	0.47	0.474	0.481	0.504	0.468	0.479
0.013	0.015	0.016	0.017	0.021	0.019	0.02	0.014	0.023	0.015
0.877	0.858	0.86	0.867	0.874	0.88	0.871	0.911	0.853	0.872
0.132	0.131	0.133	0.126	0.118	0.117	0.114	0.092	0.139	0.115
0.001	0	0	0	0.001	0	0.001	0.001	0	0
2.05	2.021	2.031	2.025	2.022	2.024	2.021	2.036	2.027	2.036
25.65	26.28	26.02	25.54	25.41	25.52	25.92	26.58	25.51	25.54
46.85	46.5	46.6	46.76	47.21	47.39	46.98	48.02	46.54	46.52
27.49	27.22	27.38	27.7	27.39	27.09	27.1	25.4	27.95	27.95
1.099	1.066	1.086	1.12	1.123	1.101	1.086	0.984	1.146	1.127
0.523	0.516	0.521	0.528	0.529	0.524	0.521	0.496	0.534	0.53

Appendix 1, Electron microprobe analyses of clinopyroxene from syenites, SLIC.

39	40	41	42	43	44	45	46	47	48
"CLI 95MYAA	"CLI 95MYAA	"CLI 95MYAA	"CLI 95MYAA	"CLI 95MYAA	"CLI 95MYAA	"CLI 95MYAA	"CLI 95MYAA	"CLI 95MYAA	"CLI 95MYAA
208-3	208-3	211-3	211-3	211-3	211-3	227-9	227-9	227-9	227-9
A3	A3	A3	A3	A4	A4	A1	A1	A1	A2
INTERIOR	AT RIM	CENTRAL	CPX AT END	CPX	AT MARGIN	CPX, CENTRAL	INTERIOR	DARK DOMAIN	CPX, DARK DOMAIN CENTRAL
Syenite	Syenite	Syenite	Syenite	Syenite	Syenite	Syenite	Syenite	Syenite	Syenite
52.12	52.21	53.27	52.92	52.46	52.31	51.67	51.99	52.72	52.6
0.03	0.07	0.1	0.09	0.08	0.09	0.33	0.35	0.4	0.37
0.64	0.63	0.41	0.43	0.45	0.4	1.06	1.23	1.09	1.07
0	0	0	0	0	0	0	0.05	0	0
15.98	15.83	13.63	13.29	13.59	13.29	15.52	15.12	9.93	11.07
8.21	8.15	10.12	10.35	10.37	10.2	8.72	8.95	12.37	11.74
0.5	0.53	0.39	0.3	0.33	0.3	0.24	0.36	0.19	0.31
20.39	20.85	20.65	20.92	20.9	21.07	19.52	19.64	22.58	22.05
0	0.01	0.01	0	0.02	0.01	0.04	0.02	0.01	0.03
2.14	1.73	2.06	2.01	2.03	2	2.74	2.73	1.2	1.52
100.01	100.01	100.64	100.31	100.23	99.67	99.84	100.44	100.49	100.76
39	40	41	42	43	44	45	46	47	48
"CLI	"CLI	"CLI	"CLI	"CLI	"CLI	"CLI	"CLI	"CLI	"CLI
95MYAA	95MYAA	95MYAA	95MYAA	95MYAA	95MYAA	95MYAA	95MYAA	95MYAA	95MYAA
208-3	208-3	211-3	211-3	211-3	211-3	227-9	227-9	227-9	227-9
A3	A3	A3	A3	A4	A4	A1	A1	A1	A2
INTERIOR	AT RIM	CENTRAL	CPX AT END	CPX	AT MARGIN	CPX, CENTRAL	INTERIOR	DARK DOMAIN	CPX, DARK DOMAIN CENTRAL
"	"	"	"	"	"	"	"	"	"
2.013	2.015	2.018	2.011	2.001	2.005	1.994	1.99	1.974	1.975
0	0	0	0	0	0	0.006	0.01	0.026	0.025
2.013	2.015	2.018	2.011	2.001	2.005	2	2	2	2
0.029	0.029	0.018	0.019	0.02	0.018	0.042	0.046	0.022	0.023
0.001	0.002	0.003	0.003	0.002	0.003	0.01	0.01	0.011	0.01
0	0	0	0	0	0	0	0.002	0	0
0.516	0.511	0.432	0.422	0.433	0.426	0.501	0.484	0.311	0.348
0.473	0.469	0.572	0.586	0.59	0.583	0.502	0.511	0.69	0.657
0.016	0.017	0.013	0.01	0.011	0.01	0.008	0.012	0.006	0.01
0.844	0.862	0.838	0.852	0.854	0.865	0.807	0.806	0.906	0.887
0.16	0.129	0.151	0.148	0.15	0.149	0.205	0.203	0.087	0.111
0	0	0	0	0.001	0	0.002	0.001	0	0.001
2.039	2.019	2.027	2.04	2.061	2.054	2.077	2.075	2.033	2.047
25.79	25.45	31.03	31.51	31.41	31.1	27.72	28.37	36.2	34.73
46.04	46.81	45.52	45.78	45.5	46.17	44.6	44.75	47.5	46.89
28.17	27.74	23.45	22.7	23.09	22.73	27.68	26.89	16.3	18.38
1.127	1.127	0.778	0.737	0.753	0.748	1.014	0.971	0.459	0.544
0.53	0.53	0.437	0.424	0.43	0.428	0.504	0.493	0.315	0.352

Appendix 1, Electron microprobe analyses of clinopyroxene from syenites, SLIC.

49	50	51	52	53	54	55	56
"CLI 95MYAA	"CLI 95MYAA	"CLI 95MYAA	"CLI 95MYAA	"CLI 95MYAA	"CLI 95MYAA	"CLI 95MYAA	"CLI 95MYAA
227-9	227-9	227-9	227-9	227-9	227-9	227-9	227-9
A2	A2	A2	A2	A5	A5	A5	A5
CPX, DARK DOMAIN CENTRAL	INTERIOR	INSIDE OUTER ZONE	BRIGHT ZONE AT MARGIN	SMALL CPX, CENTRAL	AT MARGIN	ANOTHER CPX, CENTRAL	AT MARGIN
Syenite	Syenite	Syenite	Syenite	Syenite	Syenite	Syenite	Syenite
52.83	51.75	53.26	51.61	52.34	52.23	52.41	52.21
0.33	0.41	0.38	0.3	0.53	0.32	0.43	0.39
1.07	0.94	0.85	1.06	0.87	1.13	1.03	1.17
0	0.01	0	0.01	0	0	0	0
10.56	13.65	9.39	15.42	11.8	15.15	9.91	15.44
11.79	9.59	12.46	8.66	11.14	8.7	11.89	8.8
0.23	0.3	0.18	0.38	0.26	0.33	0.29	0.27
22.36	20.17	22.94	19.81	21.6	19.35	22.22	19.69
0.02	0.01	0.02	0.03	0.01	0.02	0.01	0.03
1.41	2.27	1.2	2.61	1.59	2.69	1.42	2.85
100.6	99.1	100.68	99.89	100.14	99.92	99.61	100.85
49	50	51	52	53	54	55	56
"CLI	"CLI	"CLI	"CLI	"CLI	"CLI	"CLI	"CLI
95MYAA	95MYAA	95MYAA	95MYAA	95MYAA	95MYAA	95MYAA	95MYAA
227-9	227-9	227-9	227-9	227-9	227-9	227-9	227-9
A2	A2	A2	A2	A5	A5	A5	A5
CPX, DARK DOMAIN CENTRAL	INTERIOR	INSIDE OUTER ZONE	BRIGHT ZONE AT MARGIN	SMALL CPX, CENTRAL	AT MARGIN	ANOTHER CPX, CENTRAL	AT MARGIN
"	"	"	"	"	"	"	"
1.981	1.996	1.986	1.992	1.983	2.006	1.981	1.993
0.019	0.004	0.014	0.008	0.017	0	0.019	0.007
2	2	2	2	2	2.006	2	2
0.029	0.039	0.023	0.04	0.021	0.051	0.027	0.045
0.009	0.012	0.011	0.009	0.015	0.009	0.012	0.011
0	0	0	0	0	0	0	0
0.331	0.44	0.293	0.498	0.374	0.487	0.313	0.493
0.659	0.551	0.692	0.498	0.629	0.498	0.67	0.501
0.007	0.01	0.006	0.012	0.008	0.011	0.009	0.009
0.898	0.833	0.916	0.819	0.877	0.796	0.9	0.805
0.103	0.17	0.087	0.195	0.117	0.2	0.104	0.211
0.001	0	0.001	0.001	0	0.001	0	0.001
2.037	2.055	2.029	2.072	2.041	2.053	2.035	2.076
34.89	30.21	36.41	27.45	33.47	27.97	35.57	27.83
47.57	45.67	48.19	45.13	46.64	44.71	47.79	44.77
17.54	24.12	15.4	27.42	19.89	27.32	16.64	27.4
0.514	0.816	0.431	1.024	0.608	0.999	0.482	1.002
0.339	0.449	0.301	0.506	0.378	0.5	0.325	0.5

Appendix 1, Electron microprobe analyses of clinopyroxene from syenites, SLIC.

57	58	59	60	61	62	63	64
"CLI 95MYAA	"CLI 95MYAA	"CLI 95MYAA	"CLI 95MYAA	"CLI 95MYAA	"CLI 95MYAA	"CLI 95MYAA	"CLI 95MYAA
227-9	227-9	227-9	227-9	228-2	228-2	228-2	228-2
A5	A5	A5	A5	A1	A1	A1	A1
AT MARGIN	ZONED CPX, CENTRAL	AT MARGIN	ANOTHER CPX, CENTRAL	ZONED CPX INCLOSING PHLO	LIGHT DOMAIN	CPX INTERIOR	ADJACENT BRIGHT DOMAIN
Syenite	Syenite	Syenite	Syenite	Syenite	Syenite	Syenite	Syenite
52.34	54.48	53.86	54.31	53.93	52.5	52.93	52.36
0.38	0.1	0.12	0.1	0.11	0.17	0.1	0.25
1.15	0.17	0.74	0.31	1.21	1.65	1.49	1.42
0.03	0.13	0.23	0.2	0.21	0.2	0.18	0.18
14.67	6.53	11.48	7.11	5.82	11.33	7.35	11.47
8.84	15.1	10.79	14.38	14.09	10.33	12.98	10.26
0.35	0.16	0.23	0.15	0.05	0.14	0.11	0.18
19.69	22.69	20.98	22.95	23.51	20.32	22.54	20.32
0.02	0	0	0	0.01	0.01	0.02	0.02
2.71	0.97	2.35	0.92	1.2	2.86	1.6	2.69
100.18	100.33	100.78	100.43	100.14	99.51	99.3	99.15
57	58	59	60	61	62	63	64
"CLI	"CLI	"CLI	"CLI	"CLI	"CLI	"CLI	"CLI
95MYAA	95MYAA	95MYAA	95MYAA	95MYAA	95MYAA	95MYAA	95MYAA
227-9	227-9	227-9	227-9	228-2	228-2	228-2	228-2
A5	A5	A5	A5	A1	A1	A1	A1
AT MARGIN	ZONED CPX, CENTRAL	AT MARGIN	ANOTHER CPX, CENTRAL	ZONED CPX INCLOSING PHLO	LIGHT DOMAIN	CPX INTERIOR	ADJACENT BRIGHT DOMAIN
"	"	"	"	"	"	"	"
2.003	2.006	2.018	2.005	1.989	1.994	1.983	1.998
0	0	0	0	0.011	0.006	0.017	0.002
2.003	2.006	2.018	2.005	2	2	2	2
0.052	0.007	0.033	0.013	0.042	0.068	0.049	0.062
0.011	0.003	0.003	0.003	0.003	0.005	0.003	0.007
0.001	0.004	0.007	0.006	0.006	0.006	0.005	0.005
0.469	0.201	0.36	0.219	0.18	0.36	0.23	0.366
0.504	0.829	0.603	0.791	0.775	0.585	0.725	0.584
0.011	0.005	0.007	0.005	0.002	0.005	0.003	0.006
0.807	0.895	0.842	0.908	0.929	0.827	0.905	0.831
0.201	0.069	0.171	0.066	0.086	0.211	0.116	0.199
0.001	0	0	0	0	0	0.001	0.001
2.057	2.013	2.026	2.011	2.023	2.067	2.037	2.061
28.31	43.05	33.39	41.24	41.13	33.01	38.97	32.78
45.33	46.5	46.67	47.32	49.33	46.68	48.65	46.66
26.36	10.45	19.93	11.44	9.53	20.31	12.38	20.56
0.954	0.249	0.609	0.283	0.234	0.623	0.323	0.637
0.488	0.199	0.379	0.221	0.189	0.384	0.244	0.389

Appendix 1, Electron microprobe analyses of clinopyroxene from syenites, SLIC.

65	66	67	68	69	70	71	72	73
"CLI 95MYAA	"CLI 95MYAA	"CLI 95MYAA	"CLI 95MYAA	"CLI 95MYAA	"CLI 95MYAA	"CLI 95MYAA	"CLI 95MYAA	"CLI 95MYAA
228-2	228-2	228-2	228-2	228-2	228-2	228-2	228-2	228-2
A1	A2	A2	A3	A3	A3	A3	A3	A3
AT MARGIN	CPX CENTRAL	AT MARGIN	CPX, CENTRAL	OUTER ZONE	ANOTHER ZONED CPX, CENTR	AT MARGIN	CPX BROAD CENTRAL ZONE	AT MARGIN
Syenite	Syenite	Syenite	Syenite	Syenite	Syenite	Syenite	Syenite	Syenite
52.07	52.37	51.4	53.18	51.9	53.54	52.09	54.84	53.07
0.49	0.59	0.41	0.14	0.32	0.11	0.35	0.15	0.08
1.2	1.05	1.4	1.46	1.28	1.47	1.1	0.01	0.68
0.01	0	0.05	0.1	0.17	0.1	0.23	0.18	0.34
15.09	10.81	15.04	7.57	14.96	7.54	13.22	4.12	11.51
8.68	11.41	8.47	13.45	8.59	13.73	9.64	15.96	10.56
0.25	0.22	0.22	0.09	0.23	0.09	0.2	0	0.17
19.43	21.71	19.16	23.1	19.26	22.92	19.84	23.71	20.55
0.02	0	0	0	0.02	0	0.01	0.02	0.01
3.22	1.78	3.13	0.96	3.19	0.98	2.74	0.9	2.63
100.46	99.94	99.28	100.05	99.92	100.48	99.42	99.89	99.6
65	66	67	68	69	70	71	72	73
"CLI	"CLI	"CLI	"CLI	"CLI	"CLI	"CLI	"CLI	"CLI
95MYAA	95MYAA	95MYAA	95MYAA	95MYAA	95MYAA	95MYAA	95MYAA	95MYAA
228-2	228-2	228-2	228-2	228-2	228-2	228-2	228-2	228-2
A1	A2	A2	A3	A3	A3	A3	A3	A3
AT MARGIN	CPX CENTRAL	AT MARGIN	CPX, CENTRAL	OUTER ZONE	ANOTHER ZONED CPX, CENTR	AT MARGIN	CPX BROAD CENTRAL ZONE	AT MARGIN
"	"	"	"	"	"	"	"	"
1.993	1.98	1.991	1.977	1.996	1.979	1.998	2.011	2.016
0.007	0.02	0.009	0.023	0.004	0.021	0.002	0	0
2	2	2	2	2	2	2	2.011	2.016
0.047	0.027	0.055	0.041	0.054	0.043	0.048	0	0.03
0.014	0.017	0.012	0.004	0.009	0.003	0.01	0.004	0.002
0	0	0.002	0.003	0.005	0.003	0.007	0.005	0.01
0.483	0.342	0.487	0.235	0.481	0.233	0.424	0.126	0.366
0.495	0.643	0.489	0.745	0.492	0.756	0.551	0.872	0.598
0.008	0.007	0.007	0.003	0.007	0.003	0.006	0	0.005
0.797	0.879	0.795	0.92	0.794	0.908	0.815	0.931	0.836
0.239	0.13	0.235	0.069	0.238	0.07	0.204	0.064	0.194
0.001	0	0	0	0.001	0	0	0.001	0
2.084	2.045	2.082	2.02	2.081	2.019	2.065	2.003	2.041
27.9	34.49	27.61	39.21	27.86	39.87	30.78	45.19	33.22
44.89	47.17	44.89	48.41	44.91	47.84	45.54	48.26	46.47
27.21	18.33	27.5	12.38	27.23	12.29	23.68	6.55	20.31
0.992	0.543	1.011	0.32	0.992	0.312	0.781	0.145	0.621
0.498	0.352	0.503	0.242	0.498	0.238	0.439	0.127	0.383

Appendix 1, Electron microprobe analyses of clinopyroxene from syenites, SLIC.

74	75	76	77	78	79	80
"CLI 95MYAA	"CLI 95MYAA	"CLI 95MYAA	"CLI 95MYAA	"CLI 95MYAA	"CLI 95MYAA	"CLI 95MYAA
228-2	228-2	249-3	249-3	249-3	249-3	249-3
A3	A3	A1	A1	A1	A1	A1
ANOTHER CENTRAL	AT END	CPX LATH, CENTRAL	CPX LATH, CENTRAL	AT END, JUST INSIDE NARR	NARROW BRIGHT ZONE AT EN	NARROW BRIGHT ZONE AT EN
Syenite	Syenite	Syenite	Syenite	Syenite	Syenite	Syenite
53.63	53.49	53.41	53.07	52.86	51.6	51.88
0.13	0.12	0.19	0.16	0.21	0.21	0.23
0.4	0.83	1.09	1	1.04	1.08	1.18
0.94	0.35	0.06	0	0	0.02	0.05
8.98	10.69	10.82	10.55	10.04	13.36	13.49
11.7	11.17	11.28	11.25	11.64	9.55	9.53
0.08	0.2	0.18	0.12	0.16	0.35	0.14
20.49	20.81	21.86	22.04	22.46	20.68	20.79
0.01	0.01	0	0.01	0.01	0.02	0
2.8	2.43	1.75	1.75	1.51	2.38	2.26
99.16	100.1	100.64	99.95	99.93	99.25	99.55
74	75	76	77	78	79	80
"CLI	"CLI	"CLI	"CLI	"CLI	"CLI	"CLI
95MYAA	95MYAA	95MYAA	95MYAA	95MYAA	95MYAA	95MYAA
228-2	228-2	249-3	249-3	249-3	249-3	249-3
A3	A3	A1	A1	A1	A1	A1
ANOTHER CENTRAL	AT END	CPX LATH, CENTRAL	CPX LATH, CENTRAL	AT END, JUST INSIDE NARR	NARROW BRIGHT ZONE AT EN	NARROW BRIGHT ZONE AT EN
"	"	"	"	"	"	"
2.024	2.013	2	2.001	1.991	1.989	1.991
0	0	0	0	0.009	0.011	0.009
2.024	2.013	2	2.001	2	2	2
0.018	0.037	0.048	0.044	0.037	0.038	0.045
0.004	0.003	0.005	0.005	0.006	0.006	0.007
0.028	0.01	0.002	0	0	0.001	0.002
0.283	0.336	0.339	0.333	0.316	0.431	0.433
0.658	0.626	0.63	0.632	0.654	0.549	0.545
0.003	0.006	0.006	0.004	0.005	0.011	0.005
0.829	0.839	0.877	0.89	0.906	0.854	0.855
0.205	0.177	0.127	0.128	0.11	0.178	0.168
0	0	0	0	0	0.001	0
2.028	2.034	2.034	2.036	2.034	2.069	2.06
37.18	34.77	34.12	34.08	34.83	29.93	29.74
46.81	46.56	47.52	47.99	48.31	46.58	46.64
16.01	18.67	18.36	17.93	16.86	23.49	23.62
0.435	0.547	0.547	0.532	0.492	0.806	0.803
0.303	0.354	0.354	0.347	0.33	0.446	0.445

Appendix 1, Electron microprobe analyses of clinopyroxene from syenites, SLIC.

81	82	83	84	85	86	87	88	89
"CLI 95MYAA	"CLI 95MYAA	"CLI 95MYAA	"CLI 95MYAA	"CLI 95MYAA	"CLI 95MYAA	"CLI 95MYAA	"CLI 95MYAA	"CLI 95MYAA
249-3	249-3	249-3	249-3	249-3	249-3	249-3	254-1	254-1
A1	A1	A3	A3	A3	A4	A4	A2	A2
SMALLER CPX, CENTRAL	INTERIOR ZONE	CPX, CENTRAL	INTERIOR	AT MARGIN	CPX, CENTRAL	AT MARGIN	CPX WITH BIOTITE-PHLOGOP	AT MARGIN
Syenite	Syenite	Syenite	Syenite	Syenite	Syenite	Syenite	Syenite	Syenite
52.81	51.83	52.5	52.45	52.64	52.69	52.5	52.92	52.85
0.35	0.2	0.31	0.19	0.3	0.23	0.25	0.29	0.23
0.78	1.15	0.79	1.03	0.88	0.78	0.75	1.08	0.81
0.14	0.08	0.06	0.04	0.04	0.07	0.02	0	0
8.89	14.16	9.95	10.58	11.54	12.6	12.12	9.95	12.57
12.3	8.93	11.79	11.29	10.95	9.84	10.39	12.3	10.74
0.17	0.18	0.11	0.17	0.22	0.2	0.22	0.3	0.27
23.52	20.53	22.86	21.79	21.75	21.33	21.55	22.85	21.41
0.01	0.02	0	0.01	0	0	0	0.02	0.04
0.9	2.58	1.3	1.78	1.74	1.95	1.78	0.95	1.58
99.87	99.66	99.67	99.33	100.06	99.69	99.58	100.66	100.5
81	82	83	84	85	86	87	88	89
"CLI	"CLI	"CLI	"CLI	"CLI	"CLI	"CLI	"CLI	"CLI
95MYAA	95MYAA	95MYAA	95MYAA	95MYAA	95MYAA	95MYAA	95MYAA	95MYAA
249-3	249-3	249-3	249-3	249-3	249-3	249-3	254-1	254-1
A1	A1	A3	A3	A3	A4	A4	A2	A2
SMALLER CPX, CENTRAL	INTERIOR ZONE	CPX, CENTRAL	INTERIOR	AT MARGIN	CPX, CENTRAL	AT MARGIN	CPX WITH BIOTITE-PHLOGOP	AT MARGIN
"	"	"	"	"	"	"	"	"
1.984	1.995	1.985	1.992	1.993	2.01	2.002	1.978	1.998
0.016	0.005	0.015	0.008	0.007	0	0	0.022	0.002
2	2	2	2	2	2.01	2.002	2	2
0.019	0.047	0.02	0.038	0.032	0.035	0.034	0.026	0.034
0.01	0.006	0.009	0.005	0.009	0.007	0.007	0.008	0.007
0.004	0.002	0.002	0.001	0.001	0.002	0.001	0	0
0.279	0.456	0.315	0.336	0.365	0.402	0.386	0.311	0.397
0.689	0.512	0.664	0.639	0.618	0.559	0.591	0.685	0.605
0.005	0.006	0.004	0.005	0.007	0.006	0.007	0.009	0.009
0.947	0.847	0.926	0.887	0.882	0.872	0.88	0.915	0.867
0.066	0.193	0.095	0.131	0.128	0.144	0.132	0.069	0.116
0	0.001	0	0	0	0	0	0.001	0.002
2.019	2.07	2.035	2.042	2.042	2.027	2.038	2.024	2.037
35.97	28.23	34.88	34.33	33.12	30.52	31.79	35.85	32.37
49.44	46.65	48.61	47.62	47.29	47.55	47.4	47.88	46.38
14.59	25.12	16.51	18.05	19.59	21.93	20.81	16.27	21.25
0.413	0.901	0.479	0.534	0.603	0.73	0.667	0.468	0.671
0.292	0.474	0.324	0.348	0.376	0.422	0.4	0.319	0.402

Appendix 1, Electron microprobe analyses of clinopyroxene from syenites, SLIC.

90	91	92	93	94	95	96	97
"CLI 95MYAA	"CLI 95MYAA	"CLI 95MYAA	"CLI 95MYAA	"CLI 95MYAA	"CLI 95MYAA	"CLI 95MYAA	"CLI 95MYAA
254-1	254-1	254-1	254-1	254-1	254-1	254-1	254-1
A3	A3	A3	A3	A4	A4	A4	A4
CPX, CENTRAL	AT MARGIN	AT MARGIN	AT MARGIN	CPX CENTRAL	INTERIOR	CPX AT MARGIN	CENTRAL AGAIN
Syenite	Syenite	Syenite	Syenite	Syenite	Syenite	Syenite	Syenite
52.61	53.07	52.84	52.47	54.55	54.1	52.2	53.19
0.18	0.12	0.24	0.23	0	0.03	0.26	0.01
0.83	0.71	0.95	1.03	0.68	0.94	0.89	0.79
0	0	0	0.03	0.45	0.18	0	0.45
12.84	13.22	10.72	10.58	6.83	9.2	10.39	8.21
10.59	10.5	11.79	12.2	14.05	12.66	12.31	12.98
0.19	0.24	0.24	0.19	0.3	0.26	0.18	0.05
21.29	21.03	22.86	22.97	22.77	21.9	22.81	22.32
0.01	0.02	0.01	0.01	0.03	0.02	0	0
1.81	1.97	1.03	0.92	1.22	1.61	1.05	1.42
100.35	100.88	100.68	100.63	100.88	100.9	100.09	99.42
90	91	92	93	94	95	96	97
"CLI	"CLI	"CLI	"CLI	"CLI	"CLI	"CLI	"CLI
95MYAA	95MYAA	95MYAA	95MYAA	95MYAA	95MYAA	95MYAA	95MYAA
254-1	254-1	254-1	254-1	254-1	254-1	254-1	254-1
A3	A3	A3	A3	A4	A4	A4	A4
CPX, CENTRAL	AT MARGIN	AT MARGIN	AT MARGIN	CPX CENTRAL	INTERIOR	CPX AT MARGIN	CENTRAL AGAIN
"	"	"	"	"	"	"	"
1.995	2.003	1.982	1.97	2.004	2.004	1.97	1.996
0.005	0	0.018	0.03	0	0	0.03	0.004
2	2.003	2	2	2.004	2.004	2	2
0.032	0.032	0.024	0.015	0.029	0.041	0.009	0.031
0.005	0.003	0.007	0.006	0	0.001	0.007	0
0	0	0	0.001	0.013	0.005	0	0.013
0.407	0.417	0.336	0.332	0.21	0.285	0.328	0.258
0.599	0.591	0.659	0.683	0.769	0.699	0.692	0.726
0.006	0.008	0.008	0.006	0.009	0.008	0.006	0.002
0.865	0.851	0.919	0.924	0.896	0.869	0.922	0.897
0.133	0.144	0.075	0.067	0.087	0.116	0.077	0.103
0	0.001	0	0	0.001	0.001	0	0
2.047	2.047	2.028	2.034	2.014	2.025	2.041	2.03
32	31.79	34.44	35.21	41.02	37.72	35.64	38.6
46.24	45.76	48	47.66	47.79	46.9	47.48	47.71
21.77	22.45	17.57	17.13	11.19	15.38	16.88	13.7
0.69	0.719	0.522	0.495	0.285	0.419	0.482	0.357
0.408	0.418	0.343	0.331	0.222	0.295	0.325	0.263

Appendix 1, Electron microprobe analyses of clinopyroxene from syenites, SLIC.

	1	2	3	4	5	6	7	8	9	10	11	12	13	14	15	16	17	18	19	20	21
	*AMP	*AMP	*AMP	*AMP	*AMP	*AMP	*AMP	*AMP	*AMP	*AMP	*AMP	*AMP	*AMP	*AMP	*AMP	*AMP	*AMP	*AMP	*AMP	*AMP	*AMP
	95MYAA	95MYAA	95MYAA	95MYAA	95MYAA	95MYAA	95MYAA	95MYAA	95MYAA	95MYAA	95MYAA	95MYAA	95MYAA	95MYAA	95MYAA	95MYAA	95MYAA	95MYAA	95MYAA	95MYAA	95MYAA
	190-1	190-1	190-1	199-2	199-2	199-2	206-1	206-1	206-1	206-1	206-1	206-1	206-1	206-1	211-2	211-2	211-2	211-2	211-2	211-2	211-2
	G1	G1	G2	A1	A1	A2	A1	A1	A1	A4	A6	A6	A6	A6	A1	A1	A1	A3	A3	A3	A3
	CENTRAL	MARGIN	CENTRAL	CENTRAL	MARGIN	FGRND	CENTRAL	INTERIOR	MARGIN	AMPHIBOLE	CENTRAL	CONTwPH	AMPHIBOLE	AMPHIBOLE	CENTRAL	AT END	AT END	CENTRAL	CENTRAL	CENTRAL	INTERIOR
Rock Type	Syenite	Syenite	Syenite	Syenite	Syenite	Syenite	Syenite	Syenite	Syenite	Syenite	Syenite	Syenite	Syenite	Syenite	Granite	Granite	Granite	Granite	Granite	Granite	Granite
SiO2	52.01	54.42	52.48	49.63	49.35	55.61	52.56	52.66	54.18	54.23	52.62	52.24	52.89	52.23	47.81	48.36	46.82	54.66	51.11	47.28	47.38
TiO2	0.08	0.04	0.02	0.48	0.48	0.02	0.37	0.53	0.04	0.01	0.54	0.51	0.31	0.51	0.24	0.25	0.25	0.04	0.05	0.27	0.28
Al2O3	3.11	1.32	2.54	4.85	4.88	1.05	2.01	2.14	1.13	0.94	2.22	2.1	1.81	2.46	5.13	4.75	5.46	3.42	3.4	5.13	5.22
Cr2O3	0.03	0	0	0.01	0	0	0	0.05	0.07	0	0	0	0	0.02	0	0.01	0.03	0	0	0	0
FeO	13.83	12.34	12.53	14.43	13.93	10.48	13.23	13.14	13.26	11.94	13.68	14.08	13.56	13.77	17.26	17.14	17.91	14.14	14.1	17.35	17.69
MgO	14.99	16.18	15.68	14.36	14.41	17.84	15.03	15.18	15.33	15.73	15.13	14.74	15.25	14.69	11.91	11.71	11.27	13.23	12.95	11.6	11.79
MnO	0.11	0.16	0.17	0.17	0.17	0.05	0.2	0.13	0.18	0.13	0.13	0.13	0.08	0.26	0.52	0.74	0.7	0.81	0.67	0.9	0.63
CaO	10.85	11.09	11.64	11.22	11.25	10.58	9.2	8.2	10.85	11.38	7.95	8.45	9.39	8.9	10.82	10.35	10.39	11.19	10.94	10.58	10.72
K2O	0.8	0.46	0.66	1	0.99	0.1	1.15	1.19	0.32	0.34	1.25	1.26	0.87	1.08	1	0.97	1.06	0.48	0.48	0.99	1.03
Na2O	1.98	1.51	1.41	2.05	2.13	0.24	2.79	3.74	1.72	1.35	3.83	3.43	2.76	3.34	1.83	1.72	2.06	0.86	0.91	1.96	1.9
F	0.96	0.91	0.82	1.03	1.21	0.21	0.95	1.31	0.68	0.58	1.25	1.14	0.89	1.08	1.16	1.14	1.14	1.2	1.22	1.12	1.27
Cl	0	0	0	0.02	0.03	0	0	0	0	0	0	0	0	0	0.01	0.01	0.02	0.01	0	0.01	0
TOTAL	98.75	98.43	97.95	99.25	98.83	96.18	97.49	98.27	97.76	96.63	98.6	98.08	97.81	98.34	97.69	97.15	97.11	100.04	95.83	97.19	97.91
(=-O=F+Cl)	0.4	0.38	0.35	0.44	0.52	0.09	0.4	0.55	0.29	0.24	0.53	0.48	0.37	0.45	0.49	0.48	0.48	0.51	0.51	0.47	0.53
SUM	98.35	98.05	97.6	98.81	98.31	96.09	97.09	97.72	97.47	96.39	98.07	97.6	97.44	97.89	97.2	96.67	96.63	99.53	95.32	96.72	97.38

	1	2	3	4	5	6	7	8	9	10	11	12	13	14	15	16	17	18	19	20	21
	*AMP	*AMP	*AMP	*AMP	*AMP	*AMP	*AMP	*AMP	*AMP	*AMP	*AMP	*AMP	*AMP	*AMP	*AMP	*AMP	*AMP	*AMP	*AMP	*AMP	*AMP
	95MYAA	95MYAA	95MYAA	95MYAA	95MYAA	95MYAA	95MYAA	95MYAA	95MYAA	95MYAA	95MYAA	95MYAA	95MYAA	95MYAA	95MYAA	95MYAA	95MYAA	95MYAA	95MYAA	95MYAA	95MYAA
	190-1	190-1	190-1	199-2	199-2	199-2	206-1	206-1	206-1	206-1	206-1	206-1	206-1	206-1	211-2	211-2	211-2	211-2	211-2	211-2	211-2
	CENTRAL	AT MARGIN	ANOTHER, C	A1 AMPHIBC	A1 AT MARC	A2 FINE GRA	A1 HORNBLI	A1 INTERIOF	A1 AT MARC	A4 AMPHIBC	A6 HORNBLI	A6 IN CONT/	A6 AMPHIBC	A6 AMPHIBC	A1 AMPHIBC	A1 AT END	A1 AT END	A3 HORNBLI	A3 HORNBLI	A3 HORNBLI	A3 INTERIOF
			Formula based on 23 oxygen																		
Si	7.512	7.78	7.59	7.203	7.183	7.971	7.667	7.621	7.829	7.879	7.608	7.614	7.685	7.584	7.162	7.265	7.099	7.727	7.594	7.143	7.108
Al	0.488	0.22	0.41	0.797	0.817	0.029	0.333	0.365	0.171	0.121	0.378	0.361	0.31	0.416	0.838	0.735	0.901	0.273	0.406	0.857	0.892
Total	8	8	8	8	8	8	8	7.986	8	8	7.986	7.975	7.995	8	8	8	8	8	8	8	8
Al	0.041	0.002	0.023	0.032	0.02	0.148	0.013	0	0.022	0.04	0	0	0	0.005	0.068	0.105	0.074	0.297	0.189	0.056	0.031
Ti	0.009	0.004	0.002	0.052	0.053	0.002	0.041	0.058	0.004	0.001	0.059	0.056	0.034	0.056	0.027	0.028	0.029	0.004	0.006	0.031	0.032
Cr	0.003	0	0	0.001	0	0	0	0.006	0.008	0	0	0	0	0.002	0	0.001	0.004	0	0	0	0
Fe	1.67	1.475	1.515	1.751	1.696	1.256	1.614	1.59	1.602	1.451	1.654	1.716	1.648	1.672	2.162	2.153	2.271	1.672	1.752	2.192	2.22
Mg	3.227	3.448	3.38	3.106	3.126	3.811	3.268	3.274	3.302	3.406	3.26	3.202	3.303	3.179	2.659	2.622	2.547	2.788	2.868	2.612	2.636
Mn	0.013	0.019	0.021	0.021	0.021	0.006	0.025	0.016	0.022	0.016	0.016	0.016	0.01	0.032	0.066	0.094	0.09	0.097	0.084	0.115	0.08
Total	4.963	4.948	4.941	4.963	4.916	5.223	4.961	4.944	4.96	4.914	4.989	4.99	4.995	4.946	4.982	5.003	5.015	4.858	4.899	5.006	4.999
Ca	1.679	1.699	1.804	1.745	1.754	1.625	1.438	1.271	1.68	1.771	1.231	1.32	1.462	1.385	1.737	1.666	1.688	1.695	1.741	1.712	1.723
Na	0.554	0.419	0.395	0.577	0.601	0.067	0.789	1.049	0.482	0.38	1.074	0.969	0.778	0.94	0.532	0.501	0.606	0.236	0.262	0.574	0.553
K	0.147	0.084	0.122	0.185	0.184	0.018	0.214	0.22	0.059	0.063	0.231	0.234	0.161	0.2	0.191	0.186	0.205	0.087	0.091	0.191	0.197
Total	2.38	2.202	2.321	2.507	2.539	1.71	2.441	2.54	2.221	2.214	2.536	2.523	2.401	2.525	2.46	2.353	2.499	2.018	2.094	2.477	2.473
F	0.439	0.411	0.375	0.473	0.557	0.095	0.438	0.6	0.311	0.266	0.572	0.526	0.409	0.496	0.55	0.542	0.547	0.537	0.573	0.535	0.603
Cl	0	0	0	0.005	0.007	0	0	0	0	0	0	0	0	0	0.003	0.003	0.005	0.002	0	0.003	0
Total	0.439	0.411	0.375	0.478	0.564	0.095	0.438	0.6	0.311	0.266	0.572	0.526	0.409	0.496	0.553	0.545	0.552	0.539	0.573	0.538	0.603
Fe	25.4	22.28	22.62	26.53	25.78	18.77	25.54	25.92	24.34	21.89	26.91	27.51	25.7	26.81	32.97	33.43	34.91	27.16	27.54	33.64	33.74
Ca	25.53	25.65	26.92	26.42	26.68	24.28	22.75	20.72	25.51	26.72	20.04	21.15	22.8	22.2	26.48	25.86	25.94	27.54	27.38	26.28	26.19
Mg	49.07	52.07	50.45	47.05	47.54	56.95	51.71	53.36	50.15	51.39	53.05	51.33	51.51	50.98	40.55	40.71	39.15	45.3	45.08	40.08	40.07
Fe/Mg	0.522	0.434	0.455	0.571	0.549	0.331	0.501	0.491	0.492	0.431	0.512	0.541	0.502	0.536	0.838	0.857	0.927	0.634	0.64	0.883	0.872
Fe/Fe+Mg	0.343	0.302	0.312	0.363	0.354	0.249	0.334	0.329	0.33	0.301	0.339	0.351	0.334	0.349	0.456	0.462	0.481	0.388	0.39	0.469	0.466

Appendix 2. Electron microprobe analyses of hornblende from the SLIC.

22	23	24	25	26	27	28	29	30	31	32	33	34	35	36	37	38	39	40	41	42	43
*AMP	*AMP	*AMP	*AMP	*AMP	*AMP	*AMP	*AMP	*AMP	*AMP	*AMP	*AMP	*AMP	*AMP	*AMP	*AMP	*AMP	*AMP	*AMP	*AMP	*AMP	*AMP
95MYAA	95MYAA	95MYAA	95MYAA	95MYAA	95MYAA	95MYAA	95MYAA	95MYAA	95MYAA	95MYAA	95MYAA	95MYAA	95MYAA	95MYAA	95MYAA	95MYAA	95MYAA	95MYAA	95MYAA	95MYAA	95MYAA
211-2	211-2	211-2	211-2	211-3	211-3	211-3	211-3	211-3	211-3	211-3	211-3	211-3	211-3	211-3	211-3	249-1	249-1	249-1	249-1	249-1	254-1
A3	A4	A4	A4	A1	A1	A1	A1	A1	A1	A1	A2	A2	A2	A2	A2	A2	A2	A2	A3	A3	A1
MARGIN	CENTRAL	INTERIOR	MARGIN	AMPHIBOLE	AMPHIBOLE	INTERIOR	AMPHIBOLE	CENTRAL A	BRIGHT ZON	INNER ZONE	CENTRAL AI	AT MARGIN	ADJACENT (	ADJACENT	OUTER MAR	HORNBLEN	AT MARGIN	HORNBLEN	HORNBLEND	AT MARGIN	CENTRAL
Granite	Granite	Granite	Granite	Syenite	Syenite	Syenite	Syenite	Syenite	Syenite	Syenite	Syenite	Syenite	Syenite	Syenite	Syenite	Syenite	Syenite	Syenite	Syenite	Syenite	Syenite
47.92	47.23	46.45	46.88	52.15	51.88	52.61	51.17	51.53	48.13	51.22	51.9	51.69	49.36	50.42	51.46	48.02	47.38	48.95	46.25	47.32	53.34
0.21	0.28	0.28	0.24	0.27	0.25	0.24	0.21	0.26	0.15	0.33	0.28	0.24	0.15	0.12	0.18	0.26	0.27	0.29	0.55	0.28	0.45
5.15	5.26	5.83	5.16	2.59	2.46	2.48	2.93	2.64	5.23	2.67	2.56	2.4	3.64	3.25	2.91	5.2	5.47	4.5	6.56	5.47	2.05
0	0	0	0.03	0	0	0	0	0	0	0	0	0	0	0	0	0.02	0	0	0.02	0.05	0
17.3	17.53	17.91	17.17	14.13	14.04	13.71	15.66	14.28	15.7	13.73	13.26	13.71	16.87	14.96	15.75	17.47	17.91	16.88	18.94	17.52	12.22
11.69	11.81	11.6	11.96	14.66	15.03	14.78	13.7	14.64	13.43	14.71	15.49	15.12	13.25	14.35	13.78	11.98	11.66	12.83	11.13	11.86	16
0.68	0.6	0.48	0.61	0.36	0.38	0.14	0.36	0.38	0.35	0.26	0.32	0.29	0.48	0.31	0.4	0.2	0.3	0.27	0.27	0.25	0.19
10.48	10.4	10.78	10.65	9.09	9.09	9.05	8.94	9.19	9.33	9.25	9.13	9.12	10.1	10.07	9.14	10.5	10.54	10.74	10.63	10.72	9.09
0.99	1.01	1.1	0.96	1.09	1.09	1.12	1.22	1.06	0.88	1.19	1.15	1.1	0.92	0.85	1.26	1.12	1.13	1.12	1.26	1.12	1.05
2.05	2.1	2.15	2.17	3.19	3.36	3.39	3.22	3.3	3.38	3.18	3.27	3.09	2.58	2.42	2.95	2.51	2.29	2.27	2.45	2.37	2.86
1.15	1.18	1.22	1.32	2.07	2.03	2.21	1.86	2.02	1.77	1.96	2.13	1.96	1.6	1.78	1.72	1.23	1.15	1.23	1.19	1.37	1.24
0.01	0.02	0.01	0.01	0	0	0.01	0.01	0.02	0.01	0.01	0.01	0.01	0.02	0.02	0.02	0.09	0.02	0.01	0.06	0.02	0.01
97.63	97.42	97.81	97.16	99.6	99.61	99.74	99.28	99.32	98.36	98.51	99.5	98.73	98.97	98.55	99.57	98.6	98.12	99.09	99.31	98.35	98.5
0.49	0.5	0.52	0.56	0.87	0.85	0.93	0.79	0.86	0.75	0.83	0.9	0.83	0.68	0.75	0.73	0.54	0.49	0.52	0.51	0.58	0.52
97.14	96.92	97.29	96.6	98.73	98.76	98.81	98.49	98.46	97.61	97.68	98.6	97.9	98.29	97.8	98.84	98.06	97.63	98.57	98.8	97.77	97.98
22	23	24	25	26	27	28	29	30	31	32	33	34	35	36	37	38	39	40	41	42	43
*AMP	*AMP	*AMP	*AMP	*AMP	*AMP	*AMP	*AMP	*AMP	*AMP	*AMP	*AMP	*AMP	*AMP	*AMP	*AMP	*AMP	*AMP	*AMP	*AMP	*AMP	*AMP
95MYAA	95MYAA	95MYAA	95MYAA	95MYAA	95MYAA	95MYAA	95MYAA	95MYAA	95MYAA	95MYAA	95MYAA	95MYAA	95MYAA	95MYAA	95MYAA	95MYAA	95MYAA	95MYAA	95MYAA	95MYAA	95MYAA
211-2	211-2	211-2	211-2	211-3	211-3	211-3	211-3	211-3	211-3	211-3	211-3	211-3	211-3	211-3	211-3	249-1	249-1	249-1	249-1	249-1	254-1
A3 AT MARG	A4 HORNBLI	A4 INTERIOF	A4 AT MARG	A1 AMPHIBC	A1 AMPHIBC	A1 INTERIOF	A1 AMPHIBC	A1 CENTRA	A1 BRIGHT Z	A1 INNER ZC	A2 CENTRAL	A2 AT MARG	A2 ADJACEN	A2 ADJACEI	A2 OUTER M	A2 HORNBLE	A2 AT MARG	A2 HORNBL	A3 HORNBLE	A3 AT MARG	A1 HORNBL
7.185	7.116	7.002	7.084	7.494	7.465	7.526	7.445	7.448	7.104	7.449	7.449	7.486	7.273	7.366	7.464	7.139	7.098	7.211	6.903	7.067	7.65
0.815	0.884	0.998	0.916	0.439	0.417	0.418	0.502	0.45	0.896	0.458	0.433	0.41	0.632	0.559	0.497	0.861	0.902	0.781	1.097	0.933	0.346
8	8	8	8	7.933	7.882	7.944	7.947	7.898	8	7.907	7.882	7.896	7.905	7.925	7.961	8	8	7.992	8	8	7.996
0.095	0.05	0.038	0.003	0	0	0	0	0	0.014	0	0	0	0	0	0	0.05	0.064	0	0.056	0.029	0
0.024	0.032	0.032	0.027	0.029	0.027	0.026	0.023	0.028	0.017	0.036	0.03	0.026	0.017	0.013	0.02	0.029	0.03	0.032	0.062	0.031	0.049
0	0	0	0.004	0	0	0	0	0	0	0	0	0	0	0	0	0.002	0	0	0.002	0.006	0
2.169	2.209	2.258	2.17	1.698	1.689	1.64	1.905	1.726	1.938	1.67	1.592	1.661	2.079	1.828	1.91	2.172	2.244	2.079	2.364	2.188	1.466
2.612	2.652	2.606	2.694	3.14	3.223	3.151	2.971	3.154	2.955	3.189	3.314	3.264	2.91	3.125	2.979	2.655	2.604	2.817	2.476	2.64	3.42
0.086	0.077	0.061	0.078	0.044	0.046	0.017	0.044	0.047	0.044	0.032	0.039	0.036	0.06	0.038	0.049	0.025	0.038	0.034	0.034	0.032	0.023
4.986	5.02	4.995	4.976	4.911	4.985	4.834	4.943	4.955	4.968	4.927	4.975	4.987	5.066	5.004	4.958	4.933	4.98	4.962	4.994	4.926	4.958
1.683	1.679	1.741	1.724	1.399	1.401	1.387	1.394	1.423	1.476	1.441	1.404	1.415	1.594	1.576	1.42	1.673	1.692	1.695	1.7	1.715	1.397
0.596	0.613	0.628	0.636	0.889	0.937	0.94	0.908	0.925	0.967	0.897	0.91	0.868	0.737	0.685	0.83	0.723	0.665	0.648	0.709	0.686	0.795
0.189	0.194	0.211	0.185	0.2	0.2	0.204	0.226	0.195	0.166	0.221	0.211	0.203	0.173	0.158	0.233	0.212	0.216	0.21	0.24	0.213	0.192
2.468	2.486	2.58	2.545	2.488	2.538	2.531	2.528	2.543	2.609	2.559	2.525	2.486	2.504	2.419	2.483	2.608	2.573	2.553	2.649	2.614	2.384
0.545	0.562	0.582	0.631	0.941	0.924	1	0.856	0.923	0.826	0.902	0.967	0.898	0.746	0.822	0.789	0.578	0.545	0.573	0.562	0.647	0.562
0.003	0.005	0.003	0.003	0	0	0.002	0.002	0.005	0.003	0.002	0.002	0.002	0.005	0.005	0.005	0.023	0.005	0.002	0.015	0.005	0.002
0.548	0.567	0.585	0.634	0.941	0.924	1.002	0.858	0.928	0.829	0.904	0.969	0.9	0.751	0.827	0.794	0.601	0.55	0.575	0.577	0.652	0.564
33.55	33.77	34.18	32.94	27.22	26.76	26.55	30.39	27.38	30.43	26.51	25.23	26.19	31.58	28	30.28	33.42	34.31	31.55	36.15	33.44	23.33
26.04	25.67	26.36	26.17	22.44	22.19	22.45	22.23	22.58	23.17	22.88	22.25	22.32	24.22	24.14	22.51	25.73	25.87	25.72	25.99	26.21	22.23
40.41	40.55	39.46	40.89	50.34	51.05	51	47.38	50.04	46.4	50.61	52.52	51.48	44.2	47.86	47.21	40.85	39.82	42.74	37.86	40.35	54.44
0.863	0.862	0.89	0.834	0.555	0.538	0.526	0.656	0.562	0.671	0.534	0.492	0.52	0.735	0.597	0.658	0.828	0.876	0.75	0.969	0.841	0.435
0.463	0.463	0.471	0.455	0.357	0.35	0.345	0.396	0.36	0.401	0.348	0.33	0.342	0.424	0.374	0.397	0.453	0.467	0.429	0.492	0.457	0.303

Appendix 2. Electron microprobe analyses of hornblende from the SLIC.

44	45	46	47	
*AMP	*AMP	*AMP	*AMP	
95MYAA	95MYAA	95MYAA	95MYAA	
254-1	254-1	254-1	254-1	
A1	A1	A5	A5	
INTERIOR	MARGIN wKF	HORNBLENI	BRIGHT DOMAIN	
Syenite	Syenite	Syenite	Syenite	
52.67	52.99	52.05	52.35	
0.47	0.44	0.37	0.39	
2.09	2.14	2	2.57	
0.04	0	0	0	
12.32	13.19	13.16	13.58	
16.18	15.34	15.42	15.31	
0.22	0.13	0.22	0.24	
9.27	9.43	10.52	10.29	
1.01	0.99	0.88	0.87	
3.06	2.64	2.09	2.31	
1.42	1.07	0.97	1.04	
0.02	0.03	0	0	
98.77	98.39	97.68	98.95	
0.6	0.46	0.41	0.44	
98.17	97.93	97.27	98.51	
44	45	46	47	
*AMP	*AMP	*AMP	*AMP	
95MYAA	95MYAA	95MYAA	95MYAA	
254-1	254-1	254-1	254-1	
A1 INTERIOF	A1 AT MARG	A5 HORNBLI	A5 BRIGHT DOMAIN	
7.562	7.644	7.588	7.541	
0.354	0.356	0.344	0.436	
7.916	8	7.932	7.977	
0	0.008	0	0	
0.051	0.048	0.041	0.042	
0.005	0	0	0	
1.479	1.591	1.605	1.636	
3.462	3.298	3.351	3.287	
0.027	0.016	0.027	0.029	
5.024	4.961	5.024	4.994	
1.426	1.457	1.643	1.588	
0.852	0.738	0.591	0.645	
0.185	0.182	0.164	0.16	
2.463	2.377	2.398	2.393	
0.645	0.488	0.447	0.474	
0.005	0.007	0	0	
0.65	0.495	0.447	0.474	
23.23	25.07	24.32	25.12	
22.39	22.96	24.9	24.39	
54.38	51.97	50.78	50.48	
0.435	0.487	0.487	0.507	
0.303	0.328	0.327	0.336	

Appendix 2. Electron microprobe analyses of hornblende from the SLIC.

	1	2	3	4	5
SECTION	190-1 A1 BIOTITE	190-1 A1	190-1 A1	190-1 A4	190-1 A5
	CENTRAL	AT END	ANOTHER	PHLOGOPITE INCLUSION IN	PHLOGOPITE IN CONTACT WI
Rock Type	Syenite	Syenite	Syenite	Syenite	Syenite
SiO2	39.69	41.37	40	39.9	41.37
TiO2	1.36	0.84	0.97	1.6	0.72
Al2O3	10.97	10.88	10.99	11.27	11.26
Cr2O3	0	0	0	0	0
FeO	15.08	14	14.37	15.96	12.69
MgO	16.64	18.45	17.24	15.57	18.8
MnO	0.19	0.21	0.16	0.17	0.16
CaO	0.01	0	0	0.06	0.1
BaO	0.23	0.21	0.25	0.27	0.16
K2O	9.77	9.74	9.63	9.44	9.52
Na2O	0.04	0.06	0.06	0.07	0.12
F	2.86	2.38	2.65	2.01	2.97
Cl	0.03	0.02	0.02	0.01	0.03
TOTAL	96.87	98.16	96.34	96.33	97.9
(=-O=F+Cl)	1.21	1.01	1.12	0.85	1.26
SUM	95.66	97.15	95.22	95.48	96.64
			Formula based on 22 oxygen		
Si	5.848	5.958	5.896	5.92	5.926
Al	1.905	1.846	1.909	1.97	1.901
Total	7.753	7.804	7.805	7.89	7.827
Al	0	0	0	0	0
Ti	0.151	0.091	0.108	0.179	0.078
Cr	0	0	0	0	0
Fe	1.858	1.686	1.771	1.98	1.52
Mg	3.654	3.96	3.788	3.443	4.014
Mn	0.024	0.026	0.02	0.021	0.019
Total	5.687	5.763	5.687	5.623	5.631
Ba	0.013	0.012	0.014	0.016	0.009
Ca	0.002	0	0	0.01	0.015
Na	0.011	0.017	0.017	0.02	0.033
K	1.836	1.789	1.811	1.786	1.739
Total	1.862	1.818	1.842	1.832	1.796
F	1.333	1.084	1.235	0.943	1.345
Cl	0.007	0.005	0.005	0.003	0.007
Total	1.34	1.089	1.24	0.946	1.352
Fe	33.71	29.86	31.86	36.51	27.47
Mg	66.29	70.14	68.14	63.49	72.53
Fe/Mg	0.515	0.432	0.473	0.581	0.384
Fe/Fe+Mg	0.34	0.302	0.321	0.368	0.277

Appendix 3. Electron microprobe analyses of mica from the SLIC.

6	7	8	9	10
190-1 A5	190-1 A5	190-1 A5	190-1 A6	190-1 A6
INTERIOR "	CENTRAL ZONE IN PHOTO "	CENTRAL ZONE IN PHOTO "	PHLOGOPITE, CENTRAL "	PHLOGOPITE, CENTRAL "
Syenite	Syenite	Syenite	Syenite	Syenite
40.98	41.25	40.46	41.12	40.72
0.73	0.78	0.67	0.7	0.72
11.2	11.55	11.24	11.52	11.46
0.03	0	0	0.01	0.03
12.71	12.8	12.76	11.88	12.68
18.67	19.16	18.48	18.88	18.76
0.06	0.07	0.12	0.13	0.06
0.03	0.05	0.08	0.06	0.1
0.17	0.15	0.21	0.15	0.1
9.5	9.75	9.39	9.47	9.53
0.07	0.08	0.18	0.06	0.11
3.27	2.82	3.01	2.88	2.59
0.01	0	0.01	0.01	0.01
97.43	98.46	96.61	96.87	96.87
1.38	1.19	1.27	1.21	1.09
96.05	97.27	95.34	95.66	95.78
5.9	5.882	5.886	5.926	5.898
1.9	1.941	1.927	1.956	1.956
7.8	7.823	7.813	7.882	7.854
0	0	0	0	0
0.079	0.084	0.073	0.076	0.078
0.003	0	0	0.001	0.003
1.53	1.526	1.552	1.432	1.536
4.006	4.072	4.007	4.056	4.05
0.007	0.008	0.015	0.016	0.007
5.625	5.69	5.647	5.581	5.674
0.01	0.008	0.012	0.008	0.006
0.005	0.008	0.012	0.009	0.016
0.02	0.022	0.051	0.017	0.031
1.744	1.773	1.742	1.741	1.761
1.779	1.811	1.817	1.775	1.814
1.489	1.272	1.385	1.313	1.187
0.002	0	0.002	0.002	0.002
1.491	1.272	1.387	1.315	1.189
27.64	27.26	27.92	26.09	27.5
72.36	72.74	72.08	73.91	72.5
0.384	0.377	0.391	0.357	0.381
0.277	0.274	0.281	0.263	0.276

Appendix 3. Electron microprobe analyses of mica from the SLIC.

11	12	13	14	15
190-1 A6	199-2 A2 FINE GRAINED BIOTITE "	199-2 A2 FINE GRAINED BIOTITE "	199-2 A2 FINE GRAINED BIOTITE "	206-1 A3 FINE GRAINED PHLOGOPITE,"
PHLOGOPITE WITH AMPHIBOL"				
Syenite	Syenite	Syenite	Syenite	Syenite
40.62	38.41	40.11	37.52	38.72
0.74	1.78	1.56	1.79	1.87
11.73	12.09	11.51	11.88	11.29
0	0.06	0.03	0	0.16
13.44	15.14	15.04	15.38	16.41
18.61	15.9	16.86	15.85	15.47
0.06	0.11	0.08	0.08	0.05
0	0.07	0.06	0.07	0.01
0.16	1.19	0.65	1.16	0.27
9.48	9.08	9.56	9.05	9.34
0.06	0.04	0.07	0.06	0.03
2.65	1.56	1.76	1.5	1.87
0.02	0.06	0.03	0.04	0
97.57	95.49	97.32	94.38	95.49
1.12	0.67	0.75	0.64	0.79
96.45	94.82	96.57	93.74	94.7
5.86	5.776	5.882	5.73	5.823
1.994	2.142	1.989	2.138	2.001
7.854	7.918	7.871	7.868	7.824
0	0	0	0	0
0.08	0.201	0.172	0.206	0.211
0	0.007	0.003	0	0.019
1.621	1.904	1.844	1.964	2.064
4.002	3.564	3.685	3.608	3.468
0.007	0.014	0.01	0.01	0.006
5.71	5.69	5.714	5.788	5.768
0.009	0.07	0.037	0.069	0.016
0	0.011	0.009	0.011	0.002
0.017	0.012	0.02	0.018	0.009
1.744	1.742	1.788	1.763	1.792
1.77	1.835	1.854	1.861	1.819
1.209	0.742	0.816	0.724	0.889
0.005	0.015	0.007	0.01	0
1.214	0.757	0.823	0.734	0.889
28.84	34.82	33.36	35.25	37.31
71.16	65.18	66.64	64.75	62.69
0.407	0.538	0.503	0.547	0.597
0.289	0.35	0.335	0.354	0.374

Appendix 3. Electron microprobe analyses of mica from the SLIC.

16	17	18	19	20
206-1 A3 AT MARGIN "	206-1 A3 PHLOGOPITE LATH	206-1 A3 ANOTHER	206-1 A4 PHLOGOPITE, CENTRAL "	206-1 A4 ANOTHER, CENTRAL "
Syenite	Syenite	Syenite	Syenite	Syenite
39.3	39.49	38.94	38.38	38.19
1.46	1.89	1.8	2.06	1.93
10.89	11.24	11.21	11.69	11.35
0.16	0.01	0	0.08	0.07
16.75	16.67	17.14	16.38	16.02
15.92	15.45	15.54	15.45	15.68
0.08	0.07	0.15	0.03	0.08
0	0.01	0.04	0	0
0.19	0.2	0.24	0.63	0.53
9.57	9.56	9.35	9.41	9.33
0.07	0.05	0.02	0.09	0.11
1.96	2.02	1.75	1.92	2.01
0.01	0	0.02	0.02	0.04
96.36	96.66	96.2	96.14	95.34
0.83	0.85	0.74	0.81	0.86
95.53	95.81	95.46	95.33	94.48
5.866	5.863	5.83	5.753	5.764
1.915	1.967	1.978	2.065	2.019
7.781	7.83	7.808	7.818	7.783
0	0	0	0	0
0.164	0.211	0.203	0.232	0.219
0.019	0.001	0	0.009	0.008
2.091	2.07	2.146	2.053	2.022
3.542	3.419	3.468	3.452	3.528
0.01	0.009	0.019	0.004	0.01
5.826	5.71	5.836	5.75	5.787
0.011	0.012	0.014	0.037	0.031
0	0.002	0.006	0	0
0.02	0.014	0.006	0.026	0.032
1.822	1.81	1.786	1.799	1.796
1.853	1.838	1.812	1.862	1.859
0.925	0.949	0.829	0.91	0.96
0.003	0	0.005	0.005	0.01
0.928	0.949	0.834	0.915	0.97
37.12	37.71	38.23	37.3	36.44
62.88	62.29	61.77	62.7	63.56
0.593	0.608	0.624	0.596	0.576
0.372	0.378	0.384	0.373	0.366

Appendix 3. Electron microprobe analyses of mica from the SLIC.

21	22	23	24	25
206-1 A4 INTERIOR "	206-1 A4 AT MARGIN "	206-1 A4 PHLOGOPITE INCLUSION IN "	206-1 A4 ANOTHER PHLOGOPITE INCLU"	206-1 A4 PHLOGOPITE "
Syenite	Syenite	Syenite	Syenite	Syenite
38.26	38.62	38.95	38.43	39.87
2.38	2.13	1.77	1.93	2.33
11.54	11.2	11.02	11.01	10.76
0.17	0.02	0.02	0	0
16.53	16.58	16.74	16.42	16.49
15.16	15.54	15.64	15.44	15.47
0.08	0.08	0.06	0.06	0.14
0	0.01	0.01	0.02	0
0.94	0.62	0.34	0.53	0.19
9.17	9.27	9.49	9.23	9.58
0.06	0.04	0.07	0.07	0.09
1.94	1.75	1.91	1.83	1.96
0.02	0.03	0.03	0.02	0
96.25	95.89	96.05	94.99	96.88
0.82	0.74	0.81	0.78	0.83
95.43	95.15	95.24	94.21	96.05
5.743	5.805	5.839	5.826	5.902
2.041	1.984	1.947	1.967	1.877
7.784	7.789	7.786	7.793	7.779
0	0	0	0	0
0.269	0.241	0.2	0.22	0.259
0.02	0.002	0.002	0	0
2.075	2.084	2.099	2.082	2.041
3.392	3.481	3.495	3.489	3.413
0.01	0.01	0.008	0.008	0.018
5.766	5.818	5.804	5.799	5.731
0.055	0.037	0.02	0.031	0.011
0	0.002	0.002	0.003	0
0.017	0.012	0.02	0.021	0.026
1.756	1.777	1.815	1.785	1.809
1.828	1.828	1.857	1.84	1.846
0.921	0.832	0.906	0.877	0.918
0.005	0.008	0.008	0.005	0
0.926	0.84	0.914	0.882	0.918
37.96	37.45	37.52	37.37	37.42
62.04	62.55	62.48	62.63	62.58
0.615	0.602	0.603	0.599	0.603
0.381	0.376	0.376	0.375	0.376

Appendix 3. Electron microprobe analyses of mica from the SLIC.

26	27	28	29	30
206-1 A4 PHLOGOPITE "	208-1 A1 MICA, CENTRAL "	208-1 A1 INTERIOR "	208-1 A1 AT MARGIN "	208-1 A2 PHLOGOPITE, CENTRAL "
Syenite	Syenite	Syenite	Syenite	Syenite
40	38.96	39.63	40.06	39.58
1.82	2.03	1.74	1.33	1.85
11.13	11.18	11.51	11.2	11.31
0	0.06	0.05	0.07	0.05
17.12	17.2	16.17	15.95	16.05
15.99	15.76	16.31	16.77	16.05
0.15	0.14	0.08	0.04	0.08
0	0	0.01	0.08	0
0.11	0.34	0.17	0.12	0.31
9.24	9.42	9.44	9.24	9.59
0.06	0.06	0.06	0.07	0.05
1.9	1.67	1.69	1.81	1.75
0.02	0.02	0	0.01	0.01
97.54	96.84	96.86	96.75	96.68
0.8	0.71	0.71	0.76	0.74
96.74	96.13	96.15	95.99	95.94
5.878	5.804	5.851	5.901	5.865
1.927	1.963	2.002	1.944	1.975
7.805	7.767	7.853	7.845	7.84
0	0	0	0	0
0.201	0.227	0.193	0.147	0.206
0	0.007	0.006	0.008	0.006
2.104	2.143	1.996	1.965	1.989
3.502	3.5	3.589	3.682	3.545
0.019	0.018	0.01	0.005	0.01
5.826	5.895	5.794	5.807	5.756
0.006	0.02	0.01	0.007	0.018
0	0	0.002	0.013	0
0.017	0.017	0.017	0.02	0.014
1.732	1.79	1.778	1.736	1.812
1.755	1.827	1.807	1.776	1.844
0.883	0.787	0.789	0.843	0.82
0.005	0.005	0	0.002	0.003
0.888	0.792	0.789	0.845	0.823
37.53	37.98	35.74	34.8	35.94
62.47	62.02	64.26	65.2	64.06
0.606	0.617	0.559	0.535	0.564
0.377	0.382	0.359	0.349	0.361

Appendix 3. Electron microprobe analyses of mica from the SLIC.

31	32	33	34	35
208-1 A2 AT MARGIN "	208-1 A3 PHLOGOPITE CENTRAL "	208-1 A3 AT MARGIN "	208-1 A3 PHLOGOPITE INCLUSION IN "	208-1 A3 SECOND INCLUSION IN CPX "
Syenite	Syenite	Syenite	Syenite	Syenite
39.59	39.32	39.86	39.03	38.99
1.27	2.29	1.8	0.88	1.26
11.38	11.71	11.41	11.64	11.84
0.02	0.06	0.07	0.03	0.02
15.15	16.62	15.94	14.7	15.37
16.94	15.52	16.26	17.8	17.1
0.09	0.13	0.06	0.09	0.04
0	0	0	0.04	0.11
0.19	0.76	0.3	0.24	0.22
9.48	9.12	9.28	9.73	9.48
0.05	0.07	0.05	0.01	0.06
1.81	1.65	1.72	1.8	1.78
0	0	0.02	0	0.01
95.97	97.25	96.77	95.99	96.28
0.76	0.69	0.73	0.76	0.75
95.21	96.56	96.04	95.23	95.53
5.874	5.814	5.88	5.798	5.782
1.99	2.04	1.984	2.037	2.069
7.864	7.854	7.864	7.835	7.851
0	0	0	0	0
0.142	0.255	0.2	0.098	0.141
0.002	0.007	0.008	0.004	0.002
1.88	2.055	1.967	1.826	1.906
3.747	3.42	3.575	3.941	3.78
0.011	0.016	0.007	0.011	0.005
5.782	5.753	5.757	5.88	5.834
0.011	0.044	0.017	0.014	0.013
0	0	0	0.006	0.017
0.014	0.02	0.014	0.003	0.017
1.794	1.72	1.746	1.843	1.793
1.819	1.784	1.777	1.866	1.84
0.849	0.772	0.802	0.846	0.835
0	0	0.005	0	0.003
0.849	0.772	0.807	0.846	0.838
33.41	37.53	35.49	31.66	33.52
66.59	62.47	64.51	68.34	66.48
0.505	0.606	0.552	0.466	0.506
0.335	0.377	0.356	0.318	0.336

Appendix 3. Electron microprobe analyses of mica from the SLIC.

42	43	44	45	46
211-3 A1 MICA INCL IN AMPHIBOLE, "	211-3 A1 AT MARGIN "	215-1 A1 BIOTITE, CENTRAL "	215-1 A1 BIOTITE, CENTRAL "	215-1 A1 BIOTITE, CENTRAL "
Syenite	Syenite	Syenite	Syenite	Syenite
40.86	40.97	39.56	39.29	40.34
0.77	0.87	1.9	1.92	1.93
10.65	10.62	12.22	12.34	12.01
0	0	0	0	0
13.34	13.01	15.85	15.66	16.34
18.3	18.57	14.58	14.69	15.13
0.2	0.22	0.48	0.52	0.48
0	0	0	0.01	0
0.1	0.15	0.12	0.19	0.11
9.64	9.51	9.34	9.42	9.66
0.16	0.08	0.06	0.05	0.09
3.78	3.4	3.07	3.12	2.91
0.01	0	0.03	0.04	0.05
97.81	97.4	97.21	97.25	99.05
1.59	1.43	1.3	1.32	1.24
96.22	95.97	95.91	95.93	97.81
5.889	5.916	5.805	5.769	5.824
1.809	1.807	2.113	2.135	2.043
7.698	7.723	7.918	7.904	7.867
0	0	0	0	0
0.083	0.094	0.21	0.212	0.21
0	0	0	0	0
1.608	1.571	1.945	1.923	1.973
3.931	3.997	3.189	3.215	3.256
0.024	0.027	0.06	0.065	0.059
5.646	5.689	5.404	5.415	5.498
0.006	0.008	0.007	0.011	0.006
0	0	0	0.002	0
0.045	0.022	0.017	0.014	0.025
1.772	1.752	1.748	1.764	1.779
1.823	1.782	1.772	1.791	1.81
1.723	1.553	1.425	1.449	1.329
0.002	0	0.007	0.01	0.012
1.725	1.553	1.432	1.459	1.341
29.03	28.22	37.89	37.43	37.73
70.97	71.78	62.11	62.57	62.27
0.415	0.4	0.629	0.618	0.624
0.293	0.286	0.386	0.382	0.384

Appendix 3. Electron microprobe analyses of mica from the SLIC.

47	48	49	50	51
215-1 A2 WITH ALBITE AND KSPAR "	215-1 A2 INTERIOR "	215-1 A2 AT END "	215-1 A2 SECOND GRAIN "	215-1 A5 MICA, CENTRAL "
Syenite	Syenite	Syenite	Syenite	Syenite
39.76	40.26	39.49	40.49	39.36
1.88	1.72	1.57	1.51	1.9
12.5	12.27	13.22	12.68	12.36
0	0	0	0	0
15.09	14.08	14.25	15.01	15.77
15.36	15.85	15.34	15.87	14.86
0.45	0.43	0.4	0.34	0.47
0	0	0	0	0
0.05	0.03	0.18	0.05	0.24
9.77	10.07	9.44	9.88	9.78
0.08	0.09	0.08	0.07	0.07
3.12	3.04	2.88	3.15	2.76
0.05	0.06	0.03	0.04	0.05
98.11	97.9	96.88	99.09	97.62
1.33	1.29	1.22	1.34	1.17
96.78	96.61	95.66	97.75	96.45
5.768	5.829	5.769	5.8	5.774
2.137	2.093	2.231	2.14	2.136
7.905	7.922	8	7.94	7.91
0	0	0.045	0	0
0.205	0.187	0.172	0.163	0.21
0	0	0	0	0
1.831	1.705	1.741	1.798	1.935
3.321	3.42	3.34	3.389	3.249
0.055	0.053	0.049	0.041	0.058
5.412	5.365	5.347	5.391	5.452
0.003	0.002	0.01	0.003	0.014
0	0	0	0	0
0.023	0.025	0.023	0.019	0.02
1.808	1.86	1.759	1.805	1.83
1.834	1.887	1.792	1.827	1.864
1.431	1.392	1.331	1.427	1.28
0.012	0.015	0.007	0.01	0.012
1.443	1.407	1.338	1.437	1.292
35.53	33.26	34.26	34.67	37.32
64.47	66.74	65.74	65.33	62.68
0.568	0.514	0.536	0.543	0.613
0.362	0.339	0.349	0.352	0.38

Appendix 3. Electron microprobe analyses of mica from the SLIC.

52	55	56	57	58
215-1 A5 AT MARGIN "	227-9 A1 BIOTITE-PHLOGOPITE "	227-9 A1 BIOTITE-PHLOGOPITE "	227-9 A1 SMALL BIOTITE IN PHOTO "	227-9 A2 MICA IN CONTACT WITH CPX"
Syenite	Syenite	Syenite	Syenite	Syenite
40.25	37.92	37.99	38.08	38.33
1.9	1.58	1.82	1.8	1.83
12.57	11.71	12.05	12	11.64
0	0	0	0	0
14.95	17.54	17.26	17.48	18.77
14.9	15.36	15.42	15.36	14.96
0.43	0.2	0.26	0.19	0.29
0	0.04	0	0	0.02
0.12	0.97	0.79	0.34	0.31
9.57	9.49	9.5	9.68	9.57
0.05	0.15	0.07	0.13	0.15
3.2	2.2	2.15	2.15	2.05
0.05	0.04	0.02	0.02	0.03
97.99	97.2	97.33	97.23	97.95
1.36	0.94	0.91	0.91	0.87
96.63	96.26	96.42	96.32	97.08
5.827	5.683	5.666	5.675	5.702
2.144	2.068	2.118	2.107	2.04
7.971	7.751	7.784	7.782	7.742
0	0	0	0	0
0.207	0.178	0.204	0.202	0.205
0	0	0	0	0
1.81	2.198	2.153	2.179	2.335
3.215	3.431	3.428	3.412	3.317
0.053	0.025	0.033	0.024	0.037
5.285	5.832	5.818	5.817	5.894
0.007	0.057	0.046	0.02	0.018
0	0.006	0	0	0.003
0.014	0.044	0.02	0.038	0.043
1.767	1.814	1.807	1.84	1.816
1.788	1.921	1.873	1.898	1.88
1.465	1.043	1.014	1.013	0.964
0.012	0.01	0.005	0.005	0.008
1.477	1.053	1.019	1.018	0.972
36.02	39.05	38.58	38.97	41.31
63.98	60.95	61.42	61.03	58.69
0.579	0.648	0.638	0.646	0.715
0.367	0.393	0.389	0.392	0.417

Appendix 3. Electron microprobe analyses of mica from the SLIC.

59	60	61	62	63
227-9 A2 AT MARGIN "	227-9 A2 SMALL BIOTITE "	227-9 A5 BIOTITE-PHLOGOPITE WITH "	227-9 A5 AT END "	227-9 COARSE PHLOGOPITE, CENTRAL "
Syenite	Syenite	Syenite	Syenite	Syenite
37.76	39.23	38.61	38.25	38.95
1.77	1.72	1.76	1.65	1.46
12.17	11.21	11.75	11.93	11.67
0.04	0	0	0	0.09
18.5	17.02	17.73	17.21	13.32
15.82	15.65	15.43	15.66	17.59
0.2	0.17	0.28	0.32	0.11
0.1	0.02	0	0	0
0.31	0.25	0.76	0.31	0.5
8.46	9.68	9.79	9.75	9.89
0.11	0.12	0.12	0.08	0.15
1.5	2.23	2.33	1.94	2.7
0.02	0.03	0.05	0.03	0
96.76	97.33	98.61	97.13	96.43
0.64	0.95	0.99	0.82	1.14
96.12	96.38	97.62	96.31	95.29
5.648	5.81	5.697	5.701	5.743
2.145	1.956	2.043	2.095	2.028
7.793	7.766	7.74	7.796	7.771
0	0	0	0	0
0.199	0.192	0.195	0.185	0.162
0.005	0	0	0	0.01
2.314	2.108	2.188	2.145	1.642
3.527	3.455	3.394	3.479	3.866
0.025	0.021	0.035	0.04	0.014
6.07	5.776	5.812	5.849	5.694
0.018	0.015	0.044	0.018	0.029
0.016	0.003	0	0	0
0.032	0.034	0.034	0.023	0.043
1.614	1.829	1.843	1.854	1.86
1.68	1.881	1.921	1.895	1.932
0.71	1.045	1.087	0.915	1.259
0.005	0.008	0.013	0.008	0
0.715	1.053	1.1	0.923	1.259
39.62	37.9	39.2	38.14	29.82
60.38	62.1	60.8	61.86	70.18
0.663	0.616	0.655	0.628	0.428
0.399	0.381	0.396	0.386	0.3

Appendix 3. Electron microprobe analyses of mica from the SLIC.

64	65	66	67	68
227-9 COARSE PHLOGOPITE, CENTRAL "	227-9 PHLOGOPITE LATH, CENTRAL "	227-9 AT MARGIN "	227-9 SMALL SUBGRAIN "	228-2 A1 SMALL PHLOGOPITE INCLUSI"
Syenite	Syenite	Syenite	Syenite	Syenite
40.17	39.93	40.05	40.82	39.13
1.23	1.28	1.19	1.06	0.83
11.31	11.29	11.53	11.14	12.51
0.14	0	0.03	0.01	0.32
12.92	13.11	13.21	12.44	13.27
18.58	18.39	18.5	19.26	18.3
0.15	0.16	0.12	0.06	0.11
0	0.01	0.01	0.01	0.09
0.19	0.3	0.22	0.16	0.83
10.13	9.99	10.14	10.07	9.81
0.15	0.17	0.12	0.14	0.04
2.94	3.01	2.88	3	2.03
0.01	0.01	0	0	0
97.92	97.65	98	98.17	97.27
1.24	1.27	1.21	1.26	0.85
96.68	96.38	96.79	96.91	96.42
5.802	5.791	5.786	5.851	5.724
1.925	1.929	1.963	1.882	2.156
7.727	7.72	7.749	7.733	7.88
0	0	0	0	0
0.134	0.14	0.129	0.114	0.091
0.016	0	0.003	0.001	0.037
1.561	1.59	1.596	1.491	1.623
4	3.975	3.984	4.115	3.99
0.018	0.02	0.015	0.007	0.014
5.729	5.725	5.727	5.728	5.755
0.011	0.017	0.012	0.009	0.048
0	0.002	0.002	0.002	0.014
0.042	0.048	0.034	0.039	0.011
1.866	1.848	1.869	1.841	1.83
1.919	1.915	1.917	1.891	1.903
1.343	1.381	1.316	1.36	0.939
0.002	0.002	0	0	0
1.345	1.383	1.316	1.36	0.939
28.07	28.57	28.6	26.6	28.92
71.93	71.43	71.4	73.4	71.08
0.395	0.405	0.404	0.364	0.41
0.283	0.288	0.288	0.267	0.291

Appendix 3. Electron microprobe analyses of mica from the SLIC.

69	70	71	72
228-2 A1 SMALL PHLOGOPITE INCLUSI"	228-2 A1 PHLOGOPITE INCLUSION AT "	228-2 A1 PHLOGOPITE IN ADJACENT G"	228-2 A2 PHLOGOPITE CENTRAL "
Syenite	Syenite	Syenite	Syenite
39.22	37.27	38.17	37.51
1.49	2.14	1.97	2.09
13	11.93	11.98	11.84
0.01	0	0	0
11.89	17.52	17.68	17.2
18.16	14.38	15	14.93
0.07	0.19	0.2	0.24
0.02	0.02	0	0.01
0.4	1.01	0.47	0.72
9.83	9.53	9.66	9.66
0.14	0.07	0.08	0.09
2.18	1.57	1.76	1.74
0	0.03	0.02	0.02
96.41	95.66	96.99	96.05
0.92	0.67	0.75	0.74
95.49	94.99	96.24	95.31
5.722	5.687	5.712	5.681
2.235	2.145	2.112	2.113
7.957	7.832	7.824	7.794
0	0	0	0
0.163	0.246	0.222	0.238
0.001	0	0	0
1.451	2.236	2.212	2.179
3.949	3.271	3.345	3.37
0.009	0.025	0.025	0.031
5.573	5.778	5.804	5.818
0.023	0.06	0.028	0.043
0.003	0.003	0	0.002
0.04	0.021	0.023	0.026
1.829	1.855	1.844	1.866
1.895	1.939	1.895	1.937
1.006	0.758	0.833	0.833
0	0.008	0.005	0.005
1.006	0.766	0.838	0.838
26.87	40.6	39.81	39.26
73.13	59.4	60.19	60.74
0.37	0.691	0.669	0.656
0.27	0.409	0.401	0.396

Appendix 3. Electron microprobe analyses of mica from the SLIC.

73	74	75	76	77
228-2 A2 SMALLER GRAIN "	228-2 A2 CENTRAL "	228-2 A3 PHLOGOPITE 1, CENTRAL "	228-2 A3 PHLOGOPITE 1, CENTRAL "	228-2 A3 HIGH Ba ZONE NEAR END "
Syenite	Syenite	Syenite	Syenite	Syenite
38.54	38.3	38.28	39.13	37.96
1.95	1.97	1.74	1.63	1.81
11.8	11.64	11.64	11.87	12.05
0.02	0	0.07	0.06	0.06
16.47	17.06	16.01	16.01	16.32
15.46	15.6	15.94	16.24	15.67
0.23	0.09	0.15	0.19	0.11
0	0	0.03	0	0.03
0.56	0.42	0.38	0.37	0.83
9.92	9.62	9.89	9.73	9.35
0.06	0.09	0.11	0.11	0.07
1.93	1.82	1.97	2.03	1.9
0.03	0.01	0.01	0.01	0.02
96.97	96.62	96.22	97.38	96.18
0.82	0.77	0.83	0.86	0.8
96.15	95.85	95.39	96.52	95.38
5.744	5.731	5.735	5.77	5.699
2.073	2.053	2.055	2.062	2.132
7.817	7.784	7.79	7.832	7.831
0	0	0	0	0
0.219	0.222	0.196	0.181	0.204
0.002	0	0.008	0.007	0.007
2.053	2.135	2.006	1.974	2.049
3.435	3.479	3.56	3.569	3.507
0.029	0.011	0.019	0.024	0.014
5.738	5.847	5.789	5.755	5.781
0.033	0.025	0.022	0.021	0.049
0	0	0.005	0	0.005
0.017	0.026	0.032	0.031	0.02
1.886	1.836	1.89	1.83	1.791
1.936	1.887	1.949	1.882	1.865
0.91	0.861	0.933	0.947	0.902
0.008	0.003	0.003	0.002	0.005
0.918	0.864	0.936	0.949	0.907
37.41	38.03	36.04	35.61	36.88
62.59	61.97	63.96	64.39	63.12
0.606	0.617	0.569	0.56	0.588
0.377	0.382	0.363	0.359	0.37

Appendix 3. Electron microprobe analyses of mica from the SLIC.

78	79	80	81	82
228-2 A3 ANOTHER LATH "	228-2 A3 HIGH-Ba DOMAIN "	228-2 A4 PHLOGOPITE, CENTRAL "	228-2 A4 AT MARGIN "	228-2 A4 SECOND PHLOGOPITE, CENTR"
Syenite	Syenite	Syenite	Syenite	Syenite
38.89	38.11	40.43	39.07	40.52
1.59	1.89	1.26	1.43	1.28
11.46	12.12	11.08	11.41	10.96
0.04	0.1	0.08	0.31	0.09
16.17	16.73	12.2	13.43	12.71
16.17	15.39	18.81	17.74	18.38
0.14	0.18	0.04	0.12	0.13
0.01	0.01	0	0	0
0.4	1.41	0.13	0.21	0.14
9.93	9.37	10.01	9.69	9.72
0.06	0.07	0.14	0.11	0.07
1.9	1.81	2.68	2.2	2.4
0.01	0	0.01	0.03	0.02
96.77	97.19	96.87	95.75	96.42
0.8	0.76	1.13	0.93	1.02
95.97	96.43	95.74	94.82	95.4
5.789	5.697	5.87	5.789	5.914
2.01	2.135	1.896	1.992	1.885
7.799	7.832	7.766	7.781	7.799
0	0	0	0	0
0.178	0.212	0.138	0.159	0.14
0.005	0.012	0.009	0.036	0.01
2.013	2.092	1.481	1.664	1.551
3.587	3.429	4.07	3.918	3.999
0.018	0.023	0.005	0.015	0.016
5.801	5.768	5.703	5.792	5.716
0.023	0.083	0.007	0.012	0.008
0.002	0.002	0	0	0
0.017	0.02	0.039	0.032	0.02
1.885	1.787	1.854	1.831	1.81
1.927	1.892	1.9	1.875	1.838
0.894	0.856	1.231	1.031	1.108
0.003	0	0.002	0.008	0.005
0.897	0.856	1.233	1.039	1.113
35.94	37.89	26.68	29.81	27.95
64.06	62.11	73.32	70.19	72.05
0.566	0.617	0.365	0.429	0.392
0.361	0.381	0.267	0.3	0.282

Appendix 3. Electron microprobe analyses of mica from the SLIC.

83	84	85	86	87
228-2 A4 AT MARGIN "	245-2 A6 INTERSTITIAL MICA "	245-2 A6 ANOTHER GRAIN "	245-2 A6 IN CONTACT WITH FLUORITE"	249-3 A1 GREEN BIOTITE, CENTRAL "
Syenite	Syenite	Syenite	Syenite	Syenite
40.07	40.33	39.13	41.07	37
1.37	0.86	1.03	0.75	2
11.15	11.65	11.5	11.48	12.23
0.15	0	0	0	0.06
12.99	14.28	15.26	14.77	17.17
18.67	17.01	16.48	17.22	14.35
0.1	0.43	0.42	0.29	0.07
0.01	0.01	0.01	0.09	0
0.24	0.05	0.05	0.14	0.7
9.9	9.64	9.63	9.77	9.5
0.09	0.06	0.08	0.06	0.06
2.45	3.21	2.88	2.94	1.56
0.01	0.03	0.04	0.01	0.05
97.2	97.56	96.51	98.59	94.75
1.03	1.36	1.22	1.24	0.67
96.17	96.2	95.29	97.35	94.08
5.828	5.854	5.791	5.908	5.676
1.911	1.993	2.005	1.946	2.211
7.739	7.847	7.796	7.854	7.887
0	0	0	0	0
0.15	0.094	0.115	0.081	0.231
0.017	0	0	0	0.007
1.58	1.734	1.889	1.777	2.203
4.047	3.68	3.635	3.692	3.281
0.012	0.053	0.053	0.035	0.009
5.806	5.561	5.692	5.585	5.731
0.014	0.003	0.003	0.008	0.042
0.002	0.002	0.002	0.014	0
0.025	0.017	0.023	0.017	0.018
1.837	1.785	1.818	1.793	1.859
1.878	1.807	1.846	1.832	1.919
1.127	1.474	1.348	1.338	0.757
0.002	0.007	0.01	0.002	0.013
1.129	1.481	1.358	1.34	0.77
28.08	32.02	34.19	32.49	40.17
71.92	67.98	65.81	67.51	59.83
0.393	0.485	0.534	0.491	0.674
0.282	0.327	0.348	0.329	0.403

Appendix 3. Electron microprobe analyses of mica from the SLIC.

88	89	90	91	92
249-3 A1 INTERIOR BRIGHT ZONE "	249-3 A1 OUTER MARGIN "	249-3 A2 BIOTITE "	249-3 A3 SMALL BIOTITE "	249-3 A3 LARGE GRAIN, CENTRAL "
Syenite	Syenite	Syenite	Syenite	Syenite
36.9	38.1	38.41	38.33	36.71
2.03	1.4	1.92	2.56	2.61
12.81	12.74	12.11	12.13	12.94
0.1	0	0.01	0.08	0.01
17.23	17.76	17.75	16.85	17.52
14.54	15.23	14.62	14.17	13.85
0.1	0.13	0.1	0.19	0.17
0	0	0	0	0.01
1.55	0.19	0.65	0.59	1.88
9.27	9.63	9.86	9.85	9.13
0.06	0.03	0.06	0.05	0.16
1.51	1.53	1.67	1.51	1.44
0.03	0.03	0.04	0.03	0.03
96.13	96.77	97.2	96.34	96.46
0.64	0.65	0.71	0.64	0.61
95.49	96.12	96.49	95.7	95.85
5.607	5.695	5.743	5.76	5.581
2.294	2.244	2.134	2.148	2.318
7.901	7.939	7.877	7.908	7.899
0	0	0	0	0
0.232	0.157	0.216	0.289	0.298
0.012	0	0.001	0.01	0.001
2.19	2.22	2.22	2.117	2.228
3.293	3.393	3.258	3.174	3.138
0.013	0.016	0.013	0.024	0.022
5.74	5.786	5.708	5.614	5.687
0.092	0.011	0.038	0.035	0.112
0	0	0	0	0.002
0.018	0.009	0.017	0.015	0.047
1.797	1.836	1.88	1.888	1.77
1.907	1.856	1.935	1.938	1.931
0.726	0.723	0.79	0.718	0.692
0.008	0.008	0.01	0.008	0.008
0.734	0.731	0.8	0.726	0.7
39.94	39.55	40.52	40.02	41.51
60.06	60.45	59.48	59.98	58.49
0.669	0.659	0.685	0.675	0.717
0.401	0.397	0.407	0.403	0.417

Appendix 3. Electron microprobe analyses of mica from the SLIC.

93	94	95	96	106
249-3 A3 AT MARGIN "	249-3 A3 AT MARGIN "	249-3 A4 GREEN BIOTITE, BRIGHT DO"	249-3 A4 MAIN HOST TO HI-Ba ZONE "	254-1 A2 PHLOGOPITE INCL FLUORITE"
Syenite	Syenite	Syenite	Syenite	Syenite
37.48	37.84	36.85	37.64	38.56
2.1	2	2.38	2.25	2.19
12.02	12.1	12.24	12.22	11.74
0	0.02	0.13	0.03	0
17.26	17.91	17.32	17.54	15.91
14.11	14.4	13.95	14.43	15.73
0.09	0.11	0.12	0.11	0.28
0	0	0	0	0
0.25	0.28	1.04	0.26	0.71
9.65	9.85	9.56	9.95	10.06
0.18	0.03	0.03	0.03	0.04
1.37	1.29	1.64	1.45	2.05
0.03	0.02	0.04	0.03	0.03
94.54	95.85	95.3	95.94	97.3
0.58	0.55	0.7	0.62	0.87
93.96	95.3	94.6	95.32	96.43
5.745	5.736	5.645	5.696	5.726
2.171	2.161	2.209	2.179	2.054
7.916	7.897	7.854	7.875	7.78
0	0	0	0	0
0.242	0.228	0.274	0.256	0.245
0	0.002	0.016	0.004	0
2.212	2.271	2.219	2.22	1.976
3.223	3.254	3.185	3.255	3.481
0.012	0.014	0.016	0.014	0.035
5.689	5.769	5.71	5.749	5.737
0.015	0.017	0.062	0.015	0.041
0	0	0	0	0
0.053	0.009	0.009	0.009	0.012
1.887	1.905	1.868	1.921	1.905
1.955	1.931	1.939	1.945	1.958
0.664	0.618	0.795	0.694	0.963
0.008	0.005	0.01	0.008	0.008
0.672	0.623	0.805	0.702	0.971
40.7	41.1	41.06	40.55	36.2
59.3	58.9	58.94	59.45	63.8
0.69	0.702	0.702	0.686	0.578
0.408	0.413	0.412	0.407	0.366

Appendix 3. Electron microprobe analyses of mica from the SLIC.

107	108	109	110	111
254-1 A2 PHLOGOPITE INCL FLUORITE"	254-1 A2 DARK DOMAIN "	254-1 A2 COARSE MICA, CENTRAL "	254-1 A2 OUTER MARGIN, CENTRAL HI"	254-1 A4 PHLOGOPITE, CENTRAL "
Syenite	Syenite	Syenite	Syenite	Syenite
38.69	39.76	37.56	38.17	38.09
1.73	1.67	3.08	2.95	1.71
11.52	11.69	12.08	11.93	11.66
0	0.03	0	0.12	0.01
16.43	15.49	17.98	17.46	16.71
15.95	16.55	13.8	14.25	15.94
0.12	0.19	0.23	0.23	0.23
0.06	0	0	0	0
0.69	0.29	1.22	0.85	0.38
9.95	10.04	9.66	9.86	9.94
0.05	0.04	0.06	0.03	0.04
1.88	1.99	1.68	1.59	2.09
0.02	0.02	0.03	0.04	0.02
97.09	97.76	97.38	97.48	96.82
0.8	0.84	0.71	0.68	0.88
96.29	96.92	96.67	96.8	95.94
5.763	5.822	5.648	5.703	5.694
2.022	2.017	2.141	2.1	2.054
7.785	7.839	7.789	7.803	7.748
0	0	0	0	0
0.194	0.184	0.348	0.331	0.192
0	0.003	0	0.014	0.001
2.047	1.897	2.261	2.182	2.089
3.541	3.612	3.093	3.173	3.552
0.015	0.024	0.029	0.029	0.029
5.797	5.72	5.731	5.729	5.863
0.04	0.017	0.072	0.05	0.022
0.01	0	0	0	0
0.014	0.011	0.017	0.009	0.012
1.89	1.875	1.853	1.879	1.895
1.954	1.903	1.942	1.938	1.929
0.886	0.922	0.799	0.751	0.988
0.005	0.005	0.008	0.01	0.005
0.891	0.927	0.807	0.761	0.993
36.63	34.43	42.23	40.74	37.03
63.37	65.57	57.77	59.26	62.97
0.582	0.532	0.74	0.697	0.596
0.368	0.347	0.425	0.411	0.374

Appendix 3. Electron microprobe analyses of mica from the SLIC.

112	113	114	115	116
254-1 A4 AT MARGIN "	254-1 A4 SMALL MICAS IN FLUORITE "	254-1 A4 SMALL MICAS IN FLUORITE "	254-1 A5 SMALL MICA "	254-1 A5 AT MARGIN "
Syenite	Syenite	Syenite	Syenite	Syenite
38.19	38.73	38.6	38.89	38.19
2.13	1.67	1.89	2.12	1.85
11.77	11.61	11.39	11.8	11.8
0	0.03	0.01	0.03	0
16.51	15.44	16.1	16.1	16.1
15.19	16.5	15.7	15.5	15.32
0.13	0.08	0.14	0.05	0.04
0	0.02	0.03	0	0
0.81	0.39	0.52	0.7	0.93
9.69	9.8	9.94	9.82	9.68
0.07	0.08	0.07	0.07	0.03
1.87	2.02	1.92	1.9	1.76
0.02	0.03	0.03	0.02	0
96.38	96.4	96.34	97	95.7
0.79	0.86	0.82	0.8	0.74
95.59	95.54	95.52	96.2	94.96
5.735	5.764	5.781	5.777	5.766
2.083	2.036	2.01	2.065	2.099
7.818	7.8	7.791	7.842	7.865
0	0	0	0	0
0.241	0.187	0.213	0.237	0.21
0	0.004	0.001	0.004	0
2.073	1.922	2.017	2	2.033
3.4	3.66	3.505	3.432	3.448
0.017	0.01	0.018	0.006	0.005
5.731	5.783	5.754	5.679	5.696
0.048	0.023	0.031	0.041	0.055
0	0.003	0.005	0	0
0.02	0.023	0.02	0.02	0.009
1.856	1.86	1.899	1.86	1.864
1.924	1.909	1.955	1.921	1.928
0.888	0.951	0.909	0.893	0.84
0.005	0.008	0.008	0.005	0
0.893	0.959	0.917	0.898	0.84
37.88	34.43	36.52	36.82	37.09
62.12	65.57	63.48	63.18	62.91
0.615	0.528	0.58	0.585	0.591
0.381	0.345	0.367	0.369	0.372

Appendix 3. Electron microprobe analyses of mica from the SLIC.

117	118	36	37	38	39
263-1 A3 SMALL LATH	263-1 A3 SMALL LATH "	211-2 A1 COARSE MICA, CENTRAL "	211-2 A1 INTERIOR "	211-2 A1 AT MARGIN "	211-2 A6 "
Granite	Granite	Granite	Granite	Granite	Granite
39.74	39.39	39.85	40.72	40.81	39.67
2.13	1.93	0.91	0.96	0.83	1.14
12.55	12.33	11.05	10.94	11.07	11.62
0	0	0	0	0	0
13.53	13.43	13.22	13.59	12.88	15.05
14.99	15.08	17.04	17.27	17.77	16.16
0.5	0.33	0.32	0.37	0.29	0.39
0	0	0	0	0	0.03
0.03	0.03	0.08	0.09	0.05	0.13
9.44	9.31	9.84	9.78	9.69	9.12
0.2	0.17	0.06	0.05	0.06	0.07
4.02	4.13	3.39	2.83	2.63	2.33
0.02	0.03	0	0	0.02	0.02
97.15	96.16	95.76	96.6	96.1	95.73
1.7	1.75	1.43	1.19	1.11	0.99
95.45	94.41	94.33	95.41	94.99	94.74
5.769	5.772	5.881	5.954	5.97	5.886
2.147	2.129	1.922	1.885	1.908	2.032
7.916	7.901	7.803	7.839	7.878	7.918
0	0	0	0	0	0
0.233	0.213	0.101	0.106	0.091	0.127
0	0	0	0	0	0
1.642	1.646	1.632	1.662	1.576	1.867
3.243	3.293	3.749	3.764	3.875	3.574
0.061	0.041	0.04	0.046	0.036	0.049
5.179	5.193	5.522	5.578	5.578	5.617
0.002	0.002	0.005	0.005	0.003	0.008
0	0	0	0	0	0.005
0.056	0.048	0.017	0.014	0.017	0.02
1.748	1.74	1.852	1.824	1.808	1.726
1.806	1.79	1.874	1.843	1.828	1.759
1.846	1.914	1.582	1.309	1.217	1.093
0.005	0.007	0	0	0.005	0.005
1.851	1.921	1.582	1.309	1.222	1.098
33.62	33.32	30.33	30.63	28.91	34.32
66.38	66.68	69.67	69.37	71.09	65.68
0.525	0.512	0.446	0.454	0.416	0.536
0.344	0.339	0.308	0.312	0.294	0.349

Appendix 3. Electron microprobe analyses of mica from the SLIC.

40	41	53	54	97	98
211-2 A6 "	211-2 A6 BIOTITE "	226-1 A2 BIOTITE, CENTRAL "	226-1 A2 AT MARGIN "	251-1 A1 MINUTE MICA "	251-1 A1 MINUTE MICA "
Granite	Granite	Granite	Granite	Granite	Granite
39.23	39.55	38.8	38.52	38.68	37.88
1.01	1.16	1.43	1.41	1.83	1.85
11.85	11.59	12.14	12.17	13.75	13.92
0	0	0	0	0	0
15.1	15.28	15.23	15.05	14.69	14.34
16.57	16.3	15.62	15.86	13.95	13.35
0.35	0.43	0.36	0.51	0.42	0.43
0	0.02	0.01	0.02	0.02	0.03
0.17	0.14	0.13	0.23	0.32	0.35
8.96	9.24	9.62	9.49	9.55	9.58
0.05	0.06	0.1	0.09	0.14	0.1
2.28	2.39	2.85	2.59	3.08	2.83
0.01	0.03	0.04	0.02	0.04	0.01
95.58	96.19	96.33	95.96	96.47	94.67
0.96	1.01	1.21	1.1	1.31	1.19
94.62	95.18	95.12	94.86	95.16	93.48
5.831	5.855	5.753	5.737	5.706	5.697
2.076	2.022	2.121	2.136	2.294	2.303
7.907	7.877	7.874	7.873	8	8
0	0	0	0	0.096	0.164
0.113	0.129	0.159	0.158	0.203	0.209
0	0	0	0	0	0
1.877	1.892	1.888	1.875	1.812	1.804
3.671	3.597	3.452	3.521	3.067	2.993
0.044	0.054	0.045	0.064	0.052	0.055
5.705	5.672	5.544	5.618	5.23	5.225
0.01	0.008	0.008	0.013	0.018	0.021
0	0.003	0.002	0.003	0.003	0.005
0.014	0.017	0.029	0.026	0.04	0.029
1.699	1.745	1.819	1.803	1.797	1.838
1.723	1.773	1.858	1.845	1.858	1.893
1.072	1.119	1.336	1.22	1.437	1.346
0.003	0.008	0.01	0.005	0.01	0.003
1.075	1.127	1.346	1.225	1.447	1.349
33.83	34.47	35.36	34.74	37.14	37.6
66.17	65.53	64.64	65.26	62.86	62.4
0.523	0.541	0.56	0.551	0.608	0.621
0.344	0.351	0.359	0.355	0.378	0.383

Appendix 3. Electron microprobe analyses of mica from the SLIC.

99	100	101	102	103
A 251-1 A1 MINUTE MICA "	251-1 A3 BIOTITE DARK LAMINAR ZON"	251-1 A3 BRIGHT LINEAR ZONE "	251-1 A3 BROAD DARK DOMAIN "	251-1 A3 WIDE, RELATIVELY BRIGHT "
Granite	Granite	Granite	Granite	Granite
38.93	39.61	39.77	40.05	39.34
1.71	1.14	1.35	1.24	1.34
13.68	11.85	11.86	11.66	11.88
0	0	0	0.02	0
14.6	15.02	15.24	14.47	15.25
13.74	16.01	15.71	16.09	15.62
0.37	0.41	0.45	0.51	0.44
0.02	0	0	0	0
0.32	0.17	0.56	0.24	0.59
9.62	9.27	9.18	9.46	9.25
0.11	0.19	0.16	0.14	0.1
3.09	3.66	3.59	3.81	3.51
0.03	0.04	0.04	0.03	0.04
96.22	97.37	97.91	97.72	97.36
1.31	1.55	1.52	1.61	1.49
94.91	95.82	96.39	96.11	95.87
5.751	5.785	5.793	5.818	5.773
2.249	2.039	2.036	1.996	2.054
8	7.824	7.829	7.814	7.827
0.132	0	0	0	0
0.19	0.125	0.148	0.135	0.148
0	0	0	0.002	0
1.804	1.834	1.857	1.758	1.871
3.025	3.485	3.411	3.484	3.416
0.046	0.051	0.056	0.063	0.055
5.197	5.495	5.472	5.442	5.49
0.019	0.01	0.032	0.014	0.034
0.003	0	0	0	0
0.032	0.054	0.045	0.039	0.028
1.813	1.727	1.706	1.753	1.731
1.867	1.791	1.783	1.806	1.793
1.444	1.69	1.654	1.751	1.629
0.008	0.01	0.01	0.007	0.01
1.452	1.7	1.664	1.758	1.639
37.35	34.49	35.25	33.54	35.39
62.65	65.51	64.75	66.46	64.61
0.611	0.541	0.561	0.523	0.564
0.379	0.351	0.359	0.343	0.361

Appendix 3. Electron microprobe analyses of mica from the SLIC.

104	105
251-1 A6 BIOTITE "	251-1 A6 RELICT MICA DOMAIN "
Granite	Granite
39.16	39.55
1.76	1.48
12.18	12.18
0	0
13.56	13.29
16.13	16.33
0.42	0.42
0	0
0.11	0.04
9.59	9.39
0.1	0.06
3.07	3.01
0.02	0.02
96.1	95.77
1.3	1.27
94.8	94.5
5.768	5.819
2.114	2.112
7.882	7.931
0	0
0.195	0.164
0	0
1.67	1.635
3.541	3.581
0.052	0.052
5.458	5.432
0.006	0.002
0	0
0.029	0.017
1.802	1.762
1.837	1.781
1.43	1.401
0.005	0.005
1.435	1.406
32.05	31.35
67.95	68.65
0.486	0.471
0.327	0.32

Appendix 3. Electron microprobe analyses of mica from the SLIC.

	13	14	15	30	31	32	33	34	35	36	37	38	39	40
	"FEL	"FEL	"FEL	"FEL	"FEL	"FEL	"FEL	"FEL	"FEL	"FEL	"FEL	"FEL	"FEL	"FEL
	95MYAA	95MYAA	95MYAA	95MYAA	95MYAA	95MYAA	95MYAA	95MYAA	95MYAA	95MYAA	95MYAA	95MYAA	95MYAA	95MYAA
	190-1	190-1	190-1	199-2	199-2	199-2	199-2	206-1	206-1	206-1	206-1	206-1	206-1	206-1
	A1	A1	A4	A2	A2	A2	A2	A1	A1	A3	A3	A3	A4	A4
	KSPAR, CEN	AT MARGIN	IN CONTACT	ZONED KSP/	ZONED KSP/	BRIGHT ZON	BRIGHT ZON	KSPAR WITH	IN CONTACT	KSPAR IN FI	KSPAR IN FI	KSPAR IN FI	WITH PHLOC	WITH PHLOC
Rock Type	Syenite	Syenite	Syenite	Syenite	Syenite	Syenite	Syenite	Syenite	Syenite	Syenite	Syenite	Syenite	Syenite	Syenite
SiO2	62.6	64.78	65.22	63.32	63.56	61.81	61.57	65.05	65.37	65.54	64.58	64.74	62.1	63.31
Al2O3	19.43	19.15	18.47	18.3	18.53	19.38	19.6	18.55	18.67	18.56	19.05	18.47	18.9	19.33
CaO	0	0	0.03	0.02	0.01	0.02	0.02	0.02	0.05	0.02	0.01	0.03	0.03	0.02
BaO	2.61	1.06	0.3	1.51	1.46	3.29	3.06	0.48	0.15	0.77	0.98	0.98	2.71	2.53
K2O	13.69	14.78	14.88	15.03	15.31	12.94	13.36	14.4	14.93	14.95	14.5	14.66	13.85	13.15
Na2O	0.97	0.8	0.81	0.43	0.25	1.27	1.03	0.83	0.15	0.62	0.45	0.67	0.9	1.07
FeO	0.23	0.16	0.33	0.4	0.21	0.21	0.29	0.61	0.35	0.39	0.36	0.43	0.48	0.34
TOTAL	99.53	100.73	100.04	99.01	99.33	98.92	98.93	99.94	99.67	100.85	99.93	99.98	98.97	99.75

	13	14	15	30	31	32	33	34	35	36	37	38	39	40
	"FEL	"FEL	"FEL	"FEL	"FEL	"FEL	"FEL	"FEL	"FEL	"FEL	"FEL	"FEL	"FEL	"FEL
	95MYAA	95MYAA	95MYAA	95MYAA	95MYAA	95MYAA	95MYAA	95MYAA	95MYAA	95MYAA	95MYAA	95MYAA	95MYAA	95MYAA
	190-1	190-1	190-1	199-2	199-2	199-2	199-2	206-1	206-1	206-1	206-1	206-1	206-1	206-1
	A1	A1	A4	A2	A2	A2	A2	A1	A1	A3	A3	A3	A4	A4
	KSPAR, CEN	AT MARGIN	IN CONTACT	ZONED KSP/	ZONED KSP/	BRIGHT ZON	BRIGHT ZON	KSPAR WITH	IN CONTACT	KSPAR IN FI	KSPAR IN FI	KSPAR IN FI	WITH PHLOC	WITH PHLOC
			HCPX	ENTRAL	ENTRAL			ED AMPHIBC	H AMPHIBOL	GRAINED PH	GRAINED PH	GRAINED PH	E, FLUORIT	E, FLUORIT
Si	11.753	11.901	12.008	11.922	11.918	11.713	11.673	11.99	12.034	12.006	11.93	11.981	11.771	11.811
Al	4.247	4.099	3.992	4.06	4.082	4.287	4.327	4.01	3.966	3.994	4.07	4.019	4.221	4.189
Total	16	16	16	15.982	16	16	16	16	16	16	16	16	15.992	16
Al	0.051	0.047	0.015	0	0.013	0.041	0.052	0.019	0.084	0.012	0.076	0.008	0	0.061
Ca	0	0	0.006	0.004	0.002	0.004	0.004	0.004	0.01	0.004	0.002	0.006	0.006	0.004
Ba	0.192	0.076	0.022	0.111	0.107	0.244	0.227	0.035	0.011	0.055	0.071	0.071	0.201	0.185
K	3.278	3.463	3.494	3.61	3.662	3.128	3.231	3.385	3.506	3.493	3.416	3.46	3.348	3.129
Na	0.353	0.285	0.289	0.157	0.091	0.467	0.379	0.297	0.054	0.22	0.161	0.24	0.331	0.387
Fe	0.036	0.025	0.051	0.063	0.033	0.033	0.046	0.094	0.054	0.06	0.056	0.067	0.076	0.053
Total	3.91	3.896	3.877	3.945	3.908	3.917	3.939	3.834	3.719	3.844	3.782	3.852	3.962	3.819
Ab	9.72	7.6	7.63	4.16	2.42	12.97	10.48	8.05	1.5	5.92	4.5	6.49	8.97	10.99
Or	90.28	92.4	92.21	95.73	97.53	86.92	89.41	91.85	98.22	93.97	95.44	93.35	90.86	88.89
An	0	0	0.16	0.11	0.05	0.11	0.11	0.11	0.28	0.11	0.06	0.16	0.17	0.11

Appendix 4. electron microprobe analyses of feldspar from the syenitic and granitic phases of the SLIC.

41	42	43	44	45	46	47	48	49	50	51	52	53	54	55	56
"FEL	"FEL	"FEL	"FEL	"FEL	"FEL	"FEL	"FEL	"FEL	"FEL	"FEL	"FEL	"FEL	"FEL	"FEL	"FEL
95MYAA	95MYAA	95MYAA	95MYAA	95MYAA	95MYAA	95MYAA	95MYAA	95MYAA	95MYAA	95MYAA	95MYAA	95MYAA	95MYAA	95MYAA	95MYAA
206-1	206-1	206-1	206-1	206-1	206-1	206-1	206-1	206-1	208-1	208-1	208-1	208-3	208-3	208-3	208-3
A4	A4	A4	A5	A5	A6	A6	A6	A6	A2	A7	A7	A1	A1	A1	A1
MAIN GRAIN	ADJ HIGH-B/	ADJ HIGH-B/	KSPAR INCL	IN CONTACT	KSPAR WITH	KSPAR WITH	KSPAR WITH	KSPAR WITH	KSPAR WITH	CENTRAL	AT MARGIN	CENTRAL	CENTRAL	CENTRAL	CENTRAL
Syenite	Syenite	Syenite	Syenite	Syenite	Syenite	Syenite	Syenite	Syenite	Syenite	Syenite	Syenite	Syenite	Syenite	Syenite	Syenite
62.69	60.01	58.72	63.63	64.26	65.05	64.62	65.05	64.93	65.05	64.33	64.33	64.09	63.78	63.79	64.09
19.5	20.2	20.31	18.87	18.89	18.68	18.33	18.46	18.37	18.98	18.65	18.49	18.71	19.05	18.5	19.09
0.03	0.02	0.03	0.01	0.02	0.02	0.01	0	0	0.03	0.02	0.03	0	0.02	0.01	0.01
3.12	5.85	7.76	2.05	1.57	0.48	0.44	0.36	0.49	0.51	0.55	0.66	0.79	0.97	0.5	0.56
13.81	12.89	12.71	14.2	14.71	15.2	15.8	15.22	15.02	14.56	15.24	15.22	15.49	15.86	15.79	15.2
0.99	0.8	0.64	0.88	0.79	0.88	0.38	0.65	0.74	0.77	0.71	0.66	0.67	0.39	0.72	0.82
0.18	0.14	0.13	0.55	0.41	0.56	0.5	0.45	0.59	0.49	0.58	0.58	0.27	0.16	0.25	0.11
100.32	99.91	100.3	100.19	100.65	100.87	100.08	100.19	100.14	100.39	100.08	99.97	100.02	100.23	99.56	99.88
41	42	43	44	45	46	47	48	49	50	51	52	53	54	55	56
"FEL	"FEL	"FEL	"FEL	"FEL	"FEL	"FEL	"FEL	"FEL	"FEL	"FEL	"FEL	"FEL	"FEL	"FEL	"FEL
95MYAA	95MYAA	95MYAA	95MYAA	95MYAA	95MYAA	95MYAA	95MYAA	95MYAA	95MYAA	95MYAA	95MYAA	95MYAA	95MYAA	95MYAA	95MYAA
206-1	206-1	206-1	206-1	206-1	206-1	206-1	206-1	206-1	208-1	208-1	208-1	208-3	208-3	208-3	208-3
A4	A4	A4	A5	A5	A6	A6	A6	A6	A2	A7	A7	A1	A1	A1	A1
MAIN GRAIN	ADJ HIGH-B/	ADJ HIGH-B/	KSPAR INCL	IN CONTACT	KSPAR WITH	KSPAR WITH	KSPAR WITH	KSPAR WITH	KSPAR WITH	CENTRAL	AT MARGIN	CENTRAL	CENTRAL	CENTRAL	CENTRAL
	NE ALONG (	NE ALONG (	E GRAINED	H PHLOGOPI	HIBOLE AND	HIBOLE AND	HIBOLE AND	HIBOLE AND	OGOPITE						
11.729	11.487	11.37	11.851	11.883	11.938	11.973	11.991	11.987	11.94	11.915	11.935	11.901	11.847	11.904	11.872
4.271	4.513	4.63	4.141	4.116	4.04	4.002	4.009	3.996	4.06	4.07	4.042	4.094	4.153	4.068	4.128
16	16	16	15.992	15.999	15.978	15.975	16	15.983	16	15.985	15.977	15.995	16	15.972	16
0.028	0.044	0.004	0	0	0	0	0	0	0.045	0	0	0	0.016	0	0.039
0.006	0.004	0.006	0.002	0.004	0.004	0.002	0	0	0.006	0.004	0.006	0	0.004	0.002	0.002
0.229	0.439	0.589	0.15	0.114	0.035	0.032	0.026	0.035	0.037	0.04	0.048	0.057	0.071	0.037	0.041
3.296	3.147	3.139	3.373	3.469	3.558	3.734	3.578	3.537	3.409	3.6	3.602	3.669	3.757	3.758	3.591
0.359	0.297	0.24	0.318	0.283	0.313	0.137	0.232	0.265	0.274	0.255	0.237	0.241	0.14	0.26	0.294
0.028	0.022	0.021	0.086	0.063	0.086	0.077	0.069	0.091	0.075	0.09	0.09	0.042	0.025	0.039	0.017
3.946	3.953	3.999	3.929	3.933	3.996	3.982	3.905	3.928	3.846	3.989	3.983	4.009	4.013	4.096	3.984
9.81	8.61	7.1	8.6	7.54	8.08	3.53	6.1	6.97	7.43	6.61	6.17	6.17	3.6	6.48	7.58
90.03	91.27	92.72	91.34	92.36	91.82	96.42	93.9	93.03	92.41	93.29	93.67	93.83	96.3	93.47	92.37
0.16	0.12	0.18	0.05	0.11	0.1	0.05	0	0	0.16	0.1	0.16	0	0.1	0.05	0.05

Appendix 4. electron microprobe analyses of feldspar from the syenitic and granitic phases of the SLIC.

57	58	59	60	61	62	63	64	90	91	92	93	94	95	96	97
"FEL	"FEL	"FEL	"FEL	"FEL	"FEL	"FEL	"FEL	"FEL	"FEL	"FEL	"FEL	"FEL	"FEL	"FEL	"FEL
95MYAA	95MYAA	95MYAA	95MYAA	95MYAA	95MYAA	95MYAA	95MYAA	95MYAA	95MYAA	95MYAA	95MYAA	95MYAA	95MYAA	95MYAA	95MYAA
208-3	208-3	208-3	208-3	208-3	208-3	208-3	208-3	215-1	215-1	215-1	215-1	215-1	215-1	215-1	215-1
A2	A2	A3	A3	A3	A3	A3	A3	A2	A2	A2	A2	A2	A2	A2	A2
KSPAR, AT N	CENTRAL	KSPAR, CEN	ALBITE WITH	ALBITE WITH	ALBITE WITH	ALBITE WITH	ALBITE WITH	WITH ALBIT	BRIGHT DON	PLAGIOCLAS	INTERIOR	INTERIOR	AT MARGIN	AT MARGIN	AT MARGIN
Syenite	Syenite	Syenite	Syenite	Syenite	Syenite	Syenite	Syenite	Syenite	Syenite	Syenite	Syenite	Syenite	Syenite	Syenite	Syenite
64	65.21	63.83	68.25	66.7	67.94	68.59	63.93	64.46	63.85	66.59	66.35	66.38	68.4	66.84	67.36
18.74	18.51	18.73	19.84	19.9	19.87	19.43	19.07	18.64	19.03	21.21	21.4	21	19.88	20.53	20.32
0.02	0.02	0.02	0.22	0.33	0.24	0.06	0.02	0	0	1.8	1.86	1.35	0.39	0.86	0.8
0.85	0.2	0.41	0	0	0	0	0.9	0.23	0.95	0	0	0	0	0	0
15.39	16.55	16.36	0.07	0.11	0.1	0.11	15.34	15.42	15.53	0.21	0.13	0.1	0.12	0.06	0.1
0.6	0.11	0.15	12.25	11.7	12.43	12.36	0.5	0.62	0.43	10.2	10.44	10.61	10.7	10.41	11.02
0.15	0.23	0.01	0.25	0.3	0.16	0.13	0.12	0.16	0.03	0.11	0.04	0.03	0.1	0.08	0.1
99.75	100.83	99.51	100.88	99.04	100.74	100.68	99.88	99.53	99.82	100.12	100.22	99.47	99.59	98.78	99.7
57	58	59	60	61	62	63	64	90	91	92	93	94	95	96	97
"FEL	"FEL	"FEL	"FEL	"FEL	"FEL	"FEL	"FEL	"FEL	"FEL	"FEL	"FEL	"FEL	"FEL	"FEL	"FEL
95MYAA	95MYAA	95MYAA	95MYAA	95MYAA	95MYAA	95MYAA	95MYAA	95MYAA	95MYAA	95MYAA	95MYAA	95MYAA	95MYAA	95MYAA	95MYAA
208-3	208-3	208-3	208-3	208-3	208-3	208-3	208-3	215-1	215-1	215-1	215-1	215-1	215-1	215-1	215-1
A2	A2	A3	A3	A3	A3	A3	A3	A2	A2	A2	A2	A2	A2	A2	A2
KSPAR, AT N	CENTRAL	KSPAR, CEN	ALBITE WITH	ALBITE WITH	ALBITE WITH	ALBITE WITH	ALBITE WITH	WITH ALBIT	BRIGHT DON	PLAGIOCLAS	INTERIOR	INTERIOR	AT MARGIN	AT MARGIN	AT MARGIN
IN			PAR	PAR	PAR	PAR	PAR	D PHLOGOPI		RE TO MARG					
11.906	11.985	11.906	11.873	11.818	11.847	11.944	11.871	11.955	11.874	11.662	11.617	11.69	11.967	11.811	11.822
4.094	4.009	4.094	4.067	4.155	4.083	3.987	4.129	4.045	4.126	4.338	4.383	4.31	4.033	4.189	4.178
16	15.994	16	15.94	15.973	15.93	15.931	16	16	16	16	16	16	16	16	16
0.014	0	0.023	0	0	0	0	0.044	0.028	0.044	0.039	0.032	0.048	0.066	0.085	0.024
0.004	0.004	0.004	0.041	0.063	0.045	0.011	0.004	0	0	0.338	0.349	0.255	0.073	0.163	0.15
0.062	0.014	0.03	0	0	0	0	0.065	0.017	0.069	0	0	0	0	0	0
3.652	3.88	3.892	0.016	0.025	0.022	0.024	3.633	3.648	3.684	0.047	0.029	0.022	0.027	0.014	0.022
0.216	0.039	0.054	4.132	4.019	4.202	4.173	0.18	0.223	0.155	3.463	3.544	3.623	3.63	3.566	3.75
0.023	0.035	0.002	0.036	0.044	0.023	0.019	0.019	0.025	0.005	0.016	0.006	0.004	0.015	0.012	0.015
3.971	3.972	4.005	4.225	4.151	4.292	4.227	3.945	3.941	3.957	3.903	3.96	3.952	3.811	3.84	3.961
5.59	1	1.37	98.65	97.87	98.43	99.15	4.72	5.76	4.04	90	90.36	92.89	97.32	95.29	95.59
94.31	98.9	98.53	0.37	0.61	0.52	0.58	95.18	94.24	95.96	1.22	0.74	0.58	0.72	0.36	0.57
0.1	0.1	0.1	0.98	1.53	1.05	0.27	0.1	0	0	8.78	8.9	6.53	1.96	4.35	3.83

Appendix 4. electron microprobe analyses of feldspar from the syenitic and granitic phases of the SLIC.

98	99	100	101	102	103	104	105	106	107	108	109	119	120	121	122
"FEL	"FEL	"FEL	"FEL	"FEL	"FEL	"FEL	"FEL	"FEL	"FEL	"FEL	"FEL	"FEL	"FEL	"FEL	"FEL
95MYAA	95MYAA	95MYAA	95MYAA	95MYAA	95MYAA	95MYAA	95MYAA	95MYAA	95MYAA	95MYAA	95MYAA	95MYAA	95MYAA	95MYAA	95MYAA
215-1	215-1	215-1	215-1	215-1	215-1	215-1	215-1	215-1	215-1	215-1	215-1	227-9	227-9	227-9	227-9
A3	A3	A3	A4	A4	A4	A4	A4	A5	A5	A5	A5	A1	A1	A1	A1
KSPAR CEN	LOW-Ba CEI	BRIGHT DON	ALBITE CEN	CENTRAL, M	NARROW OU	BRIGHT ZON	OUTER ZONI	KSPAR WITI	AT MARGIN	ALBITE WITI	CENTRAL	HIGH-Ba KSI	INTERIOR	INTERIOR 2	AT MARGIN
Syenite	Syenite	Syenite	Syenite	Syenite	Syenite	Syenite	Syenite	Syenite	Syenite	Syenite	Syenite	Syenite	Syenite	Syenite	Syenite
64.46	64.35	63.67	67.98	67.76	66.01	65.11	67.85	63.91	64.19	67.48	67.71	61.31	61.53	62.84	64.45
19.07	18.66	19.41	20.65	20.81	21.31	21.46	20.61	19	19.38	20.12	20.21	20.2	19.95	19.52	19.23
0	0.01	0	1.2	0.05	1.92	1.95	0.57	0	0	0.72	0.45	0	0.02	0	0
1.13	0.14	1.31	0	0	0	0	0	0.32	1.1	0	0	4.48	4.85	2.71	1.55
14.7	15.71	15.22	0.09	0.34	0.19	0.21	0.13	15.43	15.44	0.1	0.1	11.38	11.7	12.9	13.77
0.83	0.62	0.48	10.87	11.28	10.1	10.11	10.94	0.62	0.44	10.74	11.22	1.68	1.74	1.08	1.37
0.06	0.14	0.02	0.07	0.03	0.1	0.17	0.07	0.11	0.01	0.03	0.03	0.24	0.37	0.3	0.28
100.25	99.63	100.11	100.86	100.27	99.63	99.01	100.17	99.39	100.56	99.19	99.72	99.29	100.16	99.35	100.65
98	99	100	101	102	103	104	105	106	107	108	109	119	120	121	122
"FEL	"FEL	"FEL	"FEL	"FEL	"FEL	"FEL	"FEL	"FEL	"FEL	"FEL	"FEL	"FEL	"FEL	"FEL	"FEL
95MYAA	95MYAA	95MYAA	95MYAA	95MYAA	95MYAA	95MYAA	95MYAA	95MYAA	95MYAA	95MYAA	95MYAA	95MYAA	95MYAA	95MYAA	95MYAA
215-1	215-1	215-1	215-1	215-1	215-1	215-1	215-1	215-1	215-1	215-1	215-1	227-9	227-9	227-9	227-9
A3	A3	A3	A4	A4	A4	A4	A4	A5	A5	A5	A5	A1	A1	A1	A1
KSPAR CEN	LOW-Ba CEI	BRIGHT DON	ALBITE CEN	CENTRAL, M	NARROW OU	BRIGHT ZON	OUTER ZONI	KSPAR WITI	AT MARGIN	ALBITE WITI	CENTRAL	HIGH-Ba KSI	INTERIOR	INTERIOR 2	AT MARGIN
	DOMAIN	AT MARGIN		ED	ONE			ITE AND MI		PAR					
11.901	11.937	11.82	11.796	11.814	11.622	11.554	11.832	11.885	11.848	11.877	11.866	11.596	11.601	11.774	11.862
4.099	4.063	4.18	4.204	4.186	4.378	4.446	4.168	4.115	4.152	4.123	4.134	4.404	4.399	4.226	4.138
16	16	16	16	16	16	16	16	16	16	16	16	16	16	16	16
0.05	0.016	0.066	0.019	0.089	0.043	0.041	0.067	0.048	0.063	0.05	0.039	0.099	0.034	0.084	0.033
0	0.002	0	0.223	0.009	0.362	0.371	0.106	0	0	0.136	0.084	0	0.004	0	0
0.082	0.01	0.095	0	0	0	0	0	0.023	0.08	0	0	0.332	0.358	0.199	0.112
3.462	3.717	3.604	0.02	0.076	0.043	0.048	0.029	3.66	3.635	0.022	0.022	2.745	2.814	3.083	3.233
0.297	0.223	0.173	3.657	3.813	3.448	3.478	3.699	0.224	0.157	3.665	3.812	0.616	0.636	0.392	0.489
0.009	0.022	0.003	0.01	0.004	0.015	0.025	0.01	0.017	0.002	0.004	0.004	0.038	0.058	0.047	0.043
3.9	3.99	3.941	3.929	3.991	3.911	3.963	3.911	3.972	3.937	3.877	3.961	3.83	3.904	3.805	3.91
7.9	5.66	4.57	93.77	97.82	89.49	89.27	96.47	5.76	4.15	95.86	97.27	18.33	18.42	11.29	13.14
92.1	94.29	95.43	0.51	1.94	1.11	1.22	0.75	94.24	95.85	0.59	0.57	81.67	81.47	88.71	86.86
0	0.05	0	5.72	0.24	9.4	9.51	2.78	0	0	3.55	2.16	0	0.12	0	0

Appendix 4. electron microprobe analyses of feldspar from the syenitic and granitic phases of the SLIC.

123	124	125	126	127	128	129	130	131	132	133	134	135	136	137	138
"FEL	"FEL	"FEL	"FEL	"FEL	"FEL	"FEL	"FEL	"FEL	"FEL	"FEL	"FEL	"FEL	"FEL	"FEL	"FEL
95MYAA	95MYAA	95MYAA	95MYAA	95MYAA	95MYAA	95MYAA	95MYAA	95MYAA	95MYAA	95MYAA	95MYAA	95MYAA	95MYAA	95MYAA	95MYAA
227-9	227-9	227-9	227-9	227-9	227-9	228-2	228-2	228-2	228-2	228-2	245-2	245-2	245-2	245-2	245-2
A2	A2	A5	A5	A5	A5	A1	A1	A1	A1	A1	A1	A1	A1	A2	A2
KSPAR WITH	BRIGHT DOM	ZONED, CEN	INTERIOR 1	INTERIOR HI	AT MARGIN	CENTRAL LC	INTERIOR HI	OUTER ZONE	HIGH Ba, CE	AT MARGIN	CENTRAL	INTERIOR	IN CONTACT	CENTRAL	INTERIOR
Syenite	Syenite	Syenite	Syenite	Syenite	Syenite	Syenite	Syenite	Syenite	Syenite	Syenite	Syenite	Syenite	Syenite	Syenite	Syenite
64.01	61.85	64.48	62.25	60.89	64.19	64.09	61.81	63.42	61.4	63.66	66.29	66.6	66.61	65.95	66.26
18.88	19.82	19.28	19.68	20.29	19.13	19	20.08	18.68	20.05	18.73	21.45	21.01	20.93	21.6	21.44
0	0	0	0	0.01	0	0	0.03	0.01	0.03	0.01	1.92	1.72	1.69	2.17	2.15
1.13	2.78	1.36	3.04	4.78	1.11	1.82	3.44	1.49	4.3	1.45	0	0	0	0	0
14.41	13	13.94	12.65	11.9	14.72	13.18	12.37	14.48	11.75	13.89	0.22	0.11	0.16	0.17	1.07
0.98	1.5	1.4	1.73	1.74	1.03	1.61	1.97	1.09	2.03	1.56	9.46	10.41	10.39	9.3	9.59
0.33	0.23	0.38	0.26	0.3	0.5	0.32	0.2	0.38	0.37	0.34	0.11	0.11	0.13	0.08	0.16
99.74	99.18	100.84	99.61	99.91	100.68	100.02	99.9	99.55	99.93	99.64	99.45	99.96	99.91	99.27	100.67

123	124	125	126	127	128	129	130	131	132	133	134	135	136	137	138
"FEL	"FEL	"FEL	"FEL	"FEL	"FEL	"FEL	"FEL	"FEL	"FEL	"FEL	"FEL	"FEL	"FEL	"FEL	"FEL
95MYAA	95MYAA	95MYAA	95MYAA	95MYAA	95MYAA	95MYAA	95MYAA	95MYAA	95MYAA	95MYAA	95MYAA	95MYAA	95MYAA	95MYAA	95MYAA
227-9	227-9	227-9	227-9	227-9	227-9	228-2	228-2	228-2	228-2	228-2	245-2	245-2	245-2	245-2	245-2
A2	A2	A5	A5	A5	A5	A1	A1	A1	A1	A1	A1	A1	A1	A2	A2
KSPAR WITH	BRIGHT DOM	ZONED KSP/	INTERIOR 1	INTERIOR HI	AT MARGIN	ZONED KSP/	INTERIOR HI	OUTER ZONE	HIGH Ba, CE	AT MARGIN	CENTRAL	INTERIOR	IN CONTACT	CENTRAL	INTERIOR
AND BIOTI		ENTRAL		Ba ZONE	MICA	ENTRAL LOV	Ba ZONE		AL				H QUARTZ		
11.89	11.658	11.848	11.686	11.525	11.842	11.873	11.602	11.863	11.575	11.866	11.657	11.681	11.691	11.621	11.596
4.11	4.342	4.152	4.314	4.475	4.158	4.127	4.398	4.117	4.425	4.114	4.343	4.319	4.309	4.379	4.404
16	16	16	16	16	16	16	16	15.98	16	15.98	16	16	16	16	16
0.023	0.06	0.022	0.04	0.05	0.001	0.021	0.044	0	0.029	0	0.102	0.024	0.02	0.106	0.018
0	0	0	0	0.002	0	0	0.006	0.002	0.006	0.002	0.362	0.323	0.318	0.41	0.403
0.082	0.205	0.098	0.224	0.354	0.08	0.132	0.253	0.109	0.318	0.106	0	0	0	0	0
3.414	3.125	3.267	3.029	2.873	3.464	3.114	2.962	3.455	2.825	3.302	0.049	0.025	0.036	0.038	0.239
0.353	0.548	0.499	0.63	0.639	0.368	0.578	0.717	0.395	0.742	0.564	3.225	3.54	3.536	3.177	3.254
0.051	0.036	0.058	0.041	0.047	0.077	0.05	0.031	0.059	0.058	0.053	0.016	0.016	0.019	0.012	0.023
3.923	3.974	3.944	3.964	3.965	3.99	3.895	4.013	4.02	3.978	4.027	3.754	3.928	3.929	3.743	3.937
9.37	14.92	13.24	17.21	18.17	9.61	15.66	19.46	10.26	20.76	14.58	88.7	91.05	90.91	87.64	83.52
90.63	85.08	86.76	82.79	81.77	90.39	84.34	80.38	89.69	79.07	85.37	1.36	0.63	0.92	1.05	6.13
0	0	0	0	0.06	0	0	0.16	0.05	0.17	0.05	9.95	8.31	8.17	11.3	10.35

Appendix 4. electron microprobe analyses of feldspar from the syenitic and granitic phases of the SLIC.

139	140	141	142	143	144	145	146	147	148	149	150	151	152	153	154
"FEL	"FEL	"FEL	"FEL	"FEL	"FEL	"FEL	"FEL	"FEL	"FEL	"FEL	"FEL	"FEL	"FEL	"FEL	"FEL
95MYAA	95MYAA	95MYAA	95MYAA	95MYAA	95MYAA	95MYAA	95MYAA	95MYAA	95MYAA	95MYAA	95MYAA	95MYAA	95MYAA	95MYAA	95MYAA
245-2	245-2	245-2	245-2	245-2	245-2	249-1	249-1	249-1	249-1	249-1	249-1	249-1	249-1	249-1	249-1
A2	A2	A2	A6	A6	A6	A1	A1	A1	A1	A1	A1	A1	A1	A1	A1
NEAR MARG	WITH ZONEI	ANOTHER G	KSPAR	ANOTHER G	INTERGROW	ZONED KSPA	ALTERNATI	ALTERNATI	ALTERNATI	ALTERNATI	ALTERNATI	ALTERNATI	ALTERNATI	ALTERNATI	ALTERNATI
Syenite	Syenite	Syenite	Syenite	Syenite	Syenite	Syenite	Syenite	Syenite	Syenite	Syenite	Syenite	Syenite	Syenite	Syenite	Syenite
65.88	65.02	65.14	65.15	65.56	66.89	62.57	62.84	62.46	63.18	63.57	60.77	60.91	62.91	64.08	63.38
21.27	18.56	18.61	18.4	18.56	20.92	19.36	19.82	19.62	19.5	19.43	20.24	20.26	19.35	18.92	19.58
2.14	0.01	0	0	0.01	1.87	0.02	0.02	0.03	0.03	0.02	0.04	0.01	0	0.01	0.01
0	0.27	0.2	0.29	0.19	0	2.18	3.16	3.01	2.28	2.39	4.43	4.23	2.36	1.49	2.21
0.29	15.24	15.22	15.45	14.57	0.27	14.5	13.68	13.44	13.76	13.6	13.16	12.92	13.75	14.01	13.68
9.96	0.76	0.82	0.76	1.14	10.24	0.67	1.05	1.08	1.42	1.06	1.14	1.1	1.4	1.07	1.46
0.18	0.15	0.18	0.08	0.13	0.15	0.18	0.23	0.18	0.21	0.2	0.18	0.13	0.27	0.25	0.19
99.72	100.01	100.17	100.13	100.16	100.34	99.48	100.8	99.82	100.38	100.27	99.96	99.56	100.04	99.83	100.51

139	140	141	142	143	144	145	146	147	148	149	150	151	152	153	154
"FEL	"FEL	"FEL	"FEL	"FEL	"FEL	"FEL	"FEL	"FEL	"FEL	"FEL	"FEL	"FEL	"FEL	"FEL	"FEL
95MYAA	95MYAA	95MYAA	95MYAA	95MYAA	95MYAA	95MYAA	95MYAA	95MYAA	95MYAA	95MYAA	95MYAA	95MYAA	95MYAA	95MYAA	95MYAA
245-2	245-2	245-2	245-2	245-2	245-2	249-1	249-1	249-1	249-1	249-1	249-1	249-1	249-1	249-1	249-1
A2	A2	A2	A6	A6	A6	A1	A1	A1	A1	A1	A1	A1	A1	A1	A1
NEAR MARG	WITH ZONEI	ANOTHER G	KSPAR	ANOTHER G	INTERGROW	ZONED KSPA	ALTERNATIN	ALTERNATIN	ALTERNATIN	ALTERNATIN	ALTERNATIN	ANOTHER IN	ANOTHER IN	ANOTHER IN	ANOTHER IN
	ITE				H KSPAR	ENOCRYST (	GH-LOW Ba	GH-LOW Ba	GH-LOW Ba	GH-LOW Ba	GH-LOW Ba	H-Ba ZONE	H-Ba ZONE	H-Ba ZONE	H-Ba ZONE
11.605	11.988	11.985	12.008	12.02	11.697	11.757	11.696	11.716	11.748	11.804	11.523	11.552	11.751	11.894	11.753
4.395	4.012	4.015	3.992	3.98	4.303	4.243	4.304	4.284	4.252	4.196	4.477	4.448	4.249	4.106	4.247
16	16	16	16	16	16	16	16	16	16	16	16	16	16	16	16
0.021	0.02	0.02	0.005	0.03	0.007	0.044	0.043	0.053	0.02	0.056	0.045	0.079	0.01	0.033	0.032
0.404	0.002	0	0	0.002	0.35	0.004	0.004	0.006	0.006	0.004	0.008	0.002	0	0.002	0.002
0	0.02	0.014	0.021	0.014	0	0.161	0.23	0.221	0.166	0.174	0.329	0.314	0.173	0.108	0.161
0.065	3.584	3.572	3.632	3.407	0.06	3.475	3.248	3.216	3.263	3.221	3.183	3.125	3.276	3.317	3.236
3.402	0.272	0.293	0.272	0.405	3.472	0.244	0.379	0.393	0.512	0.382	0.419	0.404	0.507	0.385	0.525
0.027	0.023	0.028	0.012	0.02	0.022	0.028	0.036	0.028	0.033	0.031	0.029	0.021	0.042	0.039	0.029
3.919	3.921	3.927	3.942	3.878	3.911	3.956	3.94	3.917	4	3.868	4.013	3.945	4.008	3.884	3.985
87.88	7.04	7.57	6.96	10.62	89.42	6.56	10.44	10.87	13.54	10.58	11.61	11.45	13.4	10.4	13.95
1.68	92.91	92.43	93.04	89.32	1.55	93.34	89.45	88.97	86.3	89.31	88.17	88.49	86.6	89.55	86
10.43	0.05	0	0	0.05	9.02	0.11	0.11	0.17	0.16	0.11	0.23	0.06	0	0.05	0.05

Appendix 4. electron microprobe analyses of feldspar from the syenitic and granitic phases of the SLIC.

155	156	157	158	159	160	161	162	163	164	165	166	167	168	169	170
"FEL	"FEL	"FEL	"FEL	"FEL	"FEL	"FEL	"FEL	"FEL	"FEL	"FEL	"FEL	"FEL	"FEL	"FEL	"FEL
95MYAA	95MYAA	95MYAA	95MYAA	95MYAA	95MYAA	95MYAA	95MYAA	95MYAA	95MYAA	95MYAA	95MYAA	95MYAA	95MYAA	95MYAA	95MYAA
249-1	249-1	249-1	249-1	249-1	249-1	249-1	249-1	249-1	249-1	249-3	249-3	249-3	249-3	249-3	249-3
A1	A1	A1	A1	A1	A2	A2	A2	A3	A3	A1	A2	A2	A2	A2	A2
ALTERNATI	ALTERNATI	INTERIOR 1	INTERIOR 2	INTERIOR 4	ALBITE, CEN	ALBITE, CEN	KSPAR MAN	KSPAR IN C	KSPAR IN C	KSPAR WITH	ZONED KSPA	ZONED KSPA	OUTER MAR	INTERIOR ZC	INTERIOR 2
Syenite	Syenite	Syenite	Syenite	Syenite	Syenite	Syenite	Syenite	Syenite	Syenite	Syenite	Syenite	Syenite	Syenite	Syenite	Syenite
62.7	63.42	62.6	62.38	64.55	67.64	67.03	64.76	65.34	66.09	64.38	62.37	61.5	62.8	63.67	62.2
19.42	19.45	19.61	19.15	18.97	19.41	20.18	19.09	18.82	18.55	19.1	19.41	19.34	19.57	19.04	19.43
0.03	0.02	0.02	0.02	0.01	0.02	0.09	0.03	0.01	0.01	0.03	0.02	0.03	0.02	0.01	0
2.32	1.79	2.73	1.82	0.64	0	0	1.09	0.33	0.35	0.84	3.73	3.84	3.52	2.01	2.97
13.95	14.57	14.15	13.98	15.02	0.02	0.01	14.5	14.82	14.97	15.01	13.58	14.13	12.57	14.61	14.06
0.89	0.99	1	0.94	0.73	11.67	12.1	0.6	0.72	0.7	1.12	1.3	0.87	1.73	1.01	0.96
0.19	0.14	0.2	0.17	0.14	0.29	0.03	0.17	0.18	0.2	0.25	0.3	0.23	0.37	0.38	0.29
99.5	100.38	100.31	98.46	100.06	99.05	99.44	100.24	100.22	100.87	100.73	100.71	99.94	100.58	100.73	99.91
155	156	157	158	159	160	161	162	163	164	165	166	167	168	169	170
"FEL	"FEL	"FEL	"FEL	"FEL	"FEL	"FEL	"FEL	"FEL	"FEL	"FEL	"FEL	"FEL	"FEL	"FEL	"FEL
95MYAA	95MYAA	95MYAA	95MYAA	95MYAA	95MYAA	95MYAA	95MYAA	95MYAA	95MYAA	95MYAA	95MYAA	95MYAA	95MYAA	95MYAA	95MYAA
249-1	249-1	249-1	249-1	249-1	249-1	249-1	249-1	249-1	249-1	249-3	249-3	249-3	249-3	249-3	249-3
A1	A1	A1	A1	A1	A2	A2	A2	A3	A3	A1	A2	A2	A2	A2	A2
ANOTHER IN	ANOTHER IN	INTERIOR 1	INTERIOR 2	INTERIOR 4	ALBITE, CEN	ALBITE, CEN	KSPAR MAN	KSPAR IN C	KSPAR IN C	KSPAR WITH	ZONED KSPA	ZONED KSPA	OUTER MAR	INTERIOR ZC	INTERIOR 2
H-Ba ZONE	H-Ba ZONE				L	L	ALBITE	CT WITH FL	CT WITH FL	AND BIOTI	RE TO MARG	RE TO MARG	CENTRAL		
11.761	11.777	11.706	11.789	11.918	11.946	11.812	11.93	11.989	12.049	11.856	11.691	11.66	11.71	11.816	11.704
4.239	4.223	4.294	4.211	4.082	4.039	4.188	4.07	4.011	3.951	4.144	4.287	4.321	4.29	4.164	4.296
16	16	16	16	16	15.985	16	16	16	16	16	15.978	15.981	16	15.98	16
0.053	0.032	0.027	0.053	0.046	0	0.002	0.074	0.058	0.034	0.001	0	0	0.01	0	0.012
0.006	0.004	0.004	0.004	0.002	0.004	0.017	0.006	0.002	0.002	0.006	0.004	0.006	0.004	0.002	0
0.171	0.13	0.2	0.135	0.046	0	0	0.079	0.024	0.025	0.061	0.274	0.285	0.257	0.146	0.219
3.337	3.451	3.375	3.37	3.537	0.005	0.002	3.407	3.468	3.481	3.526	3.247	3.417	2.99	3.458	3.374
0.324	0.356	0.363	0.344	0.261	3.996	4.134	0.214	0.256	0.247	0.4	0.472	0.32	0.625	0.363	0.35
0.03	0.022	0.031	0.027	0.022	0.043	0.004	0.026	0.028	0.03	0.039	0.047	0.036	0.058	0.059	0.046
3.921	3.995	4	3.933	3.914	4.048	4.159	3.806	3.836	3.819	4.033	4.044	4.064	3.944	4.028	4.001
8.83	9.35	9.69	9.26	6.88	99.79	99.54	5.91	6.87	6.63	10.17	12.69	8.54	17.28	9.5	9.4
91.01	90.54	90.2	90.63	93.07	0.11	0.05	93.93	93.07	93.31	89.68	87.2	91.29	82.61	90.44	90.6
0.16	0.1	0.11	0.11	0.05	0.09	0.41	0.16	0.05	0.05	0.15	0.11	0.16	0.11	0.05	0

Appendix 4. electron microprobe analyses of feldspar from the syenitic and granitic phases of the SLIC.

171	172	173	174	175	81	82	83	84	85	86	87	88	89	193	194
"FEL	"FEL	"FEL	"FEL	"FEL	"FEL	"FEL	"FEL	"FEL	"FEL	"FEL	"FEL	"FEL	"FEL	"FEL	"FEL
95MYAA	95MYAA	95MYAA	95MYAA	95MYAA	95MYAA	95MYAA	95MYAA	95MYAA	95MYAA	95MYAA	95MYAA	95MYAA	95MYAA	95MYAA	95MYAA
249-3	249-3	249-3	249-3	249-3	211-3	211-3	211-3	211-3	211-3	211-3	211-3	211-3	211-3	254-1	254-1
A2	A3	A3	A3	A4	A2	A2	A2	A2	A3	A3	A3	A4	A4	A1	A1
OUTER ZONI	KSPAR IN C(	IN CONTAC'	IN CONTACT WITH BI		KSPAR IN C(	KSPAR IN C(	BRIGHT ZON	BRIGHT ZON	KSPAR WITH	AT MARGIN	AT MARGIN	KSPAR INCL	KSPAR INCL	KSPAR INCL	INTERIOR
Syenite	Syenite	Syenite	Syenite	Syenite	Syenite	Syenite	Syenite	Syenite	Syenite	Syenite	Syenite	Syenite	Syenite	Syenite	Syenite
61.32	63.59	62.66	63.82	64.02	64.23	64.96	62.73	62.98	64.71	65.14	65.47	65.39	65.34	64.53	64.24
19.8	18.99	18.63	18.81	19.04	18.38	18.18	19.18	18.95	18.21	18.54	18.56	18.24	18.38	19.24	18.86
0.04	0.02	0.02	0.03	0.01	0	0	0	0.13	0	0	0	0	0	0	0
4.92	1.94	0.75	1.21	0.85	0.56	0.52	3.37	1.89	0.69	0.79	0.68	0.67	0.45	1.15	0.94
12.46	14.77	15.32	15.28	14.43	15.16	15.84	14.46	13.78	15.07	15.34	14.81	14.41	15.18	14.76	14.97
1.62	0.57	0.85	0.42	0.97	0.53	0.38	0.43	1.22	0.71	0.62	0.75	0.85	0.71	0.71	0.77
0.39	0.4	0.43	0.34	0.4	0.35	0.32	0.05	0.34	0.42	0.34	0.35	0.59	0.74	0.39	0.3
100.55	100.28	98.66	99.91	99.72	99.21	100.2	100.22	99.29	99.81	100.77	100.62	100.15	100.8	100.78	100.08
171	172	173	174	175	81	82	83	84	85	86	87	88	89	193	194
"FEL	"FEL	"FEL	"FEL	"FEL	"FEL	"FEL	"FEL	"FEL	"FEL	"FEL	"FEL	"FEL	"FEL	"FEL	"FEL
95MYAA	95MYAA	95MYAA	95MYAA	95MYAA	95MYAA	95MYAA	95MYAA	95MYAA	95MYAA	95MYAA	95MYAA	95MYAA	95MYAA	95MYAA	95MYAA
249-3	249-3	249-3	249-3	249-3	211-3	211-3	211-3	211-3	211-3	211-3	211-3	211-3	211-3	254-1	254-1
A2	A3	A3	A3	A4	A2	A2	A2	A2	A3	A3	A3	A4	A4	A1	A1
OUTER ZONI	KSPAR IN C(	IN CONTAC'	IN CONTACT WIT		KSPAR IN C(	KSPAR IN C(	BRIGHT ZON	BRIGHT ZON	KSPAR WITH	AT MARGIN	AT MARGIN	KSPAR INCL	KSPAR INCL	KSPAR INCL	INTERIOR
	CT WITH CP	H BIOTITE	H BIOTITE		CT WITH AM	CT WITH AM		NOTHER GRA		ALBITE	ALBITE			#NAME?	
11.579	11.841	11.827	11.884	11.874	11.973	12.015	11.782	11.813	12.001	11.977	12.006	12.039	11.992	11.87	11.9
4.406	4.159	4.144	4.116	4.126	4.027	3.962	4.218	4.187	3.98	4.017	3.994	3.957	3.975	4.13	4.1
15.985	16	15.971	16	16	16	15.977	16	16	15.981	15.994	16	15.996	15.967	16	16
0	0.008	0	0.011	0.035	0.011	0	0.026	0.001	0	0	0.017	0	0	0.04	0.017
0.008	0.004	0.004	0.006	0.002	0	0	0	0.026	0	0	0	0	0	0	0
0.364	0.142	0.055	0.088	0.062	0.041	0.038	0.248	0.139	0.05	0.057	0.049	0.048	0.032	0.083	0.068
3.001	3.508	3.688	3.629	3.414	3.605	3.737	3.464	3.297	3.565	3.597	3.464	3.384	3.554	3.463	3.537
0.593	0.206	0.311	0.152	0.349	0.192	0.136	0.157	0.444	0.255	0.221	0.267	0.303	0.253	0.253	0.277
0.062	0.062	0.068	0.053	0.062	0.055	0.049	0.008	0.053	0.065	0.052	0.054	0.091	0.114	0.06	0.046
4.028	3.93	4.126	3.939	3.924	3.904	3.96	3.903	3.96	3.935	3.927	3.851	3.826	3.953	3.899	3.945
16.46	5.54	7.77	4	9.27	5.05	3.52	4.32	11.78	6.68	5.79	7.15	8.23	6.64	6.81	7.25
83.31	94.36	92.13	95.84	90.68	94.95	96.48	95.68	87.53	93.32	94.21	92.85	91.77	93.36	93.19	92.75
0.22	0.11	0.1	0.16	0.05	0	0	0	0.69	0	0	0	0	0	0	0

Appendix 4. electron microprobe analyses of feldspar from the syenitic and granitic phases of the SLIC.

195	196	197	198	209	210	211	212	213	214	1	2	3	4	5	6
"FEL	"FEL	"FEL	"FEL	"FEL	"FEL	"FEL	"FEL	"FEL	"FEL	"FEL	"FEL	"FEL	"FEL	"FEL	"FEL
95MYAA	95MYAA	95MYAA	95MYAA	95MYAA	95MYAA	95MYAA	95MYAA	95MYAA	95MYAA	95MYAA	95MYAA	95MYAA	95MYAA	95MYAA	95MYAA
254-1	254-1	254-1	254-1	291-4	291-4	291-4	291-4	291-4	291-4	161-1	161-1	161-1	161-1	161-1	161-1
A1	A4	A4	A4	A1	A1	A1	A1	A1	A1	A1	A1	A1	A1	A1	A1
INTERIOR	KSPAR WITH	AT MARGIN	AT MARGIN	KSPAR CENT	INTERIOR BR	INTERIOR BR	OUTER ZONE	OUTER ZONE	OUTER ZONE	KSPAR, CEN	KSPAR, CEN	KSPAR, CEN	AT MARGIN	AT MARGIN	AT MARGIN
Syenite	Syenite	Syenite	Syenite	Syenite	Syenite	Syenite	Syenite	Syenite	Syenite	Granite	Granite	Granite	Granite	Granite	Granite
64.3	63.16	62.74	63.02	61.97	60.75	60.36	64.29	63.57	64.09	64.43	65.1	65.02	65.28	64.79	65.17
18.72	19.17	19.06	19.12	19.19	19.54	19.57	18.54	18.58	18.58	18.01	17.97	18.07	18.37	17.82	17.69
0	0	0	0	0.03	0.02	0.01	0.01	0.01	0.02	0.01	0	0.02	0.04	0.01	0.01
0.94	2.37	2.14	2.17	2.79	4.05	4.72	1.31	1.13	1.25	0.52	0.47	0.58	0.58	0.35	0.51
15.61	14.61	14.56	14.93	14.92	13.26	13.08	15.93	14.51	15.8	15.16	15.71	14.85	15.66	15.49	15.71
0.58	0.95	0.89	0.79	0.5	1.22	1.18	0.49	0.77	0.32	0.32	0.35	0.25	0.26	0.24	0.18
0.36	0.42	0.42	0.4	0.2	0.17	0.18	0.36	0.22	0.2	0.65	0.81	0.86	0.57	0.86	0.87
100.51	100.68	99.81	100.43	99.6	99.01	99.1	100.93	98.79	100.26	99.1	100.41	99.65	100.76	99.56	100.14
												Formula based on 32 oxygen			
195	196	197	198	209	210	211	212	213	214	1	2	3	4	5	6
"FEL	"FEL	"FEL	"FEL	"FEL	"FEL	"FEL	"FEL	"FEL	"FEL	"FEL	"FEL	"FEL	"FEL	"FEL	"FEL
95MYAA	95MYAA	95MYAA	95MYAA	95MYAA	95MYAA	95MYAA	95MYAA	95MYAA	95MYAA	95MYAA	95MYAA	95MYAA	95MYAA	95MYAA	95MYAA
254-1	254-1	254-1	254-1	291-4	291-4	291-4	291-4	291-4	291-4	161-1	161-1	161-1	161-1	161-1	161-1
A1	A4	A4	A4	A1	A1	A1	A1	A1	A1	A1	A1	A1	A1	A1	A1
INTERIOR	KSPAR WITH	AT MARGIN	AT MARGIN	KSPAR CENT	INTERIOR BR	INTERIOR BR	OUTER ZONE	OUTER ZONE	OUTER ZONE	KSPAR, CEN	KSPAR, CEN	KSPAR, CEN	AT MARGIN	AT MARGIN	AT MARGIN
	AND BIOTI			ST ZONE	T ZONE	T ZONE									
11.901	11.768	11.773	11.771	11.722	11.61	11.578	11.904	11.921	11.916	12.026	12.028	12.049	12.003	12.049	12.071
4.083	4.209	4.215	4.208	4.277	4.39	4.422	4.045	4.079	4.071	3.961	3.912	3.946	3.98	3.905	3.861
15.984	15.977	15.988	15.979	15.999	16	16	15.949	16	15.987	15.987	15.94	15.995	15.983	15.954	15.932
0	0	0	0	0	0.01	0.002	0	0.027	0	0	0	0	0	0	0
0	0	0	0	0.006	0.004	0.002	0.002	0.002	0.004	0.002	0	0.004	0.008	0.002	0.002
0.068	0.173	0.157	0.159	0.207	0.303	0.355	0.095	0.083	0.091	0.038	0.034	0.042	0.042	0.026	0.037
3.685	3.472	3.485	3.557	3.6	3.232	3.2	3.762	3.471	3.747	3.609	3.702	3.51	3.673	3.674	3.712
0.208	0.343	0.324	0.286	0.183	0.452	0.439	0.176	0.28	0.115	0.116	0.125	0.09	0.093	0.087	0.065
0.056	0.065	0.066	0.062	0.032	0.027	0.029	0.056	0.035	0.031	0.101	0.125	0.133	0.088	0.134	0.135
4.017	4.053	4.032	4.064	4.028	4.028	4.027	4.091	3.898	3.988	3.866	3.986	3.779	3.904	3.923	3.951
5.35	9	8.5	7.44	4.84	12.26	12.05	4.46	7.46	2.98	3.11	3.28	2.49	2.46	2.3	1.71
94.65	91	91.5	92.56	95	87.63	87.89	95.49	92.49	96.91	96.84	96.72	97.4	97.33	97.65	98.24
0	0	0	0	0.16	0.11	0.06	0.05	0.05	0.1	0.05	0	0.11	0.21	0.05	0.05

Appendix 4. electron microprobe analyses of feldspar from the syenitic and granitic phases of the SLIC.

7	8	9	10	11	12	16	17	18	19	20	21	22	23	24	25
"FEL	"FEL	"FEL	"FEL	"FEL	"FEL	"FEL	"FEL	"FEL	"FEL	"FEL	"FEL	"FEL	"FEL	"FEL	"FEL
95MYAA	95MYAA	95MYAA	95MYAA	95MYAA	95MYAA	95MYAA	95MYAA	95MYAA	95MYAA	95MYAA	95MYAA	95MYAA	95MYAA	95MYAA	95MYAA
161-1	161-1	161-1	161-1	161-1	161-1	197-1	197-1	197-1	197-1	197-1	197-1	197-1	197-1	197-1	197-1
A1	A2	A2	A2	A5	A5	A1	A1	A1	A1	A1	A1	A3	A3	A3	A3
AT MARGIN	BRIGHT CEN	INTERIOR	AT MARGIN	CENTRAL	AT MARGIN	CENTRAL	INTERIOR	AT MARGIN	ALBITE, CEN	INTERIOR	AT MARGIN	ALBITE, CEN	INTERIOR	AT MARGIN	AT MARGIN
Granite	Granite	Granite	Granite	Granite	Granite	Granite	Granite	Granite	Granite	Granite	Granite	Granite	Granite	Granite	Granite
64.71	63.14	64.95	64.02	64.16	64.47	64.46	63.8	64.6	68.13	68.65	68.47	67.54	67.49	67.86	68.24
17.92	18.81	18.84	19.01	18.31	18.31	18.72	18.67	18.45	19.66	19.63	19.68	20.77	19.92	20.13	20.1
0.01	0.01	0.02	0	0	0.02	0	0	0.01	0.19	0.06	0.35	1	0.55	0.66	0.26
0.28	1.06	0	0.53	0.32	0.69	0.5	0.91	0.39	0	0	0	0	0	0	0
15.88	15.81	15.99	16.2	15.97	15.82	15.19	15.77	15.28	0.01	0	0.01	0.09	0.06	0.08	0.04
0.27	0.26	0.25	0.26	0.19	0.34	0.69	0.25	0.62	11.54	11.49	11.17	10.45	10.95	10.62	10.41
1.14	0.52	0.1	0.07	0.47	0.66	0.1	0.01	0.04	0.07	0.01	0.04	0.01	0.04	0.05	0.03
100.21	99.61	100.15	100.09	99.42	100.31	99.66	99.41	99.39	99.6	99.84	99.72	99.86	99.01	99.4	99.08
7	8	9	10	11	12	16	17	18	19	20	21	22	23	24	25
"FEL	"FEL	"FEL	"FEL	"FEL	"FEL	"FEL	"FEL	"FEL	"FEL	"FEL	"FEL	"FEL	"FEL	"FEL	"FEL
95MYAA	95MYAA	95MYAA	95MYAA	95MYAA	95MYAA	95MYAA	95MYAA	95MYAA	95MYAA	95MYAA	95MYAA	95MYAA	95MYAA	95MYAA	95MYAA
161-1	161-1	161-1	161-1	161-1	161-1	197-1	197-1	197-1	197-1	197-1	197-1	197-1	197-1	197-1	197-1
A1	A2	A2	A2	A5	A5	A1	A1	A1	A1	A1	A1	A3	A3	A3	A3
AT MARGIN	BRIGHT CEN	INTERIOR	AT MARGIN	CENTRAL	AT MARGIN	CENTRAL	INTERIOR	AT MARGIN	ALBITE, CEN	INTERIOR	AT MARGIN	ALBITE, CEN	INTERIOR	AT MARGIN	AT MARGIN
									L			L		KSPAR	KSPAR
11.999	11.834	11.961	11.875	11.965	11.954	11.947	11.919	11.993	11.948	11.99	11.974	11.806	11.901	11.905	11.969
3.916	4.154	4.039	4.125	4.024	4.001	4.053	4.081	4.007	4.052	4.01	4.026	4.194	4.099	4.095	4.031
15.915	15.988	16	16	15.989	15.955	16	16	16	16	16	16	16	16	16	16
0	0	0.049	0.031	0	0	0.035	0.03	0.029	0.01	0.03	0.03	0.084	0.04	0.066	0.124
0.002	0.002	0.004	0	0	0.004	0	0	0.002	0.036	0.011	0.066	0.187	0.104	0.124	0.049
0.02	0.078	0	0.039	0.023	0.05	0.036	0.067	0.028	0	0	0	0	0	0	0
3.756	3.779	3.756	3.833	3.799	3.741	3.591	3.758	3.618	0.002	0	0.002	0.02	0.013	0.018	0.009
0.097	0.094	0.089	0.094	0.069	0.122	0.248	0.091	0.223	3.924	3.891	3.787	3.541	3.744	3.612	3.54
0.177	0.082	0.015	0.011	0.073	0.102	0.015	0.002	0.006	0.01	0.001	0.006	0.001	0.006	0.007	0.004
4.052	4.035	3.913	4.008	3.964	4.019	3.925	3.948	3.906	3.982	3.933	3.891	3.833	3.907	3.827	3.726
2.52	2.44	2.32	2.38	1.78	3.16	6.46	2.35	5.81	99.04	99.71	98.24	94.47	96.96	96.22	98.39
97.43	97.51	97.58	97.62	98.22	96.74	93.54	97.65	94.14	0.06	0	0.06	0.54	0.35	0.48	0.25
0.05	0.05	0.1	0	0	0.1	0	0	0.05	0.9	0.29	1.7	5	2.69	3.3	1.36

Appendix 4. electron microprobe analyses of feldspar from the syenitic and granitic phases of the SLIC.

26	27	28	29	65	66	67	68	69	70	71	72	73	74	75	76
"FEL	"FEL	"FEL	"FEL	"FEL	"FEL	"FEL	"FEL	"FEL	"FEL	"FEL	"FEL	"FEL	"FEL	"FEL	"FEL
95MYAA	95MYAA	95MYAA	95MYAA	95MYAA	95MYAA	95MYAA	95MYAA	95MYAA	95MYAA	95MYAA	95MYAA	95MYAA	95MYAA	95MYAA	95MYAA
197-1	197-1	197-1	197-1	211-2	211-2	211-2	211-2	211-2	211-2	211-2	211-2	211-2	211-2	211-2	211-2
A3	A3	A3	A3	A2	A2	A2	A2	A2	A2	A3	A4	A4	A5	A5	A5
AT MARGIN	KSPAR, CEN	INTERIOR	AT MARGIN	ALBITE, CEN	CENTRAL A(	INTERIOR 2	AT MARGIN,	INTERIOR 3	INTERIOR 3	KSPAR		AT MARGIN	ALBITE CEN	ALBITE CEN	AT MARGIN
Granite	Granite	Granite	Granite	Granite	Granite	Granite	Granite	Granite	Granite	Granite	Granite	Granite	Granite	Granite	Granite
68.09	64.21	64.56	64.3	68.68	68.59	64.79	69.08	64.42	67.02	65.4	64.53	64.87	67.81	67.48	67.48
19.93	18.48	18.42	18.8	19.91	19.53	22.16	20.01	18.89	20.44	18.48	18.38	18.75	20.41	20.26	19.91
0.4	0	0.01	0.01	0.28	0.11	3.12	0.69	0.01	0.92	0	0	0	0.85	0.98	0.72
0	0.59	0.43	0.87	0	0	0	0	0.72	0	0.26	0.93	0.87	0	0	0
0.06	14.97	15.76	15.56	0.05	0	0.12	0.13	15.08	0.1	14.45	14.79	13.57	0.26	0.08	0.13
10.75	0.77	0.28	0.34	10.88	11.03	9.31	10.38	0.64	10.37	0.64	0.66	0.93	9.82	11.26	11.11
0	0.55	0.11	0.03	0	0	0.16	0.2	0.15	0.2	0.16	0.37	0.26	0.2	0.17	0.14
99.23	99.57	99.57	99.91	99.8	99.26	99.66	100.49	99.91	99.05	99.39	99.66	99.25	99.35	100.23	99.49
26	27	28	29	65	66	67	68	69	70	71	72	73	74	75	76
"FEL	"FEL	"FEL	"FEL	"FEL	"FEL	"FEL	"FEL	"FEL	"FEL	"FEL	"FEL	"FEL	"FEL	"FEL	"FEL
95MYAA	95MYAA	95MYAA	95MYAA	95MYAA	95MYAA	95MYAA	95MYAA	95MYAA	95MYAA	95MYAA	95MYAA	95MYAA	95MYAA	95MYAA	95MYAA
197-1	197-1	197-1	197-1	211-2	211-2	211-2	211-2	211-2	211-2	211-2	211-2	211-2	211-2	211-2	211-2
A3	A3	A3	A3	A2	A2	A2	A2	A2	A2	A3	A4	A4	A5	A5	A5
AT MARGIN	KSPAR, CEN	INTERIOR	AT MARGIN	ALBITE, CEN	CENTRAL A(	INTERIOR 2	AT MARGIN,	INTERIOR 3	INTERIOR 3	KSPAR		AT MARGIN	ALBITE CEN	ALBITE CEN	AT MARGIN
KSPAR				L											
11.952	11.94	11.991	11.93	11.981	12.025	11.433	11.975	11.922	11.819	12.059	11.984	11.998	11.892	11.804	11.871
4.048	4.049	4.009	4.07	4.019	3.975	4.567	4.025	4.078	4.181	3.941	4.016	4.002	4.108	4.176	4.127
16	15.989	16	16	16	16	16	16	16	16	16	16	16	16	15.98	15.998
0.074	0	0.022	0.04	0.073	0.06	0.041	0.063	0.042	0.067	0.074	0.006	0.085	0.11	0	0
0.075	0	0.002	0.002	0.052	0.021	0.59	0.128	0.002	0.174	0	0	0	0.16	0.184	0.136
0	0.043	0.031	0.063	0	0	0	0	0.052	0	0.019	0.068	0.063	0	0	0
0.013	3.551	3.734	3.682	0.011	0	0.027	0.029	3.56	0.022	3.398	3.503	3.201	0.058	0.018	0.029
3.658	0.278	0.101	0.122	3.68	3.749	3.185	3.489	0.23	3.546	0.229	0.238	0.333	3.339	3.819	3.789
0	0.086	0.017	0.005	0	0	0.024	0.029	0.023	0.029	0.025	0.057	0.04	0.029	0.025	0.021
3.82	3.958	3.907	206.057	3.816	3.83	3.867	3.738	3.909	3.838	3.745	3.872	3.722	3.696	4.046	3.975
97.63	7.25	2.63	3.21	98.3	99.45	83.78	95.7	6.06	94.75	6.31	6.35	9.43	93.87	94.99	95.83
0.36	92.75	97.32	96.73	0.3	0	0.71	0.79	93.89	0.6	93.69	93.65	90.57	1.64	0.44	0.74
2.01	0	0.05	0.05	1.4	0.55	15.51	3.52	0.05	4.65	0	0	0	4.49	4.57	3.43

Appendix 4. electron microprobe analyses of feldspar from the syenitic and granitic phases of the SLIC.

77	78	79	80	110	111	112	113	114	115	116	117	118	199	200	201
"FEL	"FEL	"FEL	"FEL	"FEL	"FEL	"FEL	"FEL	"FEL	"FEL	"FEL	"FEL	"FEL	"FEL	"FEL	"FEL
95MYAA	95MYAA	95MYAA	95MYAA	95MYAA	95MYAA	95MYAA	95MYAA	95MYAA	95MYAA	95MYAA	95MYAA	95MYAA	95MYAA	95MYAA	95MYAA
211-2	211-2	211-2	211-2	226-1	226-1	226-1	226-1	226-1	226-1	226-1	226-1	226-1	263-1	263-1	263-1
A5	A5	A6	A6	A1	A1	A1	A1	A1	A1	A3	A3	A3	A1	A1	A1
Kf CENT	AT END	PLAGIOCLAS	IN CONTAC	ALBITE, CEN	INTERIOR	INTERIOR	JUST INSIDE	NARROW M/	NARROW M/	ALBITE, CEN	INTERIOR	AT MARGIN	ALBITE CEN	INTERGROW	AT MARGIN
Granite	Granite	Granite	Granite	Granite	Granite	Granite	Granite	Granite	Granite	Granite	Granite	Granite	Granite	Granite	Granite
63.02	64.28	66.67	67.84	66.67	65.53	65.98	64.57	68.01	67.08	68.63	68.21	68	68.67	68.54	65.37
19.08	18.77	21.06	20.56	21.04	22.01	22.17	22.44	20.62	20.73	20.11	20.05	20.26	19.6	19.61	21.29
0.01	0	1.44	0.96	1.25	2.7	2.73	2.92	0.57	0.72	0.15	0.19	0.57	0.33	0.15	2.07
1.58	0.74	0	0	0	0	0	0	0	0	0	0	0	0	0	0
15.4	14.82	0.09	0.18	0.1	0.25	0.19	0.18	0.13	0.12	0.11	0.02	0.09	0.01	0.04	0.23
0.25	0.51	10.81	10.81	10.93	10.3	8.76	9.91	11.45	11.48	10.91	11.77	10.83	10.65	11.82	9.84
0	0.15	0.13	0.23	0	0.1	0.14	0.16	0.06	0.06	0.13	0.01	0.11	0	0.03	0.13
99.34	99.27	100.2	100.58	99.99	100.89	99.97	100.18	100.84	100.19	100.04	100.25	99.86	99.26	100.19	98.93

77	78	79	80	110	111	112	113	114	115	116	117	118	199	200	201
"FEL	"FEL	"FEL	"FEL	"FEL	"FEL	"FEL	"FEL	"FEL	"FEL	"FEL	"FEL	"FEL	"FEL	"FEL	"FEL
95MYAA	95MYAA	95MYAA	95MYAA	95MYAA	95MYAA	95MYAA	95MYAA	95MYAA	95MYAA	95MYAA	95MYAA	95MYAA	95MYAA	95MYAA	95MYAA
211-2	211-2	211-2	211-2	226-1	226-1	226-1	226-1	226-1	226-1	226-1	226-1	226-1	263-1	263-1	263-1
A5	A5	A6	A6	A1	A1	A1	A1	A1	A1	A3	A3	A3	A1	A1	A1
KSPAR CEN	AT END	PLAGIOCLAS	IN CONTAC	ALBITE, CEN	INTERIOR	INTERIOR	JUST INSIDE	NARROW M/	NARROW M/	ALBITE, CEN	INTERIOR	AT MARGIN	ALBITE CEN	INTERGROW	AT MARGIN
		NTRAL	H BIOTITE	L			RROW OUTE	L ZONE AG/	L ZONE AG/	L				H KSPAR EX	
11.829	11.951	11.673	11.808	11.687	11.453	11.549	11.365	11.807	11.74	11.953	11.895	11.885	12.029	11.957	11.596
4.171	4.049	4.327	4.192	4.313	4.533	4.451	4.635	4.193	4.26	4.047	4.105	4.115	3.971	4.031	4.404
16	16	16	16	16	15.986	16	16	16	16	16	16	16	16	15.988	16
0.05	0.063	0.018	0.025	0.034	0	0.122	0.02	0.025	0.015	0.08	0.015	0.058	0.075	0	0.046
0.002	0	0.27	0.179	0.235	0.506	0.512	0.551	0.106	0.135	0.028	0.035	0.107	0.062	0.028	0.393
0.116	0.054	0	0	0	0	0	0	0	0	0	0	0	0	0	0
3.687	3.514	0.02	0.04	0.022	0.056	0.042	0.04	0.029	0.027	0.024	0.004	0.02	0.002	0.009	0.052
0.091	0.184	3.67	3.648	3.715	3.49	2.973	3.382	3.854	3.895	3.684	3.979	3.67	3.617	3.998	3.384
0	0.023	0.019	0.033	0	0.015	0.02	0.024	0.009	0.009	0.019	0.001	0.016	0	0.004	0.019
3.946	3.838	3.997	3.925	4.006	4.067	3.669	4.017	4.023	4.081	3.835	4.034	3.871	3.756	4.039	3.894
2.41	4.97	92.67	94.34	93.53	86.15	84.28	85.12	96.62	96.01	98.6	99.01	96.66	98.26	99.08	88.37
97.54	95.03	0.51	1.03	0.56	1.38	1.2	1.02	0.72	0.66	0.65	0.11	0.53	0.06	0.22	1.36
0.05	0	6.82	4.63	5.91	12.48	14.51	13.86	2.66	3.33	0.75	0.88	2.81	1.68	0.69	10.27

Appendix 4. electron microprobe analyses of feldspar from the syenitic and granitic phases of the SLIC.

202	203	204	205	206	207	208	187	188	189	190	191	192	176	177	178
"FEL	"FEL	"FEL	"FEL	"FEL	"FEL	"FEL	"FEL	"FEL	"FEL	"FEL	"FEL	"FEL	"FEL	"FEL	"FEL
95MYAA	95MYAA	95MYAA	95MYAA	95MYAA	95MYAA	95MYAA	95MYAA	95MYAA	95MYAA	95MYAA	95MYAA	95MYAA	95MYAA	95MYAA	95MYAA
263-1	263-1	263-1	263-1	263-1	263-1	263-1	251-1	251-1	251-1	251-1	251-1	251-1	251-1	251-1	251-1
A1	A2	A2	A4	A4	A4	A4	A4	A4	A4	A6	A6	A6	A2	A2	A2
AT MARGIN	CENTRAL	AT MARGIN	HIGH Ba ZON	HIGH Ba ZON	INTERIOR	AT MARGIN	ALBITE, CEN	INTERIOR	AT MARGIN	KSPAR, CEN	HIGH-Ba ZON	INTERGROW	OUTER EDGI	INTERIOR 2	INTERIOR 3
Granite	Granite	Granite	Granite	Granite	Granite	Granite	Granite	Granite	Granite	Granite	Granite	Granite	Granite	Granite	Granite
68.33	68.13	68.63	61.5	64.37	64.41	64.84	65.74	66.11	65.29	65.44	64.35	63.09	61.45	61.48	60.11
19.63	20.08	20.02	19.15	18.93	18.46	18.45	21.83	21.76	22.32	18.82	18.53	19.27	19.78	19.95	20.12
0.04	0.88	0.57	0.01	0	0	0.02	2.73	2.86	2.93	0.04	0.02	0.03	0.03	0.01	0.01
0	0	0	2.11	1.48	0.68	0.2	0	0	0	0.72	1.18	1.55	4.34	5.39	5.98
0	0.04	0.04	13.89	14.61	15.29	16.01	0.12	0.11	0.18	14.84	14.58	14.51	11.39	11.6	11.34
11.44	11.28	11.33	0.94	0.48	0.49	0.17	9.87	9.76	8.35	0.93	0.66	0.87	2.1	1.57	1.49
0.01	0	0	1.43	0.05	0.15	0.02	0.11	0.07	0.15	0.05	0.17	0.29	0.05	0.04	0.09
99.45	100.41	100.59	99.03	99.92	99.48	99.71	100.4	100.67	99.22	100.84	99.49	99.61	99.14	100.04	99.14

202	203	204	205	206	207	208	187	188	189	190	191	192	176	177	178
"FEL	"FEL	"FEL	"FEL	"FEL	"FEL	"FEL	"FEL	"FEL	"FEL	"FEL	"FEL	"FEL	"FEL	"FEL	"FEL
95MYAA	95MYAA	95MYAA	95MYAA	95MYAA	95MYAA	95MYAA	95MYAA	95MYAA	95MYAA	95MYAA	95MYAA	95MYAA	95MYAA	95MYAA	95MYAA
263-1	263-1	263-1	263-1	263-1	263-1	263-1	251-1	251-1	251-1	251-1	251-1	251-1	251-1	251-1	251-1
A1	A2	A2	A4	A4	A4	A4	A4	A4	A4	A6	A6	A6	A2	A2	A2
AT MARGIN	CENTRAL	AT MARGIN	HIGH Ba ZON	HIGH Ba ZON	INTERIOR	AT MARGIN	ALBITE, CEN	INTERIOR	AT MARGIN	KSPAR, CEN	HIGH-Ba ZON	INTERGROW	OUTER EDGI	INTERIOR 2	INTERIOR 3
							L					H BIOTITE	IN		
11.98	11.87	11.918	11.668	11.933	11.977	12.007	11.512	11.538	11.51	11.973	11.97	11.79	11.639	11.619	11.525
4.02	4.123	4.082	4.281	4.067	4.023	3.993	4.488	4.462	4.49	4.027	4.03	4.21	4.361	4.381	4.475
16	15.993	16	15.949	16	16	16	16	16	16	16	16	16	16	16	16
0.036	0	0.014	0	0.068	0.022	0.033	0.016	0.013	0.147	0.031	0.031	0.033	0.053	0.062	0.07
0.008	0.164	0.106	0.002	0	0	0.004	0.512	0.535	0.553	0.008	0.004	0.006	0.006	0.002	0.002
0	0	0	0.157	0.108	0.05	0.015	0	0	0	0.052	0.086	0.113	0.322	0.399	0.449
0	0.009	0.009	3.361	3.454	3.626	3.782	0.027	0.024	0.04	3.463	3.459	3.459	2.752	2.796	2.773
3.889	3.81	3.815	0.346	0.173	0.177	0.061	3.351	3.303	2.854	0.33	0.238	0.315	0.771	0.575	0.554
0.001	0	0	0.227	0.008	0.023	0.003	0.016	0.01	0.022	0.008	0.026	0.045	0.008	0.006	0.014
3.934	3.983	3.944	4.093	3.811	3.898	3.898	3.922	3.885	3.616	3.892	3.844	3.971	3.912	3.84	3.862
99.81	95.65	97.08	9.32	4.76	4.65	1.59	86.14	85.52	82.78	8.68	6.43	8.34	21.85	17.05	16.64
0	0.22	0.23	90.62	95.24	95.35	98.31	0.69	0.63	1.17	91.11	93.46	91.5	77.97	82.89	83.3
0.19	4.12	2.7	0.05	0	0	0.1	13.17	13.85	16.05	0.21	0.11	0.16	0.17	0.06	0.06

Appendix 4. electron microprobe analyses of feldspar from the syenitic and granitic phases of the SLIC.

179	180	181	182	183	184	185	186	
"FEL	"FEL	"FEL	"FEL	"FEL	"FEL	"FEL	"FEL	
95MYAA	95MYAA	95MYAA	95MYAA	95MYAA	95MYAA	95MYAA	95MYAA	
251-1	251-1	251-1	251-1	251-1	251-1	251-1	251-1	
A2	A2	A2	A2	A2	A2	A2	A4	
INTERIOR 4	INTERIOR 5	INTERIOR 5	INTERIOR 6	INNER SIDE (	ADJACENT [	ADJACENT [	ALBITE, CENTRA	
Granite	Granite	Granite	Granite	Granite	Granite	Granite	Granite	
59.59	59.63	60.03	60.46	61.04	63.98	64.15	66.32	
20.32	20.11	20.14	20.4	19.65	19.15	19.11	21.78	
0.01	0.01	0.02	0	0	0.01	0	2.89	
6.65	6.47	6.83	6.74	5.55	2.46	2.16	0	
11.2	11.28	10.69	11.21	11.79	13.51	13.15	0.12	
1.51	1.48	1.48	1.57	1.43	1.13	1.21	9.7	
0.01	0.04	0.18	0.07	0.05	0.1	0.12	0.16	
99.29	99.02	99.37	100.45	99.51	100.34	99.9	100.97	
179	180	181	182	183	184	185	186	
"FEL	"FEL	"FEL	"FEL	"FEL	"FEL	"FEL	"FEL	
95MYAA	95MYAA	95MYAA	95MYAA	95MYAA	95MYAA	95MYAA	95MYAA	
251-1	251-1	251-1	251-1	251-1	251-1	251-1	251-1	
A2	A2	A2	A2	A2	A2	A2	A4	
INTERIOR 4	INTERIOR 5	INTERIOR 5	INTERIOR 6	INNER SIDE (	ADJACENT [	ADJACENT [	ALBITE, CENTRA	
				FRAGMENT	N KSPAR	N KSPAR	L	
11.463	11.493	11.518	11.491	11.63	11.862	11.893	11.543	
4.537	4.507	4.482	4.509	4.37	4.138	4.107	4.457	
16	16	16	16	16	16	16	16	
0.07	0.06	0.072	0.06	0.042	0.046	0.068	0.01	
0.002	0.002	0.004	0	0	0.002	0	0.539	
0.501	0.489	0.513	0.502	0.414	0.179	0.157	0	
2.748	2.773	2.616	2.718	2.865	3.195	3.11	0.027	
0.563	0.553	0.551	0.579	0.528	0.406	0.435	3.273	
0.002	0.006	0.029	0.011	0.008	0.016	0.019	0.023	
3.886	3.883	3.785	3.87	3.857	3.844	3.789	3.872	
17	16.62	17.36	17.55	15.57	11.27	12.27	85.27	
82.94	83.32	82.51	82.45	84.43	88.67	87.73	0.69	
0.06	0.06	0.13	0	0	0.06	0	14.04	

Appendix 4. electron microprobe analyses of feldspar from the syenitic and granitic phases of the SLIC.

ANALYSIS	1	2	3	4	5	6	7	8	9	10	11	12
SAMPLE	184-1	184-1	184-1	184-1	213-1	213-1	213-1	213-1	213-1	213-1	213-1	213-1
	Area1 core	Area1 edge	Area3 core	Area3 edge	Area2core	Area2 mid	Area2 edge	Area1 core	Area1 edge	Area2 core	Area2 mid	Area2 edge
SIO2	41.69	41.75	41.69	41.96	39.76	40.64	41.20	40.27	39.26	39.51	40.80	39.80
TIO2	1.37	1.31	1.47	1.34	1.49	1.52	1.58	1.62	2.02	1.45	1.65	2.00
AL2O3	12.17	12.26	12.43	12.48	13.73	13.75	13.27	12.56	12.14	13.48	13.42	12.35
CR2O3	0.47	0.41	0.92	0.61	1.82	1.37	0.05	0.00	0.00	1.65	0.26	0.00
FEO	2.24	3.09	2.64	2.70	3.77	3.90	4.54	4.71	12.68	3.54	5.53	11.68
MNO	0.00	0.00	0.00	0.00	0.05	0.01	0.05	0.03	0.26	0.00	0.02	0.23
MGO	25.12	25.15	25.02	25.38	23.00	23.49	24.48	23.83	18.04	23.17	23.65	18.99
CAO	0.02	0.00	0.01	0.04	0.00	0.00	0.04	0.00	0.00	0.04	0.00	0.10
BAO	0.45	0.34	0.38	0.43	0.47	0.60	0.60	0.64	0.82	0.55	0.53	0.73
NA2O	0.16	0.18	0.14	0.15	0.08	0.09	0.18	0.23	0.10	0.08	0.22	0.16
K2O	9.92	9.60	10.21	10.00	10.20	10.13	10.03	9.83	9.48	9.98	9.83	9.32
F	2.75	3.35	3.26	3.21	1.28	1.23	1.78	1.93	1.42	1.48	1.80	1.54
CL	0.00	0.02	0.01	0.01	0.00	0.00	0.00	0.00	0.00	0.03	0.00	0.00
Subtotal	96.36	97.46	98.18	98.31	95.65	96.73	97.80	95.65	96.22	94.96	97.71	96.90
O =>F,Cl	1.16	1.42	1.37	1.35	0.54	0.52	0.75	0.81	0.60	0.63	0.76	0.65
TOTAL	95.20	96.04	96.81	96.96	95.11	96.21	97.05	94.84	95.62	94.33	96.95	96.25
Basis of 22 oxygens												
Si	5.9747	5.9591	5.9185	5.9347	5.7381	5.7844	5.8299	5.8512	5.8676	5.7492	5.8021	5.8684
Al IV	2.0253	2.0409	2.0804	2.0653	2.2619	2.2156	2.1701	2.1488	2.1324	2.2508	2.1979	2.1316
Ti	0.1477	0.1406	0.1569	0.1425	0.1617	0.1627	0.1681	0.1770	0.2270	0.1587	0.1765	0.2218
Al	0.0309	0.0221	0.0000	0.0156	0.0741	0.0916	0.0436	0.0027	0.0066	0.0617	0.0521	0.0152
Cr	0.0532	0.0463	0.1033	0.0682	0.2076	0.1542	0.0056	0.0000	0.0000	0.1898	0.0292	0.0000
Fe	0.2685	0.3689	0.3134	0.3194	0.4550	0.4642	0.5373	0.5723	1.5849	0.4308	0.6577	1.4403
Mn	0.0000	0.0000	0.0000	0.0000	0.0061	0.0012	0.0060	0.0037	0.0329	0.0000	0.0024	0.0287
Mg	5.3652	5.3499	5.2936	5.3498	4.9469	4.9827	5.1624	5.1603	4.0181	5.0247	5.0123	4.1730
Ca	0.0031	0.0000	0.0015	0.0061	0.0000	0.0000	0.0061	0.0000	0.0000	0.0062	0.0000	0.0158
Ba	0.0253	0.0190	0.0211	0.0238	0.0266	0.0335	0.0333	0.0364	0.0480	0.0314	0.0295	0.0422
Na	0.0445	0.0498	0.0385	0.0411	0.0224	0.0248	0.0494	0.0648	0.0290	0.0226	0.0607	0.0457
K	1.8137	1.7481	1.8492	1.8044	1.8780	1.8395	1.8107	1.8222	1.8076	1.8527	1.7835	1.7532
F	1.2464	1.5122	1.4637	1.4359	0.5842	0.5537	0.7966	0.8869	0.6712	0.6811	0.8096	0.7181
Cl	0.0000	0.0048	0.0024	0.0024	0.0000	0.0000	0.0000	0.0000	0.0000	0.0074	0.0000	0.0000
Tot(cat)	15.7520	15.7446	15.7766	15.7710	15.7785	15.7544	15.8224	15.8395	15.7542	15.7786	15.8039	15.7359

1 95MYAA184-1 CIRC 1 MICA CORE

Appendix 5A. Electron microprobe analyses of mica from lamprophyre and syenite dykes in the SLIC.

2 95MYAA184-1 AREA 1 MICA EDGE
3 95MYAA184-1 AREA 3 MICA CENTRE
4 95MYAA184-1 AREA 3 MICA EDGE
5 95MYAA213-1 AREA 2 MICA CENTRE
6 95MYAA213-1 AREA 2 MICA MIDDLE
7 95MYAA213-1 AREA 2 MICA EDGE
8 95MYAA213-1 AREA 1 MICA CENTRE
9 95MYAA213-1 AREA 1 MICA EDGE
10 95MYAA213-1 AREA 2 MICA CENTRE
11 95MYAA213-1 AREA 2 MICA MIDDLE
12 95MYAA213-1 AREA 2 MICA EDGE
13 95MYAA199-1 AREA 1 MATRIX MICA
14 95MYAA199-1 AREA 2 MATRIX MICA
15 95MYAA199-1 AREA 4 MATRIX MICA
17 95MYAA199-1 AREA 6 MICA CENTRE

Appendix 5A. Electron microprobe analyses of mica from lamprophyre and syenite dykes in the SLIC.

13	14	15	17
199-1	199-1	199-1	199-1
Area1 matrix	Area2 matrix	Area4 matrix	Area6 core
36.57	36.67	37.54	38.35
2.66	3.01	2.58	1.50
14.89	14.84	13.99	14.23
0.00	0.00	0.00	0.00
17.90	17.88	16.17	11.46
0.26	0.28	0.26	0.02
13.14	13.05	14.18	19.37
0.00	0.00	0.03	0.10
0.70	0.59	0.17	0.37
0.03	0.11	0.04	0.16
9.76	9.70	9.17	8.93
0.22	0.30	0.30	0.28
0.01	0.01	0.03	0.00
96.14	96.44	94.46	94.77
0.09	0.13	0.13	0.12
96.05	96.31	94.33	94.65
5.5572	5.5532	5.7129	5.6741
2.4428	2.4468	2.2871	2.3259
0.3040	0.3428	0.2953	0.1669
0.2247	0.2026	0.2229	0.1562
0.0000	0.0000	0.0000	0.0000
2.2749	2.2645	2.0580	1.4181
0.0335	0.0359	0.0335	0.0025
2.9758	2.9453	3.2160	4.2711
0.0000	0.0000	0.0049	0.0159
0.0417	0.0350	0.0101	0.0214
0.0088	0.0323	0.0118	0.0459
1.8922	1.8741	1.7804	1.6856
0.1057	0.1437	0.1444	0.1310
0.0026	0.0026	0.0077	0.0000
15.7556	15.7325	15.6329	15.7837

Appendix 5A. Electron microprobe analyses of mica from lamprophyre and syenite dykes in the SLIC.

	4	5	6	7	8	9	10
	213-1 Area 1 centre	213-1 Area 1 middle	213-1 Area 1 edge	199-1 Area 1 centre	199-1 Area 1 edge	199-1 Area 7 centre	199-1 Area 7 edge
SIO2	54.51	54.25	55.05	54.44	53.45	54.62	53.84
TIO2	0.20	0.20	0.29	0.12	0.12	0.14	0.02
AL2O3	0.49	0.56	0.61	0.91	0.54	1.01	0.39
CR2O3	0.09	0.17	0.06	0.11	0.08	0.13	0.02
FEO	3.03	2.77	3.66	3.82	8.85	3.91	8.65
MNO	0.16	0.10	0.10	0.10	0.93	0.08	1.09
MGO	18.00	17.58	17.40	17.77	12.94	17.46	12.77
CAO	22.93	23.53	23.31	22.77	23.26	22.95	23.78
NA2O	0.18	0.23	0.31	0.25	0.60	0.29	0.50
K2O	0.00	0.00	0.00	0.00	0.00	0.00	0.06
Total	99.59	99.39	100.79	100.29	100.77	100.59	101.12
	Basis of 6 oxygens						
Si	1.9878	1.9844	1.9893	1.9772	1.9906	1.9787	1.9988
Al IV	0.0122	0.0156	0.0107	0.0228	0.0094	0.0213	0.0012
Ti	0.0055	0.0055	0.0079	0.0033	0.0034	0.0038	0.0006
Al	0.0089	0.0085	0.0153	0.0162	0.0143	0.0219	0.0159
Cr	0.0026	0.0049	0.0017	0.0032	0.0024	0.0037	0.0006
Fe	0.0924	0.0847	0.1106	0.1160	0.2756	0.1185	0.2686
Mn	0.0049	0.0031	0.0031	0.0031	0.0293	0.0025	0.0343
Mg	0.9783	0.9584	0.9371	0.9618	0.7182	0.9427	0.7065
Ca	0.8960	0.9222	0.9026	0.8861	0.9282	0.8909	0.9460
Na	0.0127	0.0163	0.0217	0.0176	0.0433	0.0204	0.0360
K	0.0000	0.0000	0.0000	0.0000	0.0000	0.0000	0.0028
Tot(cat)	4.0012	4.0037	3.9999	4.0073	4.0147	4.0042	4.0112

4 95MYAA213-1 AREA 1 CPX CENTRE REPEAT
5 95MYAA213-1 AREA 1 CPX MIDDLE REPEAT
6 95MYAA213-1 AREA 1 CPX EDGE

7 95MYAA199-1 AREA 1 CPX CENTRE (DARK)
8 95MYAA199-1 AREA 1 CPX BRIGHT
9 95MYAA199-1 AREA 7 CPX CENTRE
10 95MYAA199-1 AREA 7 CPX BRIGHT

Appendix 5B. Electron microprobe analyses of clinopyroxene from lamprophyre-syenite dykes in the SLIC.

	2	3	4	5	6	7	8	9	10	11	12	13	14	15	16
SIO2	63.34	64.03	64.29	64.46	64.22	63.61	64.69	63.57	64.29	64.51	68.78	68.06	61.23	62.46	63.70
AL2O3	18.83	18.70	18.58	18.39	18.65	18.67	18.34	18.83	18.43	18.30	19.67	19.51	18.90	18.41	18.33
FE2O3	0.17	0.00	0.13	0.14	0.20	0.03	0.04	0.22	0.17	0.38	0.06	0.03	0.60	0.49	0.14
CAO	0.00	0.00	0.00	0.00	0.02	0.00	0.01	0.01	0.02	0.02	0.13	0.11	0.06	0.00	0.00
SRO	0.00	0.07	0.05	0.07	0.00	0.06	0.07	0.03	0.00	0.00	0.09	0.06	0.62	0.31	0.00
BAO	1.08	1.17	0.33	0.37	0.97	1.53	0.29	1.30	0.39	0.17	0.00	0.04	3.10	1.85	0.27
NA2O	0.19	0.19	0.19	0.17	0.19	0.23	0.21	0.26	0.17	0.14	11.70	11.79	0.66	0.50	0.17
K2O	15.86	16.11	16.40	16.47	16.41	15.95	16.21	16.06	16.33	16.41	0.12	0.16	14.02	14.87	16.44
Total	99.47	100.27	99.97	100.07	100.66	100.08	99.86	100.28	99.80	99.93	100.55	99.76	99.19	98.89	99.05
			Basis of 8 oxygens												
Si	2.9651	2.9766	2.9835	2.9902	2.9749	2.9707	2.9990	2.9615	2.9882	2.9917	2.9901	2.9858	2.9195	2.9584	2.9848
Al	1.0392	1.0249	1.0165	1.0057	1.0185	1.0279	1.0024	1.0342	1.0099	1.0005	1.0081	1.0091	1.0624	1.0280	1.0126
Fe	0.0060	0.0000	0.0045	0.0049	0.0070	0.0011	0.0014	0.0077	0.0059	0.0133	0.0020	0.0010	0.0215	0.0175	0.0049
Ca	0.0000	0.0000	0.0000	0.0000	0.0010	0.0000	0.0005	0.0005	0.0010	0.0010	0.0061	0.0052	0.0031	0.0000	0.0000
Sr	0.0000	0.0019	0.0013	0.0019	0.0000	0.0016	0.0019	0.0008	0.0000	0.0000	0.0023	0.0015	0.0171	0.0085	0.0000
Ba	0.0198	0.0213	0.0060	0.0067	0.0176	0.0280	0.0053	0.0237	0.0071	0.0031	0.0000	0.0007	0.0579	0.0343	0.0050
Na	0.0172	0.0171	0.0171	0.0153	0.0171	0.0208	0.0189	0.0235	0.0153	0.0126	0.9862	1.0029	0.0610	0.0459	0.0154
K	0.9472	0.9555	0.9710	0.9747	0.9698	0.9503	0.9587	0.9545	0.9683	0.9709	0.0067	0.0090	0.8529	0.8985	0.9828
Tot(cat)	4.9945	4.9973	5.0000	4.9995	5.0058	5.0004	4.9880	5.0065	4.9958	4.9931	5.0013	5.0151	4.9955	4.9911	5.0055

2 KSPAR IN SAMPLE RANDOM
3 95MYAA184-1 CIRC 2 K-SPAR CORE
4 95MYAA184-1 CIRC 2 K-SPAR MIDDLE
5 95MYAA184-1 CIRC 2 K-SPAR EDGE
6 95MYAA184-1 CIRC 1 REAL KSPAR CORE
7 95MYAA184-1 CIRC 1 REAL KSPAR MIDDLE
8 95MYAA184-1 CIRC 1 REAL KSPAR EDGE
9 95MYAA184-1 CIRC 3 KSPAR CORE
10 95MYAA184-1 CIRC 3 KSPAR MIDDLE
11 95MYAA184-1 CIRC 3 KSPAR EDGE
12 95MYAA184-1 CIRC 3 INTERSTITIAL PLAG
13 95MYAA184-1 CIRC 3 INTERSTITIAL PLAG
14 95MYAA213-1 AREA 1 KSPAR CENTRE
15 95MYAA213-1 AREA 1 KSPAR MIDDLE
16 95MYAA213-1 AREA 1 KSPAR EDGE
17 95MYAA213-1 AREA 2 KSPAR CENTRE (DARKEST)
18 95MYAA213-1 AREA 2 KSPAR MIDDLE (MED BRIGHT)
19 95MYAA213-1 AREA 2 KSPAR EDGE (VERY BRIGHT)
20 95MYAA213-1 AREA 2 KSPAR OUTER RIM (DARK)
21 95MYAA213-1 AREA 2 PLAG (ALBITE)
22 95MYAA213-1 AREA 1 PLAG (ALBITE)
23 95MYAA199-1 AREA 1 KSPAR (DARK)
24 95MYAA199-1 AREA 1 KSPAR EDGE(BRIGHT)
25 95MYAA199-1 AREA 1 KSPARR EDGE REPEAT

Appendix 5C. Electron microprobe analyses of feldspar from lamprophyre-syenite dykes in the SLIC.

17	18	19	20	21	22	23	24	25	26	27	28	29	30	31
62.82	61.55	61.62	64.83	68.32	68.76	64.63	64.20	64.87	64.40	64.27	65.00	66.11	67.42	65.99
18.88	19.01	19.35	17.95	19.19	19.29	18.55	19.04	18.88	18.85	18.70	21.78	21.79	20.37	21.40
0.52	0.56	0.58	0.49	0.34	0.32	0.42	0.40	0.34	0.15	0.04	0.48	0.15	0.20	0.31
0.01	0.00	0.03	0.00	0.04	0.06	0.03	0.02	0.14	0.01	0.02	2.89	2.16	0.99	2.38
0.38	0.54	0.62	0.00	0.05	0.01	0.14	0.26	0.21	0.29	0.21	0.13	0.37	0.20	0.11
2.34	3.47	3.36	0.02	0.00	0.00	0.21	1.14	0.53	0.86	0.80	0.00	0.01	0.05	0.07
2.03	0.90	1.93	0.37	11.47	11.53	0.28	0.47	0.96	0.53	0.29	9.87	10.30	11.01	10.25
12.50	13.96	12.30	16.09	0.55	0.36	16.38	15.91	14.87	15.68	15.95	0.24	0.37	0.11	0.40
99.48	99.99	99.79	99.75	99.96	100.33	100.64	101.44	100.80	100.77	100.28	100.39	101.26	100.35	100.91
2.9440	2.9171	2.9077	3.0051	2.9948	2.9982	2.9809	2.9561	2.9756	2.9723	2.9795	2.8579	2.8794	2.9469	2.8847
1.0431	1.0622	1.0764	0.9809	0.9917	0.9916	1.0086	1.0336	1.0210	1.0257	1.0220	1.1290	1.1189	1.0497	1.1029
0.0183	0.0200	0.0206	0.0171	0.0112	0.0105	0.0146	0.0139	0.0117	0.0052	0.0014	0.0159	0.0049	0.0066	0.0102
0.0005	0.0000	0.0015	0.0000	0.0019	0.0028	0.0015	0.0010	0.0069	0.0005	0.0010	0.1362	0.1008	0.0464	0.1115
0.0103	0.0148	0.0170	0.0000	0.0013	0.0003	0.0037	0.0069	0.0056	0.0078	0.0056	0.0033	0.0093	0.0051	0.0028
0.0430	0.0644	0.0621	0.0004	0.0000	0.0000	0.0038	0.0206	0.0095	0.0156	0.0145	0.0000	0.0002	0.0009	0.0012
0.1845	0.0827	0.1766	0.0333	0.9749	0.9748	0.0250	0.0420	0.0854	0.0474	0.0261	0.8414	0.8698	0.9331	0.8688
0.7474	0.8441	0.7405	0.9515	0.0308	0.0200	0.9638	0.9346	0.8702	0.9233	0.9434	0.0135	0.0206	0.0061	0.0223
4.9911	5.0053	5.0024	4.9883	5.0065	4.9982	5.0020	5.0085	4.9859	4.9976	4.9935	4.9971	5.0039	4.9946	5.0043

Appendix 5C. Electron microprobe analyses of feldspar from lamprophyre-syenite dykes in the SLIC.

26 95MYAA199-1 AREA 2 KSPAR CENTRE (DARK)
27 95MYAA199-1 AREA 4 KSPAR (UNZONED)
28 95MYAA199-1 AREA 4 PLAG (UNZONED)
29 95MYAA199-1 AREA 2 PLAG (UNZONED)
30 95MYAA199-1 AREA 2 PLAG (UNZONED) REPEAT
31 95MYAA199-1 AREA 1 PLAG (UNZONED)

Appendix 5C. Electron microprobe analyses of feldspar from lamprophyre-syenite dykes in the SLIC.

SAMPLE		BE	NA2O	MGO	AL2O3	SIO2	P2O5	K2O	CAO
95MYAA 184-1	FG LMPP	10.000	1.390	4.340	13.300	62.900	0.380	7.580	1.620
95MYAA 213-1	LMPP	5.900	3.060	4.620	12.100	60.600	0.750	6.140	3.680
95MYAA 199-1	Syenite dyke	3.800	3.080	5.470	13.400	54.400	0.580	5.220	5.680
95MYAA 269-2	MS	3.800	0.500	4.000	12.900	55.900	0.930	8.580	4.560
95MYAA 212-1	MS	3.400	2.320	5.070	12.500	55.700	1.000	7.570	5.660
95MYAA 249-3	MS	12.300	1.730	5.630	12.100	51.500	1.590	7.740	7.030
95MYAA 249-1	S	5.000	2.820	1.990	14.300	61.900	0.470	7.860	2.750
95MYAA 271-2	S	9.500	2.880	3.180	13.200	64.300	0.330	6.190	2.600
95MYAA 211-3	S	3.900	2.610	0.820	15.900	63.600	0.270	10.300	1.540
95MYAA 245-2	fg LEUCO S	5.000	4.650	0.100	13.000	74.500	-0.010	4.010	0.940
95MYAA 211-2	cg LEUCO S	6.000	4.230	0.540	16.000	64.400	0.120	7.280	1.320
95MYAA 208-1	FG MS	3.700	1.320	7.010	10.300	49.100	1.680	7.620	8.100
95MYAA 208-2	MG LEU S	3.000	1.960	0.900	15.400	61.800	0.190	11.200	2.190
95MYAA 227-7	FG MS	5.000	2.200	3.670	12.500	54.000	0.990	8.330	6.230
95MYAA 179-1	FG MS	9.000	2.030	4.170	12.700	55.900	1.020	8.640	4.260
95MYAA 208-3	MG S	11.900	3.580	0.630	15.500	63.900	0.110	8.030	1.980
95MYAA 202-3	CG S	4.400	2.690	2.660	13.400	58.000	0.840	7.840	4.250
95MYAA 202-3	CG S	8.300	4.680	0.060	12.900	75.400	-0.010	4.220	0.400
95MYAA 201-1	CGG	5.100	3.500	0.510	13.400	70.800	0.090	5.460	1.200
95MYAA 202-2	CG S	4.400	2.470	3.440	12.600	56.400	0.940	8.370	4.900
95MYAA 186-1	FGG	4.100	4.320	0.230	14.100	71.400	0.020	4.700	0.990
95MYAA 200-1	FGG	3.700	3.910	0.330	14.400	72.100	0.060	5.220	1.180
95MYAA 201-2	FGG	4.900	4.030	0.220	13.700	72.300	0.020	5.190	0.920
95MYAA 191-2	FGG	4.000	4.470	0.630	14.900	68.800	0.080	4.250	1.460
95MYAA 191-1	CGG	6.800	3.860	0.380	13.500	71.100	0.060	5.280	0.990
95MYAA 181-1	CGG	5.900	3.680	0.380	13.800	70.800	0.050	5.710	0.730
DDH 95-61 420	PORPHY	3.500	1.850	1.440	13.600	69.400	0.080	6.610	0.610
95MYAA 263-1	G	10.400	3.760	0.410	13.800	71.400	0.060	5.440	0.610
95MYAA 268-2	G	7.200	4.000	0.290	13.400	72.200	0.040	5.030	1.020
95MYAA 197-1	G	6.500	3.860	0.460	13.700	70.700	0.090	5.310	1.160
95MYAA 251-1	G	6.600	3.750	0.500	14.000	70.300	0.130	5.150	1.520
95MYAA 226-1	cg G	6.900	3.870	0.460	13.900	70.300	0.100	5.370	1.220
95MYAA 215-4	mg G	7.900	3.770	0.470	13.900	70.000	0.100	5.590	1.450
95MYAA 227-5	fg G/S	3.800	3.960	0.590	14.600	68.700	0.130	5.480	1.660

Appendix 6. Geochemistry of the various phases of the SLIC.

SC	TIO2	V	CR2O3	MNO	FE2O3	CO	NI	CU	ZN	AS
4.900	0.634	38.000	-0.010	0.030	3.240	13.000	123.000	7.300	62.000	-3.000
9.600	0.541	69.000	0.020	0.050	4.130	16.000	80.000	26.300	69.700	-3.000
15.400	0.513	105.000	-0.010	0.090	6.830	24.000	29.000	39.700	89.000	-3.000
12.000	0.831	73.000	-0.010	0.060	6.100	13.000	43.000	5.000	59.400	4.000
13.900	0.666	90.000	0.010	0.100	6.460	19.000	100.000	38.200	89.200	4.000
20.000	0.970	126.000	0.010	0.100	7.480	25.000	112.000	75.000	94.500	6.000
7.200	0.543	51.000	-0.010	0.050	4.240	7.000	22.000	5.200	52.400	5.000
6.700	0.629	51.000	-0.010	0.060	3.410	12.000	81.000	12.500	71.700	7.000
5.000	0.337	33.000	-0.010	0.020	1.870	3.000	10.000	25.700	29.800	5.000
0.600	0.024	7.000	-0.010	-0.010	1.000	-1.000	2.000	2.100	7.600	-3.000
2.200	0.351	24.000	-0.010	0.020	2.400	1.000	4.000	3.200	36.600	7.000
20.500	1.100	139.000	0.020	0.090	8.290	34.000	189.000	23.600	126.000	-3.000
5.300	0.458	45.000	-0.010	0.020	2.040	4.000	10.000	11.900	31.700	-3.000
15.000	0.768	103.000	-0.010	0.080	6.700	19.000	62.000	36.400	96.000	-3.000
11.500	0.878	92.000	-0.010	0.060	5.950	15.000	74.000	18.100	95.900	-3.000
4.300	0.286	18.000	-0.010	0.030	1.980	5.000	4.000	72.900	51.500	-3.000
10.300	0.743	82.000	-0.010	0.070	5.250	10.000	43.000	6.800	109.000	-3.000
0.800	0.046	-2.000	-0.010	-0.010	0.590	-1.000	1.000	0.600	4.800	-3.000
1.000	0.268	10.000	-0.010	-0.010	1.640	2.000	3.000	1.500	33.400	-3.000
12.800	0.756	100.000	-0.010	0.060	5.950	15.000	66.000	21.100	97.700	-3.000
1.500	0.106	5.000	-0.010	-0.010	1.050	-1.000	-1.000	0.500	32.000	-3.000
1.600	0.199	11.000	-0.010	-0.010	1.870	-1.000	-1.000	1.800	27.700	-3.000
0.800	0.092	4.000	-0.010	-0.010	0.970	-1.000	-1.000	2.000	15.700	-3.000
1.000	0.242	22.000	-0.010	-0.010	1.720	2.000	6.000	1.500	24.200	-3.000
0.900	0.196	10.000	-0.010	-0.010	1.510	-1.000	2.000	2.700	10.800	-3.000
0.800	0.188	12.000	-0.010	-0.010	1.370	2.000	2.000	2.300	19.000	-3.000
2.300	0.263	22.000	-0.010	0.020	2.430	3.000	5.000	36.300	43.600	4.000
1.500	0.236	11.000	-0.010	0.010	1.810	-1.000	3.000	6.100	20.900	4.000
1.100	0.181	10.000	-0.010	0.010	1.570	-1.000	2.000	3.400	16.600	4.000
1.300	0.207	11.000	-0.010	-0.010	1.600	-1.000	3.000	4.500	21.700	4.000
3.600	0.304	17.000	-0.010	0.030	2.150	2.000	4.000	4.000	61.700	9.000
1.300	0.209	13.000	-0.010	0.010	1.740	1.000	3.000	2.600	27.200	7.000
2.300	0.242	19.000	-0.010	0.020	1.930	2.000	6.000	6.000	53.500	5.000
3.300	0.363	28.000	-0.010	0.020	2.480	3.000	8.000	22.400	50.100	7.000

Appendix 6. Geochemistry of the various phases of the SLIC.

RB	SR	SR	Y	ZR	NB	MO	AG	CD	SN	SB
181.000	268.000	268.000	24.700	525.000	68.000	-1.000	1.100	-1.000	-10.000	-5.000
153.000	881.000	829.000	10.400	122.000	12.000	2.000	0.500	-1.000	-10.000	-5.000
138.000	2390.000	2150.000	16.600	159.000	8.000	4.000	0.200	-1.000	-10.000	-5.000
301.000	1070.000	1190.000	36.000	149.000	12.000	-1.000	-0.200	-1.000	-10.000	-5.000
296.000	1300.000	1410.000	35.000	73.000	9.000	-1.000	-0.200	-1.000	-10.000	-5.000
333.000	2240.000	2100.000	43.000	340.000	15.000	-1.000	-0.200	-1.000	-10.000	6.000
254.000	1580.000	1590.000	42.000	424.000	15.000	-1.000	-0.200	-1.000	-10.000	-5.000
275.000	702.000	650.000	26.000	461.000	28.000	-1.000	0.200	-1.000	-10.000	-5.000
364.000	1180.000	1180.000	21.000	78.000	8.000	8.000	-0.200	-1.000	-10.000	-5.000
191.000	501.000	497.000	15.000	50.000	4.000	-1.000	-0.200	-1.000	-10.000	-5.000
298.000	1670.000	1680.000	30.000	427.000	11.000	-1.000	-0.200	-1.000	-10.000	-5.000
201.000	2260.000	1900.000	32.100	133.000	11.000	-1.000	-0.200	-1.000	-10.000	-5.000
267.000	1510.000	1340.000	10.500	67.500	9.000	1.000	-0.200	-1.000	-10.000	-5.000
196.000	2450.000	2230.000	30.500	132.000	12.000	-1.000	-0.200	-1.000	-10.000	-5.000
254.000	989.000	916.000	25.600	304.000	15.000	-1.000	0.600	-1.000	-10.000	-5.000
261.000	1310.000	1310.000	13.600	145.000	12.000	-1.000	0.200	-1.000	-10.000	-5.000
202.000	1340.000	1180.000	27.700	255.000	13.000	-1.000	0.500	-1.000	-10.000	-5.000
291.000	61.200	97.000	4.800	107.000	8.000	-1.000	-0.200	-1.000	-10.000	-5.000
248.000	686.000	712.000	13.900	212.000	15.000	-1.000	-0.200	-1.000	-10.000	-5.000
247.000	1490.000	1250.000	24.900	96.500	10.000	-1.000	-0.200	-1.000	-10.000	-5.000
204.000	364.000	348.000	10.800	85.900	11.000	-1.000	-0.200	-1.000	-10.000	-5.000
212.000	430.000	419.000	11.500	219.000	13.000	-1.000	-0.200	-1.000	-10.000	-5.000
200.000	382.000	373.000	9.200	98.900	9.000	-1.000	-0.200	-1.000	-10.000	-5.000
123.000	1140.000	1070.000	7.700	134.000	5.000	-1.000	0.200	-1.000	-10.000	-5.000
180.000	653.000	632.000	8.300	189.000	8.000	-1.000	0.500	-1.000	-10.000	-5.000
206.000	683.000	628.000	9.500	201.000	6.000	-1.000	0.200	-1.000	-10.000	-5.000
219.000	326.000	309.000	17.000	211.000	8.000	2.000	-0.200	-1.000	-10.000	-5.000
322.000	573.000	536.000	18.000	201.000	13.000	-1.000	-0.200	-1.000	-10.000	-5.000
290.000	535.000	497.000	16.000	220.000	10.000	-1.000	-0.200	-1.000	-10.000	-5.000
266.000	905.000	847.000	21.000	237.000	8.000	-1.000	-0.200	-1.000	-10.000	-5.000
237.000	1290.000	1250.000	25.000	299.000	11.000	-1.000	-0.200	-1.000	-10.000	-5.000
258.000	1110.000	1070.000	21.000	240.000	10.000	-1.000	-0.200	-1.000	-10.000	-5.000
270.000	1120.000	1030.000	23.000	270.000	10.000	-1.000	-0.200	-1.000	-10.000	-5.000
186.000	1150.000	1130.000	30.000	327.000	13.000	-1.000	-0.200	-1.000	-10.000	5.000

Appendix 6. Geochemistry of the various phases of the SLIC.

BA	LA	W	PB	BI	LOI	SUM	CO2T	H2OT	FEO	ST	Fe2O3 conver
2100.000	182.000	-10.000	-2.000	-5.000	2.750	98.500	0.8	2.1	2.0	0.02	2.22268
3380.000	75.600	-10.000	303.000	-5.000	1.000	97.300	0.2	1.0	1.8	0.11	2.000412
3350.000	54.000	-10.000	321.000	-5.000	1.150	97.100	0.5	1.2	3.9	0.42	4.334226
7880.000	103.000	-10.000	-2.000	-5.000	3.950	99.400	2.1	2.0	2.3	0.02	2.556082
7260.000	104.000	-10.000	68.000	-5.000	0.650	98.700	0.1	0.8	3.8	0.11	4.223092
10200.000	128.000	-10.000	37.000	-5.000	0.650	98.000	0.1	0.9	4.3	0.10	4.778762
6350.000	126.000	-10.000	35.000	-5.000	0.500	98.400	0.3	0.6	1.5	0.04	1.66701
1470.000	128.000	-10.000	4.000	-5.000	1.650	98.800	0.5	1.4	1.9	0.01	2.111546
5750.000	50.800	-10.000	79.000	-5.000	0.400	98.500	0.2	0.3	0.6	0.04	0.666804
796.000	17.700	-10.000	74.000	-5.000	0.450	98.900	0.1	0.2	0.1	0.01	0.111134
4770.000	98.400	-10.000	58.000	-5.000	0.600	98.100	0.2	0.3	0.8	0.03	0.889072
7650.000	151.000	-10.000	21.000	-5.000	0.500	96.300	0.2	0.9	5.1	0.09	5.667834
6510.000	41.400	-10.000	35.000	5.000	0.350	97.500	0.2	0.2	1.1	0.02	1.222474
5840.000	102.000	-10.000	33.000	-5.000	0.250	96.700	0.1	0.4	3.4	0.04	3.778556
5010.000	111.000	-10.000	-2.000	-5.000	0.900	97.400	0.2	0.9	2.7	0.06	3.000618
4270.000	205.000	-10.000	71.000	-5.000	0.800	97.600	0.6	0.3	1.0	0.21	1.11134
5010.000	145.000	-10.000	59.000	-5.000	0.550	97.100	0.4	0.4	1.8	0.04	2.000412
78.000	6.300	-10.000	82.000	-5.000	0.150	98.500	0.1	0.1	0.0	0.01	0
2400.000	137.000	-10.000	81.000	-5.000	0.750	98.100	0.1	0.4	0.7	0.02	0.777938
6130.000	117.000	-10.000	33.000	8.000	0.300	97.100	0.1	0.4	3.1	0.09	3.445154
783.000	24.400	-10.000	74.000	-5.000	0.350	97.400	0.1	0.3	0.2	0.01	0.222268
1330.000	123.000	-10.000	60.000	-5.000	0.600	100.100	0.1	0.4	0.7	0.01	0.777938
733.000	56.700	-10.000	87.000	-5.000	0.600	98.200	0.1	0.3	0.3	0.01	0.333402
2070.000	52.500	-10.000	33.000	7.000	0.550	97.500	0.1	0.5	0.6	0.02	0.666804
1870.000	93.700	-10.000	39.000	-5.000	0.550	97.800	0.2	0.4	0.3	0.01	0.333402
2020.000	85.300	-10.000	49.000	-5.000	0.600	97.700	0.1	0.4	0.1	0.02	0.111134
1990.000	79.400	-10.000	25.000	-5.000	1.900	98.500	0.6	1.4	2.0	0.13	2.22268
1920.000	101.000	-10.000	64.000	-5.000	0.750	98.600	0.3	0.5	2.6	0.01	2.889484
1110.000	67.100	-10.000	69.000	-5.000	0.400	98.400	0.1	0.3	0.4	0.00	0.444536
2580.000	125.000	-10.000	60.000	-5.000	0.800	98.300	0.2	0.4	0.5	0.01	0.55567
3630.000	199.000	-10.000	102.000	-5.000	0.400	98.900	0.1	0.4	0.8	0.02	0.889072
3600.000	141.000	-10.000	69.000	-5.000	0.600	98.400	0.2	0.4	0.6	0.02	0.666804
2880.000	96.400	-10.000	107.000	-5.000	0.500	98.500	0.1	0.3	0.6	0.01	0.666804
3040.000	113.000	-10.000	68.000	-5.000	0.250	98.800	0.1	0.3	1.0	0.01	1.11134

Appendix 6. Geochemistry of the various phases of the SLIC.

Fe2O3 calc
1.017
2.130
2.496
3.544
2.237
2.701
2.573
1.298
1.203
0.889
1.511
2.622
0.818
2.921
2.949
0.869
3.250
0.590
0.862
2.505
0.828
1.092
0.637
1.053
1.177
1.259
0.207
-1.079
1.125
1.044
1.261
1.073
1.263
1.369

SAMPLE	Ba	Th	Nb	Ta	La	Ce	Nd	Sm	Zr	Hf
184-1	2117.391	74.108	32.941	2.3	174.207	369.297	150.503	22.316	598.396	14.823
213-1	3605.153	32.636	9.333	0.737	76.741	144.099	55.119	8.881	405.429	9.615
199-1	3495.769	14.254	9.879	0.621	52.223	109.72	51.299	9.093	189.291	4.405
208-1	7611.239	18.945	7.913	0.641	147.125	292.307	134.371	23.899	183.572	5.026
208-2	6271.008	5.319	10.889	0.628	104.071	218.277	108.019	20.746	217.912	5.468
227-7	5422.29	20.531	16.51	0.909	115.748	232.573	106.27	18.889	443.571	10.816
179-1	68.603	25.904	1.354	0.167	5.656	12.974	5.224	0.983	116.102	5.217
202-3	6011.212	13.563	8.364	0.744	110.36	219.62	98.889	17.356	114.4	3.991
202-2	5032.634	21.947	3.201	0.909	72.13	116.075	38.224	5.023	42.785	1.314
166-1	2108.199	17.031	2.359	0.389	52.061	94.727	33.268	4.97	153.367	3.87
191-2	4781.875	22.171	2.687	0.513	152.628	277.579	97.607	14.05	57.031	2.023
170-1	2023.737	49.617	1.789	0.245	83.241	155.943	52.151	7.26	236.762	6.196
181-1	2031.071	48.288	2.848	0.295	82.074	154.799	51.813	7.408	225.471	5.701

Appendix 7. Rare earth element analyses of selected rocks from the SLIC.

Tb	Y	Tm	Yb	Eu	Gd	Pr	Dy	Ho	Er	Lu
1.313	24.954	0.247	1.38	3.465	11.671	42.505	5.558	0.86	1.985	0.199
0.631	11.5	0.115	0.684	2.309	5.609	15.761	2.626	0.382	0.966	0.104
0.731	17.242	0.231	1.542	2.435	6.101	13.187	3.611	0.662	1.654	0.22
1.764	31.769	0.32	1.704	6.269	15.845	34.567	7.939	1.23	2.695	0.245
1.64	32.226	0.348	1.818	5.55	14.723	26.853	7.761	1.231	2.804	0.276
1.442	27.735	0.296	1.766	5.001	12.768	27.6	6.485	1.035	2.437	0.26
0.107	5.062	0.076	0.614	0.255	0.78	1.434	0.606	0.128	0.461	0.129
1.32	25.669	0.243	1.424	4.77	11.706	25.342	5.868	0.974	2.113	0.207
0.288	5.251	0.06	0.406	1.162	2.631	11.466	1.263	0.189	0.455	0.063
0.35	8.246	0.101	0.693	1.167	2.855	9.845	1.667	0.277	0.749	0.099
0.867	14.957	0.167	0.962	3.353	8.113	28.781	3.711	0.574	1.311	0.157
0.44	9.673	0.106	0.669	1.717	3.841	15.775	1.996	0.326	0.836	0.109
0.454	9.796	0.114	0.668	1.726	4.185	15.683	2.048	0.33	0.831	0.099

Appendix 7. Rare earth element analyses of selected rocks from the SLIC.

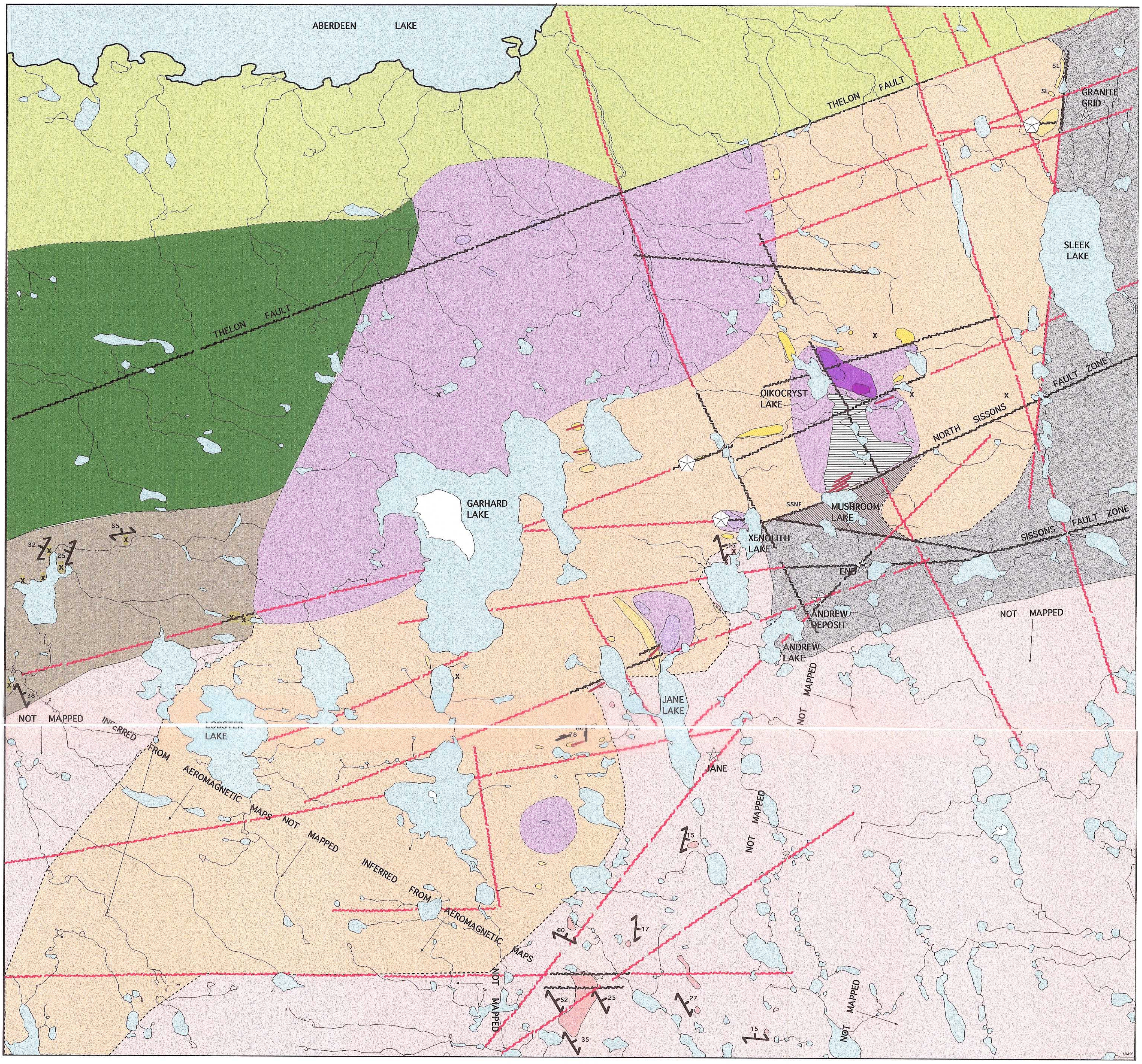

FIGURE 4
GEOLOGY OF THE SOUTHERN HALF OF THE PALEOPROTEROZOIC SCHULTZ LAKE INTRUSIVE COMPLEX, in parts of SCHULTZ LAKE, 66A/5 & ABERDEEN LAKE, 66B/8 WESTERN CHURCHILL PROVINCE.

Kilometers
0 1 2 3

ARCHEAN

Woodburn Lake Group, circa 2.80 Ga

- Unsubdivided greywacke, banded iron formation, orthoquartzite
- Metavolcanic rocks

Presumed older basement? gneisses

- Biotite +/- garnet quartzo-feldspathic paragneiss
- Layered granitic - granodioritic gneiss
- Potassic feldspar augen gneiss

PALEOPROTEROZOIC

Barrensland Group, circa 1.72 Ga

- Thelon Formation: sandstone

SCHULTZ LAKE INTRUSIVE COMPLEX, circa 1.9 - 1.84 Ga

POST- GRANITIC DYKE PHASSE

- Lamprophyre , fine-grained syenite

GRANITIC PHASE

- Glomeroporphyritic leucocratic coarse-grained flourite granite, leucocratic fine-grained granite, aplite
- Agmatitic zone: granite in syenite

SYENITIC PHASE

- Porphyritic and subporphyritic fine- to medium-grained hornblende+phlogopite +/- clinopyroxene syenite; fine-grained syenite dykes
- Melanocratic oikocrystic potassic feldspar syenite

- Foliation
- Fault , assumed
- Fault , observed
- Uranium deposit
- Proposed zones for geophysical surveys